THE UNIVERSITY
of EDINBURGH

Apoptosis-driven activation of macrophages by starry-sky B-cell lymphoma

Jorine Willems

For the degree of Doctor of Philosophy

The University of Edinburgh

2015

Acknowledgements

I would like to thank my supervisor Professor Christopher Gregory for his help, guidance, encouragement, and support during my PhD project. I am also appreciative of my second supervisor Professor Adriano Rossi for giving me scientific advice when needed. I would also like to specially thank Dr. John Pound for his advice, helpful discussions, and help with experiments, especially for doing the radioactive parts of the Cr51 release assays, and in revising the manuscript of this thesis.

Furthermore, I would like to thank various other members of the Inflammation and Cancer Group. Dr. Margaret Paterson for her help with experiments and endless help and patience for using the Attune. Lynsey Melville for carrying out and harvesting tumours from the xenograft model, as well as her help in setting up cultures of BMDM. Ben Arnold for the use of his sheep anti-lactoferrin antibody. Dr. Catriona Ford for her help with Western Blotting. Lihui Zhuang for teaching me how to prepare ESDM and collaborating on the chemotaxis and phagocytosis experiments presented here. Sofia Petrova for her well-kept lab books that helped me to set up my own qPCR experiments. Karen Colvin for printing my thesis.

I am also grateful to everyone in the Inflammation and Cancer Group for providing a pleasant atmosphere to work in.

I would also like to express my gratitude to Bruno Giotti for his help with processing and analysing quality of array databases, and Professor Tom Freeman for his help and advice on using the BioLayout Express 3^D software.

Furthermore, I would like to thank Leukaemia and Lymphoma Research for providing the funding to carry out this research.

And last, but not least, I would like to express my gratitude to my family and friends, especially Jay, for their support and patience.

Declaration

I declare that the work presented in this thesis was my original work, unless otherwise acknowledged. All sources of information are clearly stated. The work has not been submitted in any previous application for a degree.

Jorine Willems

Abstract

In high-grade 'starry-sky' non-Hodgkin's lymphoma (NHL), particularly Burkitt's lymphoma (BL), large numbers of apoptotic tumour cells are engulfed by infiltrating tumour-associated macrophages (TAM). *In situ* studies suggest that in starry-sky TAM in a xenograft model of BL various tumour-promoting, trophic, angiogenic, tissue remodelling, and anti-inflammatory pathways are activated. Furthermore, apoptotic cells have been shown to activate expression of tumour-promoting matrix metalloproteinases in macrophages. This work investigates the hypothesis that apoptotic cells or factors released from apoptotic cells induce additional aspects of the starry-sky TAM signature, which serve to promote tumour growth.

Macrophages at different stages of maturation, cultured *in vitro* in the presence of large numbers of apoptotic cells, were shown to differ in phenotype, giving credibility to the hypothesis. Less mature mouse bone marrow-derived macrophages (BMDM) were better at migrating towards apoptotic cells, whereas mature BMDM were better at phagocytosing them. Lactoferrin, which is released from cells undergoing apoptosis and inhibits the migration of neutrophils, was selected as a candidate mediator in the activation of macrophages by apoptotic cells. Lactoferrin was shown to bind viable human and murine monocytes and macrophages, however only high concentrations, which are unlikely to be physiologically or clinically relevant, were found to affect expression of starry-sky TAM genes or reduce classically-activated macrophage cytotoxicity.

The direct effect of apoptotic cells on macrophage activation was assessed. Mature BMDM were not used for these studies as their development *in vitro* in a highly apoptotic environment was judged likely to bias their activation state toward that of TAM, therefore macrophages were first classically-activated with IFN-γ and LPS. This reduced the expression of many starry-sky TAM genes, including several genes associated with responses to apoptotic cells. However, classical activation did not inhibit apoptotic cell engulfment, but rather enhanced it. Co-culture with apoptotic cells, but not viable cells, increased the gene expression of Gas6, Mrc1, Cd36,

Timp2, and Pparg, and the latter was dependent on direct interaction with macrophages rather than factors released from apoptotic cells. Furthermore, classically-activated macrophages were found to induce apoptosis in lymphoma cells, and although pre-co-culture of the macrophages with apoptotic cells did not reduce their ability to induce apoptosis, it enhanced tumour cell growth.

Macrophage deficiency of IL-4Rα or galectin-3 did not affect classically-activated macrophage responses to apoptotic cells. However, classical activation of galectin-3 deficient macrophages appeared to restore the decreased ability of galectin-3 deficient, untreated macrophages to phagocytose apoptotic cells.

Because of the unique new method of laser-capture microdissection by which starry-sky TAM signatures were established, direct comparisons with expression databases of tissue and *in vitro* cultured macrophages were not possible, but indirect comparisons suggest starry-sky TAM activation reflects the activation phenotype of a mixture of tissue macrophages. Furthermore, it highlighted phagocytosis as one of the most important pathways activated by starry-sky TAM.

Together the results presented here suggest apoptotic lymphoma cells can shape TAM activation signatures in starry-sky NHL, even when macrophages are pre-activated to induce apoptosis in lymphoma cells. This is important when considering the consequences of anti-cancer therapies that induce apoptosis or aim to redirect phagocyte activation.

Lay Summary

Although it may seem counter-intuitive, high rates of tumour cell apoptosis (cell suicide) are observed in many rapidly growing tumours. This is often accompanied by pronounced infiltration of the tumours by macrophages (multifunctional cells which can reduce inflammatory responses by engulfing dying cells). These features are clinically important as they are associated with a poor prognosis. Recent studies in mouse experimental models of lymphoma, which share these characteristics, have shown that the tumour-associated macrophages reduce inflammation and support tumour growth. This project investigated whether apoptotic lymphoma cells or factors released from them could provide the biochemical signals that induce these properties in tumour-associated macrophages. In support of this, macrophages that were cultured *in vitro* in the presence of apoptotic cells were shown to change their characteristics. Immature macrophages were better at moving towards attractive biochemical signals, but after they matured they were better at engulfing apoptotic cells. Lactoferrin, a protein released from apoptotic cells, was selected as a candidate factor that could induce these changes in macrophages. Although lactoferrin was shown to bind to macrophages, only high concentrations, which were unlikely to be physiologically or clinically relevant in the tumour, were found to affect macrophage activation. Therefore the direct effect of apoptotic cells on macrophages was assessed. Macrophages were first activated to become pro-inflammatory and capable of inducing cell death in tumour cells. Co-culture with apoptotic, but not viable tumour cells, reduced pro-inflammatory responses and induced tumour supportive pathways in macrophages. Furthermore, macrophages that had been co-cultured in direct contact with apoptotic cells supported tumour cell growth. Furthermore, comparison of gene activity in macrophages taken from tumours and normal tissues showed that proficiency for engulfment of apoptotic cells distinguished those associated with tumours. Together these results suggest that apoptotic cells can direct the pattern of activation of tumour-associated macrophages to favour tumour growth, even when the macrophages are initially stimulated to kill tumour cells. These findings are important when considering the consequences of anti-cancer therapies that induce apoptosis or aim to re-direct phagocyte activation.

Table of contents

List of Figures

List of Tables

List of abbreviations

Abca1	ATP-binding cassette transporter
ADCC	antibody-dependent cellular cytotoxicity
Anpep	Alanyl (membrane) aminopeptidase (CD13)
Apaf-1	apoptosis protease-activating factor-1
ATP	adenosine triphosphate
Axl	AXL receptor tyrosine kinase
BAFF/BLyS	B cell-activating factor of the TNF family/B lymphocyte stimulator
BAI-1	brain-specific angiogenesis inhibitor 1
BL	Burkitt's Lymphoma
BMDM	Bone marrow-derived macrophages
CALLA	common acute lymphoblastic leukaemia antigen
CCL	chemokine (C-C motif) ligands
CCL2	monocyte chemotactic protein
CD	Cluster of Differentiation
CD206	mannose receptor
Cd36	CD36 scavenger receptor
Cd93	CD93 receptor
CNS	central nervous system
CRT	calreticulin
CSF1	colony stimulating factor 1
CSF1R	colony stimulating factor 1 receptor
Ctsb	Cathepsin B
Ctsd	Cathepsin D
Ctsl	Cathepsin L
Ctss	Cathepsin S
CX3CR1	chemokine (C-X3-C motif) receptor 1
CXCL	chemokine (C-X-C motif) ligands
dATP	deoxyadenosine triphosphate
DC	dendritic cell
DLBCL	diffuse large B-cell lymphoma
DNA	deoxyribonucleic acid
DTH	delayed-type hypersensitivity
e	embryonic day
E-selectin	endothelial-leukocyte adhesion molecule 1
EBV	Epstein-Barr virus
EGF	epidermal growth factor
Emp1	Epithelial membrane protein 1
ER	endoplasmic reticulum
FADD	Fas-associated death domain protein
FGF	fibroblast growth factor
FISH	fluorescence *in situ* hybridisation

Fn1	fibronectin
Gas6	Growth arrest specific 6
GCM	tingible-body macrophages from the germinal centres of activated lymphoma nodes
GM-CSF	granulocyte-macrophage colony-stimulating factor
Gpnmb	Glycoprotein (transmembrane) NMB (osteoactivin)
GTPases	guanosine triphosphatases
H&E	haematoxylin and eosin
HGF	hepatocyte growth factor
HIV	human immunodeficiency virus
HMGB1	nonhistone chromatin protein high-mobility group box 1
Hmox1	Heme oxygenase (decycling) 1
HO-1	heme oxygenase-1
HSPG	heparan sulphate proteoglycans
i.p.	intraperitoneal
ICAM-1	intercellular adhesion molecule 1
ICAM-3	intercellular adhesion molecule 3
ICG	immunogenic cell death
IFN-γ	interferon gamma
Ig	Immunoglobulin
IGF-1	insulin-like growth factor 1
IL	interleukin
IL-1Ra	IL-1 receptor antagonist
IL-4Rα	IL-4 receptor α chain
iNOS	inducible nitric oxide synthase
Lamp2	Lysosomal associated membrane protein 2
LDL	low-density lipoprotein
Lgals3	Galectin 3
LNM	macrophages from resting lymph nodes
LPC	lysophosphatidylcholine
LPS	lipopolysaccharide
LRP1	low density lipoprotein receptor-related protein 1
MAPK	mitogen-activated protein kinase
Mertk	c-Mer tyrosine kinase
MFG-E8	milk fat globule epidermal growth factor
MHC	major histocompatibility complex
Mip-2	macrophage inflammatory protein-2
MLC	myosin light chain
Mmp12	Matrix metalloproteinase 12
Mmp2	Matrix metalloproteinase 2
Mmp3	Matrix metalloproteinase 3
MMPs	metalloproteinases
Mrc1	Mannose receptor, C type 1 (CD206)

MSR	macrophage scavenger receptor
NF-κB	nuclear factor of kappa light polypeptide gene enhancer in B cells 1
NHL	non-Hodgkin lymphoma
NK	natural killer
NO	nitric oxide
NO_2^-	nitrite
NO_3^-	nitrate
$ONOO^-$	peroxynitrite
PAF	platelet activating factor
PAMPs	pathogen-associated molecular patterns
PDGF	platelet-derived growth factor
PGE2	prostaglandin E2
Plau	Urokinase plasminogen activator
PMN	polymorphonuclear leukocytes
Pparg	Peroxisome proliferator activated receptor gamma
PS	phosphatidylserine
Psap	prosaposin
RNA	ribonucleic acid
ROCK	Rho-associated protein kinase
ROIs	Reactive oxygen intermediates
S1P	sphingosine-1-phosphate
Sepp1	Selenoprotein P plasma 1
SLE	systemic lupus erythematosus
TAM	Tumour-associated macrophages
TGF-β	transforming growth factor-β
Tgfb1	Transforming growth factor beta 1
T_H1	T helper 1
T_H2	T helper 2
TIE2	angiopoietin-1 receptor
TIM-4	T cell immunoglobulin mucin 4
Timp2	Tissue inhibitor of metalloproteinase 2
TLR	Toll-like receptor
TNFα	tumour necrosis factor α
Tregs	regulatory T cells
Trem2	Triggering receptor expressed on myeloid cells 2
UTP	uridine triphosphate
VEGF	vascular endothelial growth factor

Chapter 1 Introduction

1.1 Burkitt's Lymphoma

Burkitt's Lymphoma (BL) is a highly aggressive mature B-cell neoplasm. It makes up 40% of non-Hodgkin lymphomas (NHL) in youth under the age of 20. It presents as a rapidly enlarging mass, most commonly at extranodal sites. Three clinical variants have been described, an endemic, sporadic, and human immunodeficiency virus (HIV)-associated form. The endemic form was first described by Denis Burkitt in Uganda in 1958 (whom it was named after), and predominantly affects young children in equatorial Africa. It is still the commonest NHL in childhood across Africa, and occurs at an incidence of 40-50 per million children (Walusansa *et al.*, 2012; Molyneux *et al.*, 2012), with boys being affected twice as often as girls (Molyneux *et al.*, 2012). It is usually associated with Epstein-Barr virus (EBV) infection (more than 95% of cases), and the tumours are largely localized to the jaw, facial bones, kidneys, or abdominal region (Bornkamm, 2009; Ondrejka and Hsi, 2015). The sporadic type is less geographically defined, and its geographical distribution includes North America and Europe. It occurs most commonly in children between 3 and 12 years of age and is 3.5 times more common in boys. It accounts 30-40% of childhood non-Hodgkin lymphomas in North America and Europe, and 1-2% of adult lymphomas (Molyneux *et al.*, 2012). The sporadic form mostly presents with abdominal or bone marrow involvement in immunocompetent children, and less than a quarter of the cases show manifestations in the head or neck (Wang *et al.*, 1992; Ondrejka and Hsi, 2015). The third type is immunodeficiency-related, and is known for its association with HIV (Molyneux *et al.*, 2012).

1.1.1 Characteristics

The cell of origin in BL is controversial, with some arguing it is a germinal center B-cell and others believing it originates from a memory B cell (Molyneux *et al.*, 2012). The rate of cell division in BL is among the highest of any human tumour, and is reflected by the presence of numerous mitotic figures. Ki-67 staining, a cell cycle-specific marker, shows that typically more than 95% of the tumour cells are

progressing through the cell cycle. Additionally, BL presents with high levels of apoptotic cells, which are rapidly phagocytosed by tingible body macrophages. This leads to the characteristic "starry sky" appearance of haematoxylin and eosin (H&E) staining of histological sections of BL, where scattered, lightly stained phagocytic macrophages stand out from the background of dark blue stained tumour cells (Hecht and Aster, 2000; Molyneux *et al.*, 2012; Ondrejka and Hsi, 2015). The tumour cells usually express the B-cell-specific markers CD19 (Cluster of Differentiation 19), CD20, immunoglobulin (Ig) M, κ or λ light chain, as well as low to intermediate levels of CD10/CALLA (common acute lymphoblastic leukaemia antigen) (Hecht and Aster, 2000; Ondrejka and Hsi, 2015).

1.1.2 Mechanism

1.1.2.1 c-Myc translocation

All BL cases are characterised by the translocation of the *c-myc* gene (8q24) to the immunoglobulin heavy-chain region (14q32) (in 80% of cases), the kappa light-chain gene (2p11) (15% of cases), or lambda-chain gene (22q11). *c-myc* translocation is usually demonstrated by fluorescence *in situ* hybridisation (FISH) (Hecht and Aster, 2000; Ondrejka and Hsi, 2015), although it is not a specific marker for BL, as *c-myc* rearrangements are sometimes observed in large B-cell lymphoma, lymphoblastic lymphoma, a subset of very aggressive transformed follicular lymphomas, and a fraction of late-stage multiple myeloma (Hecht and Aster, 2000). The proximity of the translocated *c-myc* gene to the enhancer elements of one of the immunoglobulin genes leads to *c-myc* dysregulation and results in high levels of c-Myc mRNA and protein expression (ar-Rushdi *et al.*, 1983; Hayday *et al.*, 1984; Molyneux *et al.*, 2012). Another gene that is mutated in 30% of BL cases is the tumour suppressor gene p53 (Gaidano *et al.*, 1991). Mutation of p53 is thought to be a late event during BL progression and may be induced by c-Myc overexpression, as c-Myc can induce p53-dependent apoptosis (Gutierrez *et al.*, 1997) .

c-Myc encodes a basic helix-loop-helix (bHLH) transcription factor that plays an important role in cellular homeostasis. Among c-Myc targets are genes that encode

proteins that regulate cell growth, division, death, metabolism, adhesion, and motility, which are all important in cellular transformation. These effects of c-Myc are in agreement with the pathological picture of BL, as BL also exhibits high rates of growth, apoptosis and metabolism (Hecht and Aster, 2000).

1.1.2.2 Epstein-Barr Virus

EBV is a ubiquitous gamma herpesvirus that is present in over 95% of the human population and establishes a seemingly harmless latent infection in B cells (Brady *et al.*, 2008). Although the mechanism linking EBV infection to BL remains undiscovered, several observations suggest EBV infection can cause endemic Burkitt's lymphoma, including the finding that infection of EBV precedes tumourigenesis (Neri *et al.*, 1991), the ability of EBV to induce immortalisation of B cells *in vitro*, and high EBV antibody titres before disease development (Geser *et al.*, 1982). One proposed function of EBV in endemic BL is that EBV gene expression of nuclear antigens and membrane proteins can block apoptosis of B cells that have acquired a *c-myc* translocation (Molyneux *et al.*, 2012). Additionally, EBV has been shown to induce DNA damage to infected cells, promote genomic instability, and dysregulate telomere functions (Kamranvar *et al.*, 2007), which may drive tumourigenesis.

1.1.2.3 Other factors

The incidence of endemic BL in Africa has long been linked to the prevalence of malaria. Several studies suggest that malaria can interact with EBV-infected B cells, which can dysregulate EBV persistence and immunity in children. Malaria signalling through toll-like receptor 9 has been shown to induce activation of cytidine deaminase, which can induce immunoglobulin-c-myc translocations. Normal B cells will undergo apoptosis upon c-Myc overexpression, but EBV latent proteins' anti-apoptotic functions might allow B cells to tolerate *c-myc* translocations, leading to malignancy (Molyneux *et al.*, 2012).

Additionally, HIV infection has been associated with BL, and may affect B cells through chronic B cell activation and dysregulation of activation-induced cytidine deaminase. Impaired immune surveillance could promote survival of B cells that have acquired chromosomal rearrangements induced by cytidine deaminase overexpression (Molyneux *et al.*, 2012).

1.1.3 Treatment and outcome

Management of BL depends on the clinical stage of disease. Localised disease that can be completely removed surgically is usually accompanied with two cycles of moderately intensive chemotherapy. Dose and intensity of chemotherapy are increased for children with residual or later stage disease, or with central nervous system (CNS) and bone-marrow involvement. Chemotherapy regimens may include a combination of cyclophosphamide, vincristine, prednisolone, and doxorubicin, and methotrexate for high-dose treatments. These treatments are highly toxic, and initial tumour lysis is possible, but nowadays greatly reduced by the use of urate oxidase. Advanced supportive care is needed to care for patients. In low-income countries supportive care is not always sufficient, and to avoid treatment-related mortality, the intensity of treatment is determined by the amount of available supportive care and the child's tolerance of chemotherapy (Molyneux *et al.*, 2012).

The outcome for sporadic BL in high-income countries is good, with an overall cure rate of 90%. However, if relapse occurs, prognosis is poor. In low-income countries, treatment failure is higher because of lower-dose treatment, incomplete treatment, treatment-related mortality, and late presentation (Molyneux *et al.*, 2012).

1.2 Macrophages

Macrophage in Greek means "big eater" (makros "large" and phagos "to eat"). Macrophages were first described by Ilya Ilyich Mechnikov, a Russian bacteriologist, in the late nineteenth century, and named for their ability to take up microorganisms. Macrophages are found in virtually all tissues, and play critical

roles in innate immunity, as well as the initiation of adaptive immunity by recruiting lymphocytes. Furthermore, they play a critical role in development, homeostasis, and tissue repair (Gordon, 2007; Nathan, 2008; Hart *et al.*, 2008; Wynn *et al.*, 2013).

1.2.1 Origin

In embryonic vertebrates, macrophages are first detected in the yolk sac, the site of primitive haematopoiesis in embryos, at the late head-fold stage (embryonic day (e) 7.5), where they are derived directly from mesenchymal progenitor cells (Hume, 2006; Lichanska and Hume, 2000; Shepard and Zon, 2000; Wynn *et al.*, 2013). They can be identified by morphological characteristics, as well as expression of macrophage markers including colony stimulating factor 1 receptor (CSF1R), CD11b, and mannose receptor, and have been shown to phagocytose dying cells (Hughes and Gordon, 1998; Gordon and Taylor, 2005; Hume, 2006). However, they are distinct from macrophages in adult vertebrates; yolk sac macrophages lack expression of the surface marker F4/80 and the key macrophage transcriptional regulator PU.1 (Lichanska and Hume, 2000; Hume, 2006). Distribution of these primitive macrophages across the embryo has mostly been studied in zebrafish, where cells, because of zebrafish's transparency, can be more easily followed. These studies have shown that macrophage precursors in the yolk sac differentiate and then emigrate to the head mesenchyme and its circulation (Herbomel *et al.*, 1999).

Haematopoietic progenitor cells from the yolk sac then populate the primitive liver, which becomes the first site of haematopoiesis. After e11, macrophages that have differentiated from monocytic progenitor cells are found throughout the embryo (Rae *et al.*, 2007; Lichanska *et al.*, 1999; Dzierzak *et al.*, 1998; Wynn *et al.*, 2013). Macrophages derived from the liver share more similarities with the macrophages observed in adults, and the cells express F4/80, macrophage scavenger receptor (MSR) and low levels of lysozyme, and PU.1 (Morris *et al.*, 1991; Faust *et al.*, 1994; Lichanska *et al.*, 1999). The number of macrophages continues to increase at this stage, and they are found in all developing organs and tissues, including, e.g. kidney, brain, and lungs, and may make up 10 to 15% of total cells in many organs (Lichanska and Hume, 2000; Camp and Martin, 1996; Sorokin *et al.*, 1992). These

cells have been shown to be actively involved in phagocytosis of dying cells, which is most obviously shown at the development of the interdigital zone in the developing footpad (Hopkinson-Woolley *et al.*, 1994).

After birth, the bony structures are formed and the bone marrow becomes the main site of haematopoiesis (van Furth *et al.*, 1972; Pollard, 2009; Wynn *et al.*, 2013). Monocytes originate in the bone marrow from a common myeloid progenitor that is shared with neutrophils, and they are then released into the peripheral blood, where they circulate before entering tissue where they can develop into either macrophages or dendritic cells (Volkman and Gowans, 1965; Gordon and Taylor, 2005). Peripheral blood monocytes show morphological heterogeneity, such as variability of size, granularity, and nuclear morphology. Subpopulations are defined by the differential expression of markers such as CD14, CD16 (FcγRIII), CD64 (FcγRI) (Gordon and Taylor, 2005), angiopoietin-1 receptor (TIE2) (Qian and Pollard, 2010), and, in mice, Ly6c (Gordon and Taylor, 2005). This heterogeneity suggests different physiological activities of monocyte subsets and precise roles have been studied, but remain largely unclear and may be dependent on the microenvironment. Ly6c+ inflammatory monocytes appear to be recruited only to sites of infections or injury, whereas Ly6c- monocytes may be patrolling monocytes that act to maintain vessel integrity and to detect pathogens (Wynn *et al.*, 2013).

Until recently, monocytes were thought to replenish tissue macrophage populations. However, recent findings have shown that in T helper 2 (T_H2)-related pathologies, tissue macrophages were shown to undergo rapid in situ proliferation, which was controlled by interleukin 4 (IL-4) (Jenkins *et al.*, 2011). Furthermore, yolk sac-derived macrophages have been shown to persist in adult mice in several tissues, including liver Kupffer cells, and microglia (Schulz *et al.*, 2012; Ginhoux *et al.*, 2010). Langerhans cells were found to be of both yolk sac and fetal liver origin (Hoeffel *et al.*, 2012). This suggests that in addition to monocyte recruitment, macrophage populations may be replenished by tissue macrophage proliferation, and the balance between both methods may depend on the tissue and microenvironment.

Regardless of their origin, almost all macrophages are regulated by CSF1R, and its expression is required for differentiation into macrophages. CSF1R is the cognate receptor for colony stimulating factor 1 (CSF1), which in addition to the differentiation of macrophages from progenitors, also controls their proliferation and viability *in vitr*o. Additionally, granulocyte-macrophage colony-stimulating factor (GM-CSF) and interleukin 3 (IL-3) have been shown to induce the differentiation of monocytes into macrophages *in vitro* (Pollard, 2009; Hume and MacDonald, 2012; Wynn *et al.*, 2013)

1.2.2 Macrophage activation

Macrophages are very versatile, plastic cells that can adopt a wide variety of functional programmes. Which programme is activated depends on the environmental signals present in the macrophage's microenvironment. Each activation programme is characterized by the expression of certain receptors and chemokine and cytokine production, which influences the effector function of the macrophage (Mantovani *et al.*, 2004a; Wynn *et al.*, 2013; Sica and Mantovani, 2012). Traditionally, macrophages have been classified into classically activated macrophages (or M1), which is induced by interferon gamma (IFN-γ) and lipopolysaccharide (LPS) stimulation, and alternatively activated macrophages (M2), activated by IL-4 and IL-13. However, this is a simplistic presentation, and a whole spectrum of macrophages exists, which may have characteristics of either M1 or M2 or both (Mantovani *et al.*, 2002; Wynn *et al.*, 2013). Transcription profiling of resident macrophages for the 'Immunological Genome Project' has shown that there are many unique classes of macrophages (Gautier *et al.*, 2012). Here the main characteristics and functions of classically-activated and alternatively-activated macrophages, as well as the various activations associated with tumour-associated macrophages are discussed. The role of apoptotic cell interaction on macrophage activation will be discussed in section 1.3.2.

1.2.2.1 Classically-activated macrophages

The term 'classically-activated' macrophage has been used to describe macrophages that are produced during cell-mediated immune responses. Classically-activated macrophages can be induced by IFN-γ alone, or in combination with microbial stimuli, e.g. LPS, and results in a macrophage that has enhanced inflammatory, microbicidal and tumouricidal capacity, and secretes high levels of pro-inflammatory cytokines and mediators. IFN-γ can be produced by innate natural killer (NK) cells, which can produce IFN-γ in response to stress and infections, or by adaptive immune cells, in particular T helper 1 (T_H1) cells (Mosser and Edwards, 2008; Mantovani *et al.*, 2004b). Alternatively, tumour necrosis factor α (TNFα) or recognition of other pathogen-associated molecular patterns (PAMPs), such as lipoproteins, dsRNA, lipoteichoic acid, or endogenous danger signals such as heat shock proteins, can induce a classical activation profile. Classically-activated macrophages typically produce high levels of TNFα, IL-6, IL-12, and in humans also IL-23, and low levels of IL-10 (Van Ginderachter *et al.*, 2006; Sica *et al.*, 2008b; Verreck *et al.*, 2004; Urban *et al.*, 1986). IL-12 and IL-23 are strong promotors of T_H1 and T_H17 cells that can drive inflammatory responses (Sica and Mantovani, 2012). LPS activation of monocytes or macrophages results in the NF-κB-mediated (nuclear factor of kappa light polypeptide gene enhancer in B cells 1) transcription of inflammatory cytokines, including chemokine (C-X-C motif) ligands (CXCL) 1, 2, 3, 5, 8, 9, and 10, and chemokine (C-C motif) ligands (CCL) 2, 3, 4, 5, 11, 17, and 22. These chemokines amplify delayed-type hypersensitivity (DTH) reactions and resistance to intracellular pathogens and tumours (Richmond, 2002; Mantovani *et al.*, 2004b). Furthermore, IFN-γ stimulates Toll-like receptor 4 (TLR4) expression (Bosisio *et al.*, 2002).

Classically-activated macrophages exert anti-proliferative and cytotoxic activities that can lead to the killing of bacteria and tumour cells. These effects are a result of their ability to secrete reactive nitrogen and oxygen species (e.g. nitric oxide (NO), peroxynitrite, hydrogen peroxide, and superoxide) and pro-inflammatory cytokines (TNFα, IL-1β) (Van Ginderachter *et al.*, 2006; Sica *et al.*, 2008b). Nitric oxide is produced when LPS and IFN-γ-stimulated macrophages are induced to express an

inducible form of the enzyme nitric oxide synthase (iNOS), which causes the metabolism of L-arginine to NO and L-citrulline. NO is highly unstable and decomposes into other nitrogen oxides such as nitrite (NO_2^-) and nitrate (NO_3^-) or in the presence of superoxide anion to the potent oxidizing agent peroxynitrite ($ONOO^-$) (Jorens *et al*., 1995). These nitrogen oxides are major effector molecules with bactericidal (Murray and Nathan, 1999) and tumouricidal properties (Jorens *et al*., 1995; Hibbs *et al*., 1988; Higuchi *et al*., 1990; Keller *et al*., 1990). E.g. nitric oxide from macrophages was shown to induce apoptosis in P815 cells in *in vitro* co-cultures, which could be inhibited by a specific inhibitor of NO synthase (Cui *et al*., 1994). NO-induced apoptosis is thought to be a consequence of NO-induced DNA damage (Nguyen *et al*., 1992; Messmer *et al*., 1994), and mice deficient in iNOS are incapable of inhibiting lymphoma cell replication (MacMicking *et al*., 1995). Reactive oxygen intermediates (ROIs) are generated by the respiratory burst of monocytes and macrophages in the response to ligand-receptor interactions, and are involved in both antibody-dependent and independent macrophage cytotoxicity (Martin and Edwards, 1993; Aliprantis *et al*., 1996). IFN-γ stimulation of macrophages can induce apoptosis of various tumour cells, including P815 mastocytoma cells and L929 fibroblasts, which was shown by DNA laddering (Cui *et al.*, 1994). Apoptosis induction could be inhibited by an anti-TNFα neutralizing antibody (Urban *et al.*, 1986; Higuchi *et al.*, 1990; Feinman *et al.*, 1987). Furthermore, IL-1β has been shown to be cytotoxic to a human melanoma cell line, and was shown to induce apoptosis in murine thymoma cells (Onozaki *et al.*, 1985; Fratelli *et al.*, 1995). Finally, macrophages can be cytotoxic to tumour cells via the interaction of Fcγ receptors on macrophages with the Fc domain of antibodies bound to cells, so-called antibody-dependent cellular cytotoxicity (ADCC) (Adams and Hamilton, 1984).

1.2.2.2 Alternatively-activated macrophages

'Alternatively-activated' macrophages are strictly defined as those activated by the interleukins IL-4 and IL-13, but related phenotypes may also be derived by stimulation with IL-10, glucocorticoid hormones, prostaglandin E2 (PGE2) and transforming growth factor-β (TGF-β) (Sica *et al.*, 2008a; Varin and Gordon, 2009).

IL-4 and IL-13 are produced in T_H2-type responses, including allergic, cellular and humoral responses to parasites and extracellular pathogens (Van Ginderachter *et al.*, 2006; Gordon, 2003). IL-4 and IL-13 signal through the IL-4 receptor α chain (IL-4Rα), which has been shown to lead to macrophage proliferation (Jenkins *et al.*, 2013). IL-4 causes inhibition of the expression of pro-inflammatory cytokines produced by classically activated macrophages, such as TNFα (Cheung *et al.*, 1990; Bonder *et al.*, 1998) and stimulates the production of anti-inflammatory cytokines, including IL-10, IL-1 receptor antagonist (Fenton *et al.*, 1992) and type II IL-1 decoy receptor (Mantovani *et al.*, 2002; 2004a). Additionally, IL-13 inhibits production of IL-1, IL-6, and TNFα. Furthermore, IL-4 and Il-10 inhibit induction of the chemokines CXCL9 and CXCL10, and instead induce CCL18, CCL22, and CCL24. This causes a change in T cell adaptive immunity from a T_H1 type response to one characterized by an influx of naïve T cells and T_H2 or regulatory T cells (Tregs), which suppress immune responses (Mantovani *et al.*, 2002; Sica *et al.*, 2008a; Gordon, 2003). Furthermore, IL-4 and IL-13-polarized macrophages often show an increase in the expression of mannose receptor (CD206), scavenger receptor (MSR1), and major histocompatibility complex (MHC) class II molecules, which stimulate endocytosis and antigen presentation (Doyle *et al.*, 1994; Gordon, 2003; Stein *et al.*, 1992). Additionally, the effector function of alternatively activated macrophages is characterized by scavenging debris, promotion of wound healing, angiogenesis, and tissue remodelling and repair (Mantovani *et al.*, 2002; Sica *et al.*, 2008a; Duff *et al.*, 2007; Mantovani *et al.*, 2004b; Kreider *et al.*, 2007).

In contrast to classically-activated macrophages, in the presence of IL-4 and IL-13 no iNOS is induced, and L-arginine is metabolised by arginase-1, which results in the production of L-ornithine (Hesse *et al.*, 2001). This reduces the production of NO, and together with reduced levels of TNFα and IL-1, IL-4 or IL-13-activated macrophages are less cytotoxic (Chang *et al.*, 2001; Mantovani *et al.*, 2004b).

1.2.2.3 Tumour-associated macrophages

Tumour-associated macrophages (TAM) are found among the stromal cells of many cancers including breast (Mukhtar *et al.*, 2012; Mahmoud *et al.*, 2012), lung

(Montuenga and Pio, 2007), pancreatic (Mielgo and Schmid, 2013), hepatocellular carcinomas (Flecken and Sarobe, 2015), and non-Hodgkin lymphoma, e.g. diffuse large B-cell lymphoma (Wada *et al.*, 2011), Hodgkin's lymphoma (Steidl *et al.*, 2010). In the majority of cancers, TAM have been associated with poor prognosis (Leek *et al.*, 1996; Campbell *et al.*, 2011; Salvesen and Akslen, 1999; Ni *et al.*, 2015), although for some tumours they indicate good prognosis (Shimura *et al.*, 2000). Furthermore, TAM have been shown to be required for efficient metastasis of breast cancer in a murine model (Qian *et al.*, 2009). Originally thought mainly to be recruited as monocytes from the blood, macrophages have recently been shown to proliferate in various tissues (Jenkins *et al.*, 2011), and also in the tumour microenvironment of both humans (Campbell *et al.*, 2011) and mice (Ford *et al.*, 2015).

TAM activation is dependent on the tumour and other cells in the tumour stroma, but in general they have been shown to resemble alternatively-activated macrophages more than classically-activated macrophages, especially in established tumours (Wynn *et al.*, 2013). Both in the primary and metastatic sites, TAM appear to adopt a pro-tumour phenotype (Biswas *et al.*, 2013). TAM have been found to suppress the production of the pro-inflammatory cytokines TNF-α, and the interleukins IL-1, IL-6, and IL-12, which leads to suppression of T cell responses (Coussens *et al.*, 2013; Qian and Pollard, 2010). In contrast, the production of anti-inflammatory factors has been shown to be increased, including IL-10, TGF-β, CCL18, and CCL22 (Sica *et al.*, 2000; Mantovani *et al.*, 2002; Allavena *et al.*, 2008; Sica *et al.*, 2008a). TAM express high levels of mannose receptor and scavenger receptor (Allavena *et al.*, 2010; Biswas *et al.*, 2006). Moreover, TAM have been shown to promote angiogenesis, tumour cell growth, matrix remodelling, and metastasis (Qian and Pollard, 2010; Noy and Pollard, 2014), through the expression of molecules including epidermal growth factor (EGF), members of the fibroblast growth factor (FGF) family, TGF-β, platelet-derived growth factor (PDGF), insulin-like growth factor 1 (IGF-1), matrix metalloproteinases (MMPs), cathepsins, and vascular endothelial growth factor (VEGF) (Mantovani *et al.*, 2002; Sica *et al.*, 2008a; Pollard, 2004; Leek and Harris, 2002; O'Sullivan *et al.*, 1993; Burgess, 1989; Ogden

et al., 2005; Sica *et al.*, 2000; Ford *et al.*, 2015; Wynn *et al.*, 2013). Studies of both murine and human tumours have shown that TAM are poor producers of NO, as well as ROIs (Dinapoli *et al.*, 1996; Klimp *et al.*, 2001). Furthermore, TAM are poor antigen presenting cells (Mantovani *et al.*, 1992).

1.3 Apoptosis

Unwanted cell populations are removed from multicellular organisms in a regulated fashion via the process of apoptosis (Henson and Hume, 2006; Nagata *et al.*, 2010). Examples of unwanted cells include excess cells generated during development, such as cells removed to generate interdigital spaces in the mammalian footplate (Hopkinson-Woolley *et al.*, 1994) or developing thymocytes, cells infected with intracellular bacteria or viruses, and cells irreparably damaged by cytotoxic agents. Rapid removal of these cells is necessary to maintain homeostasis and to prevent autoimmunity and pathogen burden. It is estimated that one million cells undergo apoptosis every second in adult humans (Ravichandran, 2010). Removal occurs via the recognition and engulfment and degradation by phagocytes, especially professional phagocytes such as macrophages (detailed in section 1.3.2.3). In contrast to phagocytosis of bacteria, clearance of apoptotic cells does not initiate an immune response.

1.3.1 Characteristics and mechanisms

The term apoptosis was first coined by Kerr, Wyllie, and Currie to describe a mechanism of active, controlled cell death (Kerr *et al.*, 1972). Morphological characteristics of apoptosis include cell membrane blebbing, cell shrinkage, chromatin condensation, and DNA fragmentation. Later, exposure of the phospholipid phosphatidylserine (PS) on the outer membrane was described as a hallmark feature of apoptosis. Most of these events are initiated as a result of caspase-mediated cleavage of proteins (Martin *et al.*, 1996; Kothakota *et al.*, 1997; Coleman *et al.*, 2001; Sebbagh *et al.*, 2001; Ura *et al.*, 2001; Thiede *et al.*, 2005). In viable cells, caspases are normally present as inactive precursor enzymes, with little

or no protease activity, but during apoptosis these caspases get activated and orchestrate the dismantling of cellular structures, disruption of cellular metabolism, inactivation of cell-death inhibitory proteins, and activation of additional destructive enzymes (Adrain and Martin, 2001). Currently, three main pathways of apoptosis have been established in mammals, which all lead to the activation of the major effector caspases, caspase-3, caspase-6, and caspase-7. These are the intrinsic, extrinsic and granzyme-B mediated pathways.

The intrinsic pathway is, as its name suggests, mediated by signalling from within the cell. It is initiated by stimuli that evoke cell stress or (DNA) damage, such as cytotoxic drugs, heat shock, or ionizing radiation, which lead to the accumulation of danger signals in the cells. When the danger signals exceed the pro-survival signals, this leads to mitochondrial outer membrane permeabilization (Liu *et al.*, 1996). The permeability of the outer mitochondrial membrane is controlled by members of the Bcl-2 family, which include both pro-apoptotic (including Bax, Bak, and Bcl-2-homology (BH)-3-only proteins Bid, Bad, and Bim) and anti-apoptotic proteins (such as Bcl-2 and Bcl-x_L), which can generate survival or death signals, respectively (Green and Reed, 1998; Skommer *et al.*, 2010; Moldoveanu *et al.*, 2013). Permeabilization of the mitochondrial outer membrane results in the release of mitochondrial components, most importantly cytochrome *c*, into the cytosol. Cytochrome *c* can form, together with apoptosis protease-activating factor-1 (Apaf-1), deoxyadenosine triphosphate (dATP), and pro-caspase-9, a caspase-activating complex also called the apoptosome (Liu *et al.*, 1996; Acehan *et al.*, 2002). This complex activates caspase-9, which can then in turn activate the downstream effector caspases (Zou *et al.*, 1999; Creagh *et al.*, 2003; Taylor *et al.*, 2008).

In the extrinsic pathway, extracellular death ligands, including Fas ligand or TNFα, bind to transmembrane death receptors of the tumour necrosis factor receptor superfamily, which then causes the recruitment of adapter proteins such as Fas-associated death domain protein (FADD) to the internal side of the receptors (Ashkenazi and Dixit, 1998; Muzio *et al.*, 1996). This leads to the recruitment, accumulation and activation of caspase-8, which can then activate effector caspases,

leading to substrate proteolysis and cell death. Or if lower levels of caspase-8 are activated, protease-8-mediated proteolysis of Bid can activate the intrinsic pathway by promoting mitochondrial cytochrome *c* release (Scaffidi *et al.*, 1998; Luo *et al.*, 1998; Li *et al.*, 1998; Creagh *et al.*, 2003).

Another pathway that leads to apoptosis is the granzyme B-initiated caspase-activation pathway and is one of the pathways used by cytotoxic T cells and NK cells to induce apoptosis in virally infected and tumour cell targets (Froelich *et al.*, 1998). It involves the release of cytolytic granules that contain a variety of enzymes that can provoke apoptosis in their target cells. One of the proteins in the granules is perforin, a pore-forming protein that is thought to facilitate the delivery of other granule components into the target cells. The other main component of the granules is granzyme B, a serine protease that can cleave caspase-3, thereby triggering apoptosis (Darmon *et al.*, 1996; Creagh *et al.*, 2003).

1.3.2 Apoptotic cell clearance

In vivo, most apoptotic cells are found within the cytoplasm of intact cells, as they are rapidly phagocytosed (Kerr *et al.*, 1972; Surh and Sprent, 1994; Mochizuki *et al.*, 1996; Schrijvers, 2005). Phagocytosis is the engulfment and internalization of larger particles, including bacteria and dead/dying cells, followed by their processing within a membrane-bound vesicle, called the phagosome (Ravichandran and Lorenz, 2007). The principal phagocytes of apoptotic cells are macrophages, immature dendritic cells, and neutrophils (Lacy-Hulbert, 2009; Hochreiter-Hufford and Ravichandran, 2013), which e.g. clear dead and dying cells in tissues such as the spleen (during or after an immune response) or the thymus (during T-lymphocyte development). However, other, non-professional phagocytes, including fibroblasts (Hall *et al.*, 1994), epithelial cells (Juncadella *et al.*, 2013), mesenchymal cells (Wood *et al.*, 2000), and stem cells (Charrière *et al.*, 2006) are also suggested to be capable of clearing apoptotic cells.

Clearance of apoptotic cells is initiated by the attraction of phagocytes to the apoptotic cells through the release of ‘find-me’ signals, followed by the recognition

of apoptotic cells through ‘eat-me’ signals displayed on the apoptotic cell. These interactions result in the engulfment and degradation (removal) of the apoptotic cells and anti-inflammatory signalling by the phagocytes. Many pathways in these processes have been described, and below are detailed the most important ones for the phagocytosis of apoptotic cells by macrophages.

1.3.2.1 Chemoattraction: find-me signals

Various studies have shown that apoptotic cells are capable of providing migratory cues to phagocytes. These ‘find-me’ signals (Gregory and Pound, 2010) establish a chemotactic gradient that stimulates the migration of phagocytes to the apoptotic cell. Signalling factors found to be released from apoptotic cells that can effect the migration of macrophages to apoptotic cells, include the nucleotides adenosine triphosphate (ATP) and uridine triphosphate (UTP) (Elliott *et al.*, 2009; Chekeni *et al.*, 2010), the lipids lysophosphatidylcholine (LPC) (Lauber *et al.*, 2003) and sphingosine-1-phosphate (S1P) (Gude *et al.*, 2008), as well as the proteins fractalkine (Truman *et al.*, 2008) and monocyte chemotactic protein (MCP-1 or CCL2) (Kobara *et al.*, 2008). Release of ATP and UTP is mediated via the pannexin channels, which are opened during apoptosis by caspase-dependent cleavage of their carboxy-terminal tail (Chekeni *et al.*, 2010). Sensing of nucleotides appears to occur via the P2Y2 receptor on monocytes (Elliott *et al.*, 2009). Nucleotides are readily degraded by extracellular nucleotidases, so they are more likely to serve as short-range find me signals (Hochreiter-Hufford and Ravichandran, 2013). LPC release is dependent on caspase-3, and recognition of LPC is thought to occur via the G-protein-coupled receptor G2A (Peter *et al.*, 2008). Released fractalkine is sensed via chemokine (C-X3-C motif) receptor 1 (CX3CR1), which directs macrophages to the dying targets. Fractalkine release is associated with microvesicle release from apoptotic cells, which may support prolonged biological activity and increase the effective range over which it can signal (Truman *et al.*, 2008).

In addition to find-me signalling, some of these factors may serve an additional role in the context of apoptotic cell clearance. ATP released by apoptotic cells has been shown to increase binding of apoptotic cells to macrophages (Marques-Da-Silva *et*

al., 2011). Furthermore, fractalkine was found to cause the expression of milk fat globule epidermal growth factor (MFG-E8) on macrophages, which leads to enhanced apoptotic cell clearance (Miksa *et al.*, 2007), as MFG-E8 is a bridging molecule that facilitates recognition of apoptotic cells by phagocytes (described below). Find-me signals may also influence non-immunogenic responses to apoptotic cells. S1P has been shown to enhance secretion of IL-10 and PGE2 by tumour macrophages (Weigert *et al.*, 2007; Johann *et al.*, 2008) and fractalkine has been shown to stimulate pro-survival and growth-promoting effects (Boehme *et al.*, 2000; White *et al.*, 2010).

LPC, S1P and nucleotides are known to also stimulate neutrophil chemotaxis (Chen *et al.*, 2006; Florey and Haskard, 2009). However, phagocytosis of apoptotic cells is generally recognised as a non-immunogenic, non-inflammatory process, with minimal, if any, neutrophil recruitment (Savill, 1997; Savill *et al.*, 2002). The protein lactoferrin, found to be released from apoptotic cells, has been shown to inhibit the migration of neutrophils both *in vitro* and *in vivo*, but not macrophages (Bournazou *et al.*, 2009). It has been suggested that lactoferrin may be a 'keep-out' signal and that the 'decision' to migrate or not is dependent on a balance between positive 'find-me' signals, and negative 'keep-out' signals (Gregory and Pound, 2011; Gregory *et al.*, 2011).

1.3.2.2 Recognition: 'Eat-me' signals

Once in the proximity of the dying cell, phagocytes must recognise apoptotic cells and distinguish them from viable cells. Viable cells prevent their unwanted removal, whereas apoptotic cells undergo changes that allow them to be recognised and phagocytosed effectively. These 'eat-me' signals displayed by apoptotic cells are recognised by phagocytic receptors, either directly, or through soluble bridging molecules that connect the phagocytic receptors and the eat-me signals on apoptotic cells. There are many different molecules and receptors at play at the apoptotic cell-phagocyte synapse, and although they may vary between different cells or tissues, this redundancy reflects the importance of clearance of apoptotic cells.

Eat-me signals include changes in the glycosylation of surface proteins or changes in surface charge (Kinchen and Ravichandran, 2007), binding of serum proteins to the apoptotic cell, including thrombospondin and complement C1q (Ravichandran and Lorenz, 2007), the exposure of intracellular proteins such as calreticulin and annexin I (Arur *et al.*, 2003; Gardai *et al.*, 2005; Obeid *et al.*, 2007), expression of intercellular adhesion molecule 3 (ICAM-3) and low-density lipoprotein (LDL)-like moiety (Moffatt *et al.*, 1999; Fadok *et al.*, 1998b; Schlegel *et al.*, 1999). However, probably the most important of these changes is the translocation of the phospholipid phosphatidylserine (PS) from the inner to the outer membrane and its recognition by phagocyte receptors appears to be one of the most important mechanisms in clearance (Grimsley and Ravichandran, 2003; Fadok *et al.*, 2001b). In viable cells, PS is kept on the inner leaflet of the lipid bilayer via ATP-dependent translocases (Balasubramanian and Schroit, 2003). In apoptotic cells, PS becomes exposed on the outer leaflet of the lipid bilayer, which recent reports suggest is dependent on caspase activity (Segawa *et al.*, 2014). Calreticulin and annexin I co-localize with PS on the surface of apoptotic cells and enhance the uptake of targets by phagocytes (Arur *et al.*, 2003; Gardai *et al.*, 2005).

Numerous receptors are expressed on the surface of phagocytic cells that recognize these eat-me signals. Phosphatidylserine can either be directly recognized by PS-recognition receptors, which include BAI-1 (brain-specific angiogenesis inhibitor 1), TIM-4 (T cell immunoglobulin mucin 4), and Stabilin-2 (Miyanishi *et al.*, 2007; Park *et al.*, 2007; 2008a; Kobayashi *et al.*, 2007; Park *et al.*, 2008b), or indirect mechanisms that require bridging molecules. The latter include Tyro-3, Axl, and Mer, which bind PS via Gas6 and protein S, and several $\alpha_v\beta_{3/5}$ integrins, which bind MFG-E8 (milk fat globule epidermal growth factor 8) (Hanayama *et al.*, 2002; Scott *et al.*, 2001; Savill *et al.*, 1990; Nakano *et al.*, 1997; Nagata *et al.*, 2010). Other receptors for apoptotic cells include CD36, which in conjunction with the integrins $\alpha_v\beta_3$ and $\alpha_v\beta_5$ binds thrombospondin (Savill *et al.*, 1992), low density lipoprotein receptor-related protein 1 (LRP1/CD91), which binds complement C1q in conjunction with calreticulin (Ogden *et al.*, 2001), CD14, which binds ICAM3

(Devitt *et al.*, 1998), the scavenger receptors that bind oxidized low-density lipoprotein (LDL) (Gordon, 1999).

Other ways by which phagocytes can distinguish apoptotic cells from viable cells is through the display of 'don't eat-me' signals on the surface of viable cells. These include CD47 (or integrin-associated protein), recognised by its cognate receptor SIRPα (Oldenborg *et al.*, 2000). CD47 inhibits engulfment, even in the presence of PS (Tsai and Discher, 2008). CD47 expression is down-regulated or suppressed during apoptosis, thereby allowing clearance. Many leukaemias, lymphomas and solid tumours have up-regulated expression of CD47, which protects them from being phagocytosed (Jaiswal *et al.*, 2009; Majeti *et al.*, 2009; Chao *et al.*, 2011; Willingham *et al.*, 2012; Chao *et al.*, 2010). Blocking of CD47 expression by tumour cells using anti-CD47 antibodies has been shown to increase macrophages phagocytosis of tumour cells, and results in reduced tumour burden in various murine models (Willingham *et al.*, 2012; Edris *et al.*, 2012). In a xenograft murine model of NHL, anti-CD47 antibodies in combination with rituximab led to eradication of the tumour (Chao *et al.*, 2010). Currently, anti-CD47 antibody treatment is being tested in a phase I clinical trial of patients with solid tumours (Weiskopf and Weissman, 2015). Another don't-eat-me signal that has been identified is CD31 (Brown *et al.*, 2002), but it has not been studied extensively.

1.3.2.3 Removal: Engulfment and processing

Binding of apoptotic cells to phagocyte receptors initiates signalling events that lead to the activation of guanosine triphosphatases (GTPases) and subsequent cytoskeletal organization of the phagocyte membrane, which allows corpse internalization (Albert *et al.*, 2000; Gumienny *et al.*, 2001). Known GTPases associated with cytoskeletal signalling include RhoA, Cdc42, and Rac. Loss or suppression of RhoA results in increased engulfment of apoptotic cells (Tosello-Trampont *et al.*, 2003; Nakaya *et al.*, 2006). Activated RhoA increases the kinase activity of Rho-associated protein kinase (ROCK), which in turn mediates phosphorylation of myosin light chain (MLC), which promotes cell contraction. This likely inhibits the extension of pseudopods and phagocytic cup formation necessary in the early stages of

engulfment (Riento and Ridley, 2003). In contrast, Rac activation enhances engulfment, as its activation leads to Arp2/3 activation, actin polymerization, and cytoskeletal rearrangement via the Scar/WAVE complex (Miki *et al.*, 1998; Castellano *et al.*, 2000).

Following internalization, the apoptotic cell is contained within a membrane-bound compartment named the phagosome. These phagosomes become increasingly acidic, and eventually fuse with lysosomes that contain the digestive enzymes required for degradation of the apoptotic cell (Kinchen and Ravichandran, 2008). After fusion with the lysosomal network, acidic proteases and nucleases get activated and the apoptotic cell targets are degraded.

Acidification occurs in two stages. The first, early stage, results in a small drop in pH, and is not very well understood (Hackam *et al.*, 1997). In the second stage, V-type ATPases (ATP-hydrolysis-driven proton pumps) are trafficked to the phagosome to acidify its contents, through ATP hydrolysis and transporting H+ across the phagosomal membrane (Beyenbach, 2006). Acidification is essential during phagosome maturation. Only when the pH is low enough, the cathepsin family of acidic proteases becomes activated and the phagocytosed particle can begin to be degraded (Lennon-Dumenil *et al.*, 2002). Further studies to unravel phagosome maturation are under way, but Rab GTPases, in particular RAB-5 and RAB-7, appear to be important as part of a fusion pore that allows contact with other membrane-bound organelles, which potentially may allow for entry points for vesicles to deposit lysosomal proteases, or function as nodes for recycling proteins back to the plasma membrane (McBride *et al.*, 1999; Vieira *et al.*, 2003; Kinchen *et al.*, 2008).

1.3.2.4 Consequences of apoptotic cell clearance

Timely and adequate clearance of apoptotic cells prevents the release of potentially toxic or immunogenic intracellular contents from the dying cell. This is in contrast to necrotic cell death, where unregulated release of dead cell material can induce inflammatory responses (Fadok *et al.*, 2001a; Taylor *et al.*, 2008). Thus, one of the key functions of rapid clearance of apoptotic cells is to prevent an immunogenic

response as a result of uncleared dead cell material. However, if apoptotic cells are not cleared, they lose their membrane integrity and then become necrotic (a process described as 'secondary necrosis'). The intracellular contents of necrotic, permeable cells, in particular intracellular antigens and DNA, are thought to cause an inflammatory response and may cause autoimmune disorders, such as systemic lupus erythematosus (SLE) (Kawane *et al.*, 2003; Napirei *et al.*, 2000). Initial experiments where excess apoptotic cells were added to mice, or PS-mediated apoptotic cell uptake was inhibited by masking PS with an MFG-E8 mutant, were shown to produce hallmarks of autoimmunity, including autoantibody production and IgG deposition in the glomeruli (Mevorach *et al.*, 1998; Asano *et al.*, 2004). Additionally, various mouse models with genetic defects in PS-mediated recognition have confirmed that inefficient clearance of apoptotic cells can result in autoimmunity (Botto *et al.*, 1998; Scott *et al.*, 2001; Cohen *et al.*, 2002; Hanayama *et al.*, 2004; Rodriguez-Manzanet *et al.*, 2010).

However, in addition to preventing an immune response against the immunogenic dead cell contents, the engulfment and clearance of apoptotic cells results in the suppression of pro-inflammatory mediators by phagocytes, as well as the production of anti-inflammatory mediators. Recognition and phagocytosis of apoptotic cells has been found to suppress pro-inflammatory cytokine release *in vitro*, including IL-6, IL-8, IL-12, and TNFα (Voll *et al.*, 1997; Fadok *et al.*, 1998a). In addition, engulfment of apoptotic cells by macrophages has been found to activate downstream signalling pathways that cause the up-regulation and secretion of IL-10, TGF-β, platelet activating factor, and prostaglandins (Voll *et al.*, 1997; Fadok *et al.*, 1998a; McDonald *et al.*, 1999; Ogden *et al.*, 2005). IL-10 and TGF-β can induce differentiation of regulatory T-cells and T helper 2 cells that are important in the prevention of an inflammatory response (Green *et al.*, 2009).

1.4 Lactoferrin

1.4.1 Structure

Lactoferrin is a 80-kDa glycoprotein that is a component of many mammalian body fluids and secretions, including milk and colostrum, saliva, tears, semen, vaginal fluids, nasal and bronchial secretions, bile, gastrointestinal fluids, urine and plasma (García-Montoya *et al.*, 2012; Baker and Baker, 2009). Additionally, lactoferrin is found concentrated in the secondary granules of neutrophils (Baggiolini *et al.*, 1970). Its concentration is highly variable depending on the location and may range from ~1-2 mg/ml in mature milk or ~7 mg/ml in colostrum to 20-1500 ng/ml in blood plasma (Levay and Viljoen, 1995; Steijns and van Hooijdonk, 2000).

Lactoferrin is highly conserved among species. Human lactoferrin shares 95-98% sequence identity with chimpanzee lactoferrin and 70-74% with lactoferrins of other species, including pig, horse, cow, and goat (Baker and Baker, 2005). Lactoferrin is part of the transferrin family of proteins and its protein sequence has approximately 60% similarity with human serum transferrin (Metz-Boutigue *et al.*, 1984; Wally and Buchanan, 2007).

The polypeptide is folded in two globular lobes, representing its N- and C-terminal halves, which are referred to as the N-lobe and the C-lobe, and are linked by a short α-helix. Each lobe consists of an α-helix and β-pleated sheet structure with two domains (Haridas *et al.*, 1995; García-Montoya *et al.*, 2012). The N-terminal of lactoferrin is highly positively charged (Bellamy *et al.*, 1992). Each lobe can bind a metal atom in synergy with a carbonate ion (CO_3^{2-}). Lactoferrin has a very high affinity for iron (Fe^{3+}) ions (Kd ≈ 10^{-20} M) (Baker *et al.*, 2003) , but can also bind other metals with lower affinity, including Cu^{2+}, Zn^{2+}, and Mn^{2+} (Baker and Baker, 2005). It can reversibly bind Fe^{3+}, and can thus exist either free of Fe^{3+} (apo-Lf) or associated with Fe^{3+} (holo-Lf). Apo-Lf has an open conformation, while holo-Lf is a closed molecule that is more resistant to proteolysis (Wally and Buchanan, 2007).

1.4.2 Function

Lactoferrin is a pleiotropic molecule and its properties include anti-microbial and anti-inflammatory functions, as well as activity as a growth factor and it has been shown to inhibit tumour development and metastasis (Baker and Baker, 2005; García-Montoya *et al.*, 2012). Many of the proposed functions of Lf, apart from its iron binding activity, depend on its surface properties. Lactoferrin's highly positively charged domain is likely to be a major factor in its ability to bind, perhaps indiscriminately, to many different cell types and anionic molecules (Baker and Baker, 2005).

Lactoferrin's antimicrobial properties were discovered first and are most widely studied. Its antimicrobial activity is mainly driven by two mechanisms. The first involves iron sequestration at sites of infection, which deprives microorganisms of iron, thereby inhibiting bacterial growth and down-regulating bacterial expression of virulence factors (Arnold *et al.*, 1977). E.g. lactoferrin has been shown to inhibit the growth of *E. coli*, and the effect was abolished by saturating lactoferrin with iron (Bullen *et al.*, 1972). An important function of this appears to be in the protection of newborns through lactation. Milk offers the transfer of lactoferrin that can act by controlling free iron in the gut, thereby limiting microbial pathogenesis (García-Montoya *et al.*, 2012). The second mechanism by which lactoferrin's anti-microbial activity is executed is through the interaction of lactoferrin with the infectious microorganism. Its cationic domain can interact with lipopolysaccharide (LPS) on Gram-negative bacteria, which causes changes in the permeability of the cell surface, leading to cell lysis (Ellison *et al.*, 1988). Additionally, lactoferrin has been shown to enhance phagocytosis of *S. aureus* by mammary gland secretory cells (phagocytes) through opsonisation by lactoferrin (Kai *et al.*, 2002).

In addition to lactoferrin's antibacterial functions, lactoferrin also has known antiviral, antifungal, and antiparasitic functions (Weinberg, 1994; Cirioni *et al.*, 2000; García-Montoya *et al.*, 2012). Its antiviral functions are thought to be mediated through blocking of glycosaminoglycan viral receptors, thereby inhibiting contact between virus and host cell, and preventing infection (van der Strate *et al.*, 2001).

Lactoferrin's antifungal activities are mediated through altering the permeability of the cell surface, as well as through Fe^{3+} sequestration (Wakabayashi *et al.*, 2009; Kuipers *et al.*, 1999; Lupetti *et al.*, 2008).

High concentrations of lactoferrin (>100μg/ml) have been shown to promote the release of various pro-inflammatory factors, including nitric oxide, TNFα, IL-1β, IL-6, and nitrite by macrophages (Son *et al.*, 2002; Sorimachi *et al.*, 1997; Mattsby-Baltzer *et al.*, 1996; Crouch *et al.*, 1992). Furthermore, lactoferrin has been shown to increase IL-8 release from human polymorphonuclear leukocytes (Shinoda *et al.*, 1996).

In addition to the role of lactoferrin in infection, it also has key anti-inflammatory properties. Lactoferrin can modulate cytokine release by leukocytes. Bovine lactoferrin has been shown to reduce colitis in a rat model, and this was correlated with significant increases in IL-4 and IL-10 in the colon (Togawa *et al.*, 2002), whereas reductions in TNFα, IL-1β, and IL-6 were observed (Togawa *et al.*, 2002). Furthermore, pre-treatment with bovine lactoferrin has been shown to reduce TNFα and IL-6 serum levels in LPS-injected mice (Machnicki *et al.*, 1993). This may be mediated through monocytes and macrophages, as lactoferrin was shown *in vitro* to suppress the synthesis of pro-inflammatory cytokines, including TNFα, IL-1β, and IL-6, by these cells following LPS stimulation (Crouch *et al.*, 1992; Mattsby-Baltzer *et al.*, 1996; Håversen *et al.*, 2002). Additionally, human lactoferrin has been shown to reduce both mRNA and protein expression of IL-8 induced by the E. coli/sCD14 complex in human umbilical vein endothelial cells, and it prevented IL-8 binding to the proteoglycan heparin (Elass, 2002). Lactoferrin can inhibit LPS-induced expression of endothelial-leukocyte adhesion molecule 1 (E-selectin) and intercellular adhesion protein 1 (ICAM-1) on endothelial cells by interaction with LPS and soluble CD14 (Baveye *et al.*, 2000). Furthermore, lactoferrin has been shown to inhibit the migration of neutrophils and eosinophils (Bournazou *et al.*, 2009; 2010).

Lactoferrin has been shown to enhance the toxicity of NK cells against haematopoietic and breast epithelial cell lines *in vitro*, whereas high concentrations of lactoferrin appear to be toxic to the NK cells and inhibit cytotoxicity (Damiens *et al.*, 1998). Furthermore, lactoferrin has been shown to enhance antibody-dependent cellular cytotoxicity of adherent monocytes (Nishiya and Horwitz, 1982).

In addition to its anti-inflammatory abilities, lactoferrin has been shown to stimulate growth of various mammalian cells (Huang *et al.*, 2008) and it was found to be an essential growth factor for lymphocytic cell lines *in vitro* in serum-free medium (Hashizume *et al.*, 1983). Holo-recombinant human lactoferrin (holo-rhLf) has been shown to stimulate keratinocyte proliferation, which could be blocked by mitogen-activated protein kinase (MAPK) 1 inhibitor. Holo-rhLf also showed strong promoting effects on keratinocyte migration. Under starving conditions, the addition of holo-rhLf was found to increase cell viability and inhibition of apoptosis. Furthermore, holo-rhLf increased the rate of wound re-epithelialization in swine second-degree burn wounds *in vivo* (Tang *et al.*, 2010b).

Lactoferrin has also been shown to stimulate proliferation and differentiation of osteoblast cells, and to decrease their sensitivity for apoptosis (Grey *et al.*, 2006; Cornish *et al.*, 2004). This results in bone growth *in vivo*, through endocytosis and activation of p42/44 MAP kinases (Naot *et al.*, 2005). Furthermore, a rice-derived recombinant human lactoferrin has been reported to stimulate fibroblast proliferation, migration, and sustaining cell survival (Tang *et al.*, 2010a). Additionally, lactoferrin can also affect angiogenesis, and induces mRNA expression and increases protein levels of VEGF and fibroblast growth factor-2 (Nakajima *et al.*, 2011).

1.4.3 Lactoferrin and cancer

Lactoferrin has been detected in various tumours, including Hodgkin and Burkitt's lymphoma (Hoffer *et al.*, 1979), endometrial adenocarcinomas (Walmer *et al.*, 1995), sporadic renal cell carcinomas (Giuffrè *et al.*, 2007), and in neoplastic bone tissue (Ieni *et al.*, 2009).

Injections of lactoferrin into tumours has been shown to inhibit tumour growth in a murine model of fibrosarcoma, and to reduce lung metastasis (Bezault *et al.*, 1994). Furthermore, oral administration of lactoferrin has been shown to inhibit growth of squamous cell carcinoma and to potentiate chemotherapy in a murine model (Varadhachary *et al.*, 2004) and to decrease tumour growth rates in a phase I trial of patients with advanced solid tumours (Hayes *et al.*, 2005). This may be mediated through increased immunomodulatory activity, as oral administration of bovine lactoferrin has been shown to increase numbers of $CD4^+$ and $CD8^+$ T cells and NK cells in the blood of mice implanted with colon carcinoma cells, and increases in the levels of IL-18, IFN-γ and caspase-1 (Wang *et al.*, 2000).

Furthermore, lactoferrin has been associated with inducing apoptosis in tumours. Lactoferricin, an active peptide derived from lactoferrin containing its cationic domain, can induce apoptosis in Jurkat T-leukaemia cells, which was most likely the result of lactoferricin-induced cell membrane damage, and further disruption of the mitochondrial membranes by internalized lactoferricin (Mader *et al.*, 2007). Furthermore, it has been suggested that lactoferrin can inhibit Akt activation and modulates its downstream proteins phosphorylation leading to apoptosis of human stomach cancer cells (Xu *et al.*, 2010).

Additionally, lactoferrin has been shown to inhibit angiogenesis in rats, which may be mediated through suppression of VEGF (Norrby *et al.*, 2001). This was also observed in mice, where oral administration of bovine lactoferrin reduced expression of VEGF and decreased the expression of pro-inflammatory cytokines, including TNFα and IL-6, and anti-inflammatory cytokines IL-4 and IL-10, which suppressed the formation of tumours (Tung *et al.*, 2013).

1.4.4 Lactoferrin receptors

Because of its high capacity to bind proteins and membranes through its cationic N-terminal, it is difficult to identify lactoferrin receptors. Nonetheless, lactoferrin-specific receptors have been identified on leukocytes and macrophages, platelets, on bacteria, and in the gastrointestinal tract.

A receptor for lactoferrin has been described on the membranes of human foetal intestinal brush-border membranes. Competitive binding studies demonstrated specific binding of human lactoferrin. Little binding of bovine lactoferrin or human transferrin occurred (Kawakami and Lönnerdal, 1991). Furthermore, the existence of a specific receptor for lactoferrin has been suggested on mouse peritoneal cells and in particular on macrophages (Van Snick and Masson, 1976).

In the liver, lactoferrin has been shown to bind both heparan sulphate proteoglycans (HSPG), as well as the low-density lipoprotein receptor-related protein (LRP). In mutant CHO cells, lacking HSPG, the level of binding of labelled lactoferrin was reduced by ~50%, and heparinase treatment decreased binding by ~40%. Similarly, ligand blocking of LRP inhibited labelled lactoferrin degradation by ~60% (Ji and Mahley, 1994). Lactoferrin has also been shown to bind to two members of the low-density lipoprotein receptor family, low-density lipoprotein receptor-related proteins 1 (LRP1) and 2 (LRP2) on osteoblasts. Inhibition of LRP1/2 or antibody-blocking prevented endocytosis of lactoferrin and abrogated lactoferrin-induced p42/44 MAPK signalling and mitogenesis (Grey, 2004). Furthermore, LRP1 has been associated with lactoferrin binding to human keratinocytes (Tang *et al.*, 2010b).

A lactoferrin receptor has also been described on platelets, where concentrations of lactoferrin as low as 5nM could inhibit platelet aggregation (Leveugle *et al.*, 1993). Additionally, lactoferrin was shown to bind to eosinophils as determined by flow cytometry (Thomas *et al.*, 2002). Scatchard analysis of THP-1 cells differentiated into macrophages also indicated that both high and low affinity receptor sites (Kd = 0.57×10^{-6} and 3.7×10^{-6} M, respectively) are present on these cells (Eda *et al.*, 1996).

Lactoferrin has also been shown to bind to leukaemia cells. Lactoferrin binding sites were found to be distinct and unrelated to transferrin receptors on K562 cells. However, since other polycationic proteins, e.g. protamine, could inhibit lactoferrin binding to K562 cells, electrostatic forces may be responsible for lactoferrin binding to leukaemic cells (Yamada *et al.*, 1987).

Lactoferrin is known to chelate LPS and has been shown to bind soluble CD14 with high affinity, as well as bind the CD14-LPS complex (Baveye *et al.*, 2000). These findings suggest that CD14, a 55-kDa glycoprotein expressed by macrophages, may also be a receptor for lactoferrin.

1.5 Aims of the project

Massive apoptotic cell death is observed in many malignant tumours, including 'starry-sky' Burkitt's lymphoma. Despite such high rates of apoptosis, these tumours continue to grow rapidly, and apoptosis has been found to correlate with aggressive disease in NHL and many other malignancies (Ohbu *et al.*, 1995; Leoncini *et al.*, 1993; Naresh *et al.*, 2001; Sun *et al.*, 2006; Jalalinadoushan *et al.*, 2004). Free apoptotic cells are rarely observed in tumours, but are rapidly engulfed by tumour-associated macrophages. Accumulation of TAM is generally associated with poor prognosis in many cancers, and TAM have been shown to promote anti-inflammatory responses, angiogenesis, tissue remodelling, and metastasis (section 1.2.2.3).

Recently, in our laboratory, the *in situ* molecular signature of starry-sky TAM was generated (Ford *et al.*, 2015; Petrova, 2012). Transcription profiles of micro-dissected starry-sky tumour-associated macrophages (TAM) were obtained from a xenograft model of BL by laser capture of the macrophages. As controls, tingible-body macrophages from the germinal centres of activated lymphoma nodes (GCM) and resident tissue macrophages from resting lymph nodes (LNM) were acquired in the same way. Many genes were up- or down-regulated between TAM and either GCM or LNM. The published findings show that multiple pro-tumour pathways were activated in starry-sky TAM, including transcripts encoding matrix remodelling, lipid metabolism, and growth factors, as well as transcripts associated with phagocytosis functions. Selected transcripts of genes that are up-regulated in starry-sky TAM compared to GCM associated with reparatory and pro-tumour macrophage responses are shown in Table 1.1. Table 1.2 shows selected transcripts

of genes associated with macrophage responses to apoptotic cells that were up-regulated in starry-sky TAM (Ford *et al.*, 2015).

As engulfment of apoptotic cells by macrophages has been found to suppress pro-inflammatory signalling, induce anti-inflammatory signalling, and up-regulate various growth factors (see section 1.3.2.4.), it was hypothesised that apoptotic lymphoma cells, either through the release of signalling molecules, or through direct interaction with macrophages, can promote lymphomagenesis by the accumulation and activation of macrophages that are anti-inflammatory, immunosuppressive, and promote tumour growth.

In order to address this hypothesis, research presented in Chapters 3 and 4 of this thesis was aimed to address whether lactoferrin (Chapter 3), which is released from apoptotic cells (Bournazou *et al.*, 2009), or apoptotic cells, by a different mechanism, (Chapter 4) can attract monocytes and macrophages and activate them to a starry-sky TAM phenotype. Chemoattraction to lactoferrin was measured by a series of Boyden chamber experiments. The ability of lactoferrin or apoptotic cells to activate a starry-sky TAM phenotype was assessed in a series of *in vitro* co-culture experiments. Unstimulated or classically-activated macrophages were stimulated with lactoferrin or apoptotic cells, and qPCR was used to evaluate gene expression. Expression of selected starry-sky TAM-upregulated genes, as presented in Table 1.1 and Table 1.2, were assessed as a measure of starry-sky TAM activation. Additionally, gene expression of pro-inflammatory cytokines was assessed.

Research presented in Chapter 5 aimed to determine the effect of apoptotic cell interaction with classically-activated macrophages on tumour cell growth. This was assessed in a series of *in vitro* cytotoxicity assays. Finally, Chapter 6 shows research that aimed to compare the gene expression profile of starry-sky TAM to a dataset of tissue and *in vitro* cultured macrophages, to further the understanding of the underlying biological and molecular pathways involved in starry-sky TAM.

Gene	Protein	Fold change	P value
Mrc1	Mannose receptor, C type 1 (CD206)	38.2	< 0.0001
Anpep	Alanyl (membrane) aminopeptidase (CD13)	23.1	< 0.0001
Gpnmb	Glycoprotein (transmembrane) NMB (osteoactivin)	10	0.0006
Plau	Urokinase plasminogen activator	7.1	0.0001
Ctsd	Cathepsin D	6.4	0.0008
Ctsb	Cathepsin B	5.8	0.0001
Fn1	fibronectin	5.7	0.0090
Timp2	Tissue inhibitor of metalloproteinase 2	5.7	0.0002
Ctsl	Cathepsin L	5.4	0.0010
Hmox1	Heme oxygenase (decycling) 1	5.2	0.0019
Psap	prosaposin	4.2	0.0010
Mmp3	Matrix metalloproteinase 3	4	0.0407
Mmp12	Matrix metalloproteinase 12	3.5	0.0447
Mmp2	Matrix metalloproteinase 2	3	0.0007
Igf1	Insulin-like growth factor 1	2.7	0.0001
Sepp1	Selenoprotein P plasma 1	2.7	0.0005
Emp1	Epithelial membrane protein 1	2.3	0.0002
Pdgfc	Platelet derived growth factor CC	2.3	0.0080
Ctss	Cathepsin S	2.1	0.0006
Lamp2	Lysosomal associated membrane protein 2	2	0.0002
Ccl2	Chemokine (C-C motif) ligand 2	2	0.0114

Table 1.1 – Selected transcripts up-regulated by starry-sky TAM compared with GCM of genes associated with reparatory and pro-tumour macrophage responses.

Gene	Protein	Fold change	P value
Msr1	Macrophage scavenger receptor (CD204)	17	< 0.0001
Lrp1	LDL receptor-related protein (CD91)	8.4	< 0.0001
Mertk	c-Mer tyrosine kinase	7.5	< 0.0001
Cd36	CD36 scavenger receptor	5.9	0.0038
Cd93	CD93 receptor	5.9	0.0016
Lgals3	Galectin 3	5.2	< 0.0001
Abca1	ATP-binding cassette transporter	5.2	< 0.0001
Pparg	Peroxisome proliferator activated receptor gamma	4.1	0.0012
Axl	AXL receptor tyrosine kinase	3.9	0.0020
Trem2	Triggering receptor expressed on myeloid cells 2	3.5	< 0.0001
Gas6	Growth arrest specific 6	2.7	0.0058
Tgfb1	Transforming growth factor beta 1	2.3	0.0048

Table 1.2 – Selected transcripts up-regulated by starry-sky TAM compared with GCM of genes associated with macrophage responses to apoptotic cells.

Chapter 2 Materials and Methods

2.1. Cells

2.1.1. Isolation and culture of primary cells

2.1.1.1. Cultivation of mouse bone marrow-derived macrophages (BMDM)

Healthy mice (BALB/c, C57BL/6, C57BL/6 IL-4Rα KO, C57BL/6 GAL3KO) were euthanized and femurs were removed by dissection. The bones were cleaned in ethanol and placed into Phosphate Buffered Saline (PBS; Life Technologies, Paisley, UK) in a sterile hood. The ends of the bones were cut off and the bone marrow was flushed with complete RPMI medium (Gibco RPMI 1640 (Life Technologies) supplemented with 10% foetal bovine serum (FBS; Biosera Ltd. Ringmer, UK), 2mM L-glutamine (Life Technologies), 100U/ml penicillin and 100µg/ml streptomycin (PAA Laboratories Ltd)) using a 20ml syringe (BD Bioscience, Oxford, UK) and a 26-gauge needle (BD Bioscience) into a 50ml conical tube (BD Bioscience). Chunks of bone marrow were then broken up by drawing the cells up and down through a 23-gauge needle (BD Bioscience), avoiding the creation of bubbles. Cells were centrifuged at 350 x g for 5 minutes at room temperature and the supernatant discarded. Cells were resuspended in 15ml complete RPMI medium supplemented with 100ng/ml recombinant human CSF1 (rhCSF1; R&D Systems, Abington, UK) and added to 100mm square Petri dishes (Sterilin) and cultured at 37˚C, 5% CO_2. On day 4, 10 ml complete RPMI medium supplemented with 100ng/ml rhCSF1 was added to the cells. Alternatively, when indicated, BMDM were cultured in X-VIVO-10 medium (Lonza, Basel, Switzerland), supplemented with 2mM L-glutamine, 100U/ml penicillin, 100µg/ml streptomycin and 100ng/ml rhCSF1. On day 7 or 8, matured BMDM were detached by spraying the cells with a 19-gauge needle and 20ml syringe. Cells were counted and used for experiments. Approximately 5-15 million BMDMs were harvested per dish.

2.1.1.2. Isolation of human blood leukocytes

Human leukocytes were isolated from the peripheral blood of healthy volunteers who provided written consent (Lothian Research Ethics Committee approvals no. 08/S1103/38). Peripheral venous blood was drawn from an antecubital vein, transferred to polypropylene tubes containing 3.8% (w/v) sodium citrate (Sigma-Aldrich, Dorset, UK) and gently mixed for anticoagulation. Blood was centrifuged at 350 x g for 20 minutes (min) to separate platelet rich plasma (PRP) from the cellular components. PRP was transferred to sterile glass tubes containing 40mM $CaCl_2$ (Sigma-Aldrich) and incubated at 37˚C for 2 hours until a clot formed. Autologous serum was then incubated for 45 min at 56˚C to heat-inactivate complement, followed by centrifugation at 2000 x g for 10 min to remove any precipitate. Autologous serum was then stored at 4˚C and used as required in the culture of monocytes. The cellular components of the blood were then resuspended in Dextran (Pharmacia, Buckinghamshire, UK; final concentration 0.6% (w/v)) and left to stand undisturbed for 15-30 min to allow sedimentation of erythrocytes. The leukocyte-rich upper-layer was collected and the cells were gently resuspended in 0.9% Saline (Baxter, Northampton, UK) and pelleted at 350 x g for 6 min at 20˚C. In the meantime, three different concentrations of Percoll (50%, 63% and 73%) were prepared from the stock (Pharmacia) in phosphate buffered saline (PBS, Ca^{2+}/Mg^{2+}-free). 3ml 63% Percoll was carefully layered over 3ml 73% Percoll in a conical 15ml polypropylene tube. The leukocyte pellet was resuspended in 3ml of 50% Percoll and was layered on top of the gradient. Following a 20-min centrifugation at 700 x g at 20˚C, mononuclear leukocytes were harvested from the 50%/63% interface, and the polymorphonuclear leukocytes (PMN) from the 63%/73% interface and washed twice in PBS (200 x g, 5min at 20˚C). PMN were systemically analysed by cytospin and Quick-Diff stain (Reagena Ltd, Toivala, Finland), and neutrophils represented > 95% of the population. The cells were used directly for assays. Mononuclear phagocytes were resuspended at $4x10^6$ cells/ml in serum-free Iscove's Modified Dulbecco's Medium (IMDM; Life Technologies) containing 100U/ml penicillin, 100µg/ml streptomycine, and 2mM glutamine (IMDM + P/S + L-glut) and incubated for 1 hour at 37˚C, 5% CO_2. The medium and any non-adherent cells were then removed. Fresh IMDM + P/S + L-glut, supplemented with 10% heat-inactivated

autologous serum, was added and the cells were matured for 7 days to generate human monocyte-derived macrophages (HMDM).

2.1.2. Culture of cell lines

2.1.2.1. Human Burkitt's lymphoma cell lines

The human (EBV-negative) BL cell lines BL2 and BL2-bcl2 (BL2 cells stably transfected with Bcl2 to suppress apoptosis) (Wang *et al.*, 1996) were cultured in suspension in 50% X-VIVO medium (50% Gibco RPMI 1640, 50% X-VIVO 20 medium (Lonza), supplemented with 50 U/ml penicillin and 50µg/ml streptomycin) at 37˚C, 5% CO_2.

2.1.2.2. Mouse Burkitt's lymphoma-like cell line

λ-MYC (MycEd1) cells were derived from λ-MYC transgenic mice by Dr. J. Pound and cultured in suspension at 37°C, 5% CO_2, in 45% Dulbecco's Modified Eagle Medium (DMEM (high glucose); Life Technologies), 45% IMDM, supplemented with 10% hybridoma selected foetal calf serum (FCS; PAA Laboratories Ltd), 2mM L-glutamine, 25µM 2-mercaptoethanol (Life Technologies), 100 units/ml penicillin, and 100µg/ml streptomycin.

2.1.2.3. Human monocyte-like cell lines

THP-1 cells were cultured at 37˚C, 5% CO_2, in RPMI medium supplemented with 10% Fetal Bovine Serum (FBS), 2mM glutamine, 100 units/ml penicillin, and 100µg/ml streptomycin. MonoMac6 cells were cultured in the same medium, further supplemented with 1x non-essential amino acids (PAA Laboratories Ltd) and OPI media supplement HYBRI-MAX (containing final working concentrations of 1mM oxaloacetate, 0.45 mM pyruvate, and 0.2 U/ml insulin; Sigma-Aldrich)

2.1.2.4. Human myelogenous leukaemia cell line

K562 cells were cultured at 37˚C, 5% CO_2, in complete RPMI medium.

2.1.2.5. Culture of embryonic-stem cell derived macrophages (ESDM)

Murine embryonic stem cell line E14, derived from the 129/Sv mouse strain was cultured in ESC cell culture medium $GMEM_{SR}$ (Glasgow's Modified Eagle Medium (GMEM), supplemented with 10% (v/v) FBS, 1% (v/v) non-essential amino acids, 2mM L-glutamine, 1mM sodium pyruvate (Life Technologies), 0.1mM 2-mercaptoethanol, 100U/ml leukaemia inhibitory factor (LIF; R&D Systems)) at 37˚C, 5% CO_2. Embryonic stem cells (ESC) were seeded at $1x10^6$ cells/10ml media in gelatinized T25 cm^2 flasks and were passaged when the cells were confluent. At the start of the macrophage differentiation procedure (day 0), $6x10^5$ trypsin-dissociated E14 ESC were seeded in $ESDM_{Diff}$ (GMEM supplemented with 10% (v/v) FBS (pre-screened for optimal haematopoietic differentiation (Jackson *et al.*, 2010)), 1% (v/v) non-essential amino acids, 2mM L-glutamine, 1mM sodium pyruvate, 0.1mM 2-mercaptoethanol, 1ng/ml IL-3 (Stem Cell Technologies, Grenoble, France)) in 95 mm bacteriological-grade round Petri dishes and formed various sized embryonic bodies (EB) over the next few days. To prevent adherence of larger aggregates, EB were transferred to new Petri dishes on day 4 and day 6, and on day 8 they were transferred to a 95 mm round gelatin-coated tissue culture dish. EB adhered to the tissue culture plastic and over the next few days started to release non-adherent macrophage precursor cells into the medium. At day 10 the non-adherent cells were harvested, centrifuged and resuspended in 20mL $ESDM_{Cult}$ (GMEM containing 10% (v/v) FBS (pre-screened for optimal haematopoietic differentiation), 1% (v/v) non-essential amino acids, 2mM L-glutamine, 1mM sodium pyruvate, 0.1mM 2-mercaptoethanol, 15% (v/v) L929 CM, 100U/ml penicillin, 100µg/ml streptomycin) and plated onto 95 mm round bacteriological Petri dishes. Cells adhered to the plastic and proliferated into CD68, CD11b, and F4/80-positive cells (Zhuang *et al.*, 2012) and were cultured for 2-6 days, as indicated. 10ml $ESDM_{Diff}$ culture medium was added to the original EB plates, and every 2 days after that, up to a total number of 20 days, non-adherent macrophage-like cells were harvested and cultured in the same way.

2.1.2.6. Culture of L929 cells and production of L929 cell-conditioned medium

The mouse lung fibroblast line L929 (Burgess, Metcalf et al. 1985) expresses high concentrations of CSF1 and is widely used as a source of CSF1. L929 cells were thawed and cultured in L929 cell culture medium (D-MEM: F12 with Glutamax (Life Technologies) supplemented with 10% FCS (Biosera Ltd), 100 U/ml penicillin (PAA Laboratories Ltd), and 100µg/ml streptomycin (PAA Laboratories Ltd). Cells were passed every 3 to 4 days when confluent using trypsin/EDTA to detach the cells. To harvest conditioned medium, cells were cultured for 3 additional days after they become confluent. Supernatant was collected from the adherent monolayer of cells and filtered through a 0.22µm membrane (Merck Millipore, Livingston, UK) to remove cell debris, and stored at -20˚C.

2.2. Animal Models

All animal procedures and husbandry were performed under a license from the UK Home Office according to regulations described in the Animals (Scientific Procedures) Act 1986. BL2 and BL2-bcl2 cells were resuspended in Hanks' Balanced Salt Solution (HBSS, PAA Laboratories Ltd, Yeovil, UK; w/o Ca^{2+}/Mg^{2+}) and $10x10^6$ cells were injected subcutaneously into the right flank of 6-8 week-old BALB/c SCID mice (injection volume 200µl). The diameter of the developing tumour was measured daily in two dimensions using callipers. When tumours grew larger than 12mm in either dimension, the mice were humanely sacrificed and tumours were excised, snap-frozen in liquid nitrogen and stored at -80˚C until further processed.

2.3. Detachment of ESDM and BMDM for flow cytometry

Cell culture medium was removed from the dishes and macrophages were washed twice with Hanks' Balanced Salt Solution (HBSS, w/o Ca^{2+}/Mg^{2}/phenol red; PAA Laboratories Ltd) and incubated in detachment buffer (Hanks BSS supplemented with 5mM EDTA (Fisher Scientific Ltd, Loughborough, UK) and 0.2% w/v low-

endotoxin bovine serum albumin (BSA, PAA) at 4˚C for 20 min before being detached by gentle scraping using a Cell Lifter (Corning, Ewloe, UK).

2.4. Induction and evaluation of apoptosis

2.4.1. Induction of apoptosis by UV-irradiation

Apoptosis was induced by exposing BL2 or λ-MYC cells in 50% X-VIVO medium to 100mJ/cm^2 of UVB light (17 minutes) using the UVIcab CV006 minicabinet (UVItec Limited, Cambridge, UK). Following exposure to UVB, cells were returned to the incubator (37˚C, 5% CO_2) for 2 (λ-MYC cells) or 3 hours (BL2 cells) before being used in *in vitro* macrophage-tumour cell co-cultures or cytotoxicity assays. For interaction and phagocytosis assays, the UVB-irradiated cells were returned to the incubator (37˚C, 5% CO_2) for 20 hours before being used.

2.4.2. Induction of apoptosis by cold-shock

BL2 cells were harvested, washed once in serum-free RPMI 1640 (Gibco's RPMI 1640 supplemented with 100 U/ml penicillin, 100µg/ml streptomycin, and 2mM L-glutamine) and resuspended at 5x10^6 v cells/ml in HypoThermosol (BioLife Solutions, Bothell, WA, USA) in a polypropylene tube (BD Bioscience) and incubated at 4˚C for 18 hours. Cells were then washed twice in serum-free RPMI 1640 and resuspended at 2x10^6 cells/ml in $ESDM_{Cult}$ medium and cultured for 90 min at 37˚C, 5% CO_2 to allow apoptosis to occur.

2.4.3. Induction of apoptosis by high-density stress

BL2 cells were harvested, washed twice with PBS and once with serum-free RPMI medium. Cells were then resuspended in serum-free RPMI medium at 100x10^6 cells/mL and cultured at 37˚C for 1 hour. After 1 hour, cells were harvested and supernatant was collected by sequential centrifugation (both at 4˚C) at 400 x g for 5 min to remove cells, and at 870 x g for 10 min to remove cell debris. High-density culture under these conditions triggers synchronous apoptosis in 40-50% of BL2 cells (Zhuang *et al.*, 2012).

2.4.4. Assessment of apoptosis by Annexin V/Propidium iodide staining

$2x10^5$ cells were washed once in 2ml PBS, then resuspended in 100µl Annexin V Binding Buffer (AxV-BB; 140mM NaCl (Fisher Scientific), 10mM HEPES (Sigma-Aldrich), 2.5mM $CaCl_2$ (Sigma-Aldrich)) and incubated at 4˚C for 15 min with 1µl Annexin V Alexa Fluor-488 (Life Technologies). 300µl AxV-BB was added and Annexin V binding was analysed by flow cytometry and compared to unstained controls. 10µl (20µg/ml) PI (Sigma-Aldrich) was added 1 minute before analysis.

2.5. Cytokine assays

TNFα, IL-6, and CCL2 release from BMDM was measured using the Mouse Inflammation Cytometric Bead Array (CBA) kit or Flex Sets (BD Biosciences) according to manufacturer's instructions. Additionally, the kit can also detect IL-10, IL-12p70, and IFN-γ. This study focused on TNFα, IL-6 and MCP-1/CCL2, as the other cytokine concentrations were very low or undetectable in the samples. The kit contains six bead populations with distinct fluorescence, making it possible to identify individual beads using flow cytometry. Each capture bead in the kit has been conjugated with capture antibodies, specific for the above analytes. The unknown sample is incubated simultaneously with the capture beads (which binds to recognized analytes) and the detection reagents (a mixture of phycoerythrin (PE)-conjugated antibodies). Together they form sandwich complexes (capture bead + analyte + detection reagent), which provide a fluorescent signal in proportion to the amount of bound analyte. These complexes can be measured using flow cytometry to identify particles with fluorescence characteristics of both the bead and the detector. This study used a 96-well format of this assay, which could be analysed using a BD Accuri™ C6 Flow Cytometer and FACS Array software. The lower limit of detection was ~ 20pg/ml.

2.6. Nitrite release

Nitrite release was determined using the Griess reaction. The Griess reaction is based on the quantitative conversion of sulfanic acid to a diazonium salt by reaction with nitrite in acid solution. The diazonium salt is then coupled to N-(1-

naphthyl)ethylenediamine, forming an azo dye that can be sprectrophotometrically quantitate based on its absorbance at 548 nm. On a 96-well plate, in each well 20µl of Griess reagent (Life Technologies; containing N-(1-naphthyl)ethylenediamine and sulfanic acid, which are added to together immediately before the experiment) is added to 80µl sample and incubated for 10 minutes at room temperature. Absorbance was read using the Varioskan microplate reader (Thermo Scientific) at 548nm. A standard curve was prepared from absorbance levels of known sodium nitrite concentration standards, and nitrite concentration of samples was calculated.

2.7. Western Blotting

2.7.1. Whole cell lysate preparation

Cells were centrifuged at 300 x g for 5 min at 4˚C. Supernatants were removed and cells were then lysed with 80µl lysis buffer (10mM HEPES, 1mM EDTA (Fisher Scientific), 1% triton-X-100 (Sigma-Aldrich)) and 4µl protease inhibitors (Sigma-Aldrich) were added. Samples were then vortexed intensively for 30 seconds and incubated on ice for 30min in a 1.5ml Eppendorf (Eppendorf, Stevenage, UK). Lysate was cleared by centrifugation at 18,000 x g for 10 min at 4˚C. Resultant supernatants were transferred to fresh Eppendorfs and stored at -20˚C.

Protein concentration of the lysates was determined using Bradford dye reagent (Bio-Rad, Hertfordshire, UK). 10µl lysate dilutions were mixed with 190µl 1 in 5 diluted dye in water, incubated for 10 min at room temperature before the absorbance was read at 595 nm wavelength using the Varioskan plate reader. Protein concentrations for the samples were determined by comparison to a standard curve prepared in parallel with the samples from serial dilutions of human IgG standards of known concentration (Sigma-Aldrich).

For each sample, 30µg protein was then mixed with NuPAGE LDS sample buffer (Life Technologies) containing NuPAGE reducing agent (Life Technologies). Samples were denatured for 10 min at 70˚C prior to loading to the gel.

2.7.2. Electrophoresis and Western Blotting

Electrophoretic sample separation and their transfer to nitrocellulose membranes was performed using the Life Technologies NuPAGE system and reagents, according to manufacturer's protocol. Denatured samples, prepared as described above, were loaded into NuPAGE pre-cast 4-12% Bis-Tris gels. SeeBlue Plus2 pre-stained standard (Life Technologies) was used as the molecular weight standard. Protein separation was performed in NuPAGE MOPS SDS running buffer at 200V for approximately 40 min. Proteins were then transferred onto Hybond-P polyvinylidene fluoride transfer membranes (PVDF) in NuPAGE transfer buffer containing 10% methanol (VWR, Lutterworth, UK) and anti-oxidant (Life Technologies) at 30V for 75 min. Blots were blocked for 1hr in PBS containing 0.1% Tween-20 (Sigma-Aldrich) and 5% milk (instand dried skimmed milk, Tesco, Edinburgh, UK). Blots were then incubated with 0.5µg/ml primary antibody, anti-Akt1 Ab (4D6) (Abcam, Cambridge, UK) in PBS/0.1% Tween-20/5% milk at 4˚C overnight. Blots were washed 6x 5 min with PBS/0.1% Tween-20, before blots were incubated with 1µg/ml anti-mouse-Ig-horseradish peroxidase (GE Healthcare, Buckinghamshire, UK) in PBS/0.1% Tween/5% milk for 1 hour at room temperature. Blots were washed 6x 10 min in PBS/0.1% Tween-20, followed by one 30-min wash in PBS. Blots were then developed using ECL reagents (GE Healthcare). Chemiluminescence was detected on photographic film (GE Healthcare).

To confirm that equal amounts of protein were present on the membrane, membranes were washed in stripping buffer (0.87% NaCl (w/v), 0.75% glycine (w/v), pH 2.6) for 2 hours. Blots were then washed for 5 min in PBS, before being blocked at room temperature (RT) in PBS/0.1% Tween-20/5% milk. Blots were then incubated with 0.2µg/ml anti-beta actin primary antibody (Sigma-Aldrich, A1978), in PBS/0.1% Tween-20/5% milk for 30 min at RT. Blots were washed 6x for 5 min with PBS/0.1% Tween-20, before blots were incubated with 0.1µg/ml anti-mouse-Ig-horseradish peroxidase in PBS/0.1% Tween/5% milk for 30 min at room temperature. Blots were washed 6x 10 min in PBS/0.1% Tween-20, followed by one 30-min wash in PBS. Blots were developed as before.

2.8. Limulus amoebocyte lysate (LAL) assay

Lactoferrin was routinely checked for endotoxin content by the chromogenic LAL assay (Lonza) following manufacturer's protocol. The principle of the assay depends on the ability of Gram-negative bacterial endotoxin to catalyse the activation of a pro-enzyme in the Limulus Amebocyte Lysate (LAL). The initial rate of activation is determined by the concentration of endotoxin present. The activated enzyme catalyzes the splitting of pNA from the colourless substrate Ac-Ile-Glu-Ala-Arg-pNA. Released pNA can be measured photometrically at 405-410nm after the reaction is stopped with stop reagent. The correlation between the absorbance and the endotoxin concentration is linear in the 0.1-1.0 EU/ml range. The concentration of endotoxin in a sample can be calculated from the absorbance values of endotoxin standards. Disposable endotoxin-free glass assay tubes were used (Cambrex). 50µl of standard or diluted sample was dispensed into assay tubes in a 37˚C waterbath. At time 0 (T=0), 50µl of LAL was added to each assay tube and the solutions were mixed thoroughly. At T=10 minutes, 100µl of substrate solution was added and mixed thoroughly. At T=16 minutes, 100µl of stop reagent (25% v/v glacial acetic acid in water) was added and mixed before the absorbance was read at 405 on the Varioskan plate reader. Reagents were pipetted in the same order from tube to tube to ensure exact timing for each reaction tube in order to determine the proper endotoxin concentration.

2.9. Interaction and phagocytosis assay

2.9.1. Flow cytometry based phagocytosis assay

The ability of ESDM to phagocytose apoptotic BL2 cells was tested using a method based on a published flow cytometric phagocytosis assay (Jersmann *et al.*, 2003). BL2 cells were washed twice in serum-free RPMI medium and $20x10^6$ cell were stained with 4µl PKH26 Red Fluorescent Cell Linker dye (Sigma-Aldrich), followed by a 4-min incubation at 25˚C. The reaction was stopped by addition of 2ml FCS and cells were centrifuged and then washed three times in complete RPMI medium. PKH26 stained BL2 cells were then washed once more in serum-free RPMI and apoptosis was induced by cold-shock as described in section 2.4.2.

$5x10^6$ detached ESDM at various stages of maturation were stained with 1µl PKH67 Green Fluorescent Cell Linker dye (Sigma-Aldrich) for 4 min at 25˚C. The reaction was stopped by the addition of 500µl FCS and cells were centrifuged and washed three times in complete RPMI medium. ESDM were resuspended at $4x10^6$ cells/ml in $ESDM_{Cult}$ and 500µl was added to each well of a 48-well plate (Nunc A/S, Roskilde, Denmark) and incubated overnight.

Before the start of the assay, medium was removed from the ESDM by aspiration and cells were washed gently with PBS before 500µl of BL2 cells ($2x10^6$ per ml, PKH26-stained induced to undergo apoptosis by cold-shock as described above) was added. The plate was incubated for 1hr at 37˚C, 5% CO_2 to allow phagocytosis to proceed. ESDM alone and BL2 cells alone were used as controls. All samples were tested in triplicate. After incubation, medium was removed and wells were washed gently with PBS. 500µl trypsin/EDTA (PAA Laboratories Ltd) was added to each well, followed by a 15-min incubation at 37˚C and a 15 min incubation on ice to detach ESDM from the surface. Cells were harvested from each well by vigorous pipetting for analysis on the Beckman Coulter Epics-XL-MCL flow cytometer.

2.9.2. Microscopy-based interaction and phagocytosis assay

The ability of BMDM to interact with and phagocytose apoptotic lymphoma cells was tested in a microscopy-based assay. BL2 or λ-MYC cells were induced to undergo apoptosis by exposure to UVB irradiation, as described in section 2.4.1, followed by a 20-hour culture at 37˚C, 5% CO_2. d7 BMDM were prepared on the day of the assay. BMDM were harvested from bacteriological plates, resuspended at $0.2x10^6$ viable cells/ml and 200µl (= 40,000 cells) was added to each well of a pre-cleaned glass side (Henley-Essex; cleaned by incubating the slides in 100% ethanol (VWR) for 30 min, followed by air-drying in the hood for 10-20 min). If BMDM were to be pre-cultured with 10U/ml IFN-γ (R&D Systems) and 0.5ng/ml LPS (Sigma-Aldrich; (rough strains) from S. enterica serotype Minnesota Re595), this was added to the BMDM as they were added to the slides. Slides were placed in Square Petri dishes (Sterilin) and incubated for 2-4 hrs (4hrs if pre-treated with IFN-

γ and LPS or controls) at 37˚C, 5% CO_2 to let the cells adhere to the slides. After a 20 hr incubation of UVB-irradiated cells, BL2 cells were harvested in to a Falcon Tube. Slides with BMDM were dipped three times each in two changes of serum-free to remove media and pre-treatments. Slides were then quickly dried around the wells using cotton buds, carefully avoiding touching the wells, and 200µl apoptotic cells (containing 400,000 cells) were added to each well or media alone was added and the slides were incubated at 37˚C, 5% CO_2. When assays were done in the presence of lactoferrin, 0.1-50µg/ml human milk-derived lactoferrin (Sigma-Aldrich) was added to the apoptotic cells before cells were added to the slides. Slides were then incubated for 1 hour at 37˚C, 5% CO_2. For interaction assays, after the 1-hour co-culture, non-adherent cells were washed off by dipping the slides 5 times in two changes of ice-cold PBS, before fixing the slides in 100% methanol for 20 min. For phagocytosis assays, non-adherent cells were washed off by dipping the slides 5 times in each of two changes of serum-free RPMI medium at room temperature, before adding 200µl trypsin-EDTA to each well to proteolytically remove apoptotic cells bound to the macrophage surface. After incubation in trypsin-EDTA for 5 minutes, unbound cells were washed off by dipping 5x in two changes of ice-cold PBS and slides were fixed in 100% methanol for 20 min and then dried. Cells were then stained using standard May-Grünwald-Giemsa protocol.

May-Grünwald-Giemsa protocol:

A 50x May-Grünwald/Giemsa buffer was prepared by adding 200mM Na_2HPO_4 (Fisher Scientific) to 190ml 200mM NaH_2PO_4 (Fisher Scientific) until the pH was 5.6. The volume was then adjusted to 1 litre with distilled water. A 1x working solution was prepared by dilution of the stock in distilled water, and May-Grünwald (Sigma-Aldrich) and Giemsa (Merck Millipore) stains were diluted 1/3 and 1/10 with 1x buffer, respectively. Slides were then immersed in diluted May-Grünwald stain for 4.5 min. Slides were washed by dipping 3x in 1x buffer. Slides were then immersed in diluted Giemsa buffer for 9.5 min and washed as before by dipping 3x in 1x buffer. A final wash was performed by dipping 3x in distilled water. Slides were allowed to dry completely before a coverslip was mounted on using Histomount (Fisher Scientific).

The number of macrophages interacting with 0, 1, or 2 or more apoptotic cells were then counted using an Olympus CX40 microscope, and the percentage of macrophages interacting with/phagocytosing apoptotic cells was counted. The interaction index was calculated as the product of the percentage of macrophages interacting with apoptotic cells and the average number of apoptotic cells interacting per interacting macrophage.

2.10. Chemotaxis assay

Chemotaxis assays were performed using a transfilter migration assay using polyvinyl uncoated Transwell^{TM} inserts (5μm pore size, Corning BV Life Sciences, Amsterdam, Netherlands) placed in wells of 24-well plates. RPMI 1640 supplemented with 2mM L-glutamine, 100IU/mL penicillin and 100μg/ml streptomycin and 0.1% low-endotoxin BSA (PAA Laboratories Ltd) was used as the chemotaxis assay medium. Cell supernatants or chemotactic reagents, including fMLF (Sigma-Aldrich), ATP (Sigma-Aldrich), recombinant mouse C5a (R&D Systems), and human milk-derived lactoferrin (Sigma-Aldrich), were tested for their chemoattractant activity, and 600μl of each was added to the lower well. Cells to be tested ($2x10^5$ ESDM, BMDM, or THP-1, or $1x10^5$ neutrophils) were added on top of the transwell filter (in 100μl) and incubated at 37˚C, 5% CO_2 for 1 hour (BMDM and neutrophils) or 4 hrs (ESDM and THP-1 cells). After the indicated incubation period, non-migrated cells were removed from the upper surface of the transwells using cotton buds and the transwells were fixed in 100% methanol for 10min, air-dried, and stained with Quick-Diff Blue (Dade) for 20 min. The number of cells that had migrated to the lower side of the transwell was determined using an inverted microscope (Axiovert 25, Carl Zeiss) and was calculated as the mean number of migrated cells per high power field (400x magnification) from 5 random areas. Duplicates were run for each experiment. Alternatively, migrated THP-1 cells did not stick to the lower well and migrated to the lower chamber. Cells were gently resuspended by 10x pipetting, and transferred to a 1.5ml Eppendorf. 2x 100μl was counted from each well using the Attune Acoustic Focusing Cytometer (Life

Techologies) and the total mean number of migrated cells per well was calculated. Duplicates were run for each treatment.

2.11. Flow cytometry

2.11.1. Extracellular staining

$0.2x10^6$ v. cells were centrifuged at 300 x g, for 5 min at 4˚C to remove supernatants. Cells were then incubated in 100µl blocking buffer (PBS + 5% normal goat serum (NGS; Biosera) + 10% normal mouse serum (NMS; Biosera)) to block Fc receptors for 30min at 4˚C. Primary antibody or isotype was then added at the final concentrations indicated in Table 2.1 and incubated for 40 min at 4˚C. Following incubation, cells were washed twice with 2ml fluorescence activated cell sorting (FACS) buffer (PBS + 5% NGS) by centrifugation at 300 x g for 5 min at 4˚C. If incubation with a secondary fluorescence-tagged antibody was necessary, cells were incubated in 100µl FACS buffer for 30 min at 4˚C with fluorescence-tagged secondary antibody added at the final concentrations indicted in Table 2.1. Cells were then washes twice with 2ml FACS buffer by centrifugation at 300 x g for 5 min at 4˚C, before being resuspended in 500µl FACS buffer for analysis by flow cytometry.

	Primary antibody	Secondary antibody
CD206	5µg/ml rat IgG2a anti-mouse CD206 Alexa Fluor-488 conjugated (AbD Serotec, MCA2235A488T)	/
CD206 isotype	5µg/ml Rat IgG2a negative isotype control (AbD Serotec, MCA1124)	/
F4/80	2µg/ml rat IgG2a anti-mouse F4/80 Alexa Fluor-488 conjugated (Life Technologies, MF48020)	/
F4/80 isotype	2µg/ml rat IgG2a negative isotype control Alexa Fluor-488 conjugated (Invitrogen, R2a20)	/
CD204	1.5µg/ml recombinant human IgG1 anti-CD204-FITC conjugated (Miltenyi Biotec, REA148)	/
CD204 isotype	1.5µg/ml recombinant human IgG1 control-FITC conjugated (Miltenyi Biotec, REA293)	/
CD11b	0.5µg/ml rat IgG2b anti mouse CD11b Alexa Fluor 488 conjugated (AbD Serotec, MCA 74A488)	/
CD11b isotype	0.5µg/ml rat IgG2b negative control Alexa Fluor 488 conjugated (AbD Serotec, MCA 1125A488)	/
CD11c	2.5µg/ml Armenian hamster IgG anti-mouse CD11c –FITC conjugated (eBioscience, clone N418)	/
CD11c isotype	2.5µg/ml Armenian hamster IgG isotype control – FITC conjugated (eBioscience, clone eBio299Arm)	/
LRP1	1µg/ml mouse IgG1 anti-human LRP1 (AbD Serotec, clone A2Mralpha-2)	4µg/ml goat anti-mouse IgG Alexa Fluor 488 (Life Technologies, A11029)
LRP1 isotype	1µg/ml purified mouse IgG1 (Biolegend, clone MG1-45)	4µg/ml goat anti-mouse IgG Alexa Fluor 488 (Life Technologies, A11029)
CD14	36µg/ml mouse anti-human CD14 (61D3, produced in our laboratory)	8µg/ml goat anti-mouse IgG Alexa Fluor 488 (Life Technologies, A11029)

Table 2.1 Antibodies used for extracellular/membrane staining for flow cytometry

2.11.2. Detection of lactoferrin binding

Fc receptors on $0.2x10^6$ cells were blocked as above. Human milk-derived lactoferrin (Sigma-Aldrich) or recombinant human lactoferrin (Sigma-Aldrich), both either unconjugated or Alexa Fluor 488-conjugated, was then added at final concentrations of 5 or 20µg/ml and incubated for 1 hour at 4˚C (or room temperature as indicated).

Excess lactoferrin was washed away by 2 washing steps at 300 x g for 5min with 2ml FACS buffer. Cells incubated with Alexa Fluor-488 conjugated lactoferrin were resuspended in 500µl FACS buffer and analysed by flow cytometry. For cells incubated with unconjugated lactoferrin further incubations with primary and secondary antibodies were necessary. 10µg/ml sheep anti-Lf antibody (produced in our laboratory by Ben Arnold) was added to the cells in 100µl FACS buffer and incubated for 40 min at 4˚C. Following incubation, cells were washed twice with 2ml FACS buffer and resuspended in 100µl FACS buffer for incubation with donkey anti-sheep Alexa Fluor 488 antibody (Life Technologies, A22015) at a final concentration of 8µg/ml. Cells were then washed twice with 2ml FACS buffer, before being resuspended in 500µl FACS buffer for analysis by the Attune Acoustic Focusing Cytometer and software.

2.11.3. Competition assays

d7 BMDM (50,000) were centrifuged at 300 x g, for 5 min at 4˚C to remove supernatants. Cells were then incubated in 100µl human IgG blocking buffer (PBS + 0.5% low endotoxin BSA) + 100µg/ml human IgG to block Fc receptors for 50 min at 4˚C. Lactoferrin at a final concentration of 2µg/ml and 0.1-100µg/ml anti-MSR1 antibody (rat anti-mouse CD204 mAb (AbD Serotec, clone 2F8)) or isotype control (purified rat (Serotec, clone IR863) were then added simultaneously and the cells were incubated for 60 min at 4˚C. Cells were then washed twice with PBS + 0.5% BSA. Following washes, cells were resuspended in 100µl hIgG blocking buffer and incubated with 10µg/ml sheep anti-Lf antibody for 40 min at 4˚C. Cells were washed twice with PBS + 0.5% BSA, resuspended in 100µl hIgG blocking buffer and incubated with 8µg/ml donkey anti-sheep Alexa Fluor 488 antibody for 30 min at 4˚C. Cells were then washed twice with PBS + 0.5% BSA and resuspended in 400µl PBS + 5% NGS for analysis by the Attune Acoustic Focusing Cytometer and software.

2.12. *In vitro* macrophage-tumour cell co-cultures

2.12.1. Direct contact co-cultures

d7 BMDM were washed twice with HBSS, on Petri dishes, and resuspended in 25ml standard RPMI medium and incubated for 18 hours at 37˚C, 5% CO_2. The next day, non-adherent cells were removed, and PBS was added to the dishes. Adherent cells were then dislodged using a 19g needle and syringe. Cells were washed once in 50% X-VIVO medium (if stained with violet proliferation dye as indicated below) or once in serum-free RPMI medium (if unstained) and resuspended at $0.5x10^6$ cells/ml in 50% X-VIVO medium. 2.5ml of cells was added per round 6mm tissue culture dish (Corning; = $1.25x10^6$ BMDM) and supplemented with 2.5ml 50% X-VIVO medium. Pre-treatments of 10U/ml IFN-γ and 0.5ng/ml LPS were added at this time. Cells were then incubated for 4 hrs at 37˚C, 5% CO_2 to let the BMDM adhere to the dishes. In the mean time, apoptotic or viable lymphoma cells were prepared. BL2, BL2-bcl2 and λ-MYC lymphoma cells were harvested and washed once in PBS followed by a wash in serum-free RPMI. Cells were then resuspended at $2.5x10^6$ cells/ml in 50% X-VIVO. Cells were then transferred to tissue culture flasks (Nunc) and either left untreated or subjected to 100mJ UVB irradiation to induce apoptosis, as explained in section 2.4.1. Cells were then incubated for 3 hrs (BL2 and BL2-bcl2 cells) or 2 hrs at 37˚C, 5% CO_2. After the 4-hour incubation, BMDM were gently washed 3x with cold PBS, before 5ml untreated or UVB-exposed lymphoma cells were added ($12.5x10^6$ cells) per dish. Dishes were incubated for 24 hrs at 37˚C, 5% CO_2. After 24 hours, supernatants were collected from the plates. Supernatants were cleared from cells by a 5 min 300 x g spin, and from cell debris by a 1200 x g spin for 10 min, both at 4˚C. Supernatants were collected into Eppendorf tubes and stored at -80˚C until analysed for cytokine or nitrite content. Lymphoma cells were washed away from the dishes by 3 washes with ice-cold PBS and BMDM were lysed against the dish for RNA extraction as detailed in section 2.15.2.

For BMDM co-cultures in which the BMDM would later be analysed by flow cytometry, BMDM were stained with the fluorescent CellTrace Violet Cell Proliferation dye (Life Technologies) according to manufacturer's protocol, prior to adding the cells to the tissue culture dishes. Pre-treatments and co-cultures were then

performed as explained above. At the end of the assay, lymphoma cells were washed away by 3 washes with ice-cold PBS, and BMDM were then harvested for flow cytometry using detachment buffer (as explained in section 2.3).

2.12.2. Contact-free co-cultures

Contact-free co-cultures were set up similar as direct contact co-cultures. In short, $1.25x10^6$ BMDM were added to wells of 6-well plates, and incubated for 4 hrs in the presence or absence of IFN-γ and LPS. In the mean time, BL2 and BL2-bcl2 cells were washed, resuspended at $4x10^6$ cells/ml, and subjected to 100mJ UVB or left untreated. After a 4-hour incubation, BMDM were gently washed 3x with cold PBS, before 1.9ml 50% X-VIVO medium was added to each well. 0.4µm pore size Millipore Cell Culture plate inserts 30mm (Sigma-Aldrich) were then added to some wells, and 3.1ml lymphoma cells (containing $12.5x10^6$ cells/ml) were added on top of the transwell inserts or added directly to the media (for controls). Following 24-hour co-culture, supernatants were collected from transwells and dishes and cleared as explained above. BMDM were washed 3x with ice-cold PBS as before and lysed against the plates for RNA extraction.

2.13. Lactoferrin treatment of BMDM and neutrophils

2.13.1. Lactoferrin treatment of BMDM

BMDM were prepared as described in section 2.12.1 and $1x10^6$ BMDM were incubated per well on a 6-well plate in serum-free RPMI supplemented with 1% X-VIVO 20 medium (1% X-VIVO medium). BMDM were incubated for 3hrs before 0-100µg/ml human lactoferrin (AbD Serotec, PHP239) was added and the BMDM were incubated a further 16 hrs at 37˚C, 5% CO_2. At the end of the assay, BMDM were gently washed 3x with ice-cold PBS before the cells were lysed against the plate for RNA extraction as explained in section 2.15.2.

2.13.2. Lactoferrin treatment of neutrophils

Neutrophils were isolated from peripheral blood as described in section 2.1.1.2, and resuspended at $2x10^6$ v. cells/ml in serum-free RPMI containing 0.1% BSA (low endotoxin). 200nM fMLF (Sigma-Aldrich) and/or 10µg/ml human milk-derived lactoferrin (Sigma-Aldrich) or 10µg/ml human transferrin (Sigma-Aldrich) was then added simultaneously and incubated for 2 hours at 37˚C, 5% CO_2. Lysates were prepared and analysed for AKT1 by Western Blotting as described in section 2.7.

2.14. Cytotoxicity assays

2.14.1. Violet Ratiometric Membrane Asymmetry Probe-based cytotoxicity assay

d7 BMDM were washed twice with HBSS on Petri dishes and resuspended in 25ml complete RPMI medium and incubated overnight at 37˚C, 5% CO_2. 18 Hours later, non-adherent cells were removed, and PBS was added to the dishes. Adherent cells were then dislodged using a 19g needle and syringe. Cells were stained with PKH67 Green Fluorescent Cell Linker dye according as explained in section 2.9.1 and washed twice in 50% X-VIVO medium and resuspended at $0.4x10^6$ cells/ml. Pre-treatments of 10U/ml IFN-γ and 0.5ng/ml LPS were added at this time. 500µl cells were then added per well on 24-well tissue culture plates (Nunc) (= $0.2x10^6$ cells) and incubated for 4 hrs at 37˚C, 4% CO_2. In the mean time, apoptotic or viable lymphoma cells for pre-treatments were prepared. BL2, BL2-bcl2 and λ-MYC lymphoma cells were harvested and washed once in PBS followed by a wash in serum-free RPMI. Cells were then resuspended at $4x10^6$ cells/ml in 50% X-VIVO medium. Cells were transferred to tissue culture flasks (Nunc) and either left untreated or were subjected to 100mJ UVB irradiation to induce apoptosis (see section 2.4.1). Lymphoma cells were then incubated for 3 hrs (BL2 and BL2-bcl2 cells) or 2 hrs (λ-MYC cells) at 37˚C, 5% CO_2. After a 4-hour incubation of BMDM, 500µl lymphoma cells (= $2x10^6$ cells) or media was added to the macrophages. Plates were incubated for 24 hours at 37˚C, 5% CO_2.

The next day, new (target) BL2 lymphoma cells were taken from fresh cultures and washed with PBS before being stained with PKH26 Red Fluorescent Cell Membrane

dye, using **3x** the recommended concentration by the manufacturer and washed in FBS and complete RPMI 1640 medium, followed by 2 washes in 50% X-VIVO medium and resuspended at $0.4x10^6$ cells/ml in 1% X-VIVO medium. After 24 hours co-culture with viable and apoptotic lymphoma cells, BMDM were gently washed 3x with warm PBS to remove non-adherent lymphoma cells. 500µl of PKH-26 labelled BL2 cells (= 200,000 cells) were then added to the BMDM and co-cultured for 20h at 37˚C, 5% CO_2. After a 20-hour co-culture with target BL2 cells, all cells were dislodged from the plates by repeated pipetting. 200µl cells from each well was transferred to Eppendorfs, and 0.2µl of F2N12S, and 0.2µl of SYTOX AADvanced dead cell stain from the Violet Ratiometric Membrane Asymmetry Probe/Dead Cell Apoptosis kit (Life Technologies) were added approximately one minute before analysis by the Attune Acoustic Focusing Cytometer and software.

2.14.2. Chromium-51 release cytotoxicity assay

BMDM were prepared and plated at 400,000 cells/well and pre-treated with or without IFN-γ and LPS as described for the Violet Ratiometric Membrane Asymmetry Probe-based cytotoxicity assay described above, but BMDM were not stained with PKH67 dye. Following 4-hour pre-treatment with or without 10U/ml IFN-γ and 0.5ng/ml LPS, 500µl X-VIVO 20 medium was added and the macrophages were incubated for a further 24 hours at 37˚C, 5% CO_2. The next day, fresh (target) BL2 lymphoma cells were taken from culture and washed with PBS and $3x10^6$ BL2 cells were resuspended in 1ml 50% X-Vivo/50% RPMI containing 250µCi Cr51 (PerkinElmer Inc, Beaconsfield, UK) and incubated for 1 hour at 37˚C. Cells were washed twice in 50% X-vivo/50% RPMI and resuspended in 10ml 50% X-VIVO and cultured for 1 hour at 37˚C to allow diffusion of loosely bound Cr51. Cells were washed a further 3x in 50% X-VIVO medium. BMDM were then gently washed 3x with PBS and Cr51-labelled target cells were added to the BMDM at the following effector:target cell ratios: 100:1, 50:1, 20:1, 10:1, at a final volume of 500µl/well in 1% X-VIVO medium. Effector and target cells were co-cultured for 4, 8, or 24 hours. Effector cells without target cells (to measure background), and target cells without effector cells (to measure spontaneous release of Cr51) were included for each time point. 100% lysis controls were prepared by adding 9 volumes of water

to labelled targets and incubating for 4 hours. After the indicated incubation time, 250µl of supernatant was collected from each well using a Gilson pipette and transferred to sealed tube for gamma counting using the 1470 WIZARD gamma counter (Wallac, PerkinElmer).

2.15. RNA extraction, evaluation and reverse transcription

2.15.1. Isolation of total RNA from frozen tissue

Tissue was placed in 600µl RLT buffer containing 10% β-mercaptoethanol (RNeasy Qiagen kit). 2.8mm ceramic (zirconium oxide) beads were then added and the tissue lysed and homogenized using Precellys 24 equipment (Bertin Technologies, Izasa, Spain) at 5000 x g for one 20-second cycle. Lysed tissue was transferred to RNase-free microtubes (Eppendorf) and 700µl 70% ethanol was then added and RNA extracted using the RNeasy Qiagen kit as explained below.

2.15.2. Isolation of total RNA from cultured cells

BMDM were lysed directly on the tissue culture wells by adding 350µl RLT buffer (RNeasy mini kit, Qiagen) containing 10% β-mercaptoethanol and cell lysates were collected into 1.5ml ml RNase-free microtubes. In the case of non-adherent lymphoma cells, $5x10^6$ cells were first pelleted by centrifugation at 300 x g for 5 min. Supernatants were discarded, and cells resuspended in 350µl RLT buffer containing 10% β-mercaptoethanol (Sigma-Aldrich). RLT lysis buffer is a highly denaturing guanidine-thiocyanate-containing buffer, which inactivates RNases to ensure purification of intact RNA.

Samples were vortexed for 3 minutes to ensure homogenization of lysates. 350µl 70% ethanol was then added to provide binding conditions. Samples were then transferred to RNeasy Mini spin columns and RNA was extracted following the manufacturer's protocol. This involves various washing steps to wash away contaminants effectively before purified RNA was extracted by elution with RNase-free water. Quantity and quality of RNA was assessed using the NanoDrop 1000

spectrophotometer (Thermo Scientific). Samples were then DNase treated using Amplification Grade DNase 1 (Sigma-Aldrich) and stored at -80˚C.

2.15.3. cDNA synthesis by reverse transcription

200ng of total RNA was reverse transcribed into cDNA using SuperScript™ III First-Strand Synthesis Supermix for qRT-PCR (Life Technologies). 200ng of RNA was mixed with 10µl 2x RT Reaction mix, 2µl RT Enzyme mix, and RNase-free water up to 20µl. Reactions were then incubated for 10 minutes at 25˚C, followed by 30 minutes at 50˚C, and reactions were terminated by incubation at 85˚C for 5 minutes, before they were chilled on ice. 1 µl of *E. coli* RNase H was then added and incubated at 37˚C for 20 minutes to inactivate RNases, and cDNA was stored at -20˚C until use.

2.16. Real-time quantitative PCR (qPCR)

Real-time qPCR was performed in an ABI 7500 FAST qPCR system using SYBR Green I Dye chemistry (Life Technologies) and gene specific primers. Primer sequences were obtained from Primer Bank (http://pga.mgh.harvard.edu/primerbank/) and qPrimerDepot (http://mouseprimerdepot.nci.nih.gov/) online databases. Primers were ordered from Eurofins MWG Operon (Ebersberg, Germany). Because SYBR Green dye can bind to any double-stranded DNA product, including non-specific primer-dimer products, all primers were first validated and routinely assessed for production of a single product by including the dissociation stage at the end of the qPCR program (see Table 2.2 for details of the qPCR program).

Step	Activity	Temperature (˚C)	Duration
1	Enzyme activation	95	20 seconds
2	Denaturation	95	3 seconds
3	Annealing/Extension	60	30 seconds
4	Repeat steps 2-3 (39x)	-	-
5	Dissociation step	increasing	-

Table 2.2 Real-time qPCR fast programme settings for ABI 7500 Fast instrument (Applied Biosystems).

Reactions were set up in white 96-well optical Thermo-Fast qPCR plates (Fisher Scientific). 80-100ng of cDNA (depending on the assay) was added to 6µl of FAST SYBR Green master mix (Life Technologies), 1µl forward primer (2.5µM), 1µl reverse primer (2.5µM), and RNase-free water up to 12µl. No RT (reverse transcription) and no template controls were routinely included in runs to assess any genomic DNA or non-specific amplification. Samples and controls were set up in duplicate wells.

Relative mRNA expression for genes of interest was assessed by comparison to a calibrator sample, following normalization to the reference genes α-tubulin (Tuba1b), heat shock protein 90 (Hsp90), hypoxanthine guanine phosphoribosyl transferase Hprt, and beta-2 microglobulin (B2m) using the ΔΔCT method (described in Applied Biosystems User Bulletin No. 2 (P/N 4303859) and (Livak and Schmittgen, 2001) in Excel. Appropriateness of reference genes was tested using NormFinder (version 20) (Andersen *et al.*, 2004). The relative quantitation data are presented in graphs showing $\log_2$ expression ratio relative to control samples with error bars corresponding to the standard error of the mean (SEM).

Optimisation of qPCR amplification efficiency

Additionally, qPCR efficiency for each primer set was determined by generating standard curves on cDNA synthesised from RNA pooled from mixed murine tissue (extracted as described in section 2.6.1). qPCR reactions were carried out with serial dilutions of cDNA template on the ABI 7500FAST qPCR system. Standard curves and primer dissociation curves were drawn by ABI SDS 1.4 software. Amplification

efficiency for each primer set was determined from the slope of the standard curve as well as the coefficient of determination (R^2). Only primer sets with amplification efficiencies of 90-110% (-3.1 and -3.6) and R^2>0.97 were used. Table 2.3 shows the slope and R^2 values for all primers that were used, along with information on primer sequences and Genbank accession number.

Gene	Genbank accession	Primer sequence (5' → 3')	Amplicon size (bp)	Slope	R^2
Abca1	NM_013454	F: AAAACCGCAGACATCCTTCAG R: CATACCGAAACTCGTTCACCC	124	-3.26	0.97
Anpep	NM_008486	F: ATGGAAGGAGGCGTCAAGAAA R: CGGATAGGGCTTGGACTCTTT	180	-3.34	0.98
Arg1	NM_007482	F: CTCCAAGCCAAAGTCCTTAGAG R: AGGAGCTGTCATTAGGGACATC	185	-3.26	0.98
Axl	NM_009465	F: ATGGCCGACATTGCCAGTG R: CGGTAGTAATCCCCGTTGTAGA	155	-3.36	0.98
B2m	NM_009735	F: ACCCGCCTCACATTGAAATCC R: GGCGTATGTATCAGTCTCAGTG	146	-3.43	0.99
CCL2	NM_011333	F: TTAAAAACCTGGATCGGAACCAA R: GCATTAGCTTCAGATTTACGGGT	121	-3.27	0.99
Cd36	NM_007643	F: AGATGACGTGGCAAAGAACAG R: CCTTGGCTAGATAACGAACTCTG	83	-3.35	0.99
Cd68	NM_009853	F: CCTCGCCTAGTCCAAGGTC R: GGATTCGGATTTGAATTTGGGCT	102	-3.44	0.99
Cd93	NM_010740	F: ATCTCAACTGGTTTGTTCCTGC R: ACTCTTCACGGTGGCAAGATT	186	-3.55	0.99
Csf1r	NM_001037859	F: GGACCTACCGTTGTACCGAG R: CAAGAGTGGGCCGGATCTTT	85	-3.34	0.99
Ctsb	NM_007798	F: TCCTTGATCCTTCTTTCTTGCC R: ACAGTGCCACACAGCTTCTTC	176	-3.50	0.99
Ctsd	NM_009983	F: GCTTCCGGTCTTTGACAACCT R: CACCAAGCATTAGTTCTCCTCC	113	-3.53	0.99
Ctsl	NM_009984	F: ATCAAACCTTTAGTGCAGAGTGG R: CTGTATTCCCCGTTGTGTAGC	136	-3.38	0.99
Ctss	NM_021281	F: CCATTGGGATCTCTGGAAGAAAA R: TCATGCCCACTTGGTAGGTAT	155	-3.35	0.97
Emp1	NM_010128	F: TTGGTGCTACTGGCTGGTCT R: CATTGCCGTAGGACAGGGAG	169	-3.58	0.99
Emr1	NM_010130	F: TGACTCACCTTGTGGTCCTAA R: CTTCCCAGAATCCAGTCTTTCC	111	-3.38	0.99
Fn1	NM_010233	F: TTCAAGTGTGATCCCCATGAAG R: CAGGTCTACGGCAGTTGTCA	154	-3.49	0.99
Gas6	NM_019521	F: TGCTGGCTTCCGAGTCTTC R: CGGGGTCGTTCTCGAACAC	186	-3.40	0.96
Gpnmb	NM_053110	F: TGCCAAGCGATTTCGTGATGT R: GCCACGTAATTGGTTGTGCTC	76	-3.11	0.99
Hmox1	NM_010442	F: AAGCCGAGAATGCTGAGTTCA R: GCCGTGTAGATATGGTACAAGGA	100	-3.148	0.98
Hprt	NM_013556	F: TCAGTCAACGGGGACATAAA R: GGGGCTGTACTGCTTAACCAG	141	-3.56	0.99
Hsp90ab1	NM_008302	F: GTCCGCCGTGTGTTCATCAT R: GCACTTCTTGACGATGTTCTTGC	168	-3.55	0.99

Gene	Genbank accession	Primer sequence (5' → 3')	Amplicon size (bp)	Slope	R^2
Igf1	NM_010512	F: GCAACACTCATCCACAATGC R: AGCTGGACCAGAGACCCTTT	148	-3.53	0.99
Il12a	NM_008351	F: CAATCACGCTACCTCCTCTTTT R: CAGCAGTGCAGGAATAATGTTTC	181	-3.11	0.99
Il6	NM_031168	F: TAGTCCTTCCTACCCCAATTTCC R: TTGGTCCTTAGCCACTCCTTC	76	-3.25	0.99
Lamp2	NM_010685	F: TGGCTCAGCTTTCAACATTTCC R: TGCCAATTAGGTAAGCAATCACT	278	-3.56	0.98
Lgals3	NM_010705	F: GTACAGCTAGCGGAGCGG R: CGGATATCCTTGAGGGTTTG	110	-3.18	0.99
Lrp1	NM_008512	F: ACTATGGATGCCCCTAAAACTTG R: GCAATCTCTTTCACCGTCACA	102	-3.28	0.98
Mertk	NM_008587	F: CTCCTGAGCCCGTCAATATCT R: AGACCAGGTACGGTTAGGACA	94	-3.10	0.99
Mmp12	NM_008605	F: TTTGGATTATTGGAATGCTGC R: ATGAGGCAGAAACGTGGACT	106	-3.488	0.98
Mmp2	NM_008610	F: CAAGTTCCCCGGCGATGTC R: TTCTGGTCAAGGTCACCTGTC	171	-3.51	0.99
Mmp3	NM_010809	F: TCTGGGCTATACGAGGGCAC R: ACCCTTGAGTCAACACCTGGA	232	-3.19	0.96
Mrc1	NM_008625	F: CTCTGTTCAGCTATTGGACGC R: CGGAATTTCTGGGATTCAGCTTC	132	-3.599	0.98
Msr1	NM_031195	F: TTCAAACTCAAAAGCCGACCT R: GTTGCCATGCTGAAATTCTGG	60	-3.29	0.98
Nos2	NM_010927	F: ACATCGACCCGTCCACAGTAT R: CAGAGGGGTAGGCTTGTCTC	177	-3.85	0.99
Pdgfc	NM_019971	F: ACATTTGATGAGAGATTTGGGCT R: CAGCGTCCTAAAACACTTCCAT	104	-3.2	0.99
Plau	NM_008873	F: GCGCCTTGGTGGTGAAAAAC R: TTGTAGGACACGCATACACCT	100	-3.35	0.99
Pparg	NM_011446	F: GGAAGACCACTCGCATTCCTT R: GTAATCAGCAACCATTGGGTCA	121	-3.33	0.99
Psap	NM_011179	F: CCTGTCCAAGACCCGAAGAC R: CAAGGAAGGGATTTCGCTGTG	137	-3.40	0.99
Timp2	NM_011594	F: TCAGAGCCAAAGCAGTGAGC R: GCCGTGTAGATAAACTCGATGTC	142	-3.34	0.99
Tnf	NM_013693	F: CAGGCGGTGCCTATGTCTC R: CGATCACCCCGAAGTTCAGTAG	89	-3.19	0.99
Trem2	NM_031254	F: CTGGAACCGTCACCATCACTC R: CGAAACTCGATGACTCCTCGG	183	-3.45	0.99
Tuba1b	NM_011654	F: AGTAGAGCTCCCAGCAGGC R: TCTCACCCTCGCCTTCTAAC	104	-3.38	0.99

Table 2.3 – Sequences and amplification efficiency of mouse primers used in real-time qPCR.
Gene symbols, Genbank IDs, forward (F) and reverse (R) oligonucleotide sequences and amplicon size in base pairs (bp) are shown. Amplification efficiency is presented in terms of standard curve slope and R^2 values.

2.17. Bovine lactoferrin removal from medium

2.17.1. Preparation of anti-bovine lactoferrin-coupled nanoparticles

First anti-bovine lactoferrin antibody (clone 2G10, produced in our laboratory) was covalently bound to magnetic nanomag®-D particles (250nm diameter; Micromod, Rostock, Germany) using carbodiimide chemistry. 1ml of nanomag®-D particles in a 1.5ml microtube were placed on a magnet for 5 minutes. Supernatant was aspirated and the nanomag®-D particles were resuspended in 900µl 0.1M 2-(4-morpholino)ethanesulphonic acid (MES) buffer (Sigma). A 1M MES buffer stock was prepared by mixing with 0.5M Na_2CO_3 to get pH 6.3. 100µl of 1mg/ml 1-ehtyl-3-(3-dimethylaminopropyl)-carbodiimide hydrochloride (EDC) and 2mg/ml N-hydroxysuccinimide (NHS) dissolved in N,N-Dimethylformamide (DMF) was then added to the nanomag®-D particles to activate them. The microtube containing the particles was mixed end-over-end on a Dynal sample mixer for 1 hour at RT. Two washes were then performed as follows. The microtube was placed on the magnet for 5 minutes. Supernatant was aspirated off and the nanomag®-D particle resuspended in 1ml 0.1M MES. After two washes in this way, the microtube was placed back on the magnet for 5 minutes and supernatant removed. 1ml of 1mg/ml anti-bovine lactoferrin in PBS was then added to and mixed with the nanomag®-D particles on the Dynal sample mixer for 3 hours at RT. After 3 hours, the reaction was quenched by adding 111µl 25mM glycine, and mixed for a further 30 minutes. nanomag®-D particles were then washed twice with PBS on the magnet as described earlier. Anti-bovine lactoferrin-coupled nanoparticles were then resuspended in 1mL PBS and stored at 4˚C until used.

2.17.2. Removal of bovine lactoferrin from FBS

Bovine lactoferrin was then removed from FBS in sequential separation steps as follows. 2G10-coupled nanoparticles were vortexed for 30 seconds. 100µl nanoparticles were transferred to each microtube and washed once in 1ml PBS on the magnet. Suspension was removed and FBS diluted 1:1 in RPMI 1640 was added and mixed with the anti-bovine lactoferrin-coupled nanomag®-D particles. It was incubated and mixed for 40 min at RT on the Dynal sample mixer. Tubes were then

placed on the EasySep magnet for 5 minutes. Suspension was removed and transferred to microtubes containing new beads and incubated again for 40 min. This was repeated once more (total of 3 incubations with nanoparticles). After 3 incubations with the anti-bovine lactoferrin-coupled nanomag®-D particles, the suspension was transferred to 1.5ml Eppendorfs and the diluted FBS, from which bovine lactoferrin was removed was stored at 4˚C. Success of lactoferrin removal was measured by sandwich ELISA as detailed below.

2.18. Sandwich ELISA for bovine lactoferrin detection:

Wells of a 96-well plate were coated with 50µl 1µg/ml capture antibody (sheep anti-bovine lactoferrin (Bethyl, Montgomery, TX, USA, A10-126A) in coating buffer (0.05M carbonate/bicarbonate pH 9.6). The plate was sealed and incubated overnight at 4˚C. The next day, wells were emptied and blocked with PBS containing 5% normal goat serum (PBS:NGS) for 1 hour. Wells were blotted dry and washed 3 times with PBS containing 0.05% Tween-20 (PBS-T). 50µl bovine lactoferrin (Sigma-Aldrich) standards of 2000ng/ml - 1.95ng/ml and samples to be tested were then added to each well and incubated for 1 hour at 37˚C. Wells were washed 3x with PBS-T and 50µl 2µg/ml mouse anti-bovine lactoferrin (clone 2G10) was added and incubated for 1 hour at 37˚C. Wells were then washed 3 times with PBS-T and 50µl HRP-conjugated goat anti-mouse IgG detection antibody (Sigma-Aldrich, A3673) and incubated for 1 hour at 37˚C. Wells were washed 3x with PBS-T and 100µl OPD substrate (SIGMAFast OPD-HCL tablets; Sigma-Aldrich) were added to each well and incubated for 10-30 min at RT. The reaction was stopped by adding 50µl HCL per well and OD was read at 492nm on the Varioskan plate reader.

2.19. Bioinformatics analysis

Monocyte, macrophage, and dendritic cell expression datasets were searched on the National Center for Biotechnology Information's (NCBI) Gene Expression Omnibus (GEO; http://www.ncbi.nlm.nih.gov/geo/), a public functional genomics data repository. Datasets were selected based on the following criteria: 1, chip platform (Affymetrix Mouse Gene 1.0 ST Array), 2, cell type studied; 3, availability of raw

data (.cel) files, and 4, availability of at least 2 replicates of each cell type within each study. An annotated list including all the samples was made, and information regarding the study and cell type for each sample was entered to make the interpretation of the data easier. The raw data files (.cel) were downloaded for each selected study and the quality and compatibility of the raw data was assessed using the arrayQualityMetrics package in Bioconductor (http://www.bioconductor.org). The data were scored on the basis of 7 metrics. Any array suggested to be an outlier on more than one metric was removed from the dataset. Furthermore, datasets that comprised extra time points, treatments or knock-outs were removed to simplify the dataset. Each remaining dataset was then normalized independently, using the robust multi-array average (RMA) expression measure (Irizarry *et al.*, 2003), and any outlier datasets were removed. The final macrophage dataset contained all the samples that had passed the quality and compatibility assessments. Probesets of the microarrays were annotated using the latest annotation available from Bioconductor (March 2014) to link the AffyIDs to better understandable gene names. Using a Pearson threshold cut off of r=0.80, a network graph was generated of the data using BioLayout Express^{3D}. Using the Markov Cluster (MCL) Algorithm, the graph was then clustered non-subjectively into clusters of genes that share similarities in their expression, with the MCL inflation value set to 2.2. Alternatively, the graph was clustered by dataset. For the largest clusters and other clusters of interest, the gene transcripts were analysed for functions using the Functional Annotation Clustering tool on the Database for Annotation, Visualization, and Integrated Discovery (DAVID; http://david.abcc.ncifcrf.gov/) (Huang *et al.*, 2009a; b). Additionally, individual genes were analysed using BioGPS, a gene annotation portal (www.biogps.com).

2.20. Statistical analysis

Results from experiments are presented as means ± standard error of the mean (SEM), unless otherwise indicated. Data analysis and statistical analysis was performed using GraphPad Prism version 6 (GraphPad, La Jolla, USA). Data was statistically analysed using a paired or unpaired t-test, one-way ANOVA followed by

Dunnett's post test, or two-way ANOVA followed by Tukey's post test. P values of 0.05 or less were considered statistically significant.

Chapter 3 Exploration of the role of lactoferrin in shaping starry-sky TAM activation signature

3.1 Introduction

Lactoferrin is an 80 kDa iron-binding glycoprotein found in exocrine secretions and secondary granules of neutrophils. Its numerous functions include antimicrobial, anti-inflammatory and trophic activities (García-Montoya *et al.*, 2012; Vogel, 2012). Furthermore, lactoferrin has been identified to be released from apoptotic cells, including apoptotic Burkitt's lymphoma cells, and it was shown to specifically inhibit chemotaxis of neutrophils and eosinophils, but not mononuclear phagocytes, both *in vitro* and *in vivo* (Bournazou *et al.*, 2009; 2010). Moreover, recombinant human lactoferrin was reported to have the ability to attract monocytes (la Rosa *et al.*, 2008).

Various chemoattractants released from apoptotic cells have been shown not only to be capable of recruiting macrophages, but to also prepare them for apoptotic cell clearance. Indeed, ATP released by apoptotic cells increases binding of apoptotic cells to macrophages (Marques-Da-Silva *et al.*, 2011) and fractalkine was found to cause the expression of milk fat globule epidermal growth factor (MFG-E8) on macrophages, which leads to enhanced apoptotic cell clearance (Miksa *et al.*, 2007). Additionally, find-me signals may also influence non-immunogenic responses to apoptotic cells. Fractalkine has been shown to stimulate growth-promoting and survival effects (Boehme *et al.*, 2000; White *et al.*, 2010), and S1P can enhance secretion of IL-10 and PGE2 by tumour macrophages (Weigert *et al.*, 2007; Johann *et al.*, 2008).

Apart from regulating chemotaxis of phagocytes, lactoferrin has also been shown to affect clearance and immunogenic responses of macrophages. Opsonisation of *S. aureus* and parasites by lactoferrin can enhance their phagocytosis by mammary

gland secretory cells (Kai *et al.*, 2002) and macrophages (Lima and Kierszenbaum, 1985), respectively. In addition, lactoferrin can down-regulate LPS-induced cytokine production in human monocyte cell lines, including down-regulation of TNFα, IL-1β, IL-6, and IL-8 (Håversen *et al.*, 2002).

Because of its multifaceted functions, it was hypothesised that lactoferrin released from apoptotic lymphoma cells can promote lymphomagenesis through the recruitment and activation of mononuclear phagocytes that are anti-inflammatory, immunosuppressive, and promote tumour growth and tissue remodelling.

The study presented in this chapter first tests the ability of lactoferrin to attract human and murine monocytes in a modified Boyden chamber assay. It then goes on to investigate the binding of lactoferrin to various monocytes and macrophages, and to see if lactoferrin affects binding of apoptotic cells to macrophages. Because of the presence of lactoferrin in serum, the effect of bovine lactoferrin in serum on macrophage function is investigated, before the effect of lactoferrin on macrophage function is tested. Gene expression of selected starry-sky TAM transcripts (Table 1.1 and Table 1.2) is analysed in the presence and absence of lactoferrin by qPCR. Finally, the ability of lactoferrin to inhibit macrophage-mediated cytotoxicity is tested. The chapter concludes with a study to investigate whether Akt1 is involved in lactoferrin-induced inhibition of neutrophil migration.

3.2 Results

3.2.1 Lactoferrin is not a chemoattractant for monocytes

The ability of lactoferrin to attract monocytes and macrophages was tested in a modified Boyden chamber assay. Chemoattractants were added to the lower chamber and 4-day matured bone marrow-derived macrophages (BMDM) from BALB/c mice were placed on top of the membrane. The BMDM were then allowed to migrate to the lower side of the membrane for 1 hour at 37˚C. At the end of the assay the inner side of the membranes was cleaned, followed by fixation with methanol and staining of the membranes with Quick-Diff Blue. The number of migrated cells per high

power field (HPF) was counted for 10 random areas from duplicate membranes. The results are presented in Figure 3.1a. Large numbers of BMDM were found to migrate to the control chemoattractant recombinant mouse C5a (rmC5a), but no BMDM migration was observed to any of the concentrations of human milk-derived lactoferrin.

To validate these results with human cells, the human monocyte-like cell line THP-1 was employed. THP-1 cells were placed on top of the membranes and allowed to migrate to the chemoattractant in the lower membrane for 4 hours at 37˚C. Migration was measured by counting the THP-1 cells that had migrated to the lower well at the end of the assay using a flow cytometer. The results are shown in Figure 3.1b. Similar to BMDM, large numbers of THP-1 cells appeared to migrate towards the control chemoattractant ATP, but no migration was observed to lactoferrin. Together, these results suggest that lactoferrin is not a chemoattractant for monocytes.

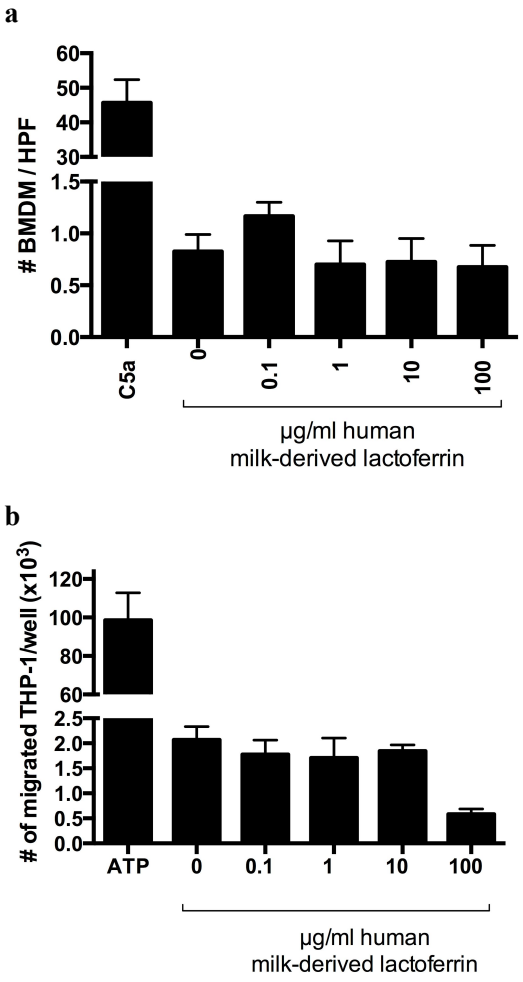

Figure 3.1 – Monocytes do not migrate to lactoferrin.
Migratory responses of monocytes to 0-100µg/ml human milk-derived lactoferrin were measured in a modified Boyden chamber assay. (a) 4-day matured BMDM were allowed to migrate to human milk-derived lactoferrin or 10ng/ml rmC5a (positive control). Data are means + SEM for the number of migrated cells per high power field (HPF) for 10 random areas (n=4). (b) THP-1 cells were allowed to migrate to human milk-derived lactoferrin or 0.9µM ATP (positive control). Data are means + SEM for the number of cells migrated to the lower chamber (n=2).

3.2.2 Lactoferrin binds to macrophages

Having shown that lactoferrin does not appear to play a role in the attraction of mononuclear phagocytes to apoptotic cells, the focus of the research was then turned to the second aim of determining whether lactoferrin is involved in regulating macrophage activation in starry-sky non-Hodgkin lymphomas. First, the ability of lactoferrin to bind to monocytes and macrophages was tested. Lactoferrin was added to the human monocyte-like cell line MonoMac6 (MM6) and incubated for 1 hour at

4˚C. Bound lactoferrin was detected on a flow cytometer following consecutive staining with a sheep anti-lactoferrin antibody and an AlexaFluor® 488 conjugated anti-sheep secondary antibody and compared to BMDM that had not been incubated with lactoferrin. Figure 3.2a shows the flow cytometry plot. A small shift in fluorescence detection was observed when MM6 cells were incubated with lactoferrin suggesting that lactoferrin was binding to the cells. Binding of lactoferrin using this method was also repeated with primary BMDM, as shown in Figure 3.2b. The shift in fluorescence detection for BMDM incubated with lactoferrin compared to those incubated without this glycoprotein was even stronger, confirming that lactoferrin could indeed bind to macrophages.

To improve the process of detection, for further studies investigating lactoferrin binding to macrophages, Alexa Fluor® 488-conjugated human milk-derived lactoferrin and human recombinant lactoferrin were used. Binding of lactoferrin to human monocyte-derived macrophages (HMDM) was confirmed in this way (Figure 3.2c).

Binding of lactoferrin to MM6 cells was repeated with Alexa Fluor® 488-conjugated recombinant human lactoferrin too and this confirmed lactoferrin interaction with BMDM as shown in Figure 3.2d. When more lactoferrin was incubated with MM6 cells for 3 hours at room temperature, more lactoferrin was observed to bind to the MM6 cells. Binding saturation was not achieved at 1 mg/ml.

Having validated that lactoferrin could bind to and interact with monocytes and macrophages, an attempt was then made to elucidate how lactoferrin was binding to these cells. The N-terminal end of lactoferrin is highly positively charged (Bellamy *et al.*, 1992) and has a high binding capacity for proteins and membranes (Baker and Baker, 2005). This makes it very difficult to identify lactoferrin receptors. Nonetheless, lactoferrin receptors have been proposed on monocytes and macrophages. Lactoferrin, known to chelate LPS, has been shown to bind soluble CD14 with high affinity, as well as bind the CD14-LPS complex (Baveye *et al.*, 2000). These findings suggest that CD14, a 55-kDa glycoprotein expressed by

macrophages, may be a receptor for lactoferrin. Furthermore, low-density lipoprotein receptor-related protein 1 (LRP-1) has been reported as a receptor for lactoferrin on osteoblast cells and lactoferrin was found to promote cell proliferation and survival (Grey, 2004). Interestingly for this study, LRP-1 is a receptor involved in the recognition of apoptotic cells and found to be highly up-regulated in starry-sky TAM (Table 1.2) (Ford *et al.*, 2015).

Because of its potential biological significance, the first candidate receptor for binding lactoferrin that was assessed was LRP1. LRP1 expression on > 90% of human primary macrophages was confirmed by detection with an anti-human LRP1 antibody (Figure 3.3). Further investigations to find out if human lactoferrin binding to macrophages could be blocked by the presence of excessive anti-LRP1 antibody were attempted, but no signs of blocking were observed and the antibody that was used to measure LRP1 expression was not known to block competitive binding. Unfortunately, anti-LRP1 antibodies that had been used in other blocking studies (Ogden *et al.*, 2001; Vandivier *et al.*, 2002) could not be obtained.

The next lactoferrin receptor candidate having high potential for being involved in lactoferrin binding to monocytes and macrophage that was tested was CD14. For previous studies in the laboratory, the myelogenous leukaemia cell line K562 had been transfected with CD14 and these cells were employed to test whether lactoferrin could bind to the CD14 on these cells (Tennant *et al.*, 2013).

First the CD14-transfected and parental K562 cells were tested for their expression of CD14. The results are shown in Figure 3.4a and confirm that CD14-transfected K562 cells indeed expressed CD14 receptor whereas the parental cells did not. Both cells were then incubated with 0, 50, or 200µg/ml human lactoferrin for 1 hour at 4˚C, and lactoferrin binding was detected using the sheep anti-human lactoferrin polyclonal antibody and secondary antibody staining. Detection of lactoferrin binding to both the parental and CD14-transfected K562 cells was low and no difference in binding was observed between the wild type (WT) and the CD14-tranfected K562 cells as shown in Figure 3.4b. These results suggest that the CD14

receptor is most likely not involved in lactoferrin binding to monocytes and macrophages.

Another receptor highly expressed by starry-sky TAM is macrophage scavenger receptor 1 (MSR1) and this receptor was also tested for its ability to bind lactoferrin. BMDM were incubated simultaneously with 20µg/ml human milk-derived lactoferrin and increasing concentrations of an anti-MSR1 antibody known to inhibit the uptake of acetylated low-density lipoproteins and divalent cation-independent adhesion (Fraser *et al.*, 1993). Lactoferrin binding was then detected by consecutive staining with a sheep anti-human lactoferrin polyclonal antibody and secondary antibody, both of which did not detect the anti-MSR1 antibody (not shown). If lactoferrin was indeed binding to the MSR1 receptor on macrophages, high concentrations of the anti-MSR1 antibody were expected to compete with lactoferrin for binding to MSR1 and reduce lactoferrin detection. 92% of the BMDM were found to express MSR1, but incubation with increasing amounts of anti-MSR1 antibody did not inhibit lactoferrin binding to the BMDM (Figure 3.5). These results suggest that MSR1 is most likely not the receptor that binds lactoferrin. However, the possibility remains that the anti-MSR1 antibody used does not inhibit binding of lactoferrin MSR1 receptor.

As it proved difficult to identify a receptor for lactoferrin on monocytes and macrophages the focus of the research was then shifted to identify if lactoferrin interaction with monocytes and macrophages affects macrophage function and phenotype.

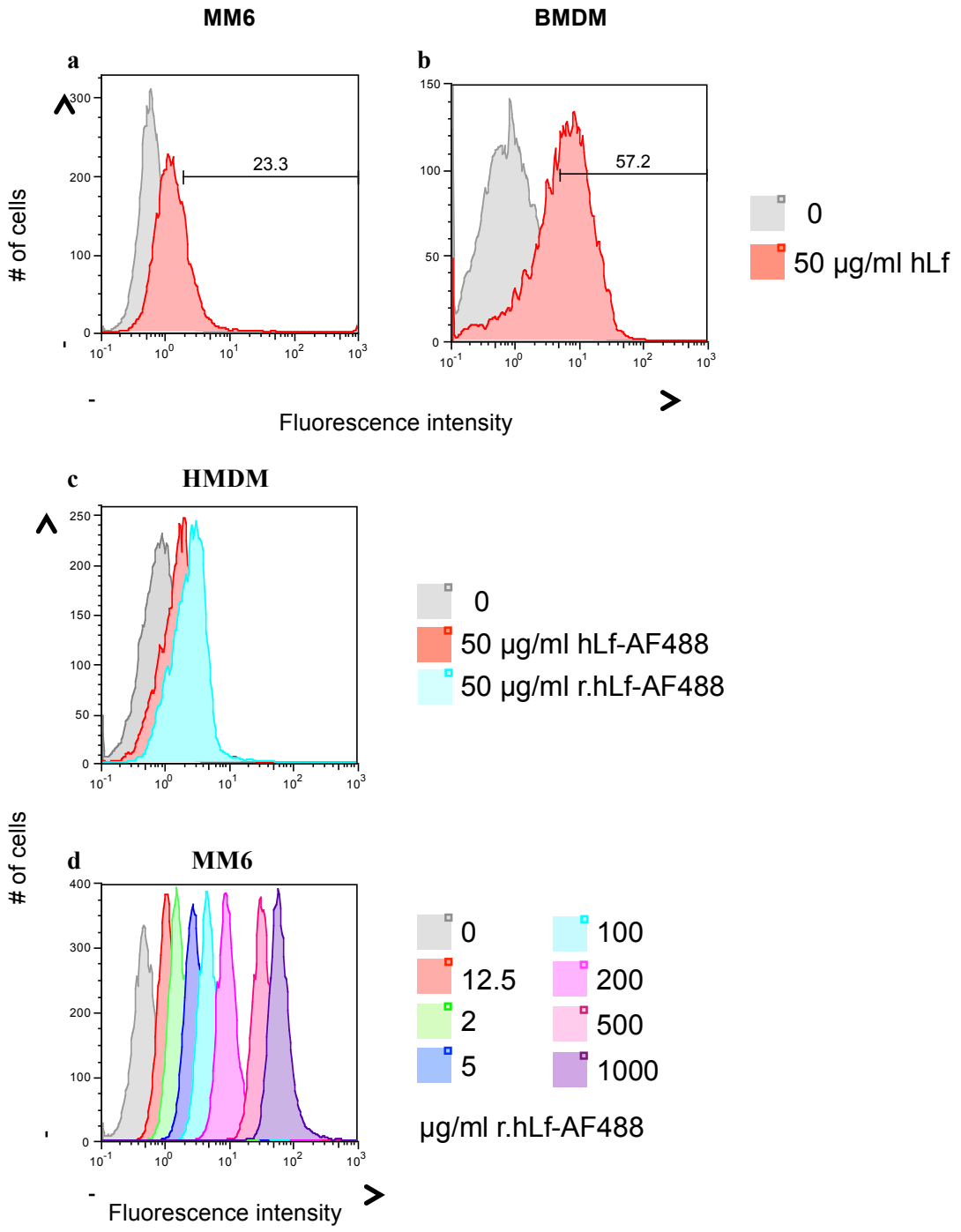

Figure 3.2 – Lactoferrin binds to monocytes and macrophages.
MM6 (a) or BMDM (b) cells were incubated at 4˚C for 1h with or without 50µg/ml human milk-derived lactoferrin (hLf). Binding of lactoferrin was detected by successive staining with a sheep anti-human lactoferrin polyclonal antibody and anti-sheep Ig Alexa Fluor® 488 antibody. Gates indicate percentage of total viable cells that are stained positive. (c) HMDM were incubated with 200µg/ml human milk-derived lactoferrin or recombinant human lactoferrin conjugated to Alexa Fluor® 488 (hLf-AF488 and r.hLf-AF488, respectively) for 1 hour at 4˚C. (d) MM6 cells were incubated with 1-100µg/ml r.hLf-AF488 for 3h at room temperature. a-d show green fluorescence detection in the viable cell gate. Results depicted are representative of 3 (a-c) or 1 (d) independent experiments.

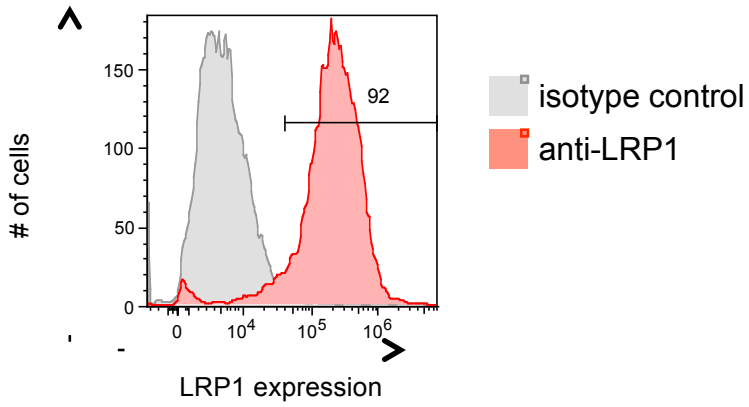

Figure 3.3 – LRP1 is expressed by HMDM.
Expression of LRP1 on HMDM was detected by successive staining with an anti-LRP1 antibody or isotype control and goat anti-mouse IgG Alexa Fluor 488 antibody. Green fluorescence detection is shown for the viable cell gate. Gates indicate percentage of total viable cells that are stained positive. Result presented is representative of three independent experiments.

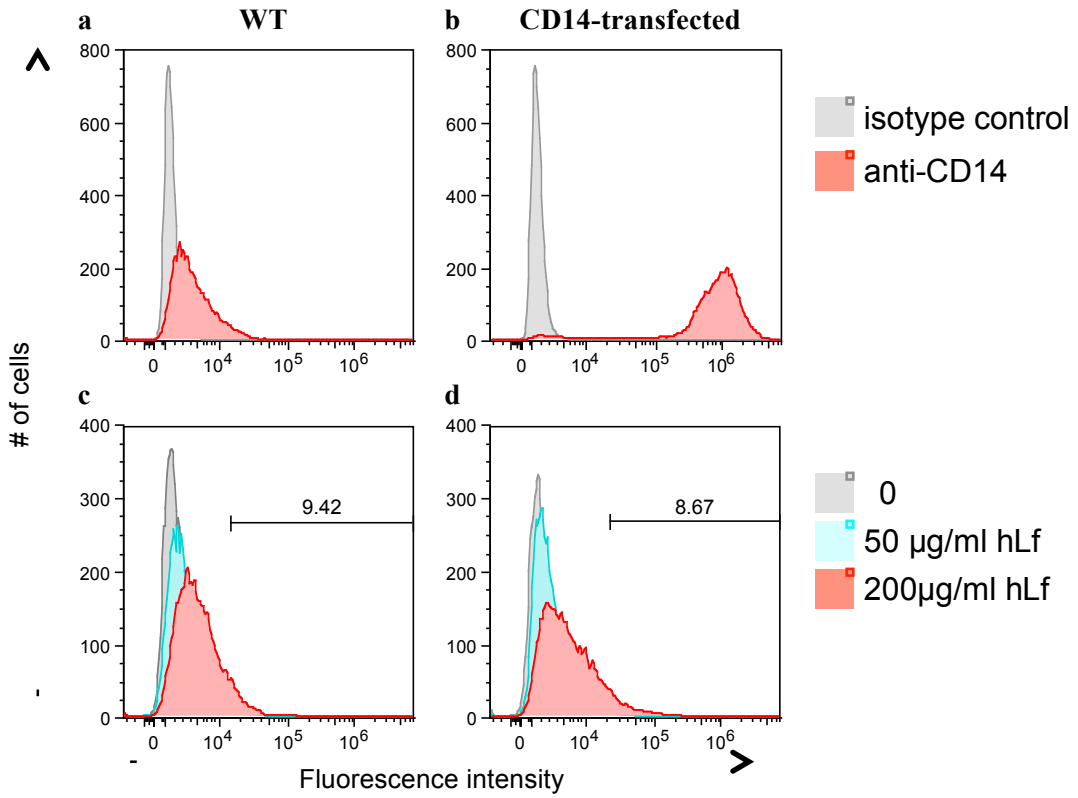

Figure 3.4 – Lactoferrin does not bind to CD14 receptor.
CD14 expression on parental (a) and CD14-transfected (b) K562 cells was detected using an anti-human CD14 antibody. Binding of lactoferrin to parental (c) and CD14-transfected (d) K562 cells was detected by successive staining with a sheep anti-lactoferrin polyclonal antibody and anti-sheep IgG Alexa Fluor® 488 antibody after the cells had been incubated with 50 or 200µg/ml human milk-derived lactoferrin for 1 hour at 4˚C. (a-d) show green fluorescence detection in the viable scatter gate. Gates indicate percentage of total viable cells that are stained positive by comparison with unstained cells. Results depicted are representative of two independent experiments.

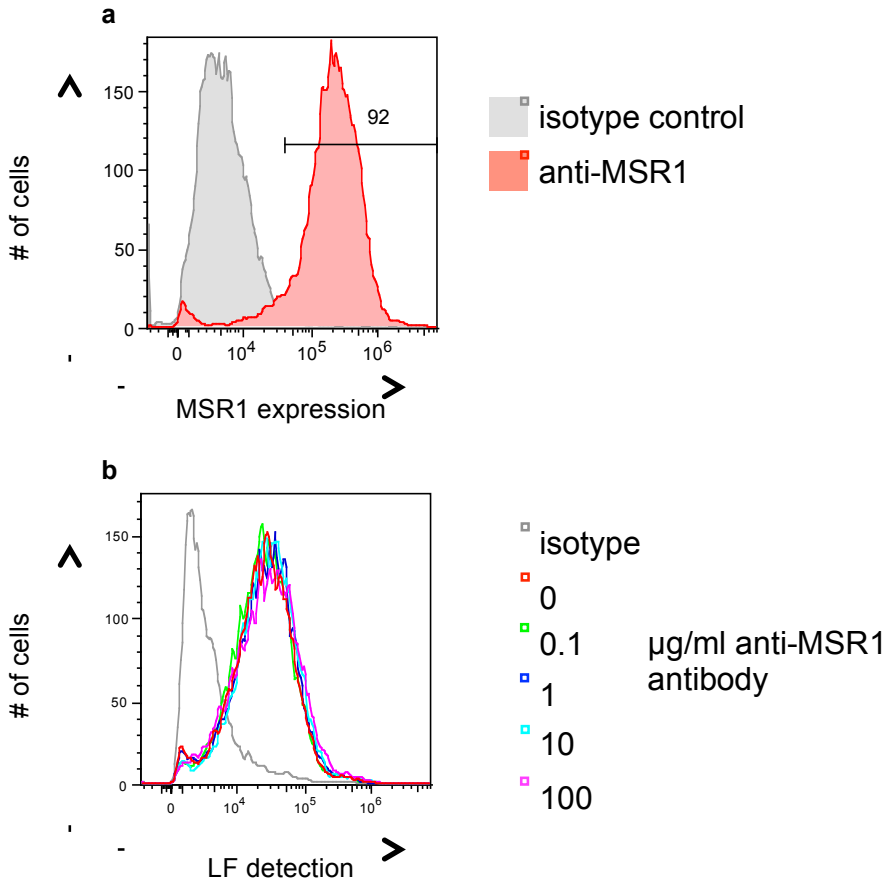

Figure 3.5 – anti-MSR1 antibody does not block lactoferrin binding to monocytes and macrophages.
(a) Expression of MSR1 on CD1 BMDM was detected using a rat anti-mouse MSR1 antibody and anti-rat Ig Alexa Fluor® 488 secondary antibody. Gates indicate percentage of total viable cells that are stained positive. Result shown is representative of three independent experiments. (b) The ability of anti-MSR1 antibody to block lactoferrin binding to macrophages was tested by incubating the cells simultaneously with a constant amount of human milk-derived lactoferrin (20µg/ml) and increasing concentrations of anti-MSR1 antibody. Binding of lactoferrin was detected by successive staining with a sheep anti-lactoferrin polyclonal antibody and anti-sheep Ig Alexa Fluor® 488 antibody. Results are shown from one experiment.

3.2.3 Lactoferrin does not enhance apoptotic cell-macrophage interaction

Previous studies have suggested that chemoattractants released by apoptotic cells can enhance binding and phagocytosis of apoptotic cells by macrophages. Fractalkine, a chemokine and intercellular adhesion molecule, has been found to cause the expression of milk fat globule epidermal growth factor (MFG-E8) on macrophages, which leads to enhanced apoptotic cell clearance (Miksa *et al.*, 2007). Furthermore,

ATP released by apoptotic cells increases binding of apoptotic cells to macrophages (Marques-Da-Silva *et al.*, 2011). Additionally, lactoferrin has been found to increase the phagocytosis of parasites (Lima and Kierszenbaum, 1985). It was therefore investigated if lactoferrin could also act as an opsonin and increase the interaction with and phagocytosis of apoptotic cells by macrophages.

Mature BMDMs were harvested from Petri dishes and cultured on glass slides for two hours, before a one-hour co-culture with apoptotic lymphoma cells and 0 - 50µg/ml of human milk-derived lactoferrin. Apoptosis had been induced by UVB-irradiation followed by a 20-hour incubation at 37˚C before cells were added to the macrophages. To measure interaction, unbound cells were washed off and macrophages were fixed and stained. The percentage of macrophages interacting with apoptotic cells was counted for 10 independent high power fields on duplicate wells. Results are presented in Figure 3.6 and indicate a possible trend of decreased, rather than increased, interaction between macrophages and apoptotic cells when increasing concentrations of lactoferrin were present during the assay, although this was not statistically significant. Additionally, the interaction index was calculated as the product of the percentage of macrophages interacting with apoptotic cells and the average number of apoptotic cells interacting per macrophage. A similar pattern was observed as for the percentage of macrophages interacting with apoptotic cells, and for macrophages and apoptotic cells interacting in the presence of 10µg/ml lactoferrin, the interaction index was significantly different from the control.

Similar observations were made by another member of this laboratory for phagocytosis assays performed in the presence of lactoferrin, but these were also not statistically significant (Benjamin Arnold, personal communication). These findings leave the possibility that lactoferrin may bind to (and block) a receptor that is involved in apoptotic cell recognition. However, as the pathways by which macrophages recognize apoptotic cells are redundant, presumably because of its high importance in development and homeostasis, this does not lead to significant changes in macrophage-apoptotic cell interaction and uptake.

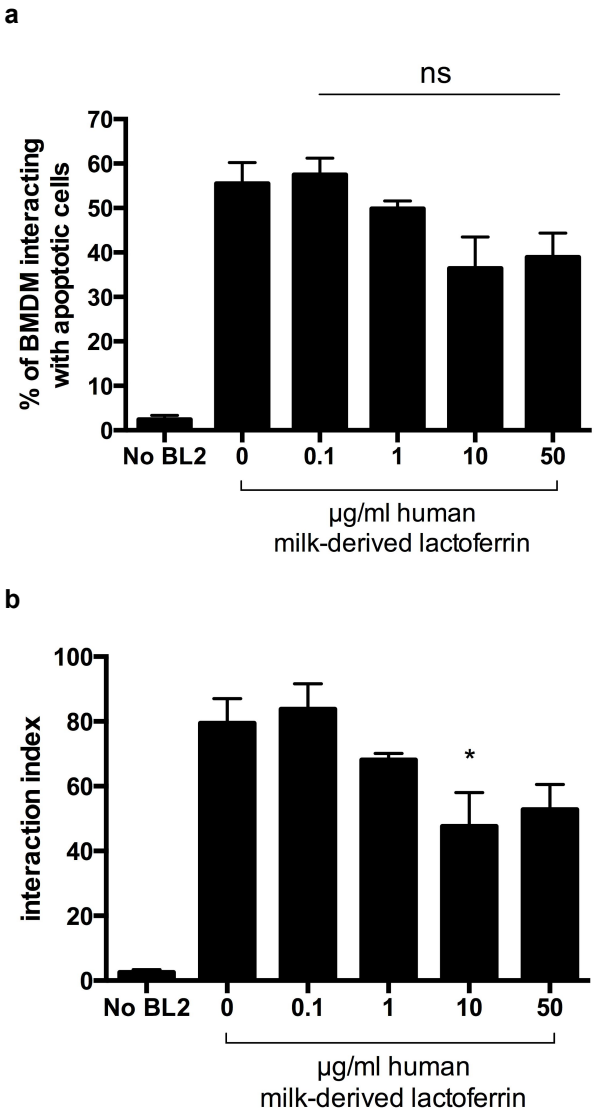

Figure 3.6 – Lactoferrin does not enhance BMDM-apoptotic cell interaction.
BMDM were assessed for their ability to interact with apoptotic Burkitt lymphoma (BL2) cells in the presence or absence of human milk-derived lactoferrin in a microscopy-based phagocytosis assay. BMDM incubated in the absence of apoptotic Burkitt lymphoma cells (no BL2) are also shown. (a) Data are means + SEM for the percentage of BMDM demonstrating interaction with apoptotic BL2 cells (n=4). (b) Data are means + SEM for the interaction index, calculated as: (number of macrophages interacting with apoptotic cells/total number of macrophages) x (average number of apoptotic cells interacting per macrophage) x 100 (n=4). Statistical analysis was performed using one-way ANOVA with Dunnett's multiple comparison test. * $p<0.05$.

3.2.4 Lactoferrin in culture medium does not affect BMDM maturation

Further investigations would focus on the effect lactoferrin may have on macrophage phenotype and mature BMDM were planned to be used for these studies. However, the medium in which BMDM are cultivated includes foetal bovine serum (FBS),

which contains bovine lactoferrin. Because bovine lactoferrin is highly similar to human lactoferrin (Baker and Baker, 2009; García-Montoya *et al.*, 2012) and may affect the phenotype of BMDM, a bovine lactoferrin-free BMDM cultivation medium was preferred.

First, BMDM cultivation in serum-free media was tested. The femurs of mice were flushed and the resuspended cells incubated in either serum-free X-VIVO™ 10 medium or RPMI 1640 medium with 10% FBS, both supplemented with 100ng/ml recombinant human CSF1 (rhCSF1) for 7 days. More medium was added on day 4. After 7 days of maturation, the morphology and phenotype of the BMDM cultivated in either medium was compared. As can be seen in Figure 3.7a, no differences in morphology were observed. However, different scatter properties were observed when analysed by flow cytometry (Figure 3.7b). In addition the expression of F4/80, CD11b, and mannose receptor (CD206), macrophage markers and receptors was measured by flow cytometry (Figure 3.7c-f). Expression of CD11c, a marker for dendritic cells, was measured as a control. Although the BMDM matured in serum-free medium expressed the same macrophage markers as the control BMDM, the expression levels appeared lower. CD11c was not expressed by either of the BMDM cultures.

Because the culture of BMDM in serum-free medium gave morphologically and phenotypically different BMDM cultures, an approach by which lactoferrin would be removed from the standard medium was preferred. A method was designed that is depicted in Figure 3.8 and is explained in detail in Materials and Methods. In short, anti-bovine lactoferrin antibody was covalently bound to magnetic nanomag®-D particles (250nm diameter) using carbodiimide chemistry. The particle-antibody complex was then incubated with 50% FBS/50% RPMI 1640 for 1 hour at room temperature to allow binding of bovine lactoferrin. The formed bovine lactoferrin-antibody-nanoparticle complexes could then be separated from the media by applying a magnet that drew all the nanoparticles to one side of the tube, allowing the bovine lactoferrin-free medium to be carefully removed. The success of the

removal of bovine lactoferrin from the media was measured using a sandwich ELISA and is summarised in Table 3.1.

Before removal of bovine lactoferrin, FBS contained on average 50ng/ml lactoferrin, which, as FBS makes up 10% of BMDM culture medium, would lead to concentrations of approximately 5ng/ml in the culture medium. After separation, lactoferrin concentrations in 50% FBS/ 50% serum-free RPMI were below the detection levels of 8ng/ml, or effectively bringing the concentration of lactoferrin in FBS down to below 15.8ng/ml, which brings the final concentration of lactoferrin in the culture medium down to below 1.6ng/ml.

It was then tested whether the removal of bovine lactoferrin from BMDM cultivation medium affected the expression of macrophages markers by BMDM (Figure 3.9). BMDM were matured with either standard medium, or with culture medium from which lactoferrin had been depleted to below 1.6 ng/ml. Following a 7-day maturation, F4/80 and CD11b were found to be expressed highly by both the BMDM matured in standard and in lactoferrin-reduced medium, and no differences were found. Mannose receptor and MSR1, both highly expressed in many macrophages including starry-sky TAM, showed similar high expression by BMDM matured in either culture medium. CD11c was not expressed by either of the BMDM cultures.

Because no differences in the expression of a variety of macrophage markers and receptors could be found between BMDM that were cultivated in low-bovine lactoferrin or standard BMDM cultivation medium, it was assumed that the low quantities of bovine lactoferrin present in the standard BMDM culture medium did not affect BMDM phenotype. Therefore, the laborious process of reducing the bovine lactoferrin concentration in FBS was omitted for the following experiments and BMDM were cultivated under standard culture conditions.

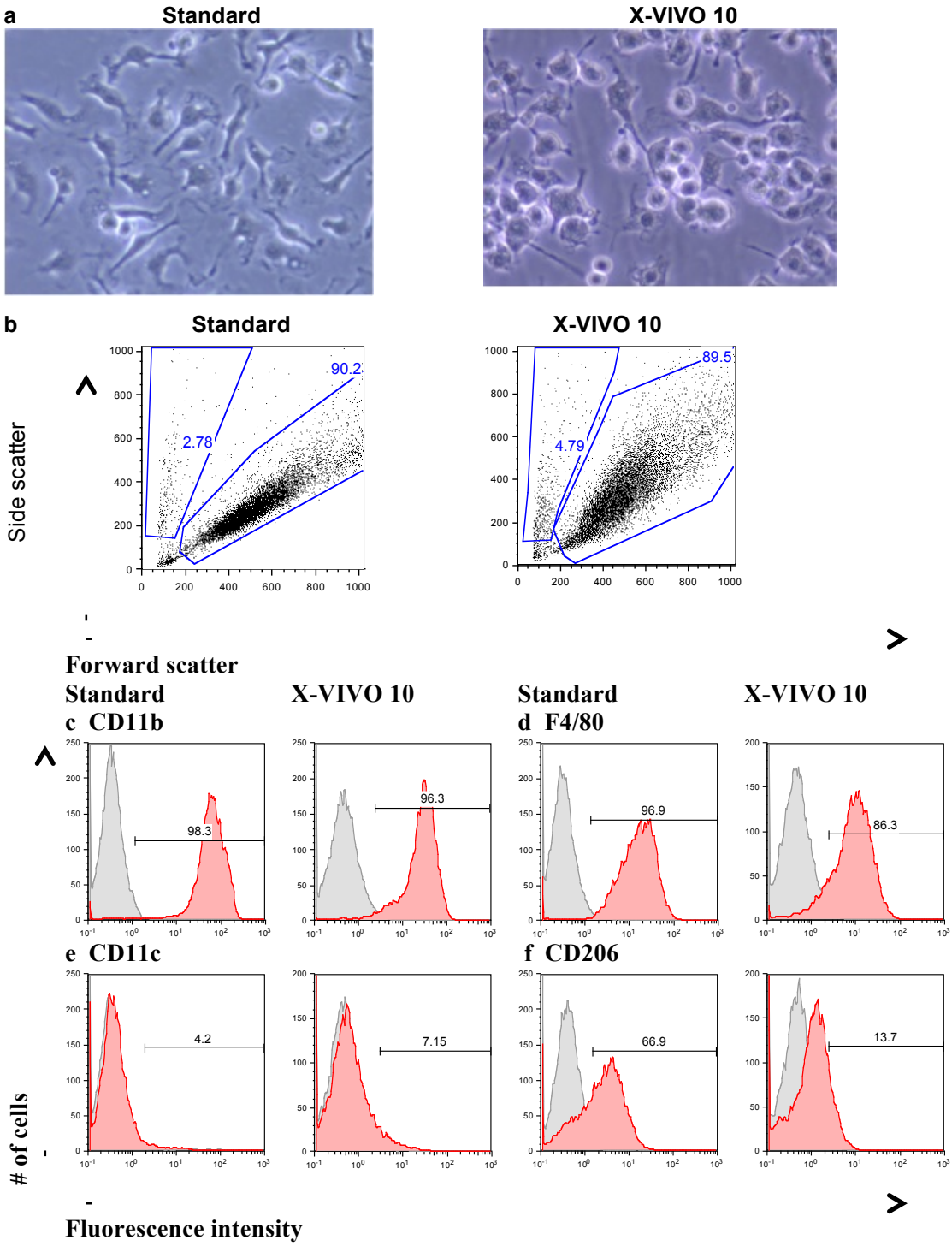

Figure 3.7 – Morphology and phenotype of BMDM cultured in serum-containing and serum-free media.

(a) Images of d7 BMDM from CD-1 mice were cultured in serum-containing BL-medium and serum-free X-VIVO 10 medium. Images were taken using an inverted microscope at 400x magnification. (b) Forward and side scatter plots of d7 BMDM cultivated in serum-containing BL-medium and serum-free X-VIVO 10 medium. Expression of (c) CD11b, (d) F4/80, (e) CD11c (e), and (f) CD206 (red) or isotype controls (grey) was detected on BMDM using Alexa-Fluor 488-tagged antibodies, or FITC-tagged antibody (CD11c). Green fluorescence detection in the viable gate is shown. Gates indicate percentage of total viable cells showing positive staining.

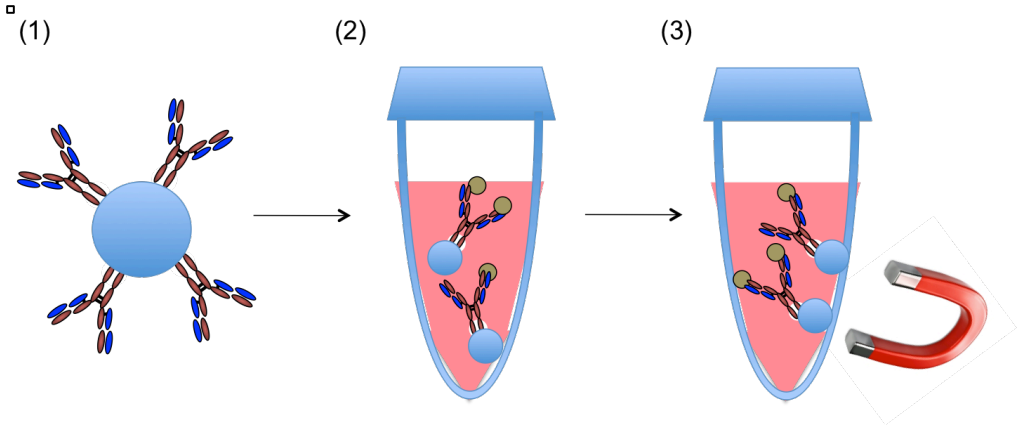

Figure 3.8 – Schematic drawing of protocol to remove bovine lactoferrin from FBS.
(1) Anti-bovine lactoferrin is covalently bound to magnetic nanomag®-D particles. (2) The particle-antibody complex is incubated with 50% FBS/50% RPMI 1640 for one hour at room temperature to allow binding of bovine lactoferrin. (3) The antibody-magnetic particle complexes with or without bovine lactoferrin bound are separated from the media by applying a magnet that draws the magnetic particles to one side of the tube, allowing the bovine lactoferrin-free medium to be carefully removed. Images are not to scale.

Medium	Bovine lactoferrin conc. (ng/ml)
FBS	~ 50
50% FBS/ 50% RPMI after lactoferrin removal	< 8
BMDM culture medium	~ 5
BMDM culture medium after lactoferrin removal	< ~1.6

Table 3.1 – Bovine concentration in FBS and BMDM culture medium before and after bovine lactoferrin removal.

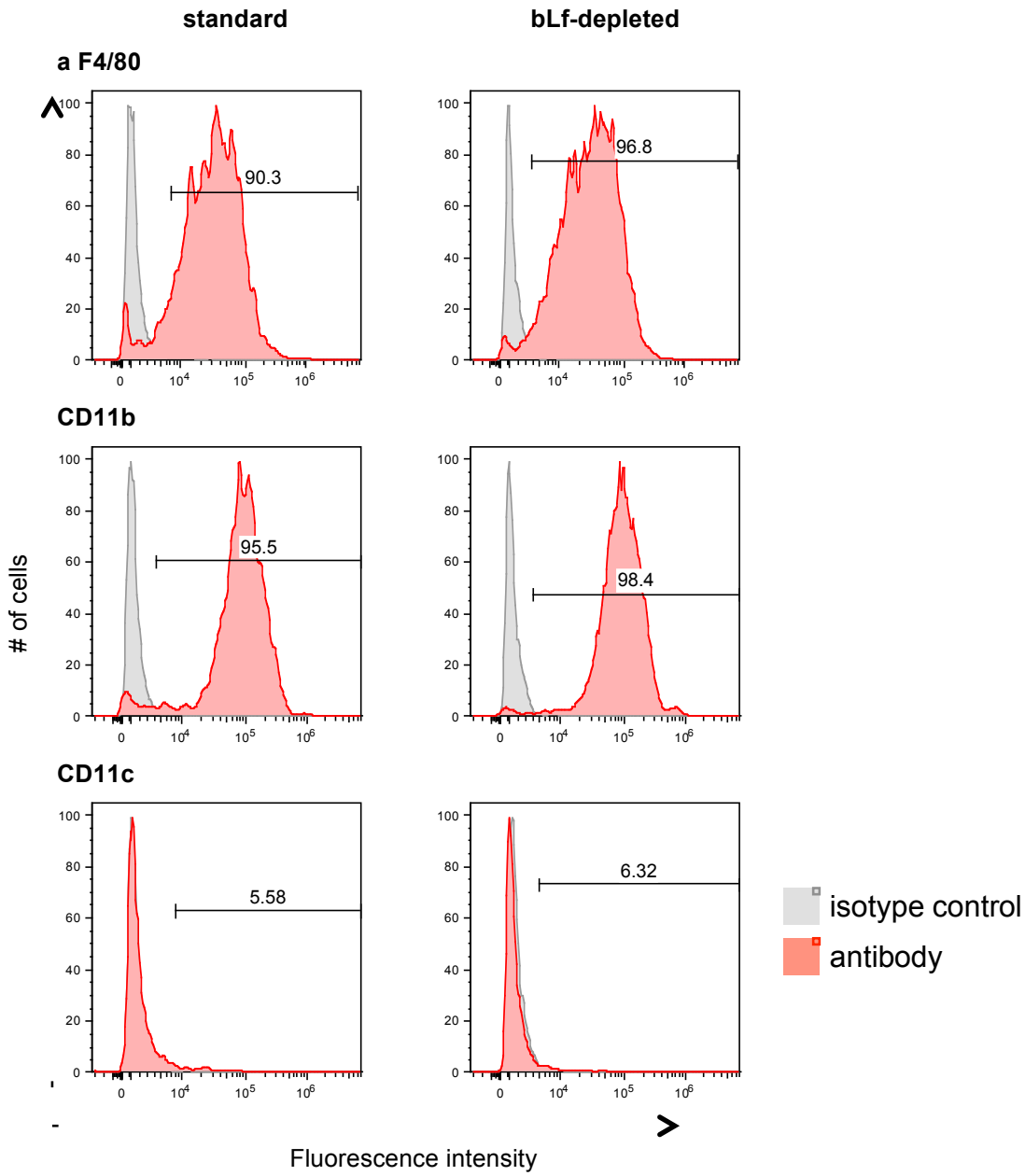
standard
bLf-depleted
a F4/80
90.3
96.8
CD11b
95.5
98.4
CD11c
5.58
6.32
# of cells
Fluorescence intensity
isotype control
antibody

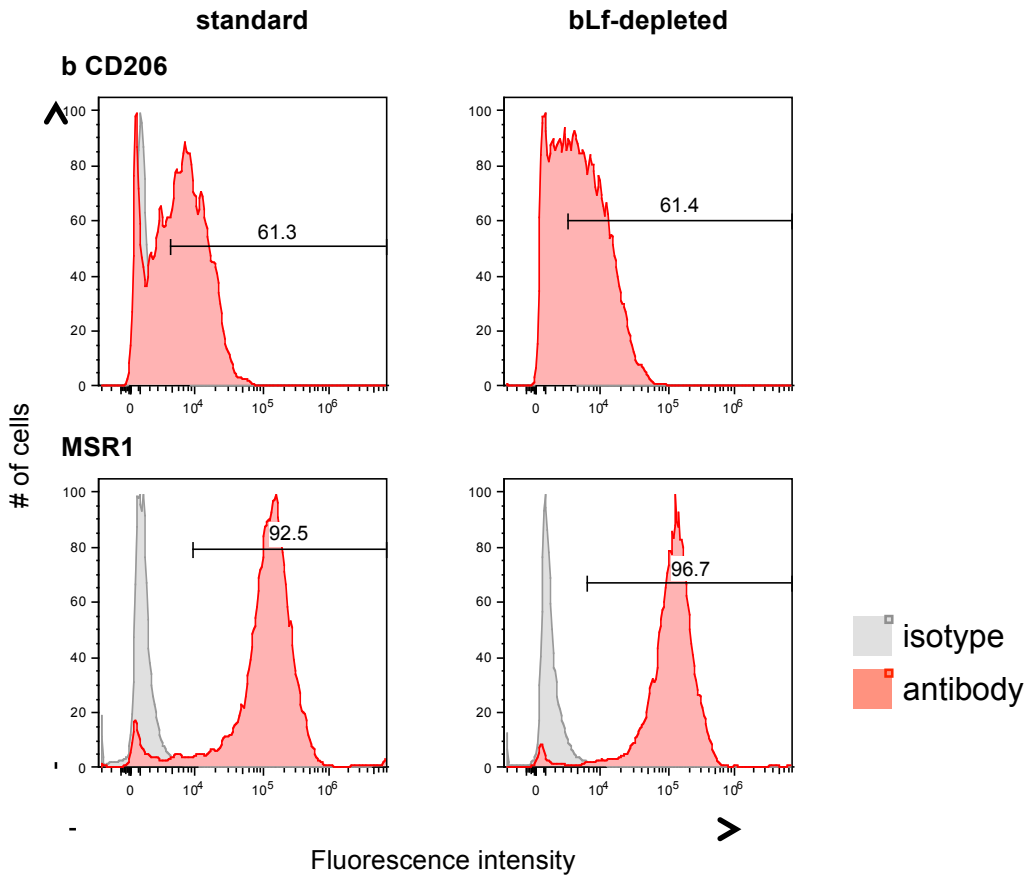

Figure 3.9 – Bovine lactoferrin reduction in culture medium does not affect the maturation of BMDM.
(a) Expression of F4/80, CD11b, CD11c, and (b) CD206, and MSR1 by d7 BMDM that were matured in standard or lactoferrin-depleted cell culture medium, detected using Alexa Fluor 488-labelled antibodies or FITC-labelled antibodies (CD11c and MSR1). Green fluorescence detection in the viable gate is shown. Gates indicate percentage of viable cells that are stained positive. Results are representative of two independent experiments.

3.2.5 High concentrations of lactoferrin affect macrophage activation status

Having established that the low concentration of bovine lactoferrin present in BMDM cultivation medium does not affect BMDM phenotype, it could then be tested whether lactoferrin released from apoptotic cells may affect the gene expression and phenotype of starry-sky TAM.

As described in Section 1.5, starry-sky TAM were found to have increased expression of genes that are involved in reparatory and growth functions, as well as genes that are associated with apoptotic cell recognition and engulfment. In order to

investigate the effect of lactoferrin on the expression of these genes by macrophages, mature BMDM were incubated with 1-100µg/ml human milk-derived lactoferrin for 16 hours and the expression of these genes was compared to control BMDM. Only 2-fold increases or decreases were considered meaningful. The results are shown in Figure 3.10.

Culture with 1 or 10µg/ml human milk-derived lactoferrin was not found to affect the gene expression of any of the genes tested. Most of the genes tested were also unaffected by an even higher concentration of lactoferrin, 100µg/ml, but a few genes were found to be significantly up- or down-regulated. Of the reparatory and pro-tumour growth genes, Mrc1 (mannose receptor) was down-regulated upon culture with 100µg/ml human milk-derived lactoferrin. Mmp2, previously shown to be up-regulated in macrophage cell lines upon co-culture with apoptotic cells (Ford *et al.*, 2015), appears to be up-regulated by incubation with larger amounts of lactoferrin (10 – 100 µg/ml), but this was not found to be statistically significant within the number of repeats. Furthermore, Igf1 was found to be significantly down-regulated, although the effective down-regulation was less than 2-fold. Additionally, two genes associated with apoptotic-cell responses were found to be differentially expressed upon culture with 100µg/ml lactoferrin. The gene expression of Axl was significantly increased, whereas the expression of Gas6 was found to be significantly decreased.

High concentrations of lactoferrin have been reported in colostrum and mature milk, 1-2 and ~7mg/ml, respectively (Levay and Viljoen, 1995; Steijns and van Hooijdonk, 2000), and lactoferrin concentrations are expected to be high at inflammatory sites, most likely through release from the secondary granules of neutrophils. Although it is difficult to measure lactoferrin concentrations at inflammatory sites, faecal lactoferrin has been shown to be a sensitive and specific marker for detecting inflammation in chronic inflammatory bowel disease. Patients with Crohn's Disease had average lactoferrin concentrations of 440µg/g faecal weight, and patients with ulcerative colitis had average lactoferrin concentration of 1125 µg/g faecal weight, compared to concentration of 1.45µg lactoferrin/g faecal weight for healthy controls

(Kane *et al.*, 2003). However, high concentrations have not been reported in the tumour microenvironment. Given our results indicating that a concentration of lactoferrin of 100µg/ml was required to affect the expression of tested starry-sky TAM genes, the low concentration of lactoferrin released from apoptotic cells in Burkitt's lymphoma tumours (Bournazou *et al.*, 2009) is unlikely to be responsible for the TAM phenotype of macrophages in those tumours. As lactoferrin has repeatedly been reported to have anti-inflammatory effects on macrophages, this was investigated next.

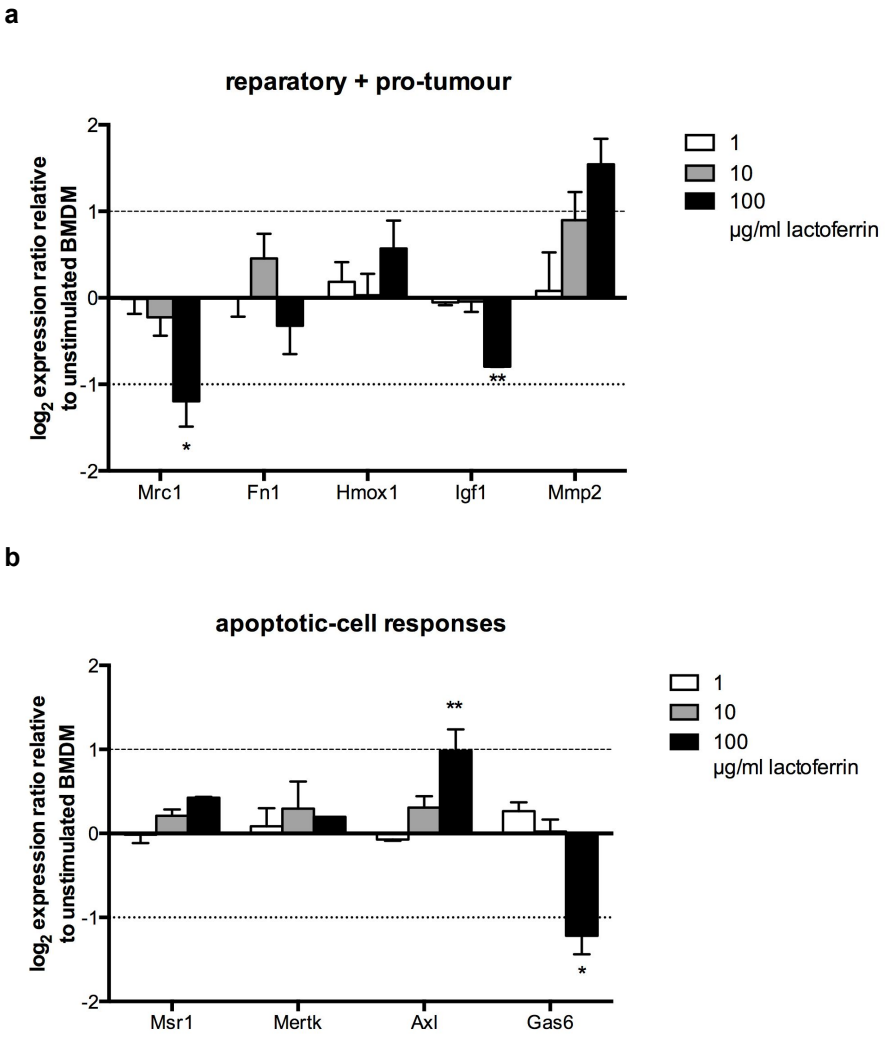

Figure 3.10 - BMDM responses to lactoferrin
BMDM were cultured for 24 hours with 0-100 µg/ml human milk-derived lactoferrin. mRNA expression of selected genes was assessed and normalized using the reference gene Tuba1b. Expression is presented as log[2] ratio relative to unstimulated BMDM. Data are means ± SEM for 3 independent experiments (or 2 experiments for 100µg/ml lactoferrin). The lines at y=1 and y=-1 indicate a 2-fold increase or decrease of expression, respectively. Statistical analysis was performed on the raw data using one-way ANOVA with Dunnett's multiple comparisons test. * $p<0.05$, ** $p<0.01$.

3.2.6 High concentrations of Lf reduce macrophage cytotoxicity

Research in our laboratory has shown that lactoferrin can exert anti-inflammatory effects by inhibiting the migration of neutrophils and eosinophils (Bournazou *et al.*, 2009; 2010). Additionally, human lactoferrin has been shown to enhance the production of anti-inflammatory cytokines by macrophages, including IL-10, IL-4, and TGF-β (Togawa *et al.*, 2002; Zimecki *et al.*, 2005). Furthermore, human lactoferrin was found to suppress the pro-inflammatory response of macrophages to

LPS by reducing the mRNA and cytokine expression of TNFα, IL-1β, IL-6, and IL-8 (Håversen *et al.*, 2002). Classically-activated macrophages have previously been shown to be capable of killing cells and this effect could be reduced by co-culture with apoptotic cells (Reiter *et al.*, 1999). Here it was investigated whether lactoferrin released from apoptotic cells may also reduce macrophage cytotoxicity and thereby protect tumour cells from being killed by activated macrophages.

A cytotoxicity assay was designed as explained in Figure 3.11. In short, BMDM were matured for 7 days and then labelled with the fluorescent green membrane marker PKH67 and stimulated with IFN-γ and LPS for 24 hours. After the 24 hours incubation, the BMDM were washed to remove IFN-γ and LPS, and the cells were incubated with 0-100μg/ml human milk-derived lactoferrin for 24hrs. After the combined 48 hours of total pre-treatments, lactoferrin was washed away, and target BL2 lymphoma cells, labelled with the CellTrace Violet fluorescent proliferation marker, were then added to the macrophages and co-cultured for 48 hours. After 48 hours, all cells were removed from the plates by repeated pipetting and viable target cell numbers were counted by flow cytometry.

As can be seen in Figure 3.12, co-culture of target cells with untreated BMDM did not affect viable target cell numbers compared to the target cells that had been cultured alone. In contrast, when target cells were co-cultured with IFN-γ and LPS-stimulated BMDM, significantly fewer viable target cells remained. This suggests that macrophages were cytotoxic to the target cells. Additionally, increased phagocytosis was observed (Figure 3.12b) and it is likely that cytotoxicity and phagocytic clearance might be happening in parallel. Treatment of BMDM with 1-100μg/ml human milk-derived lactoferrin following IFN-γ and LPS stimulation, did not appear to affect viable target cell numbers when they were co-cultured.

As lactoferrin treatment following IFN-γ and LPS-stimulation did not appear to affect macrophage cytotoxicity to BL cells, it was then tested whether lactoferrin treatment of BMDM prior to IFN-γ and LPS-stimulation could affect the killing effect classically-activated BMDM have on target lymphoma cells. BMDM were

first incubated with 0-100μg/ml human milk-derived lactoferrin, which was washed away after 24 hours, when BMDM were stimulated with IFN-γ and LPS for 24 hours. Macrophage cytotoxicity was then measured as before. Pre-treatment with 1-10μg/ml human milk-derived lactoferrin did not appear to affect the ability of the BMDM to kill lymphoma target cells (Figure 3.13). However, pre-treatment of BMDM with the highest tested concentration of lactoferrin, 100μg/ml, was found to have significantly increased numbers of viable lymphoma target cells, suggesting it was able to suppress the ability of BMDM to kill target lymphoma cells.

As a concentration of 100μg/ml lactoferrin is unlikely to be physiologically relevant in the tumour microenvironment, it was decided to take a step back and investigate if there may be other components released from apoptotic cells that could prevent macrophage cytotoxicity. PKH67-labelled BMDM were incubated with either 10x apoptotic lymphoma cells or supernatants derived from these apoptotic cells, known to contain lactoferrin but also other signalling factors released from apoptotic cells. Apoptosis was induced by exposure of the cells to 100mJ UVB irradiation, followed by a 3-hour incubation, which induced apoptosis in the majority of cells. After this 3-hour incubation, cells and supernatants were separated by centrifugation and individually co-cultured with BMDM for 24 hours. Lymphoma cells were then washed away and BMDM activated with IFN-γ and LPS for 24 hours. Macrophage cytotoxicity was tested as before by the addition of labelled target cells. The results are presented in Figure 3.14 and indicate that pre-exposure to apoptotic cells, but not supernatants derived from apoptotic cells, can increase target cell viability. Because apoptotic cells are known to bind LPS (Ellison *et al.*, 1988), it remains unclear whether this result is due to reduced macrophage cytotoxicity, or if remaining apoptotic pre-treatment cells prevent LPS from contributing to the activation of macrophages, and this will be further explored in Chapter 5.

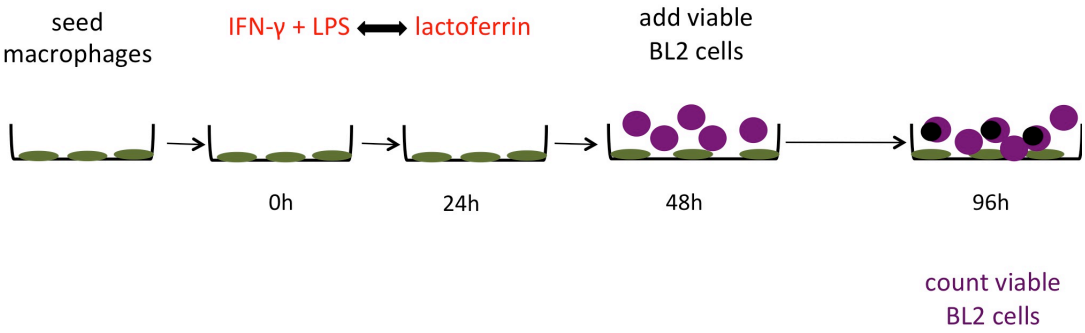

Figure 3.11 – Schematic drawing of BMDM cytotoxicity assay.
7-day matured BMDM were labelled with the green membrane marker PKH67, seeded onto 48-well plates and stimulated with IFN-γ and LPS for 24 hours. After the 24 hours incubation, IFN-γ and LPS were washed away and the BMDM were incubated with 0-100µg/ml human milk-derived lactoferrin for 24 hours. Alternatively, IFN-γ + LPS and lactoferrin treatments were added in reverse order. After the 48 hours of total pre-treatments, BMDM were washed again and co-cultured with target BL2 lymphoma cells, labelled with a CellTrace Violet proliferation marker, for 48 hours. After the 48-hour co-culture all cells were removed from the plates by repeated pipetting and viable target cell numbers ($blue^+/green^-$) were counted by flow cytometry.

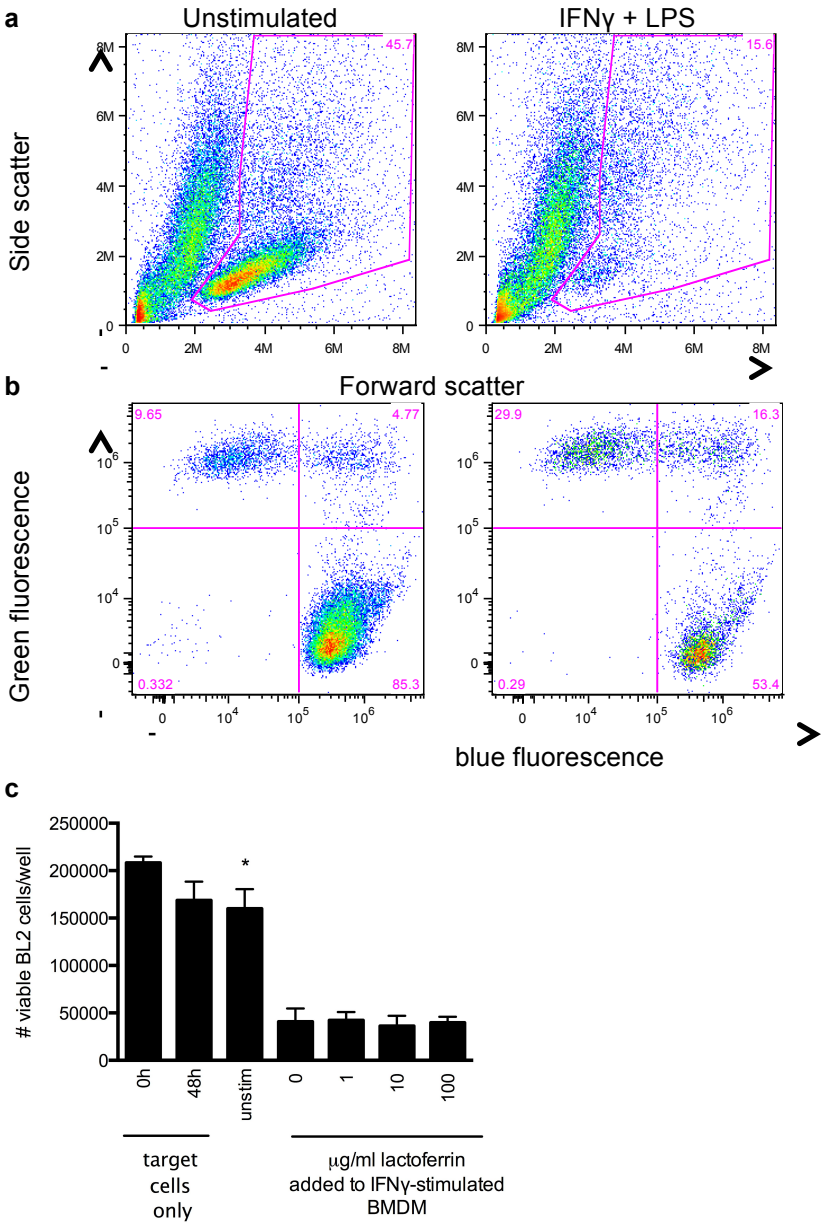

Figure 3.12 – Lactoferrin treatment does not reverse macrophage cytotoxicity.
BMDM were classically activated by IFN-γ and LPS for 24 hours before BMDM were washed and stimulated with 0-100μg/ml human milk-derived lactoferrin. Cytotoxicity of BMDM was then assessed by counting the presence of viable target BL (stained with CellTrace Violet) cells after a 48-hour co-culture. Flow cytometry forward and side scatter plots (a) and green (BMDM) / blue (target cell) fluorescence plots (b) of cytotoxicity assays are presented for unstimulated BMDM and BMDM pre-stimulated with IFN-γ and LPS followed by a 24-hour rest period. Gates in (a) indicate viable cell gate. (c) Bar-chart indicating the number of viable target BL2 cells at the beginning and end of the cytotoxicity assay for target cells cultured alone or for target cells co-cultured with unstimulated (unstim) or IFN-γ and LPS-stimulated BMDM, further treated with lactoferrin. Data are means + SEM for the number of viable gate target BL2 cells counted per well (n=3). Statistical analysis was performed using one-way ANOVA with Dunnett's multiple comparison test and is shown compared to target cells co-cultured with IFN-γ and LPS-stimulated BMDM. *$p<0.05$.

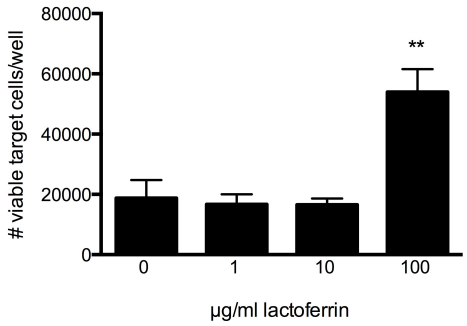

Figure 3.13 – Pre-treatment with a high concentration of lactoferrin inhibits macrophage cytotoxicity.
BMDM were stimulated with 0-100µg/ml human milk-derived lactoferrin for 24 hours before they were washed and treated with IFN-γ + LPS for 24 hours. Cytotoxicity of BMDM was then determined by counting the presence of viable target BL cells (as described in Figure 3.11) after a 48-hour co-culture. Bar-chart indicates the number of viable target BL2 cells remaining after co-culture with untreated or lactoferrin pre-treated BMDM followed by IFNγ and LPS stimulation. Data are means + SEM for the number of viable target BL2 cells counted per well (n=3). Statistical analysis was performed using one-way ANOVA with Dunnett's multiple comparison test. ** $p<0.01$

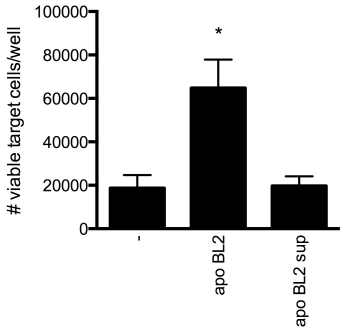

Figure 3.14 – Pre-treatment with apoptotic cells, but not supernatants from apoptotic cells, reduces macrophage cytotoxicity.
BMDM were stimulated with 10x apoptotic BL2 cells or supernatants from 10x apoptotic BL2 cells three hours after apoptosis was induced by UVB-irradiation. BMDM were then washed and classically activated by IFN-γ + LPS for 24 hours. Cytotoxicity of BMDM was then assessed by counting the presence of viable target BL cells after a 48-hour co-culture. Bar-chart indicates the number of viable target BL2 cells for target cells co-cultured with untreated or apoptotic cell/supernatant treated BMDM followed by IFN-γ and LPS stimulation. Data are means ± SEM for the number of viable gate target BL2 cells counted per well (n=3) as described in Figure 3.12. Statistical analysis was performed using one-way ANOVA with Dunnett's multiple comparison test. * $p<0.05$

3.2.7 Lactoferrin and transferrin can inhibit reduction of Akt1 expression upon neutrophil activation

The findings that the low concentrations of lactoferrin released from apoptotic cells are unlikely to contribute to the attraction and activation of TAM led us to conclude that the main role of lactoferrin released from apoptotic tumour cells is likely to be the prevention of neutrophil migration to the tumour microenvironment, thereby preventing an anti-tumour pro-inflammatory response. However, although lactoferrin was found to inhibit the migration of neutrophils to several chemoattractants (Bournazou *et al.*, 2009), the signalling pathway involved has not been established. Research published during this project suggested the involvement of AKT1, a member of the protein kinase AKT family, which has been implicated with modulating immune defence in infection and autoimmunity (Liu *et al.*, 2013). Protein kinase AKT1 (or PKBα) was found to be the dominant isoform of AKT in neutrophils and was down-regulated upon bacterial infection and neutrophil activation. AKT1 deficiency was found to worsen disease progression and lead to increased recruitment of neutrophils in two infection mouse models. Further investigations found that AKT1 negatively regulated neutrophil recruitment and activation through a STAT1-dependent pathway. These results indicated the AKT1-STAT1 signalling axis as a pathway by which lactoferrin may inhibit neutrophil migration.

To test this hypothesis neutrophils were incubated simultaneously with formyl Methionyl-Leucyl-Phenylalanine (fMLF) and lactoferrin for 2 hours. Cell lysates were examined using Western blotting for the expression of AKT1. Neutrophil activation with fMLF was found to reduce expression of AKT1 compared to unactivated neutrophils, confirming the results of Liu et al (Figure 3.15). As predicted, when lactoferrin was added to neutrophils at the same time as fMLF, this prevented the down-regulation of AKT1 expression by fMLF. Because inhibition of neutrophil migration had previously been shown to be specific for lactoferrin, and was not shared by closely-related transferrin, neutrophils were also incubated with fMLF and transferrin simultaneously. Interestingly, culture of neutrophils with fMLF and transferrin also prevented down-regulation of AKT1 by fMLF, showing that

lactoferrin-induced inhibition of neutrophil migration is not mediated by AKT1. Curiously, culture of neutrophils with lactoferrin alone down-regulated expression of AKT1 compared to unstimulated neutrophils.

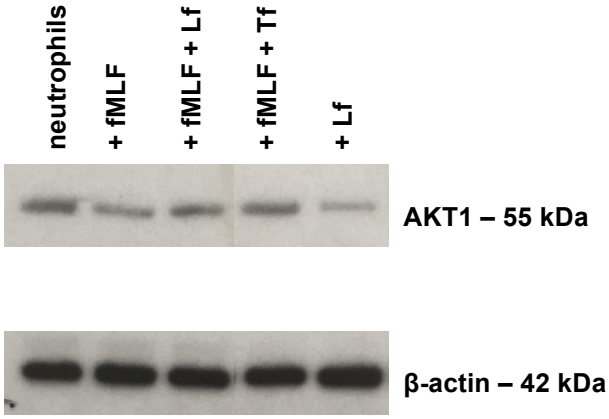

Figure 3.15 – Lactoferrin and transferrin inhibit neutrophil AKT1 downregulation by fMLF.
Western blot analysis of AKT1 protein levels in neutrophils following culture with or without fMLF and/or human milk-derived lactoferrin (Lf) or human transferrin (Tf) for two hours. Membranes were stripped and reprobed with β-actin antibody to assess sample loading. Blot shown is representative of three independent experiments.

3.3 Discussion

In this chapter the role of lactoferrin in shaping macrophages in the tumour microenvironment was tested. Lactoferrin had previously been found to be released from various tumour cells undergoing apoptosis, and could inhibit the migration of neutrophils to the tumour microenvironment (Bournazou *et al.*, 2009), which could potentially inhibit an inflammatory response at the tumour site that could decrease tumour growth. Because of its many pleiotropic properties (García-Montoya *et al.*, 2012), lactoferrin was proposed to not only inhibit the migration of neutrophils to the tumour site, but also affect the infiltration of macrophages and to influence their activation into anti-inflammatory and tumour-promoting starry-sky TAM.

First the ability of lactoferrin to attract monocytes was tested using both murine primary cells and a human monocytic cell line, but neither of the cells did elicit a chemotactic response towards lactoferrin, even though lactoferrin has been reported to have the ability to attract monocytes at similar concentrations as tested here (100ng/ml – 10µg/ml) (la Rosa *et al.*, 2008).

To further investigate whether lactoferrin could influence macrophage activation into anti-inflammatory and tumour-promoting starry-sky TAM, it was tested whether lactoferrin could bind to monocytes and macrophages as had been previously shown for THP-1 cells (Håversen *et al.*, 2002). A variety of murine and human macrophages were found to bind human milk-derived lactoferrin or human recombinant lactoferrin, and this appeared not to be saturated at high concentrations of lactoferrin.

Results presented here showed a trend, although not significant, that increasing concentrations of lactoferrin could reduce interaction between macrophages and apoptotic cells. This leaves the possibility that lactoferrin may be binding to a receptor involved in apoptotic-cell clearance and could thereby reduce the ability of apoptotic cells to bind to macrophages. However, this reduction might never be significantly visible, as macrophages have redundant pathways and receptors for the uptake of apoptotic cells. LRP1, a receptor involved in apoptotic-cell recognition, is the most likely candidate macrophage receptor for binding lactoferrin, as it has been shown to bind lactoferrin on osteoclasts (Grey, 2004). Unfortunately, tools to investigate lactoferrin binding to LRP1, including blocking antibodies, were not available during this project. Two other apoptotic cell receptors were investigated. Lactoferrin binding to K562 cells transfected with CD14 was assessed, because soluble CD14 has been shown to bind lactoferrin (Baveye *et al.*, 2000; Elass, 2002), but did not show binding of lactoferrin to CD14. Furthermore, blocking of the macrophage scavenger receptor (MSR1) on HMDM with an antibody previously shown to inhibit divalent cation-independent adhesion and the uptake of acetylated low-density lipoproteins (Fraser *et al.*, 1993) did not affect lactoferrin binding to HMDM. Further investigation into a lactoferrin receptor on macrophages needs to be

done, however, given lactoferrin's ability to bind with low affinity through its cationic N-terminal (Baker and Baker, 2005) and the observations here that the interaction between lactoferrin and MM6 cells could not be saturated at high concentrations, there might not be a specific receptor for lactoferrin on macrophages.

Further studies investigated whether lactoferrin could induce the expression of starry-sky TAM genes in macrophages. A range of concentrations of lactoferrin were tested, similar to those previously found to affect neutrophil activation (Bournazou *et al.*, 2009). However, only the highest concentration of lactoferrin of 100μg/ml was found to have an effect on the expression of SS-TAM genes. Mrc1, Mmp2, and Axl, were found to be up-regulated, whereas Gas6 was down-regulated.

In addition, it was investigated whether lactoferrin plays a role in preventing induction of or driving macrophages away from a classically activated phenotype that is capable of suppressing BL cell growth. Classically-activated macrophages were shown to reduce the number of viable target cells in co-culture assays. Classically-activated macrophages have been shown to induce apoptosis in tumour cells through release of TNFα, nitrogen oxides, reactive oxygen intermediates, and IL-1β (Cui *et al.*, 1994; Higuchi *et al.*, 1990; Feinman *et al.*, 1987; Jorens *et al.*, 1995; Martin and Edwards, 1993; Onozaki *et al.*, 1985), and it is therefore likely that macrophages directly induced cell death. However, the macrophage-mediated cytotoxic effects could also be indirect, through inhibition of growth (cytostasis) or anti-survival effects, or a combination of these. Cytostasis has been shown *in vitro* by human monocytes and macrophages (Mantovani *et al.*, 1979). Cytostatic effects were responsible for the elimination of rat tumour cells *in vitro* by non-specifically-activated macrophages (Keller, 1973). Co-culture led to pronounced morphological changes in the tumour cells, including shrinkage of cells, as well as substantial reduction in tumour cell numbers. Furthermore, reduced 3H-thymidine incorporation indicated decreased proliferation of the tumour cells. This cytostatic effect was found to be dependent on cell-to-cell contact (Keller, 1973). Additionally, the reduction of lymphoma cells could be (partially) due to the engulfment of (apoptotic) lymphoma cells, as an increase was observed, and cytotoxicity and cell removal may be going

on in parallel. The cytotoxic function of classically-activated macrophages will be further investigated in Chapter 5.

Our studies showed that lactoferrin cannot reverse macrophage cytotoxicity and that only pre-exposure to high concentrations of lactoferrin may reduce macrophage cytotoxicity. However, it cannot be ruled out that the observed effect is due to LPS binding to lactoferrin already bound to macrophages (and not washed away), as lactoferrin is known to bind LPS (Baveye *et al.*, 2000), thereby preventing full classical activation. No direct controls were included to test the direct effect of lactoferrin on target cell survival or death, but experiments performed by another member of our laboratory did not show an effect of lactoferrin on lymphoma cell viability (personal communication; Benjamin Arnold). Although high concentrations of lactoferrin have been reported at inflammatory sites, such high concentrations of lactoferrin are unlikely to be physiologically or clinically relevant in the tumour microenvironment. This was confirmed by the inability of supernatants from apoptotic cells, known to contain lactoferrin released from apoptotic cells, to reduce macrophage cytotoxicity. In contrast, pre-exposure of macrophages to apoptotic cells was found to reduce the cytotoxicity of macrophages towards tumour cells.

Taken together, these results suggest that cell contact with apoptotic cells, rather than signalling factors released from apoptotic cells, including lactoferrin active in the supernatant, is necessary to affect macrophage activation. Chapter 4 will therefore investigate the effects of apoptotic tumour cells in regulating macrophage activation in 'starry-sky' non-Hodgkin lymphomas towards an immunomodulatory, antimicrobial, anti-inflammatory, and trophic phenotype. Furthermore, Chapter 5 will look further at the ability of apoptotic cells to affect macrophage cytotoxicity.

A paper published during the course of this project showed that fMLF activation of neutrophils causes the down-regulation of AKT1 and that AKT1 depletion in murine infection models increases neutrophil migration and activation. This suggested that AKT1 negatively regulated neutrophil migration and it was proposed that lactoferrin may inhibit neutrophil migration through inhibition of AKT1 down-regulation by

activation signals such as fMLF. Indeed, lactoferrin was found to reverse the down-regulation of AKT1 caused by fMLF activation, however, this effect was not unique for lactoferrin and transferrin was found to have a similar effect on AKT1 expression. As transferrin had previously been shown not to inhibit neutrophil migration (Bournazou *et al.*, 2009), it appeared unlikely that inhibition of neutrophil migration by lactoferrin was regulated through AKT1. However, downstream signalling of STAT1 should be investigated to confirm this.

Chapter 4 Apoptotic lymphoma cells can contribute to a starry-sky TAM activation signature of macrophages

4.1 Introduction

One of the most important functions of phagocytosis is the clearance of apoptotic cells to prevent the release of toxic and immunogenic intracellular contents from the dying cell, thereby inhibiting inflammatory responses or tissue damage. Moreover, clearance of apoptotic cells results in the production of anti-inflammatory mediators and suppression of pro-inflammatory mediators by macrophages, further preventing inflammation (Voll *et al.*, 1997; Fadok *et al.*, 1998a). The importance of highly controlled elimination of apoptotic cells during development and homeostasis is clear from the redundancy in signals on apoptotic cells and receptors on phagocytes (Gregory and Pound, 2010). Additionally, studies in Drosophila have highlighted the importance of apoptotic cell removal, as it was shown that hemocytes (Drosophila macrophages), during later stages of development, prioritize responding to wounds over developmental cues (Moreira *et al.*, 2010). Furthermore, ineffective clearance has been shown to cause inflammatory responses, and may cause autoimmune diseases (Kawane *et al.*, 2003; Napirei *et al.*, 2000).

Massive cell death is a feature of many malignant tumours, although these tumours often continue to grow rapidly. Apoptotic cells are rapidly engulfed by tumour-associated macrophages, which have been associated with poor prognosis, and can promote anti-inflammatory responses, angiogenesis, tissue remodelling, and metastasis (Gregory and Pound, 2011). Recently, the *in situ* molecular signature of starry-sky TAM, known to engulf many apoptotic cells, was generated in our laboratory in a murine xenograft model of Burkitt's lymphoma, and many genes that were up-regulated by starry-sky TAM were associated with reparatory, pro-tumour, and phagocytic responses (Ford *et al.*, 2015). Given the ability of apoptotic cells to

control macrophage inflammatory responses, it was suggested that apoptotic cells could also influence other aspects of macrophage activation. Thus, it was hypothesised that apoptotic cells can promote lymphomagenesis through the activation of macrophages that are anti-inflammatory, immunosuppressive, and promote tumour growth and tissue remodelling.

The study presented in this chapter investigates, through a series of *in vitro* experiments, whether apoptotic cell co-culture with unstimulated or classically-activated macrophages can influence macrophage gene expression of selected starry-sky TAM genes (Table 1.1 and Table 1.2). Additionally, it is tested whether apoptotic cell co-culture can influence gene and protein expression of selected anti-inflammatory cytokines. Furthermore, it is investigated if the effects of apoptotic cells on macrophages are dependent on direct cell interaction, or can also be mediated through signalling of factors released from apoptotic cells. Finally, the involvement of IL-4Rα and galectin-3 in apoptotic cell-mediated signalling is analysed.

4.2 Results

4.2.1 'Young' macrophages are more responsive to chemotactic signals, whereas 'old' macrophages are more phagocytic

One of the main functions of macrophages is the phagocytosis of apoptotic cells. *In vivo*, apoptotic cells are rarely observed as they are rapidly engulfed by macrophages. Apoptotic cells release chemotactic signals that act as cues for monocytes and macrophages to migrate towards these apoptotic cells and allow for their rapid engulfment. As part of published experiments carried out in collaboration with Lihui Zhuang to compare the phenotype of embryonic stem cell-derived macrophages (ESDM) and their precursors, less mature ('young') ESDM and more mature ('old') ESDM were compared for their chemotactic and phagocytic responses. ESDM differentiation is explained in detail in materials and methods and has been published (Zhuang *et al.*, 2012).

For chemotaxis assays, ESDM were prepared as explained in materials and methods and were matured on Petri dishes for 0, 2, or 6 days, followed by one day in Teflon pots, and were designated ESDM d0, ESDM d3, or ESDM d7, respectively. Chemotaxis assays were performed using the modified Boyden chamber assay described in Chapter 3 and the results are shown in Figure 4.1a. ESDM d0 showed a larger number of cells migrating to the chemotactic peptide C5a than ESDM d3 or ESDM d7. Furthermore, ESDM d0 showed more migration of cells to supernatants from high-density cultured BL2 cells, than ESDM d3 cells, and ESDM d7 did not show any migration at all.

The ability of ESDM at different stages of maturation to phagocytose apoptotic cells was tested in a flow cytometry-based phagocytosis assay modified from a study of human monocyte-derived macrophages (Jersmann *et al.*, 2003). Briefly, 0, 2 or 6-day matured ESDM were labelled with the PKH67 dye and incubated on plates overnight. The next day, ESDM were washed and incubated with cold shock-induced apoptotic human Burkitt's lymphoma (BL2) cells for one hour at 37˚C. After the incubation, wells were washed and ESDM were detached from the wells and from non-engulfed apoptotic BL2 cells by trypsin/EDTA. Cells were harvested from each well for analysis by flow cytometry.

Green fluorescence indicated the macrophages, whereas red fluorescence indicated the presence of apoptotic cells. Double-positive red/green events mostly likely indicated macrophages that had phagocytosed apoptotic cells, as trypsin/EDTA treatment did not release apoptotic cells from these macrophages. The percentage of macrophages that had engulfed apoptotic cells were calculated and results are presented in Figure 4.1. ESDM d0 showed the lowest ability to phagocytose apoptotic BL2 cells, but this was increased in proportion to the time for which the ESDM were matured.

To repeat these observations in a different cell system, bone marrow-derived macrophages (BMDM) at different stages of maturation were used. Figure 4.2a compares the chemotactic response of BMDM at different stages of maturation

towards the chemotactic peptide C5a. 'Younger' BMDM, were matured for 4 days, and were designated 'BMDM d4'. 'Older', more mature BMDM were matured for 7 days, and were designated 'BMDM d7'. Although 'older' BMDM d7 had not completely lost their ability to migrate, a significantly larger number of BMDM d4 macrophages migrated towards C5a compared with BMDM d7.

It was then investigated whether BMDM d4 and BMDM d7 also differed in their phagocytic response. BMDM were harvested from Petri dishes and cultured on glass slides for two hours, before co-culture with UVB-irradiation-induced apoptotic lymphoma cells for one hour. To measure interaction, unbound cells were washed off and macrophages were fixed. The percentage of macrophages interacting with apoptotic cells was calculated. No difference in interaction between BMDM d4 and BMDM d7 was observed (Figure 4.2b). However, when non-engulfed apoptotic cells were removed by trypsin treatment, and the percentage of phagocytosing macrophages was calculated, a significant difference was observed between BMDM d4 and BMDM d7, with a larger percentage of BMDM d7 engulfing apoptotic cells (Figure 4.2c).

Taken together, these results show that the activation state of macrophages changes during maturation. Young macrophages readily migrate towards apoptotic cells, but as they matured, their ability to migrate was reduced, whereas their ability to phagocytose apoptotic cells was increased. These results were in agreement with other studies that found that macrophages are better phagocytes of apoptotic cells than monocytes (Newman *et al.*, 1982; Callahan *et al.*, 2003). As ESDM and BMDM are matured in the presence of large numbers of apoptotic cells, these findings support the hypothesis that interaction of BMDM with apoptotic cells and factors released from apoptotic cells can influence macrophage function and activation state.

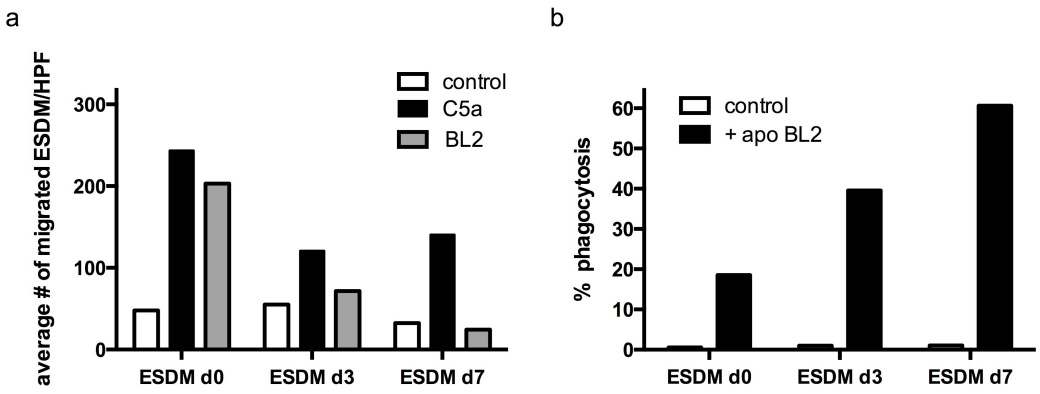

Figure 4.1 – As ESDM mature their ability to respond to a chemotactic signal is reduced, whereas their ability to phagocytose apoptotic cells increases.
(a) Migratory responses of 0, 3, and 7-day matured ESDM to 10ng/ml C5a and supernatants from high-density cultured BL2 cells. Data are means for the number of migrated cells per high power field (HPF) for 10 random areas (n=2). (b) Ability of 0, 3, and 7-day matured ESDM to phagocytose cold shock-induced apoptotic BL2 cells in a flow cytometric-based phagocytosis assay. Data are means for the percentage of ESDM demonstrating phagocytosis of apoptotic BL2 cells and untreated controls (n=2).

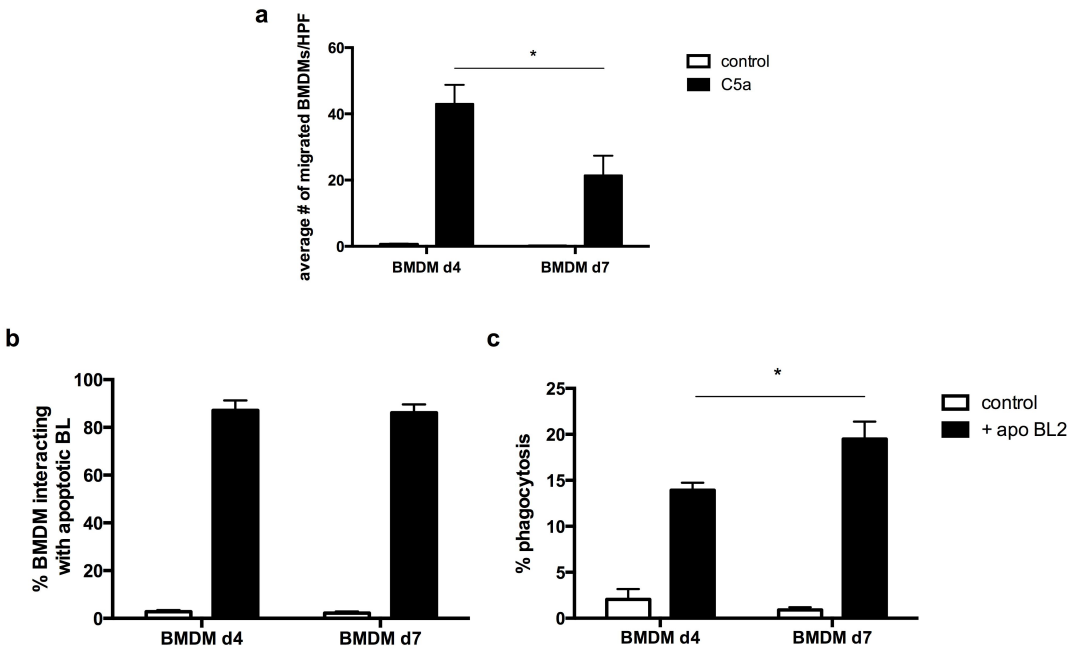

Figure 4.2 – 'Younger', less mature BMDM respond better to a chemotactic stimulus than 'older', more mature BMDM, which have a higher ability to phagocytose apoptotic cells.
(a) Migratory responses of 4 and 7-day matured BMDM to 10ng/ml C5a were measured in a modified Boyden chamber assay. Data are means + SEM for the number of migrated cells per high power field (HPF) for 10 random areas (n=4). BMDM were assessed for their ability to (b) interact with and (c) phagocytose apoptotic BL2 cells in a microscopy-based phagocytosis assay. Data are means + SEM for the percentage of BMDM demonstrating interaction or phagocytosis of apoptotic BL2 cells and untreated controls. (n=4). Statistical analysis was performed using a paired t test. *$p<0.05$.

4.2.2 Comparison of TAM phenotype in an apoptosis-suppressed lymphoma model to the phenotype of starry-sky TAM

To investigate the role apoptotic cells play in regulating the activation of anti-inflammatory, pro-angiogenic, and tissue signalling macrophages, first gene expression of TAM from starry-sky tumours were compared to TAM from tumours in which apoptosis had been suppressed.

Burkitt's lymphoma cells, or their Bcl-2 transfected counterparts, in which apoptosis is suppressed (Skommer *et al.*, 2010; Wang *et al.*, 1996), were injected into the flank of severe combined immunodeficient (SCID) BALB/C mice. Suppression of apoptosis has been shown to constrain tumour cell proliferation, reduce tumour angiogenesis, and reduce the accumulation of macrophages *in vivo* in this model of

starry-sky NHL (Ford *et al.*, 2015). Snap-frozen masses from fully-grown tumours were lysed and RNA was extracted and converted to cDNA. Expression of genes of interest was measured by qPCR. Because the primers used were chosen to specifically bind to murine and not human mRNA, only gene expression of murine cells was measured. To account for the difference in macrophages numbers in the BL2 and Bcl-2-transfected tumours, gene expression was normalized to Csf1r expression, a marker for macrophages. Figure 4.3 shows a heatmap comparing the signature of selected genes in BL2 and BL2-Bcl-2 xenograft tumours. No differences in the signature were observed, with genes similarly expressed in both.

Because the presence of apoptotic tumour cells in the Bcl-2-transfected model was reduced, but not abolished, and the presence of other apoptotic cells could not be ruled out, it could not be concluded that the activation signature of TAM in both models was independent of apoptotic cell interaction, especially since the TAM in the Bcl-2-transfected model were also found to have engulfed apoptotic cells, although fewer than their parental counterparts (Ford *et al.*, 2015). Therefore, a different approach was needed to assess whether interaction with apoptotic cells or apoptosis-independent properties of lymphoma cells are responsible for the activation of TAM.

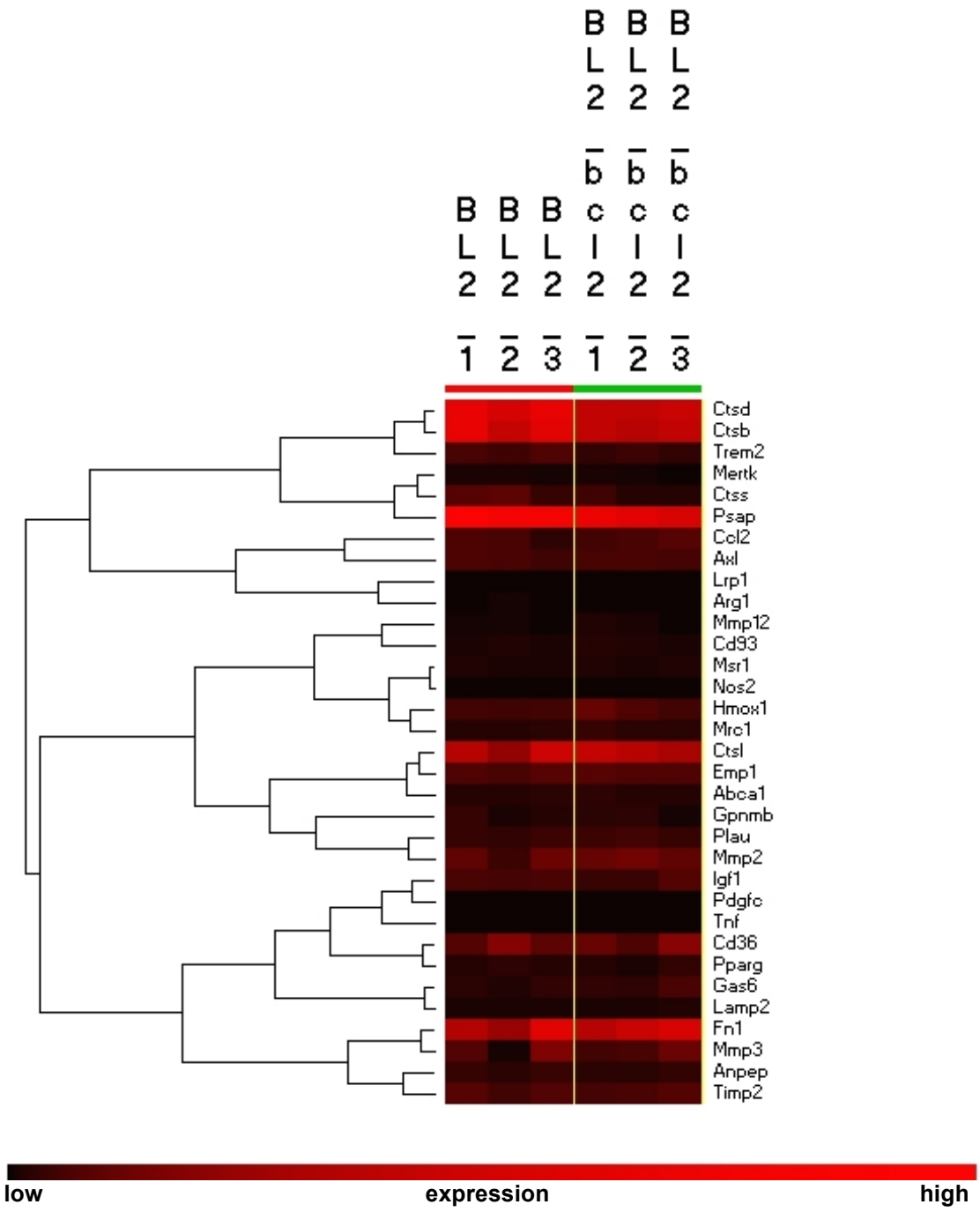

Figure 4.3 – Heatmap comparing murine mRNA expression of selected genes in BL2 and BL2-Bcl-2 xenograft tumours.
Snap-frozen tumours from SCID mice transplanted with BL2 cells and their Bcl-2-transfected counterparts were analysed for murine mRNA expression of selected genes by qPCR. Gene expression was normalized to the macrophage gene Csf1r to account for the difference in macrophage numbers in the tumours. The heatmap was made using PermutMatrix software.

4.2.3 Assessment of the effect of apoptotic cell co-culture on macrophage activation

In order to assess whether apoptotic cell-interaction is responsible for the activation signature of starry-sky TAM, the effect of macrophage co-culture with apoptotic lymphoma cells was assessed in an *in vitro* setting. Additionally, WT BMDM were compared to BMDM from mice deficient in the IL-4 receptor α-chain (IL-4Rα knockout (KO) mice), which is a component of the receptors for both IL-4 and IL-13, and thus associated with alternative activation of macrophages (Colegio *et al.*, 2014; Wang and Joyce, 2010). Furthermore, IL-4 signalling through IL-4Rα has recently been shown to induce macrophage proliferation (Jenkins *et al.*, 2013). IL-4Rα KO BMDM were included because published *in vivo* xenograft BL experiments showed that IL-4Rα KO mice displayed slower tumour growth than WT mice (Ford *et al.*, 2015), and we wanted to investigate whether this was due to differential macrophage activation because of a lack of IL-4Rα expressed by the macrophages present in those tumours.

In addition to stimulating proliferation, differentiation, and survival of macrophages, CSF1 has been shown to generate phagocytic macrophages that promote tissue repair and extracellular proteolysis, activations states that are also associated with starry-sky TAM (Davies *et al.*, 2013; Hume and MacDonald, 2012). Thus, following 7-day maturation of BMDM, CSF1 was removed for 18 hours to reduce the effects of CSF1 on the BMDM. WT or IL-4Rα KO C57BL/6 mice were then co-cultured for 24 hours with or without apoptotic BL2 cells. Gene expression of the macrophage markers Cd68, Csf1r, and Emr1 (F4/80) remained high in these cells (not shown). Apoptosis of BL2 cells was triggered by 100mJ UVB-irradiation and cells were incubated for three hours to induce apoptosis before they were added to the macrophages. Simultaneous staining with Annexin V (AxV) and propidium iodide (PI) shows that the majority of cells were apoptotic when added to the BMDM, and by the end of the assay almost all cells had undergone apoptosis and were secondary necrotic (Figure 4.4c).

Both the expression of mannose receptor (CD206) and F4/80 by macrophages was slightly increased upon co-culture with apoptotic BL2 cells (Figure 4.4a). IL-4Rα KO BMDM showed similar modest increases of F4/80 expression upon co-culture with apoptotic BL2 cells, but not for mannose receptor.

Secondly, it was investigated whether co-culture with apoptotic cells induced expression of interleukins 4 or 13 (IL-4 or IL-13) or the inflammatory cytokines TNFα, IL-12p70, IL-6, IL-10, CCL2, and IFN-γ, but none were found to be expressed above detection levels of ~75ng/ml by either the WT or the IL-4Rα KO macrophages (not shown).

Additionally, qPCR was used to investigate whether co-culture with apoptotic cells changed the expression of selected starry-sky TAM genes by the macrophages (Figure 4.4b). Up- or down-regulation was considered meaningful if the difference was more than 2-fold. Hmox1 and Ccl2 were found to be significantly up-regulated upon co-culture with apoptotic cells. In contrast, Fn1, Mmp12, and Plau were found to be down-regulated, although only down-regulation of IL-4Rα KO BMDM upon apoptotic cell co-culture for Plau and Mmp12 was found to be significant. No differences were observed in the response of IL-4Rα KO BMDM to co-culture with apoptotic BL2 cells compared to WT BMDM.

The same experiment was repeated using transgenic λ-MYC cells from a model of aggressive B-cell lymphoma in mice, which displays similar starry-sky morphology with TAM accumulation after transplantation into immunocompetent mice (Kovalchuk *et al.*, 2000). λ-MYC cells were induced to undergo apoptosis by exposure to UVB followed by a 2-hour culture before the cells were co-cultured with WT and IL-4Rα BMDM for 24 hours. UVB-irradiation induced apoptosis in ± 20% of the cells after 2 hours and by the end of co-culture almost all cells had undergone apoptosis and were necrotic (Figure 4.5c). Flow cytometric analysis of the expression of mannose receptor and F4/80 on WT and IL-4Rα BMDM showed similar modest increases upon co-culture with apoptotic λ-MYC cells as were observed upon co-culture with apoptotic BL2 cells (Figure 4.5a). Again, expression

levels of IL-4, IL-13, and inflammatory cytokines were assessed but did not rise above the detection levels of the assay. qPCR analysis revealed the up-regulation of Ccl2, and the down-regulation of Mmp12, Fn1, Anpep, Abca1, and Lrp1, although only down-regulation of IL-4Ra KO BMDM upon apoptotic cell co-culture for Abca1 and Fn1 was found to be significant. No significant differences between the responses of WT and IL-4Rα KO BMDM were found.

Overall the results presented here indicate small increases for mannose receptor and F4/80 expression, and modest (just above the two-fold cut-off level) up-regulation of Hmox1 and Ccl2 and a trend of down-regulation of Mmp12, Fn1, Plau, Lrp1, and Abca1 gene expression in BMDM as a result of co-culture with apoptotic lymphoma cells. These results show much smaller effects of co-culture with apoptotic cells on macrophages than might be expected given this laboratory's published findings that co-culture with apoptotic cells, but not viable cells, could significantly up-regulate gene expression of Mmp2 and Mmp12 by macrophage cell lines up to 10-fold and this up-regulation was confirmed at the protein level (Ford *et al.*, 2015). However, one of the main draw-backs in the experiments carried out here is that BMDM are matured in the presence of large numbers of apoptotic cells, which may already affect gene expression to a more TAM-like phenotype during maturation. In contrast, macrophage cell lines such as RAW264.7 and J774 as used by Ford et al. (2015) are cultured mostly free from apoptotic cells. Because apoptotic cells could not be reliably removed from BMDM cultivation cultures, a different approach needed to be found to assess the effect of apoptotic cells on primary macrophage activation.

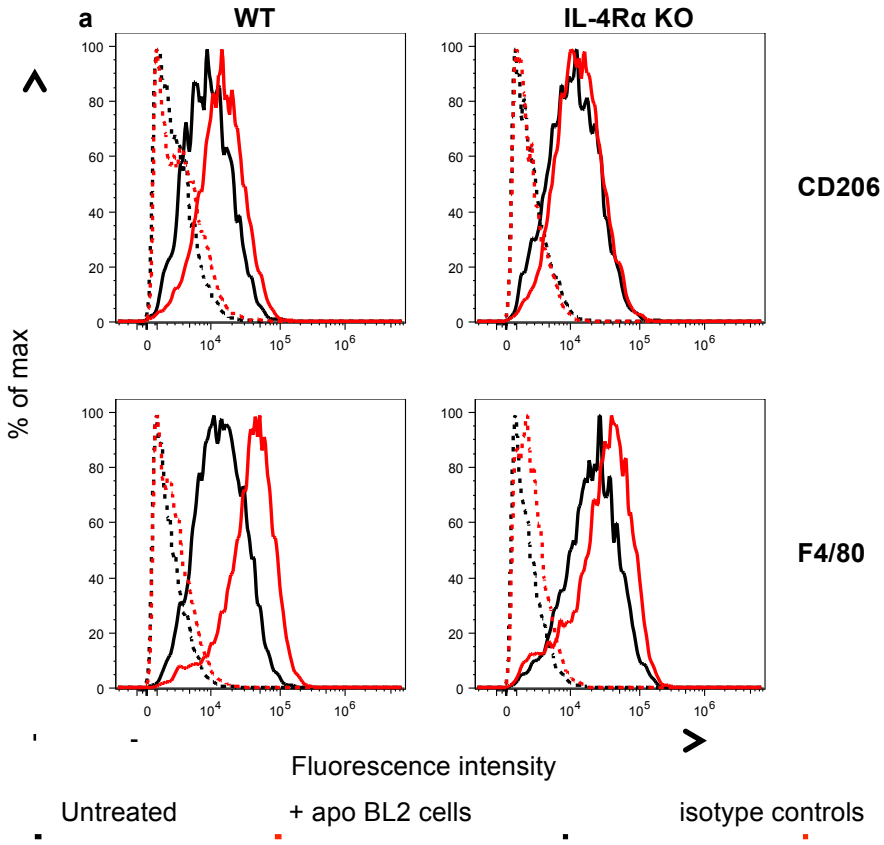
a
WT
IL-4Rα KO
CD206
F4/80
% of max
Fluorescence intensity
Untreated
+ apo BL2 cells
isotype controls

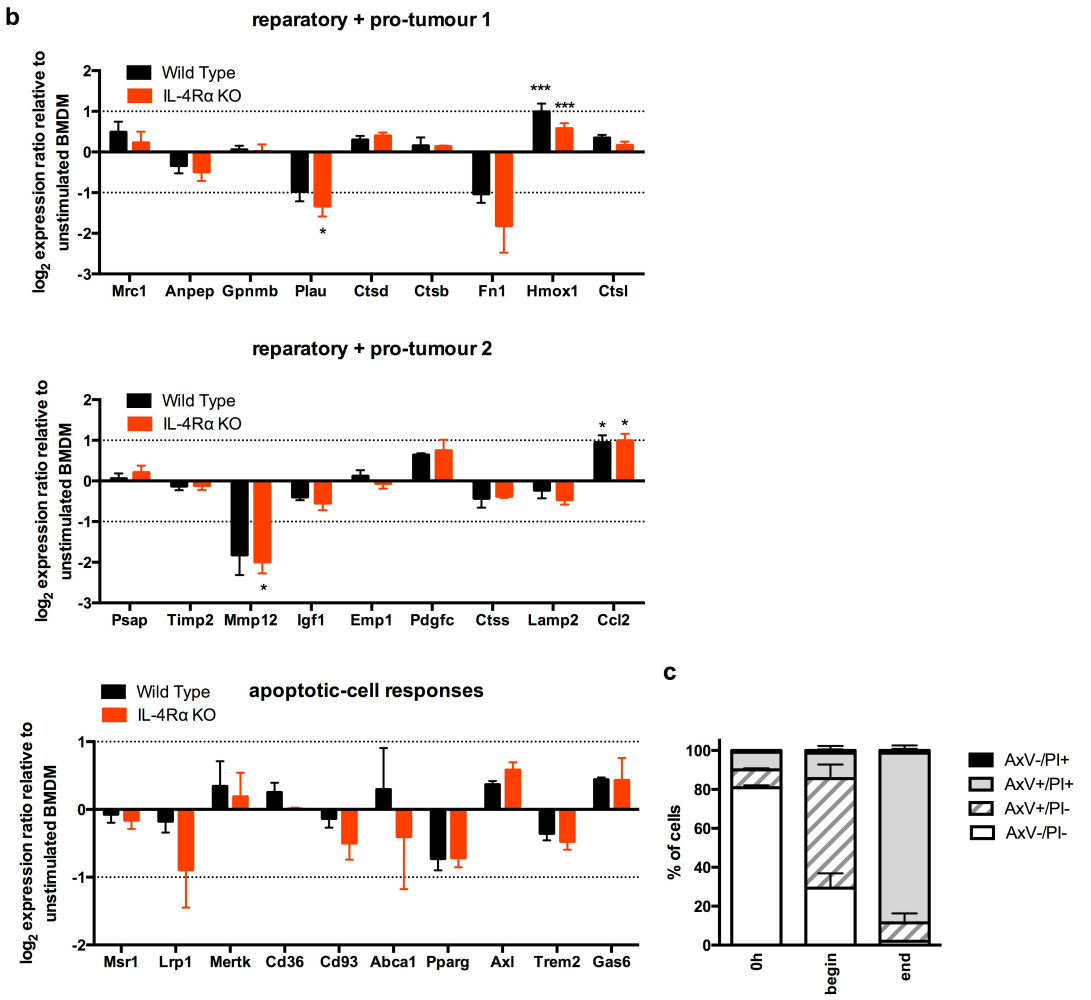

Figure 4.4 – Phenotype of BMDM from WT and IL-4Rα KO mice after co-culture with apoptotic BL2 cells.

BMDM from WT or IL-4Rα knockout C57BL/6 mice were co-cultured for 24h with or without apoptotic BL2 cells (apo BL2). At the end of the assay BMDM were assessed for (a) cell surface expression of mannose receptor (CD206) and F4/80 measured by flow cytometry using antibody Alexa Fluor 488 conjugates. (b) mRNA expression of selected genes was assessed following co-culture and normalized using the reference genes Tuba1b, Hsp90, and Hprt. Expression is presented as mean log[2] ratio relative to BMDM control. Data are means ± SEM for 3 independent experiments. The dotted lines at y=1 and y=-1 indicate a 2-fold increase or decrease of expression, respectively. Statistical analysis was performed on the raw data using two-way ANOVA with Tukey's multiple comparison test and is shown for + apo BL2 compared to BMDM control. *p<0.05, ***p<0.001. No significant differences were found between WT and IL-4Rα KO BMDM. (c) Assessment of BL2 cell viability was assessed by flow cytometry by simultaneous staining with Annexin V (AxV) and propidium iodide (PI) of control lymphoma cells at 0h and at the beginning and end of co-culture with BMDM. Data are means + SEM.

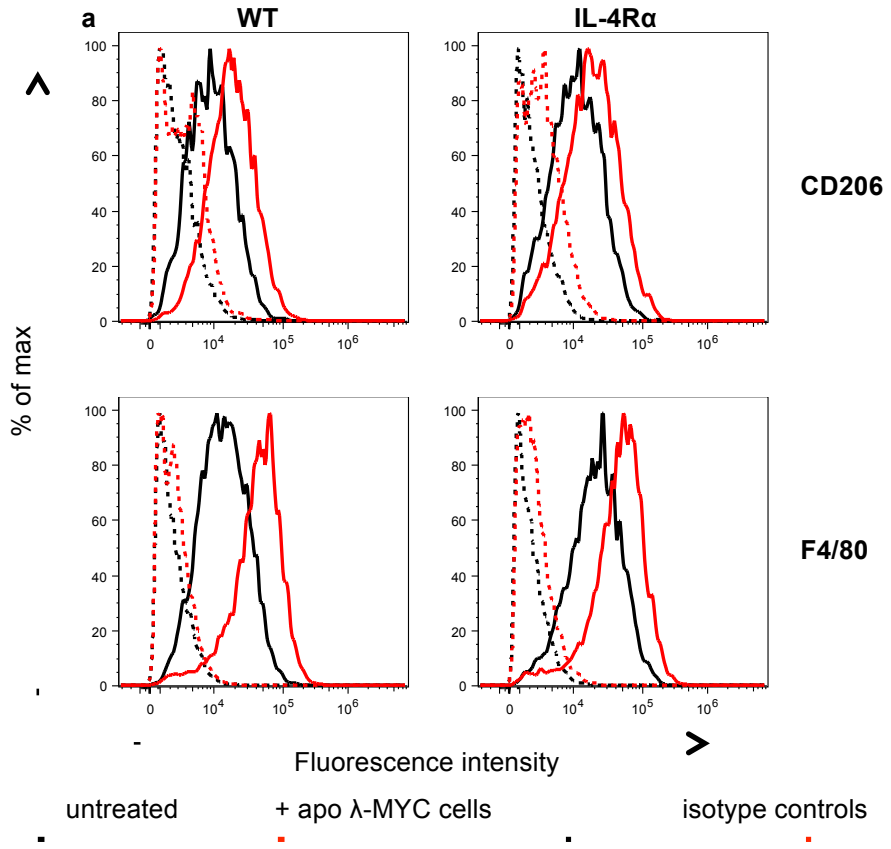
a
WT
IL-4Rα
CD206
F4/80
% of max
Fluorescence intensity
untreated
+ apo λ-MYC cells
isotype controls

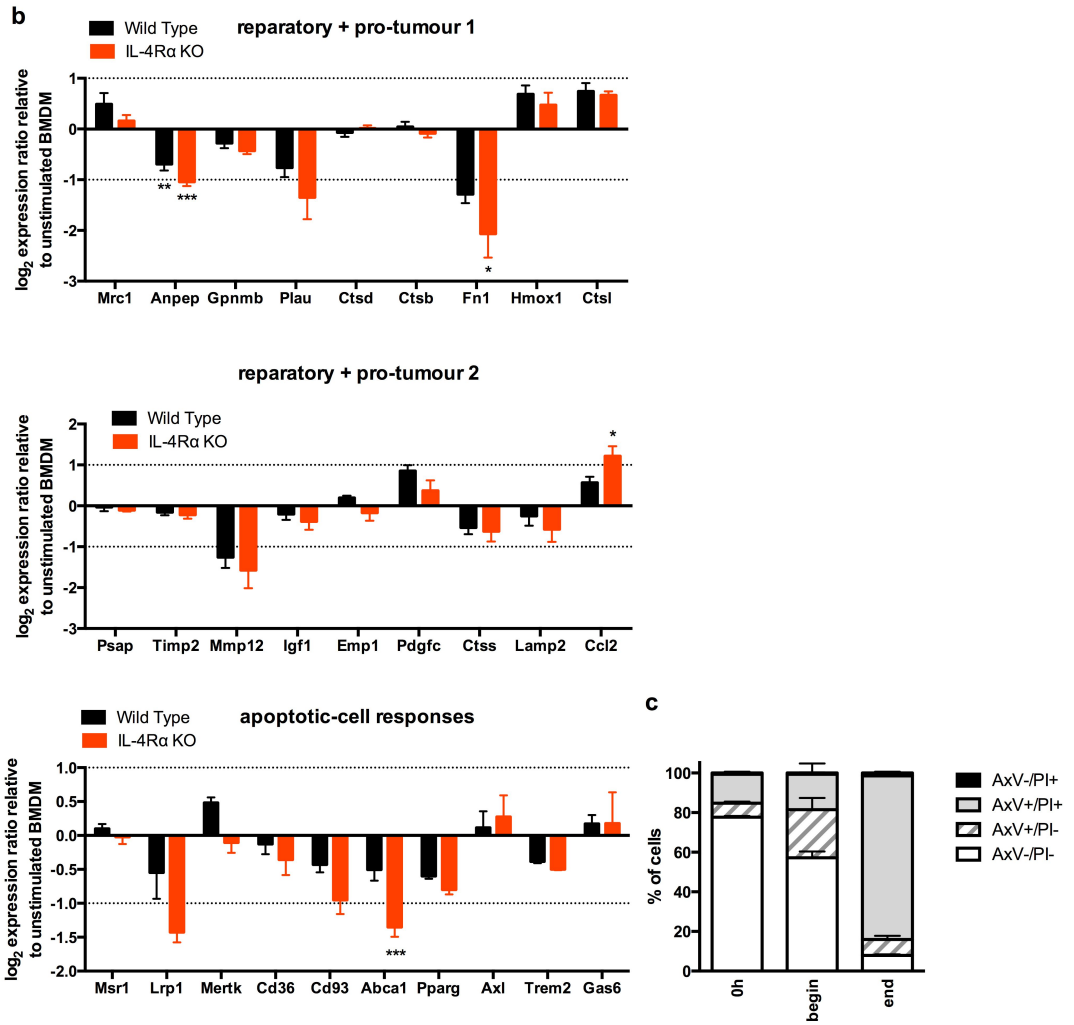

Figure 4.5 – Phenotype of BMDM from WT and IL-4Rα KO mice after co-culture with apoptotic λ-MYC cells.

BMDMs from WT or IL-4Rα KO C57BL/6 mice were co-cultured for 24h without or with apoptotic λ-MYC cells (apo λ-MYC). (a) At the end of the assay BMDM were assessed for cell surface expression of mannose receptor (CD206) and F4/80 as described for Figure 4.4(a). (b) mRNA expression of selected genes was assessed following co-culture and normalized using the reference genes Tuba1b, Hsp90, and Hprt. Expression is presented as mean log[2] ratio of BMDM + apo λ-MYC relative to BMDM control. Data are means ± SEM for 3 independent experiments. The dotted lines at y=1 and y=-1 indicate a 2-fold increase or decrease of expression, respectively. Statistical analysis was performed on the raw data using two-way ANOVA with Tukey's multiple comparison test and is shown for + apo λ-MYC compared to BMDM control. *p<0.05, **p<0.01, ***p<0.001. (c) Assessment of λ-MYC cell viability was assessed by flow cytometry by simultaneous staining for Annexin V (AxV) and propidium iodide (PI) of control lymphoma cells at 0h and at the beginning and end of co-culture with BMDM the beginning and end of the co-culture assay. Data are means + SEM for 3 independent experiments.

4.2.4 Classical activation affects macrophage gene expression and increases phagocytosis of apoptotic cells by macrophages

In an attempt to shift the baseline phenotype of BMDM toward a less apoptotic cell-influenced phenotype, the effect of classical activation on BMDM phenotype was assessed. Mature BMDM were stimulated for 4 hours with 10U/ml IFN-γ and 0.5ng/ml LPS. BMDM were then rested for a further 24 hours before gene expression of selected TAM-genes was assessed. Additionally, the activation state of the IFN-γ and LPS-stimulated BMDM was assessed by expression of Tnf and Il6, and the Arg1/Nos2 ratio was assessed, all indicators of classical or alternative activation of macrophages (Van Ginderachter *et al.*, 2006; Urban *et al.*, 1986; Jorens *et al.*, 1995).

As predicted, classical activation of BMDM indeed decreased the expression of most of the starry-sky-TAM markers (Figure 4.6). Genes that were significantly down-regulated include the reparatory and pro-tumour genes Mrc1, Plau, Ctsd, Fn1, Ctsl, Timp2, Igf1, and Emp1, as well as the following genes that are associated with apoptotic cell responses: Cd36, Pparg, Trem2, and Gas6. CD93 also appeared to be down-regulated, but this was not significant within the number of repeats. In contrast, genes associated with inflammatory responses, including Tnf and Il6 were significantly up-regulated. Furthermore, several genes that were found to be up-regulated in TAM were also up-regulated upon classical activation, including the reparatory and pro-tumour genes Hmox1, Mmp3, and Ccl2, as well as the apoptotic cell response genes Msr1 and Axl. Mmp2, and Pdgfc also appeared to be up-regulated, but this was not significant within the number of repeats. Expression of Anpep, Gpnmb, Psap, Lamp2, and the cathepsins Ctsd, Ctsb, and Ctss were not affected by classical activation. The Arg1/Nos2 ratio was significantly down-regulated following IFN-γ and LPS-stimulation of BMDM, confirming that the macrophages were classically-activated.

Because classical activation reduced the expression of many genes involved in apoptotic cell recognition and phagocytosis, it was tested whether classically activated BMDM could still bind and phagocytose apoptotic cells. BMDM were

matured for 7 days, plated onto glass slides classically activated with IFN-γ and LPS for 4h prior to co-culture with apoptotic BL2 cells for one hour. No differences in binding were found, but, classically-activated macrophages were significantly better at phagocytosing apoptotic BL2 cells compared to their non-activated counterparts (Figure 4.7). Binding and phagocytosis of apoptotic λ-MYC cells by untreated and classically-activated BMDMs was only tested once, but followed the same trend as binding and phagocytosis of apoptotic BL2 cells (Figure 4.8).

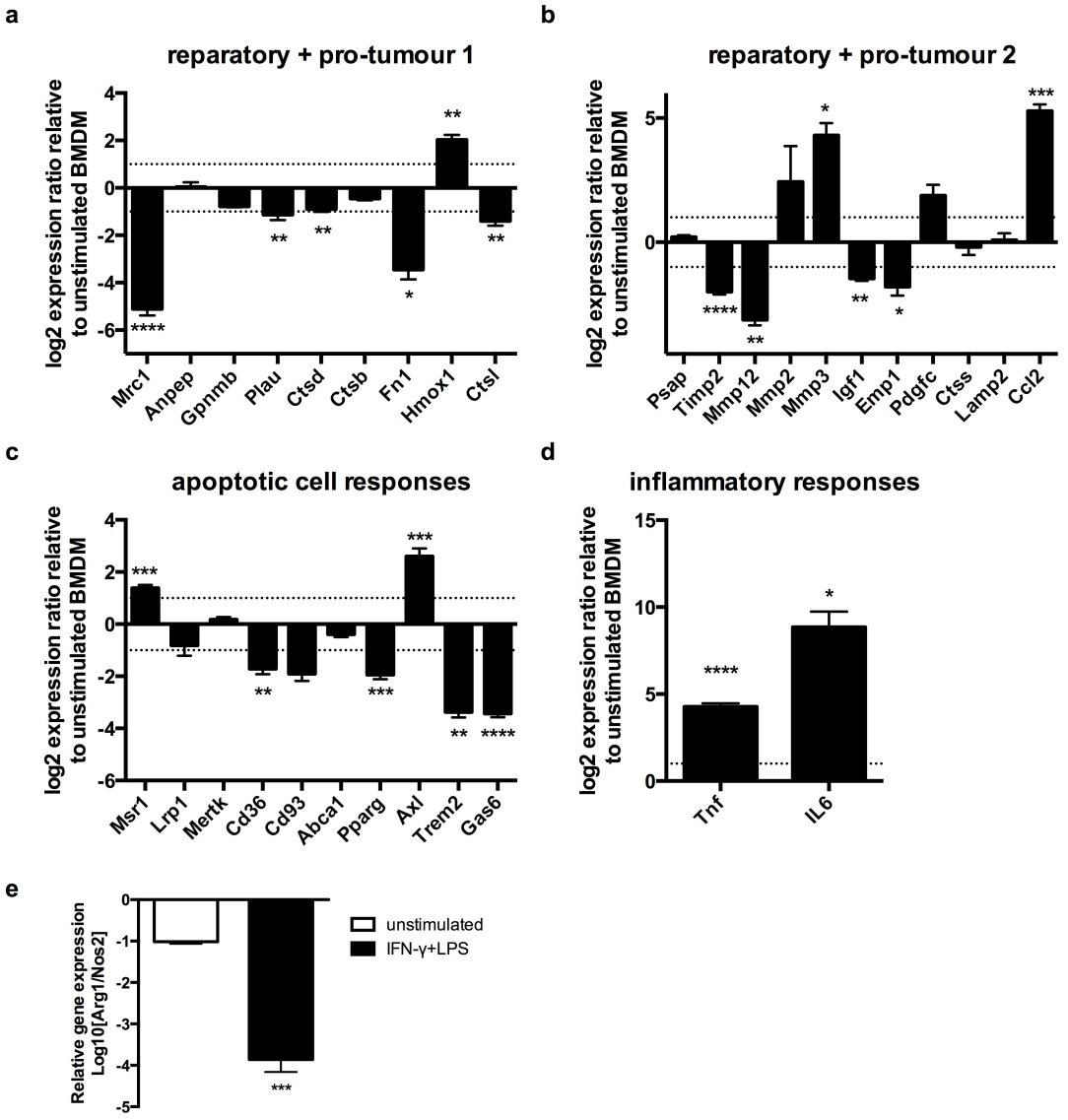

Figure 4.6 – BMDM responses to classical activation.
BMDM were cultured for 4 hours with 10U/ml IFN-γ and 0.5ng/ml LPS followed by a 24-hour resting period. (a-d) mRNA expression of selected genes was assessed and normalized using the reference genes Tuba1b, Hsp90, Hprt, and B2m. Expression is presented as log[2] ratio of IFN-γ and LPS-stimulated BMDM relative to un-stimulated BMDM. Data are means ± SEM for 3-8 independent experiments (or 2 experiments for Cd93 and MMP2). The dotted lines at y=1 and y=-1 indicate a 2-fold increase or decrease of expression, respectively. Statistical analysis was performed on the raw data using a paired t test and compared IFN-γ and LPS-stimulated BMDM to un-stimulated BMDM. * $p<0.05$, ** $p<0.01$, *** $p<0.001$, **** $p<0.0001$. (e) Log[Arg1/Nos2] expression ratio for unstimulated and IFN-γ and LPS-stimulated BMDM. ***$p<0.001$ (unpaired t test).

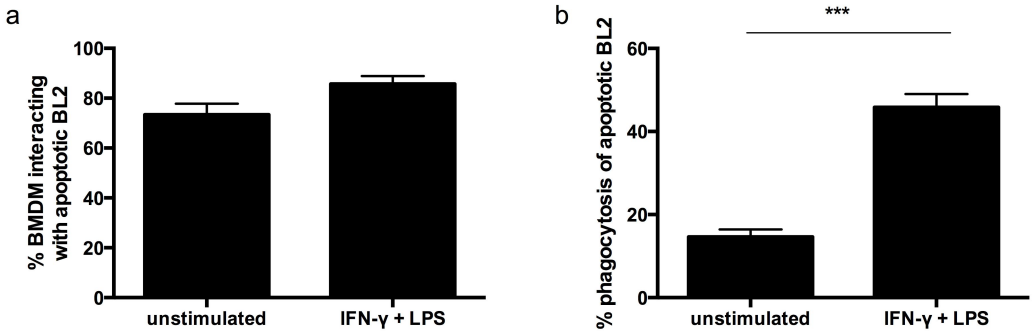

Figure 4.7 – IFN-γ and LPS-stimulated BMDM show increased ability to phagocytose apoptotic BL2 cells.
7-day matured untreated and IFN-γ and LPS-stimulated BMDM were assessed for their ability to (a) interact with and (b) phagocytose apoptotic BL2 cells in a microscopy-based phagocytosis assay. Data are means + SEM for the percentage of BMDM demonstrating interaction or phagocytosis of apoptotic BL2 cells and untreated controls. Statistical analysis was performed using a paired t test. ***$p<0.001$.

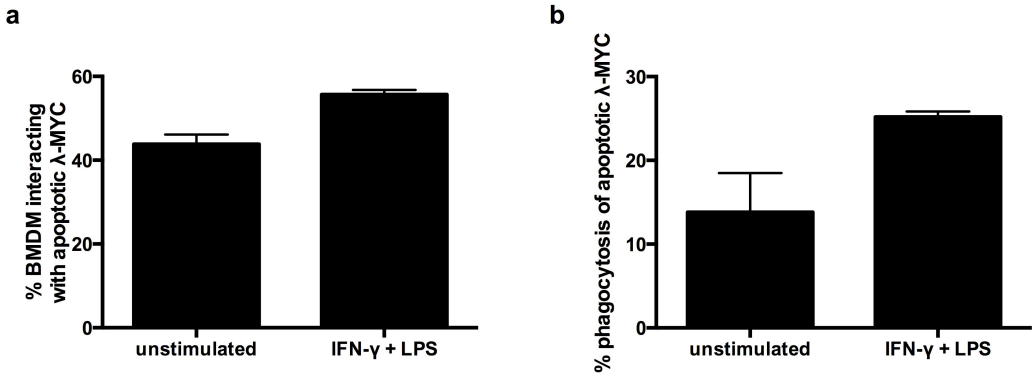

Figure 4.8 – IFN-γ and LPS-stimulated BMDM show increased ability to phagocytose apoptotic λ-MYC cells.
7-day matured untreated and IFN-γ and LPS-stimulated BMDM were assessed for their ability to (a) interact with and (b) phagocytose apoptotic λ-MYC cells. Data are means of duplicates + SD for the percentage of BMDM demonstrating interaction or phagocytosis of apoptotic BL2 cells and untreated controls for one experiment.

4.2.5 Co-culture of classically-activated macrophages with apoptotic lymphoma cells changes macrophage phenotype

Thus having established that classical activation of BMDM by IFN-γ and LPS did down-regulate expression of some starry-sky TAM genes, but did not negatively affect phagocytosis of apoptotic cells, the investigation could be returned to the question of whether co-culture with apoptotic cells affects macrophage gene expression.

BMDM were classically activated for 4 hours with IFN-γ and LPS before co-culture with apoptotic lymphoma cells for 24 hours. Classical stimuli were washed away before apoptotic cells were added, as LPS is known to bind to apoptotic cells, which could interfere with the experiment. Gene expression of classically-activated BMDM co-cultured with either apoptotic BL2 or λ-MYC cells is shown in Figure 4.9.

Co-culture with apoptotic BL2 cells significantly increased the expression of Timp2, Cd36, Pparg, and Gas6 by classically-activated macrophages more than two-fold. Expression of Mrc1 was also increased, but this was not significant. The expression of Mmp3, Tnf, and Il6 was found to be significantly more than two-fold decreased upon co-culture with apoptotic BL2 cells. Furthermore, the [Arg1/Nos2] ratio was significantly increased (Figure 4.9e).

Co-culture with apoptotic MYC-Ed1 cells also decreased the expression of Tnf and IL6, and in addition to that significantly decreased the expression of Axl, Mmp12, Anpep, and Plau.

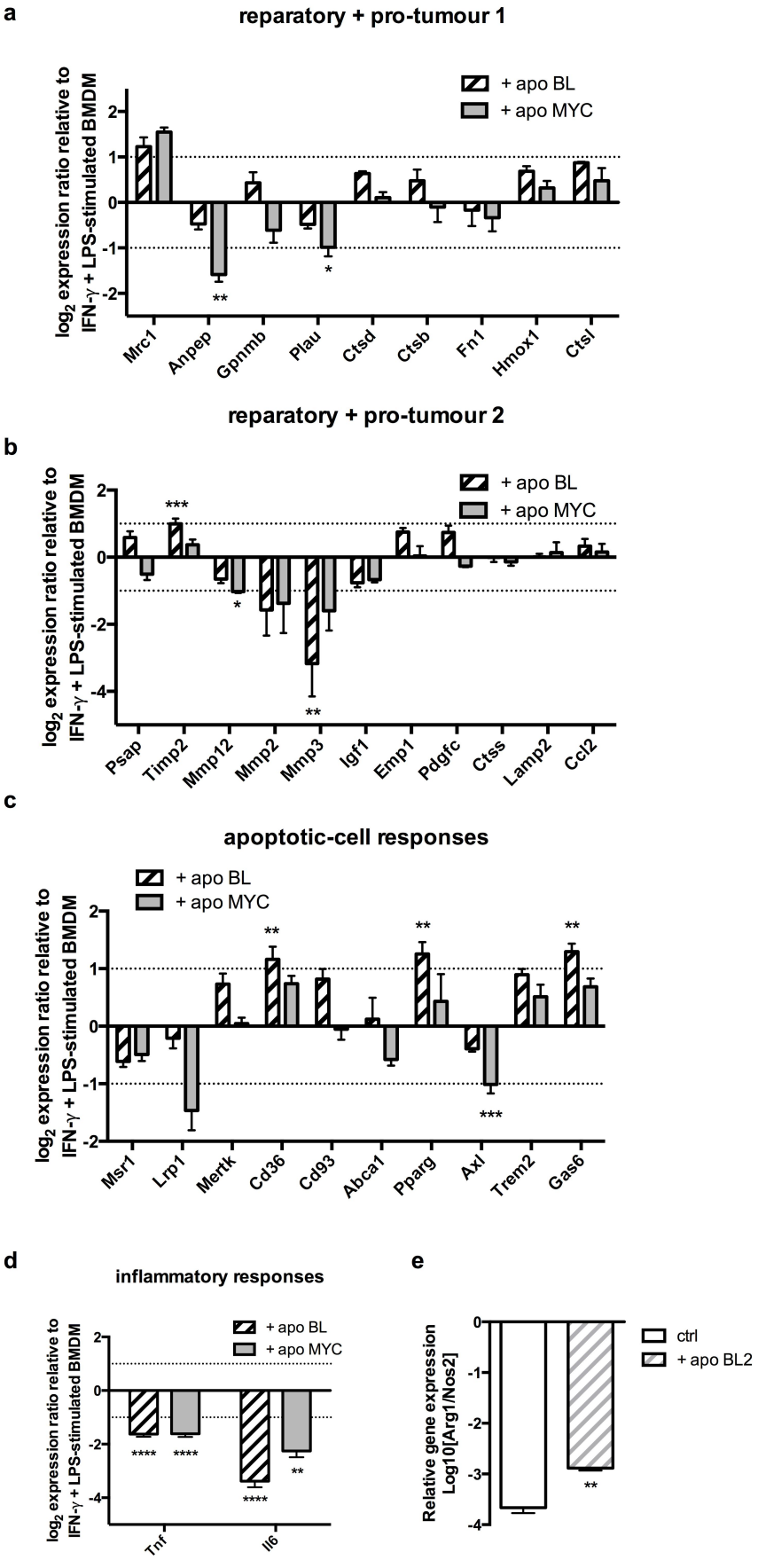
a
reparatory + pro-tumour 1
log2 expression ratio relative to IFN-γ + LPS-stimulated BMDM
+ apo BL
+ apo MYC
Mrc1
Anpep
Gpnmb
Plau
Ctsd
Ctsb
Fn1
Hmox1
Ctsl
b
reparatory + pro-tumour 2
Psap
Timp2
Mmp12
Mmp2
Mmp3
Igf1
Emp1
Pdgfc
Ctss
Lamp2
Ccl2
c
apoptotic-cell responses
Msr1
Lrp1
Mertk
Cd36
Cd93
Abca1
Pparg
Axl
Trem2
Gas6
d
inflammatory responses
Tnf
Il6
e
Relative gene expression Log10[Arg1/Nos2]
ctrl
+ apo BL2

Figure 4.9 – Gene transcription responses of classically activated-macrophages to co-culture with apoptotic BL2 and apoptotic MYC-Ed1 cells.
4-hour IFN-γ + LPS-stimulated BL6 BMDM were co-cultured for 24 hours with or without apoptotic BL2 or apoptotic λ-MYC cells. Apoptosis of the BL2 and λ-MYC cells was triggered by 100mJ UVB irradiation. mRNA expression of selected genes was assessed following co-culture and normalized using the reference genes Tuba1b, Hsp90, Hprt, and B2m. Expression is presented as log[2] ratio relative to IFN-γ and LPS-stimulated BMDM. Means are ± SEM for 3-7 independent experiments. The dotted lines at y=1 and y=-1 indicate a 2-fold increase or decrease of expression, respectively. Statistical analysis was performed on raw data using one-way ANOVA and Dunnett's multiple comparison test. *p<0.05, **p<0.01, ***p<0.001, ****p<0.0001. (e) Log[arginase/Nos2 expression ratio] for IFNγ and LPS-stimulated BMDM cultured with or without apoptotic BL2 cells. Statistical analysis was performed using a non-paired t test. **p<0.01.

4.2.6 Apoptotic, but not viable lymphoma cells, can change the phenotype of classically-activated macrophages

Having found that co-culture with apoptotic lymphoma cells can induce up- or down-regulation of starry-sky TAM genes by classically activated BMDM, it was then investigated whether these differences were due specifically to co-culture with apoptotic cells or if co-culture with untreated viable lymphoma cells could produce a similar effect. An identical experiment was carried out, but in addition to co-culture with UVB-induced apoptotic cells, IFN-γ and LPS-stimulated macrophages were also co-cultured with untreated BL2 cells and Bcl-2-transfected lymphoma cells, which are inhibited from undergoing apoptosis. AxV/PI-staining of control BL2 cells at the beginning and end of the co-culture show that almost all the UVB-exposed BL2 cells underwent apoptosis during the course of the assay. In contrast, only half of the untreated BL2 cells, and 2-3% of the Bcl-2-transfected cells underwent apoptosis during the assay (Figure 4.10a).

Figure 4.10b compares the gene expression of Gas6, Mrc1, Cd36, Pparg, Timp2, Tnf, and Il6 for IFN-γ and LPS-activated macrophages stimulated with or without apoptotic or untreated BL2 cells. As shown before, Gas6, Mrc1, Cd36, Pparg, and Timp2 expression was significantly down-regulated upon IFN-γ and LPS-stimulation, but this was significantly reversed when the macrophages were co-cultured with apoptotic cells following classical activation. This reversal was found to be specific to co-culture with apoptotic cells, as co-culture with unstimulated BL2

or Bcl-2-transfected cells did not significantly affect the down-regulation of IFN-γ and LPS-stimulated macrophages. Only for Pparg could untreated BL2 cell cultures, of which half the cells would undergo apoptosis during the course of the assay, also up-regulate Pparg expression, but Bcl-2-transfected cells could not.

Similar results were obtained for the gene expression of inflammatory cytokines Tnf and Il6 (Figure 4.10b). Both genes were shown to be up-regulated by IFN-γ and LPS-stimulation, but expression was reduced when this classical stimulus was followed by co-culture with apoptotic cells. Co-culture with unstimulated BL2 or Bcl-2-transfected cells could not reduce Tnf expression. Moreover, untreated BL2 and Bcl-2-transfected cells even significantly increased the expression of Tnf by classically-activated BMDM. For Il6 even co-culture with untreated BL2 and Bcl-2-transfected cells could significantly decrease Il6 expression, but it seemed to follow a trend with a higher decrease in Il6 expression when there were more apoptotic cells in the co-culture cells, and expression of Il6 of classically-activated BMDM co-cultured with BL2 or Bcl-2-tranfected BL2 cells was significantly different from those co-cultured with apoptotic cells.

The release of the cytokines TNFα and IL-6 by macrophages under the different culture conditions was then tested using a cytokine bead array kit and results are shown in Figure 4.10c. Levels of TNFα and IL-6 released by untreated BMDM were below detection levels, but IFN-γ and LPS-activated BMDM released both TNFα and IL-6. Interestingly, not only apoptotic BL2 cells, but also untreated and Bcl2-transfected BL2 cells could bring down the TNFα and IL-6 levels of IFN-γ and LPS-activated BMDM. As a control, IL-6 and TNFα release from apoptotic, untreated, and Bcl-2-transfected BL2 cells was also tested, but no expression above the detection level was observed (not shown).

The same experiment was repeated with λ-MYC cells for the genes that were found to be down-regulated by classically-activated BMDM upon co-culture with apoptotic lymphoma cells. However, as Bcl-2-transfected λ-MYC cells were not available, the effect of apoptotic cells on IFN-γ and LPS-stimulated macrophages was only

compared to untreated λ-MYC cells. However, λ-MYC cells show high levels of spontaneous apoptosis (Figure 4.11a). The experiment was only done twice, but no differences were observed for the expression of Axl, Plau, Tnf, or Il6. For Plau, interestingly, co-culture with untreated λ-MYC cells appeared to decrease expression of Plau even further than co-culture with apoptotic cells did (Figure 4.11b).

To verify these results at the protein level, the release of the cytokines TNFα and IL-6 was tested for IFN-γ and LPS-stimulated BMDM co-cultured with apoptotic λ-MYC cells as well. Similarly, not only apoptotic, but also untreated λ-MYC cells appeared to bring down the TNFα and IL-6 levels of IFN-γ and LPS-activated BMDM (Figure 4.11c). Apoptotic or untreated λ-MYC cells alone could not induce release of TNFα or IL-6 (not shown).

All primers had been selected based on the prediction that they would not pick up mRNA of human genes. However, to test that this was indeed the case, gene expression of these genes was also measured in apoptotic and untreated BL2 cells and Bcl-2-transfected cells using the same primers. Because the housekeeping genes were also specific for murine genes (and no expression was detected in any of the BL2 cells), the expression of each gene by the lymphoma cells was depicted relative to expression of the same amount of cDNA from IFN-γ and LPS-stimulated BMDM (Figure 4.12a). For most genes no expression was detected above the detection threshold of the assay, or very small amounts were measured, which could be considered insignificant compared to the expression measured from classically-stimulated macrophages.

Because the primers used for detecting gene expression in the macrophages could potentially also pick up expression by murine λ-MYC cells with the apoptotic cells, expression of each gene was also tested in the λ-MYC cells, but here also only very low amounts were detected (Figure 4.12b).

The results presented here show that co-culture with apoptotic lymphoma cells, but not viable lymphoma cells, could increase the expression of TAM genes Timp2,

Cd36, Pparg, and Gas6 in classically-activated BMDM. Furthermore, the expression of Tnf and Il6 is decreased by co-culture of classically-activated BMDM with apoptotic cells, but not by viable cells (Tnf) or only partially (Il6). No differences in effect between apoptotic and untreated λ-MYC cells were observed and both can decrease the expression of Axl, Plau, Tnf, and Il6 by classically-activated macrophages.

Surprisingly, cytokine release by classically-activated BMDM stimulated with apoptotic or viable lymphoma cells did not follow the same trend as their gene expression. There could be a timing issue here, and TNFα and IL-6 cytokine release measured at a later time point might reflect gene expression better. Another possibility is that BL2 cells were interacting with TNFα or IL-6, thereby obscuring the cytokine release measured. To this end, apoptotic and untreated lymphoma cells were co-cultured with 0, 190, or 951 pg/ml TNFα or IL-6 for 24 hours before levels of TNFα and IL-6 were measured in the supernatants (Figure 4.13). Similar cytokine levels were detected for cytokines alone or for those in cultures with apoptotic or untreated lymphoma cells. This suggests that the discrepancy between IL-6 and TNFα expression results at the gene level compared to the protein level are most likely not due to viable cells interacting with released cytokines.

a

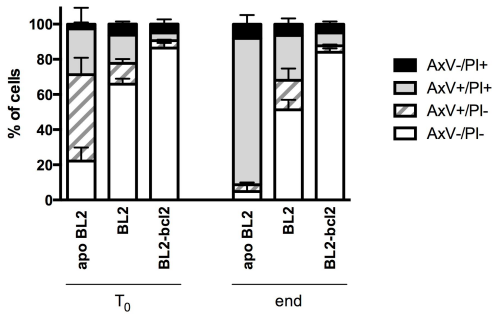

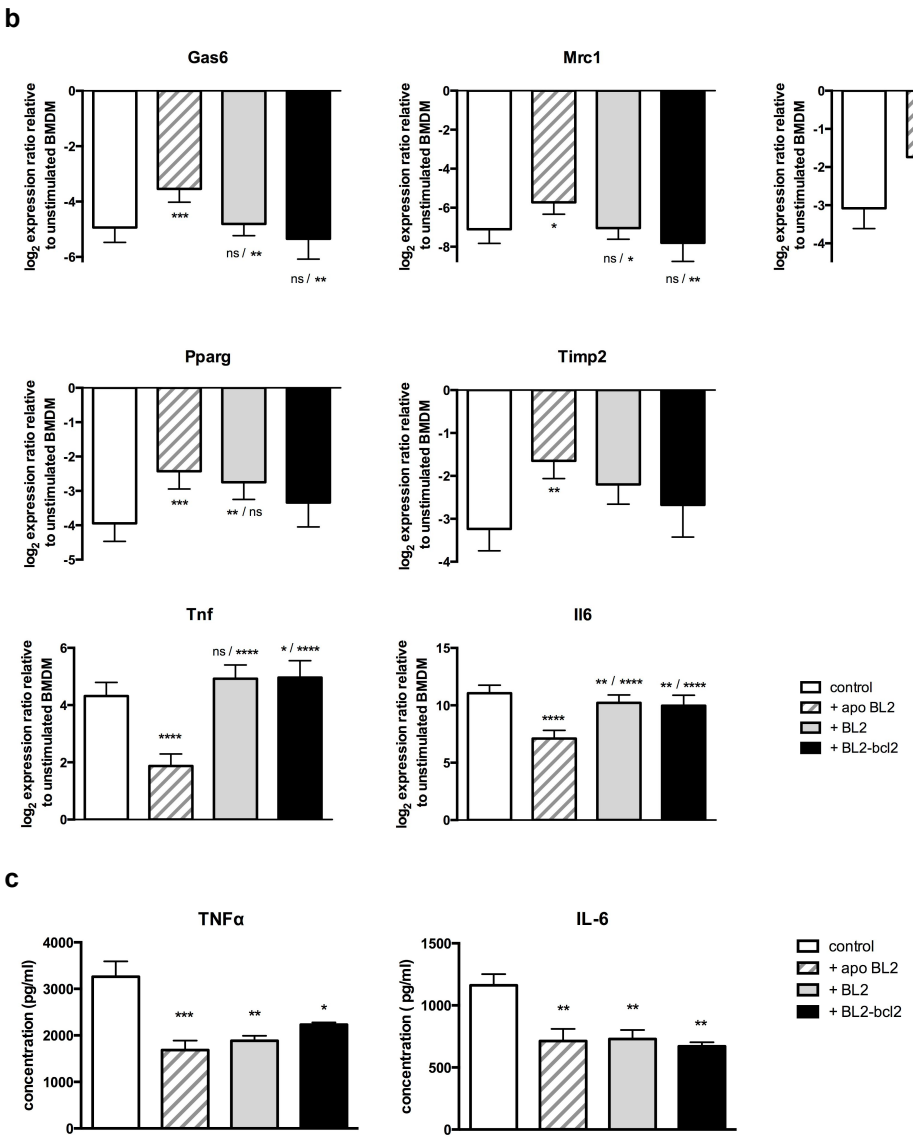

Figure 4.10 – Co-culture with apoptotic BL2 cells, but not viable BL2 cells, affects the phenotype of classically-activated macrophages.
4-hour IFN-γ + LPS-stimulated Balb/c BMDM (control) were co-cultured for 24 hours with apoptotic (apo BL2), untreated BL2, or untreated Bcl-2-transfected BL2 cells. Apoptosis of the BL2 cells was triggered by 100mJ UVB irradiation. (a) Assessment of BL2 cell viability was assessed by flow cytometry by simultaneous staining for Annexin V (AxV) and propidium iodide at the time BL2 cells were added to the macrophages (T_0) and at the end of the assay (end). Data are means + SEM. (b) mRNA expression of selected genes was assessed following co-culture and normalized using the reference genes Tuba1b, Hsp90, Hprt, and B2m. Expression is presented as as log[2] ratio relative to unstimulated BMDM. Data are means ± SEM for n=6 for all treatments, except n=4 for Bcl-2-tranfected cells. Statistical analysis was performed on the raw data using one-way ANOVA with Tukey's multiple comparisons test and are shown first compared to "control" and second to "+ apo BL2 cells". * $p<0.05$, ** $p<0.01$, *** $p<0.001$, **** $p<0.0001$. (c) Release of TNFα and IL-6 cytokines into the supernatant at the end of the assay was assessed using a cytometric bead array kit. Data are means + SEM for n=6, except n=4 for BL2-transfected cells. Statistical analysis was performed using one-way ANOVA with Tukey's multiple comparisons test and are shown compared to "control". * $p<0.05$, ** $p<0.01$, *** $p<0.001$.

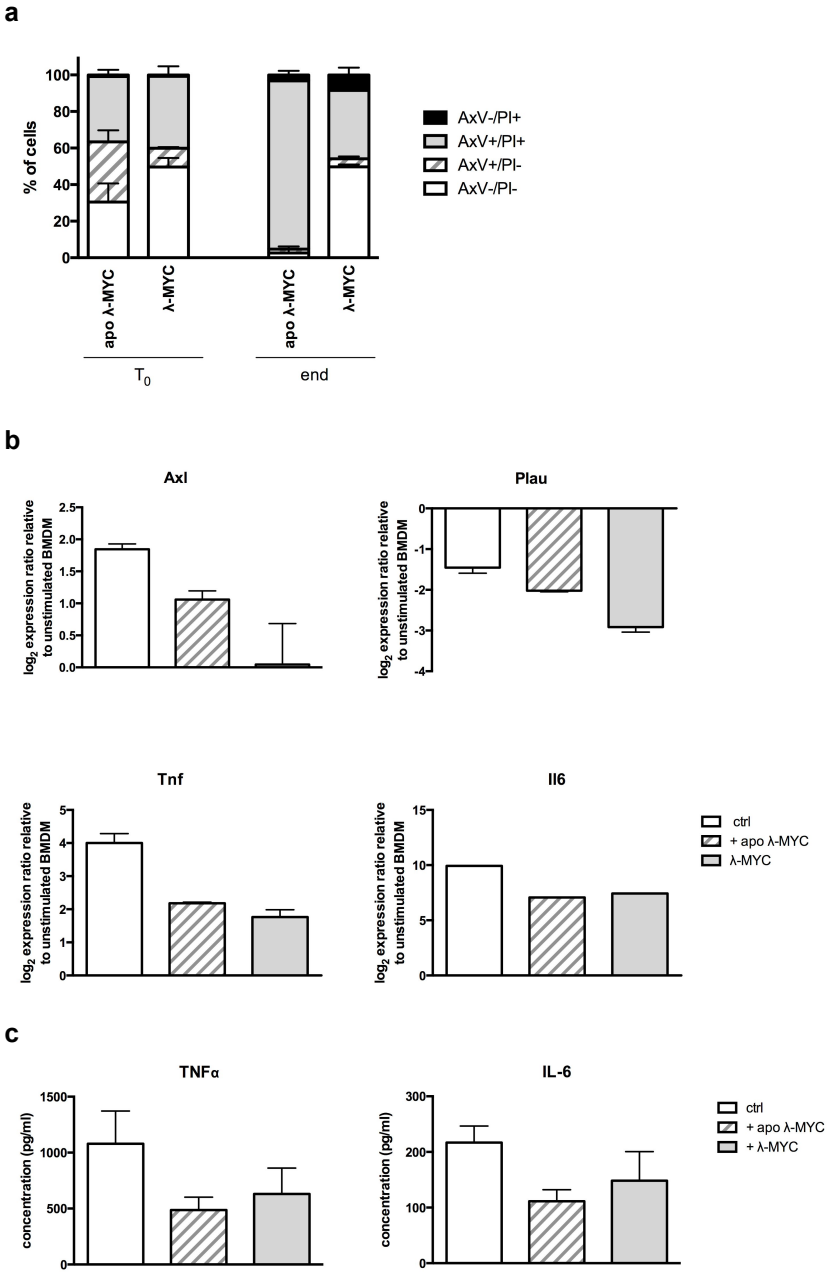
a
% of cells
AxV-/PI+
AxV+/PI+
AxV+/PI-
AxV-/PI-
apo λ-MYC
λ-MYC
T0
end
b
Axl
Plau
Tnf
Il6
log2 expression ratio relative to unstimulated BMDM
ctrl
+ apo λ-MYC
λ-MYC
c
TNFα
IL-6
concentration (pg/ml)
ctrl
+ apo λ-MYC
+ λ-MYC

Figure 4.11 - Gene expression responses of classically-activated macrophages to co-culture with apoptotic and viable MYC-Ed1 cells

4-hour IFN-γ + LPS-stimulated C57BL/6 BMDM were co-cultured for 24 hours with apoptotic or untreated λ-MYC cells. Apoptosis of the λ-MYC cells was triggered by 100mJ UVB irradiation. (a) Assessment of λ-MYC cell viability was assessed by flow cytometry by simultaneous staining with Annexin V (AxV) and propidium iodide at the time λ-MYC cells were added to the macrophages (begin) and at the end of the assay (end). Data are means + SEM. (b) mRNA expression of selected genes was assessed by qPCR following co-culture and normalized using the reference genes Tuba1b, Hsp90, Hprt, and B2m. Expression is presented as log[2] ratio relative to unstimulated BMDM. Data are means ± SEM for n=2 for all treatments, except n=1 for Il6. (c) Release of TNFα and IL-6 cytokines into the supernatant at the end of the assay was assessed using a cytometric bead array kit. Data are means + SEM for n=2.

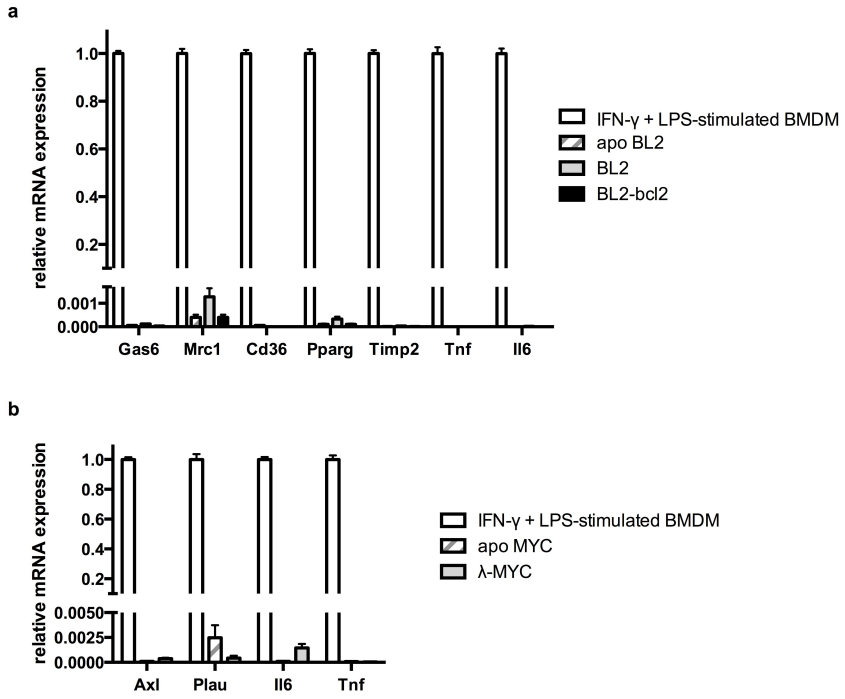

Figure 4.12 - mRNA expression of apoptotic lymphoma cells compared to IFN-γ and LPS-stimulated BMDM.

mRNA expression of selected genes by control apoptotic and untreated (a) BL2 cells and (b) λ-MYC cells from co-culture assays was assessed by qPCR and compared to expression by IFN-γ and LPS-stimulated BMDM. Expression by lymphoma cells is presented relative to expression by IFN-γ and LPS-stimulated BMDM when equal amounts of cDNA were analysed. Data are means + SEM for two independent experiments.

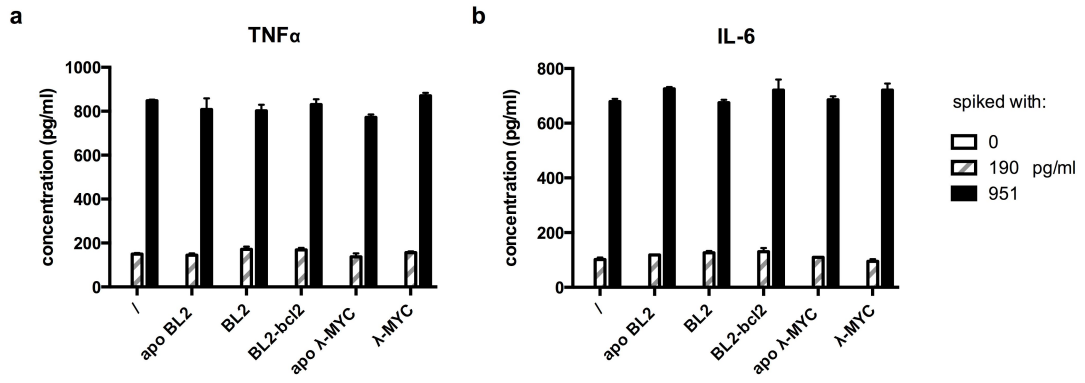

Figure 4.13 – Cytokine concentrations of apoptotic and viable lymphoma cells spiked with TNFα and IL6.
Apoptotic or viable BL2 and MYC cells were incubated with 0, 190, or 951 pg/ml TNFα or IL-6 for 24 hours after which concentrations of (a) TNFα and (b) IL-6 were assessed. Data are means + SEM for two independent experiments.

4.2.7 Some TAM genes are regulated by direct interaction with apoptotic cells and others by soluble factors released from apoptotic cells

Next it was investigated if the effects of co-culture with apoptotic cells on gene expression by classically-activated BMDM as observed for a subset of starry-sky TAM and inflammatory genes was due to the release of signalling molecules from apoptotic cells or whether macrophage-apoptotic cell interaction was necessary. To this end, similar assays were carried out, but IFN-γ and LPS-stimulated BMDM were co-cultured either directly with apoptotic or untreated lymphoma cells in the same well, or the macrophages and lymphoma cells were separated by a 0.44μm pore-size membrane, which allows small soluble particles to pass, but not cells. The results for classically-activated BMDM co-cultures with BL2 cells are shown in Figure 4.14. No significant differences of expression were observed for Gas6, Mrc1, Cd36, Timp2, Tnf, and Il6, between co-cultures with or without the membrane, suggesting that the effects that co-culture with apoptotic cells were due to soluble particles released from apoptotic cells. In contrast, co-culture of classically-activated BMDM with apoptotic cells in the presence of the membrane, inhibited the reduction in Pparg expression, suggesting that the effect here is due to direct contact between apoptotic cells and macrophages. Furthermore, cytokine expression of TNFα was

also not affected by the separation of BMDM and apoptotic cells during co-culture, but cytokine expression of IL-6 was.

This experiment was also repeated with λ-MYC cell co-cultures. It was only done twice, but the presence of the membrane did not appear to affect expression of any of the genes tested, including Axl, Plau, Tnf, and Il6, and neither was cytokine expression of TNFα or IL-6 affected.

From these experiments it can be concluded that macrophage-apoptotic cell contact was necessary to induce changes in Pparg expression in classically-activated macrophages, but that soluble factors released from apoptotic cells were most likely responsible for changes in Gas6, Mrc1, Cd36, Timp2, and Tnf expression. Further testing is needed to elucidate if apoptotic cell contact is necessary to affect Il6 expression.

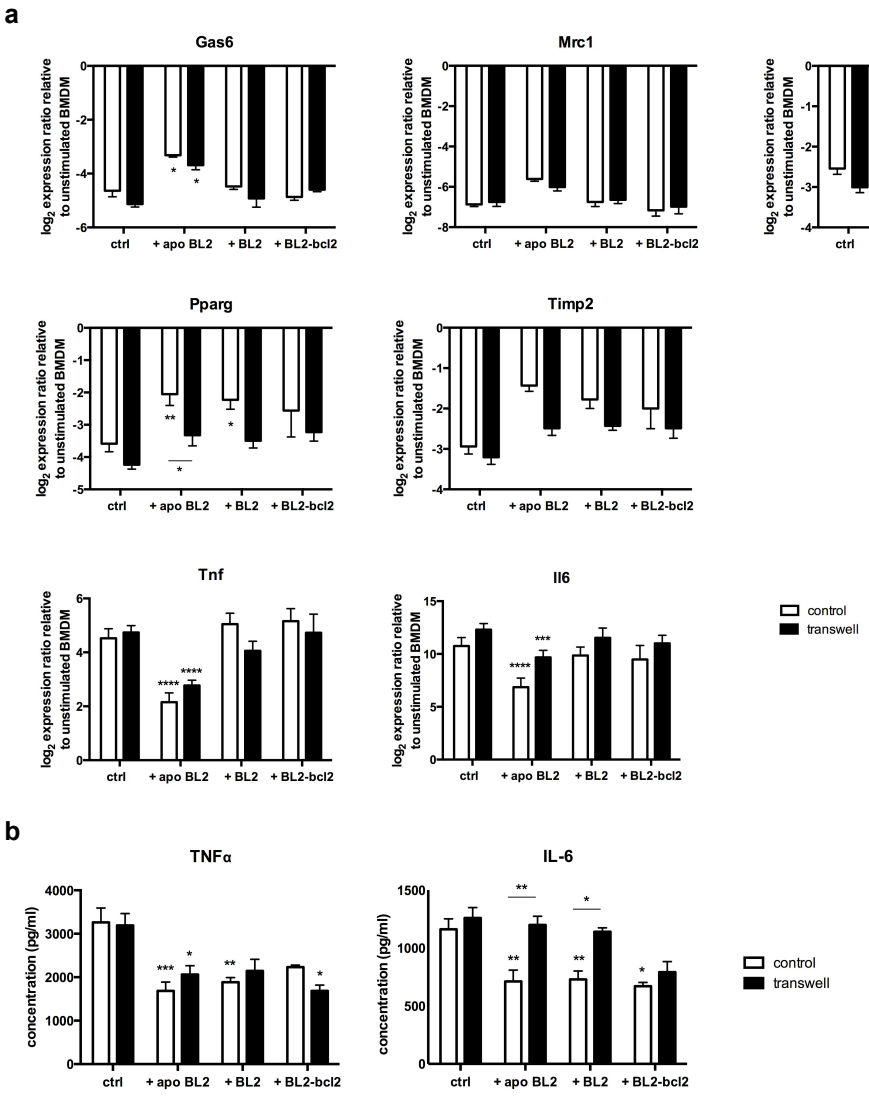

Figure 4.14 – Separation of apoptotic lymphoma cells and classically-activated macrophages during co-culture affects Pparg signalling and release of IL-6.
4-hour IFN-γ + LPS-stimulated Balb/c BMDM were co-cultured for 24 hours with apoptotic or untreated BL2 or untreated Bcl-2-transfected cells, either added directly to the macrophages, or separated by a 0.44μm transwell. Apoptosis of the BL2 cells was triggered by 100mJ UVB irradiation. (a) mRNA expression of selected genes was assessed following co-culture and normalized using the reference genes Tuba1b, Hsp90, Hprt, and B2m. Expression is presented as log[2] ratio relative to unstimulated BMDM. Data are means ± SEM for n=4 for all treatments, except n=2 for Bcl-2-transfected cells. Statistical analysis was performed on the raw data using two-way ANOVA with Tukey's multiple comparisons test. * $p<0.05$, ** $p<0.01$, *** $p<0.001$, **** $p<0.0001$. (b) The release of TNFα and IL-6 cytokines by BMDM was assessed using a cytometric bead array kit. Data are means ± SEM for n=4, except n=2 for Bcl-2-transfected cells. Statistical analysis was performed using two-way ANOVA with Tukey's multiple comparisons test. * $p<0.05$, ** $p<0.01$, *** $p<0.001$.

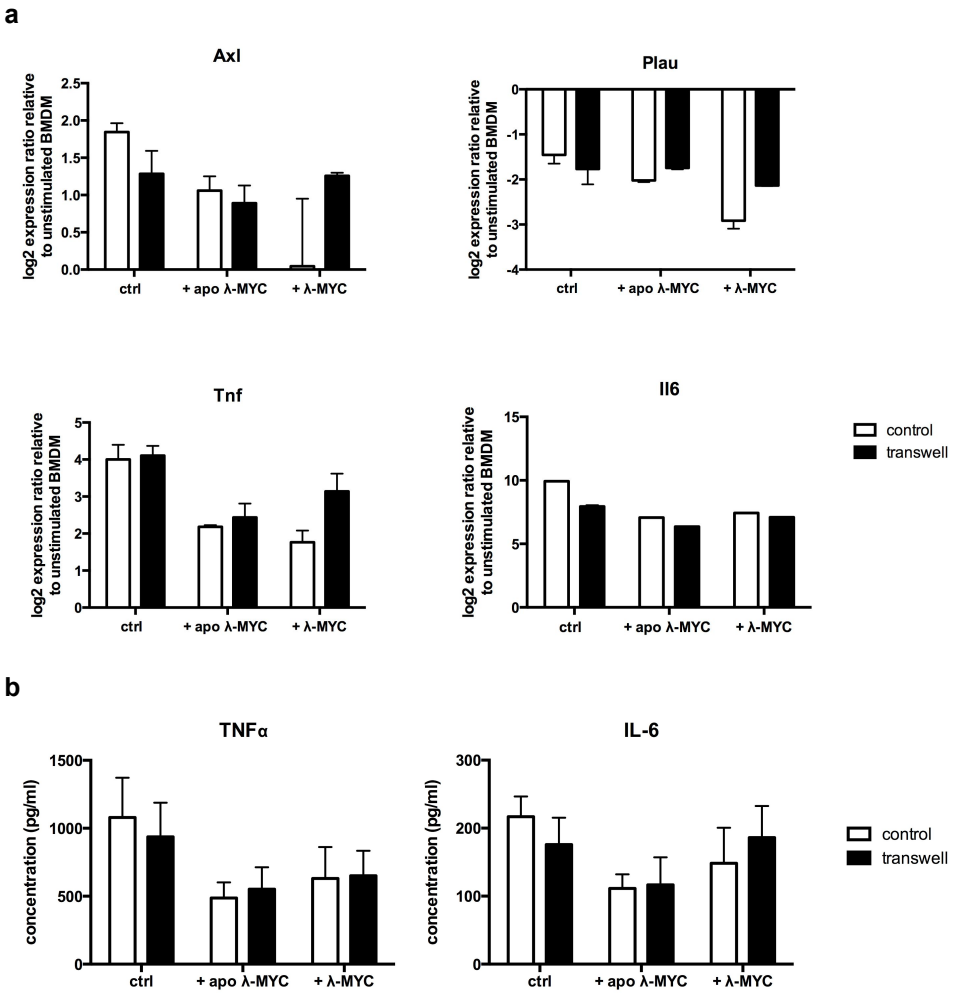

Figure 4.15 – Gene and cytokine expression responses of classically-activated macrophages to co-culture with apoptotic or untreated λ-MYC cells in the absence or presence of a transwell

4-hour IFN-γ + LPS-stimulated C57BL/6 BMDM were co-cultured for 24 hours with apoptotic or untreated λ-MYC cells, either added directly to the macrophages, or separated by a 0.44μm transwell. Apoptosis of the λ-MYC cells was triggered by 100mJ UVB irradiation. (a) mRNA expression of selected genes was assessed following co-culture and normalized using the reference genes Tuba1b, Hsp90, Hprt, and B2m. Expression is presented as log[2] ratio relative to unstimulated BMDM. Data are means ± SEM for n=2, except n=1 for Il6. (b) The release of TNFα and IL-6 cytokines by BMDM was assessed using a cytometric bead array kit. Data are means ± SEM for n=2.

4.2.8 Investigation into macrophage receptors involved in gene expression effects induced by apoptotic cell co-culture

Many receptors are involved in the recognition of apoptotic cells and factors released from apoptotic cells. In our published *in vivo* studies, IL-4Rα KO mice were found to show delayed tumour growth in the λ-MYC tumour model (Ford *et al.*, 2015).

Therefore it was investigated whether this was (partially) mediated through the lack of IL-4Rα expression on the macrophages in these tumours through prevention of the up-regulation of starry-sky TAM genes by apoptotic cells. Classically-activated WT or IL-4Rα KO C57BL/6 BMDM were co-cultured with apoptotic BL2 or λ-MYC cells. Expression levels are shown relative to control IFN-γ and LPS-stimulated cells, but no differences were observed between WT and IL-4Rα KO BMDM (Figure 4.16 and Figure 4.17). Furthermore, TNFα and IL-6 cytokine release was assessed, but no differences were observed in their expression either (Figure 4.18).

In addition, expression of genes associated with IL-4Rα-dependent 'alternative activation' in starry-sky TAM compared to germinal center macrophages was investigated, including the expression of Arg1, Retnla, Lyve1, Chil1, Ccl7, Mrc1, Ccl2 (Wang and Joyce, 2010; DeNardo *et al.*, 2009). Only expression of Mrc1 was found to be up-regulated in starry-sky TAM. Furthermore, all genes except for Mrc1 were expressed at low levels (Figure 4.19). Together these findings strongly suggest that IL-4Rα does not play a role in regulating starry-sky TAM activation.

Secondly, the role of galectin-3 in starry-sky TAM activation was investigated. Galectin-3 is a β-galactoside-binding lectin that is highly expressed and secreted by macrophages, and is up-regulated when monocytes differentiate into macrophages (Liu *et al.*, 1995). Preliminary studies in our laboratory have demonstrated a reduced ability of galectin-3 knockout (LGALS3 KO) mice to produce tumours in the λ-MYC murine lymphoma model. Thus it was investigated whether the lack of galectin-3 could affect gene expression of classically-activated macrophages induced by apoptotic cells. No differences were found in the gene expression of TAM-genes or cytokine expression of TNFα and IL-6 in LGALS3 KO BMDM compared to WT, suggesting that galectin-3 may not play a role in the activation signature of TAM (Figure 4.20).

Additionally, the ability of LGALS3 KO BMDM to interact and engulf apoptotic BL2 cells was investigated. Results are presented in Figure 4.21. No difference was observed in interaction, but LGALS3 KO BMDM had a significantly reduced ability

to phagocytose apoptotic cells. These findings are in agreement with published studies that galectin-3-deficient cells exhibited reduced phagocytosis of apoptotic thymocytes *in vitro* and attenuated clearance of apoptotic thymocytes by peritoneal macrophages *in vivo* (Sano *et al.*, 2003). Similar observations were made for LGALS3 KO BMDM interaction with and engulfment of apoptotic λ-MYC cells (Figure 4.22). Interestingly, although only tested once, classical activation of LGALS3 KO BMDM also appeared to increase the macrophages' ability to phagocytose apoptotic cells (Figure 4.23).

These latter results suggest that IFN-γ and LPS-stimulation of BMDM may be able to restore the reduced phagocytic ability induced by loss of galectin-3. Therefore, the gene and cytokine expression responses of apoptotic cells cultured with classically-activated macrophages presented here may not fully reflect the effects of apoptotic cells on macrophages in tumour models in LGALS3 KO mice.

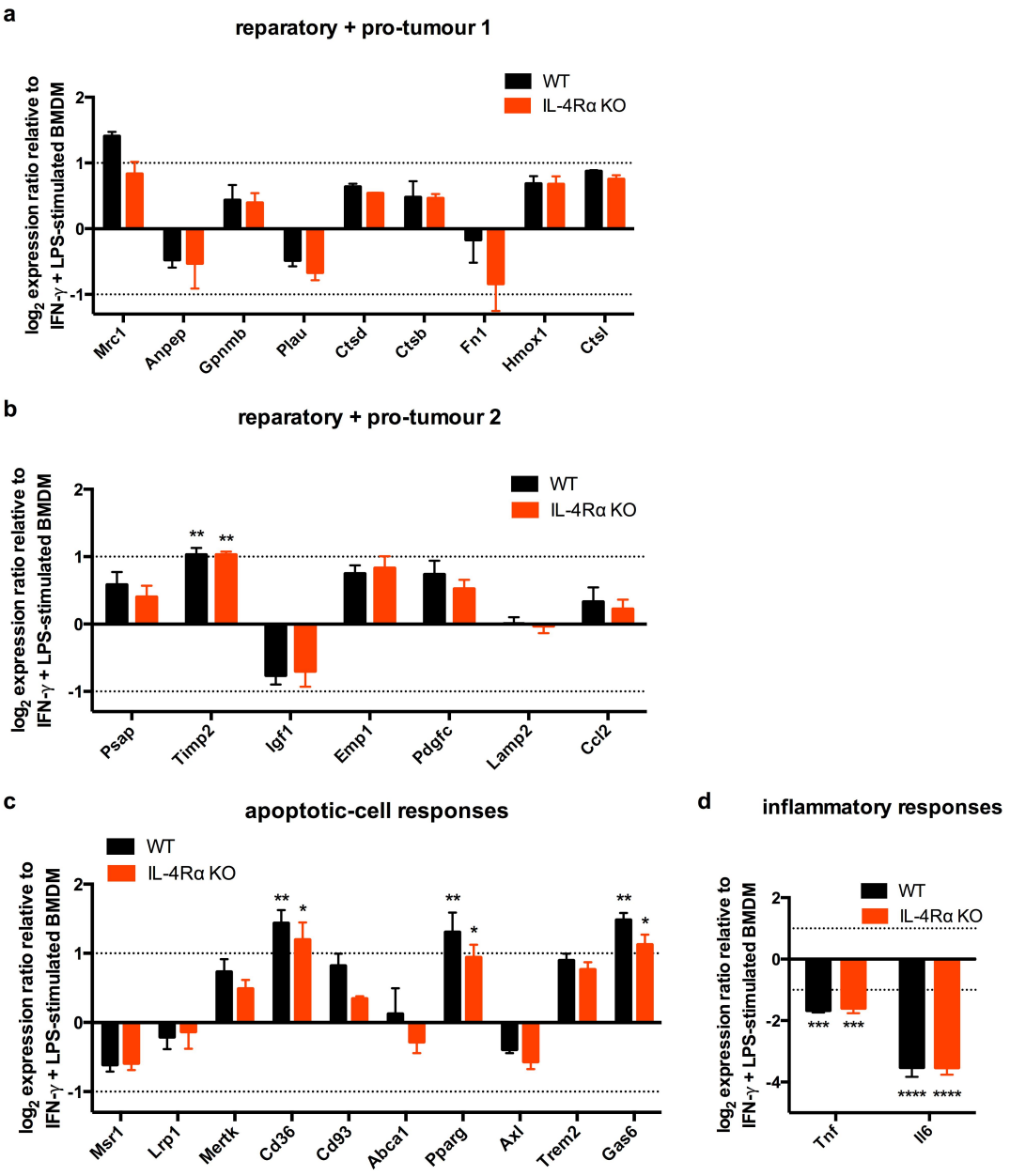

Figure 4.16 - Loss of IL-4Rα does not affect starry-sky TAM gene expression of classically-activated BMDM co-cultured with apoptotic BL2 cells.
4-hour IFN-γ + LPS-stimulated BMDM from WT or IL-4Rα knockout C57BL/6 mice were co-cultured for 24 hours with or without apoptotic BL2 cells. Apoptosis of the BL2 cells was triggered by 100mJ UVB irradiation. (a-d) mRNA expression of selected genes was assessed following co-culture and normalized using the reference genes Tuba1b, Hsp90, Hprt, and B2m. Expression is presented for "IFN-γ + LPS-stimulated BMDM + apo BL2" as log[2] ratio relative to "IFN-γ + LPS-stimulated BMDM". Data are means ± SEM for n=2-5. Statistical analysis was performed on the raw data using two-way ANOVA with Tukey's multiple comparison test and is shown for "IFN-γ + LPS-stimulated BMDM + apo BL2" versus 4-hour IFN-γ + LPS-stimulated BMDM. *p<0.05, **p<0.01, ***p<0.001, ****p<0.0001. No significant differences between WT and IL-4Rα were observed.

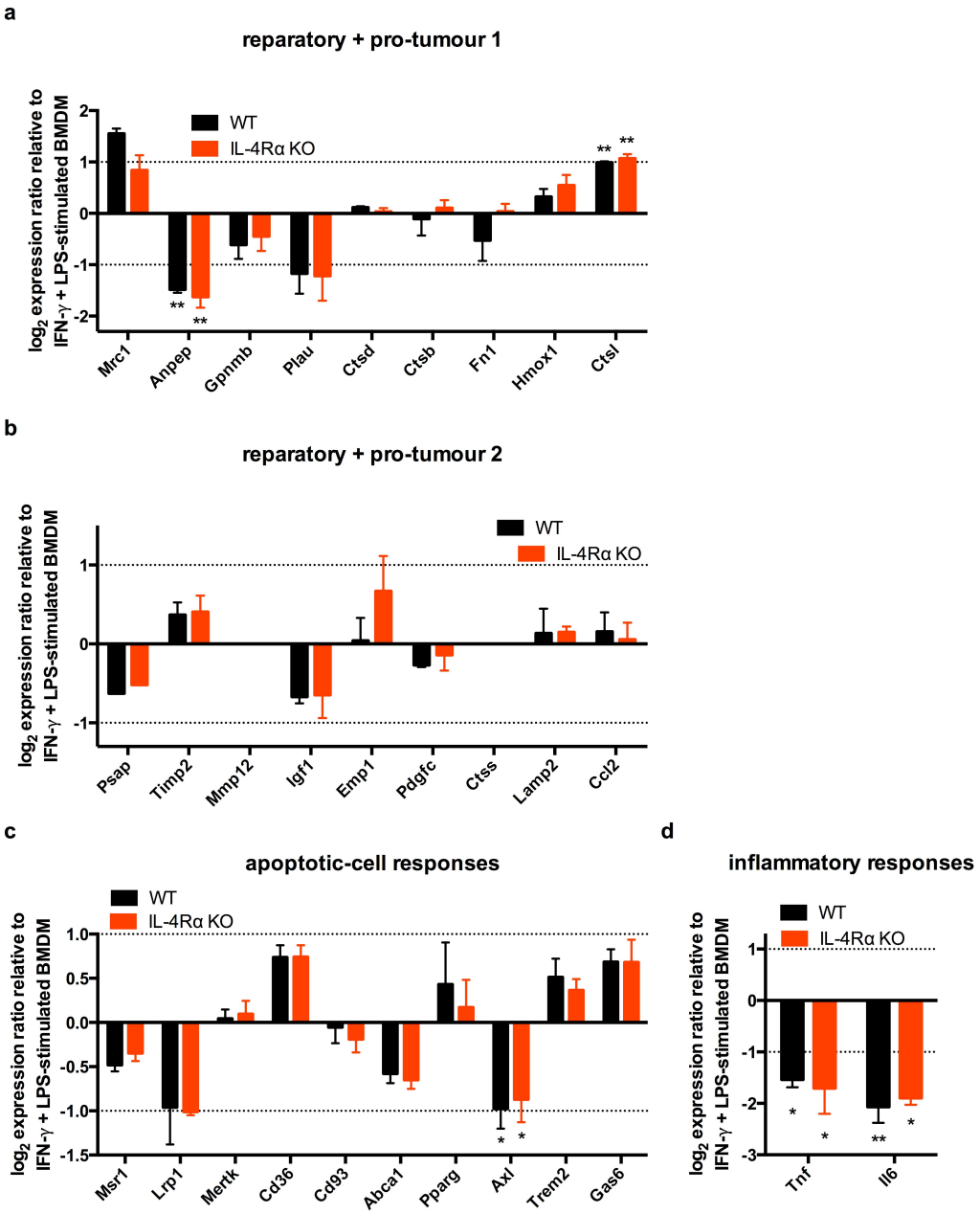

Figure 4.17 – Loss of IL-4Rα does not affect starry-sky TAM gene expression of classically-activated BMDM co-cultured with apoptotic λ-MYC cells.
4-hour IFN-γ + LPS-stimulated BMDM from WT or IL-4Rα knockout C57BL/6 mice were co-cultured for 24 hours with or without apoptotic λ-MYC cells. Apoptosis of the λ-MYC cells was triggered by 100mJ UVB irradiation. (a-d) mRNA expression of selected genes was assessed following co-culture and normalized using the reference genes Tuba1b, Hsp90, Hprt, and B2m. Expression is presented for "IFN-γ + LPS-stimulated BMDM + apo λ-MYC" as log[2] ratio relative to "IFN-γ + LPS-stimulated BMDM". Data are means ± SEM for n=2-5. Statistical analysis was performed on the raw data using two-way ANOVA with Tukey's multiple comparison test and is shown for "IFN-γ + LPS-stimulated BMDM + apo λ-MYC" versus 4h IFN-γ + LPS-stimulated BMDM. *p<0.05, **p<0.01. No significant differences between WT and IL-4Rα were observed.

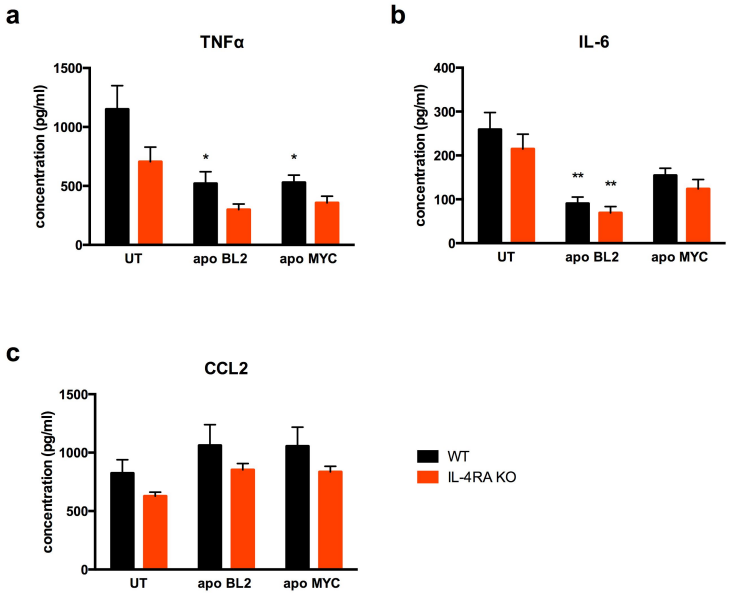

Figure 4.18 – Loss of IL-4Rα does not affect inflammatory cytokine expression of classically-activated BMDM co-cultured with apoptotic lymphoma cells.
4-hour IFN-γ + LPS-stimulated BMDM from WT or IL-4Rα knockout C57BL/6 mice were co-cultured for 24 hours with or without apoptotic BL2 or apoptotic λ-MYC cells. Apoptosis of the BL2 and λ-MYC cells was triggered by 100mJ UVB irradiation. Release of (a) TNFα, (b) IL-6, and (c) CCL2 cytokines by BMDM was assessed using a cytometric bead array kit. Data are means ± SEM for n=5-6. Statistical analysis was performed using two-way ANOVA with Tukey's multiple comparison test. *$p<0.05$ and **$p<0.01$.

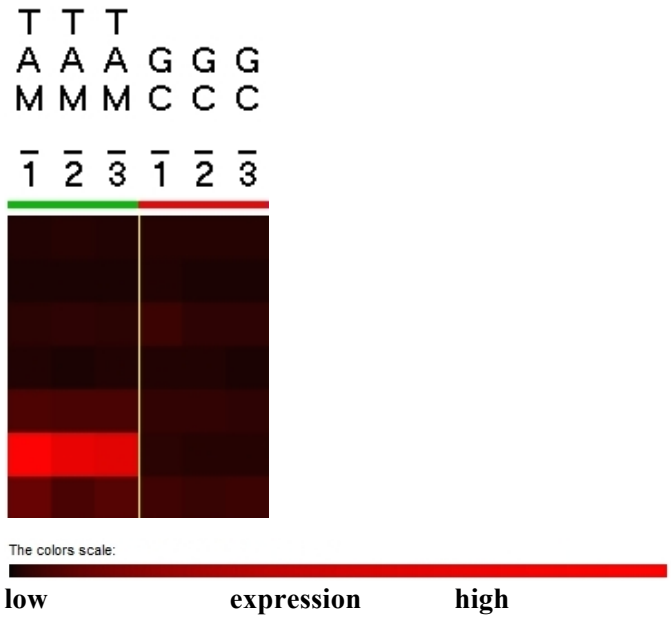

Figure 4.19 – Heat map comparing murine mRNA expression of alternative activation genes of starry- sky TAM and GC macrophages.
Gene expression comparison of selected 'alternative activation' genes for laser-captured micro-dissected starry-sky TAM and GC macrophages. Intensities shown are of normalised data.

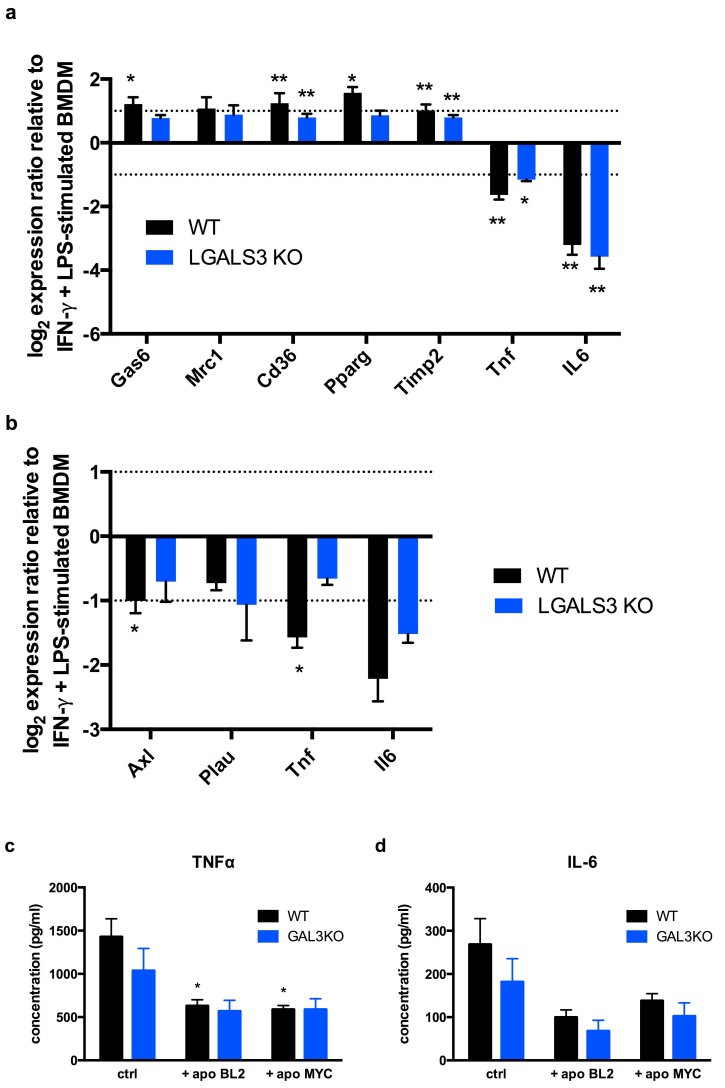

Figure 4.20 – Loss of galectin-3 does not affect activation of classically-activated BMDM co-cultured with apoptotic lymphoma cells.
4-hour IFN-γ + LPS-stimulated BMDM from WT or LGALS3 knockout C57BL/6 mice were co-cultured for 24 hours with or without apoptotic (a) BL2 or (b) λ-MYC cells. Apoptosis of the λ-MYC cells was triggered by 100mJ UVB irradiation. (a-b) mRNA expression of selected genes was assessed following co-culture and normalized using the reference genes Tuba1b, Hsp90, Hprt, and B2m. Expression is presented for "IFN-γ + LPS-stimulated BMDM + apo λ-MYC" as log[2] ratio relative to "IFN-γ + LPS-stimulated BMDM". Data are means ± SEM for n=4. Statistical analysis was performed on the raw data using two-way ANOVA with Tukey's multiple comparison test and is shown for "IFN-γ + LPS-stimulated BMDM + apo" versus 4h IFN-γ + LPS-stimulated BMDM. *p<0.05, **p<0.01. Release of (c) TNFα and (d) IL-6 cytokines by BMDM was assessed using a cytometric bead array kit. Data are means ± SEM for n=4. Statistical analysis was performed using two-way ANOVA with Tukey's multiple comparison test. *p<0.05. No significant differences between WT and LGALS3 KO BMDM were observed.

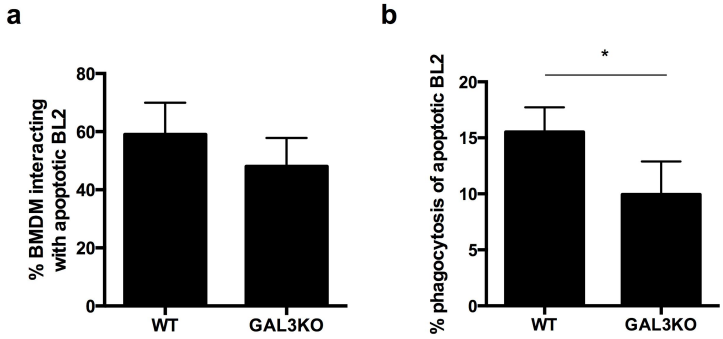

Figure 4.21 – GAL3KO BMDM have a decreased ability to phagocytose apoptotic BL2 cells.
7-day matured WT and GAL3KO BMDM were assessed for their ability to (a) interact with and (b) phagocytose apoptotic BL2 cells in a microscopy-based phagocytosis assay. Data are means + SEM for the percentage of BMDM demonstrating interaction or phagocytosis of apoptotic BL2 cells and untreated controls (n=4). Statistical analysis was performed using a paired t test. *p<0.05.

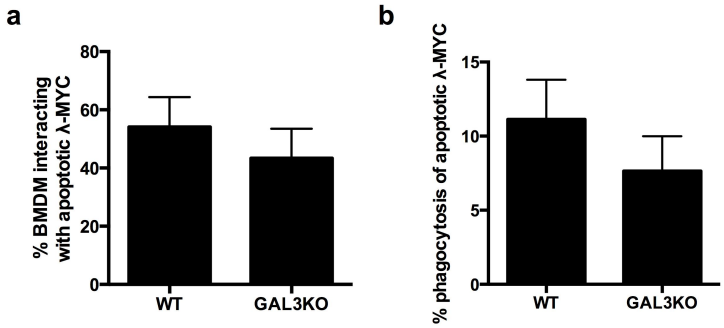

Figure 4.22 – GAL3KO BMDM have a decreased ability to phagocytose apoptotic λ-MYC cells.
7-day matured WT and GAL3KO BMDM were assessed for their ability to (a) interact with and (b) phagocytose apoptotic λ-MYC cells in a microscopy-based phagocytosis assay. Data are means + SEM for the percentage of BMDM demonstrating interaction or phagocytosis of apoptotic λ-MYC cells and untreated controls (n=2).

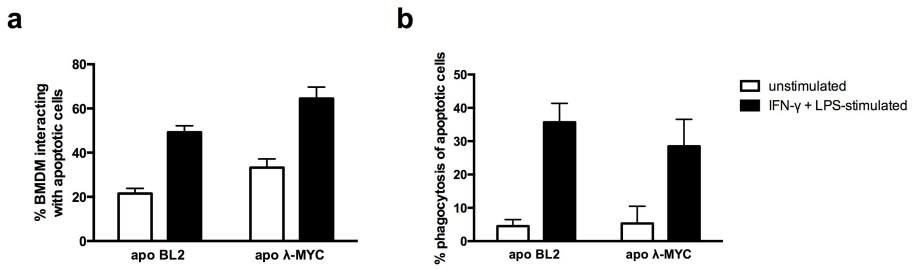

Figure 4.23 – IFN-γ and LPS stimulation enhances interaction and phagocytosis of apoptotic cells by LGALS3 KO BMDM.
7-day matured untreated and IFN-γ and LPS-stimulated GAL3KO BMDM were assessed for their ability to (a) interact with and (b) phagocytose apoptotic BL2 and λ-MYC cells in a microscopy-based phagocytosis assay. Data are means of duplicates ± s.d. for the percentage of BMDM demonstrating interaction or phagocytosis of apoptotic BL2 or λ-MYC cells and untreated controls for one experiment.

4.3 Discussion

Work described in this chapter investigated the role apoptotic cells play in shaping the phenotype of macrophages in the Burkitt's lymphoma tumour microenvironment. Published research by this laboratory investigated gene expression profiling of laser-captured starry-sky TAM to establish their activation signature *in situ*, and it was shown that TAM in this model of starry-sky NHL signalled via multiple tumour-promoting reparatory, trophic, angiogenic, tissue remodelling, and anti-inflammatory pathways. Furthermore, suppression of apoptosis in this model showed constrained tumour cell proliferation, reduced tumour angiogenesis, and reduced the accumulation of macrophages *in vivo* (Ford *et al.*, 2015). Apoptotic cells have been shown to modulate their tissue microenvironments and can inhibit immunological and inflammatory responses and promote signalling pathways by acting on phagocytes, notably macrophages (Sica *et al.*, 2008b; Allavena *et al.*, 2008; Mantovani *et al.*, 2002). Starry-sky TAM are found to have engulfed many apoptotic cells, and the work presented here contributed to the published research by investigating whether apoptotic cells can help drive starry-sky TAM signature (Ford *et al.*, 2015).

First the ability of 'young' and 'mature' ESDM and BMDM to respond to migratory signals and to phagocytose apoptotic cells was investigated. 'Young' macrophages were found to respond better to migratory signals, including supernatants from apoptotic cells. In contrast, 'mature' macrophages were better phagocytes, as a higher percentage of mature macrophages engulfed apoptotic cells. As both ESDM and BMDM mature in the presence of apoptotic cells, it is possible that apoptotic cell signalling and interaction with macrophages may influence the ability of macrophages to migrate towards and engulf apoptotic cells, as well as other aspects of its phenotype.

To further assess the effect of apoptotic cell interaction with macrophages on macrophage activation, the activation signature of starry-sky TAM from a murine model of Burkitt's lymphoma and a tumour model in which apoptosis of tumour cells was suppressed were compared. Primers were selected that would only recognize the expression of murine genes and gene expression was normalized against Csf1r expression, a macrophage marker, to account for the lower number of macrophages present in the tumour model in which apoptosis is suppressed (Ford *et al.*, 2015). However, although macrophages appear to be the dominant stromal cells present in starry-sky tumours and many of the genes of interest are known to be expressed by macrophages, these genes are not specific for macrophages, thus it should be kept in mind that some of the expression shown could potentially be from other stromal cells present in the tumour. The results were initially surprising, as they gave identical signatures of TAM in both tumour models. However, apoptosis is merely suppressed in the tumour cells in these models and not completely inhibited. Furthermore, apoptosis of other cells in the tumour environment cannot be ruled out. Moreover, although the number of macrophages accumulating in the apoptosis-suppressed tumour model is significantly lower, macrophages are still present, although they are generally smaller and have engulfed fewer apoptotic cells (Ford *et al.*, 2015). This suggests that the smaller number of TAM in these tumours could still be activated through the interaction with the smaller numbers of apoptotic cells present. Alternatively, the activation status of accumulated TAM could be independent from apoptosis and be attributable to other properties of the lymphoma

cells. In order to elucidate which of these possibilities is responsible for the starry-sky TAM activation signature, assays were carried out in which primary macrophages were co-cultured with apoptotic or untreated lymphoma cells and their activation status was assessed.

The use of primary cells was preferred over the use of macrophage-lineage cell lines derived from malignant tumours, as primary macrophages may more closely resemble their tissue counterparts. However, since macrophages are highly responsive to their environments, culture conditions may heavily affect their activation state. BMDM are cultivated in the presence of many apoptotic cells, which disappear by the end of the maturation period. It is highly likely that the interaction of macrophages in the culture with these apoptotic cells affects their activation state and could already induce expression of TAM genes. Furthermore, macrophage colony-stimulating factor 1 (CSF1) was added to the cultures, which is known to stimulate macrophage proliferation, differentiation and survival by signalling through the CSF1 receptor (Hume and MacDonald, 2012; Davies *et al.*, 2013). Additionally, *in vitro* data suggests that CSF1 stimulation may generate actively phagocytic macrophages, promote tissue repair and extracellular proteolysis, and suppress cell-mediated immunity (Hume and MacDonald, 2012), which are some of the same features associated with starry-sky TAM. Although some starry-sky TAM genes were found to be affected by apoptotic cell co-culture with BMDM, including up-regulation of Ccl2, and Hmox1, and down-regulation of Mmp12, Fn1, Plau, Anpep, Abca1, and Lrp1, taken together, this may explain why apoptotic cell co-culture with BMDM only had minimal effects on the expression of TAM signature genes, even when CSF1 was removed prior to the start of the assay. Alternatively, the possibility also remains that interaction with apoptotic cells does not affect BMDM activation.

Thus, as mature BMDM may already closely resemble starry-sky TAM, ideally less mature BMDM would be used to investigate if apoptotic cells can affect expression of starry-sky TAM genes. Unfortunately, there would not be enough macrophages to perform the assays if they were taken a few days earlier and a different approach was

sought. IFN-γ and LPS stimulation of macrophages is known to induce microbicidal and tumouricidal capacity, as well as pro-inflammatory signalling in macrophages, including expression of TNFα, IL-6, and IL-12 (Mantovani *et al.*, 2004a; Van Ginderachter *et al.*, 2006; Urban *et al.*, 1986; Mosser and Edwards, 2008). It was hypothesised that classical activation of macrophages could also reduce the expression of starry-sky TAM genes and indeed many TAM genes were found to be down-regulated upon activation with IFN-γ and LPS, including the reparatory and pro-tumour genes Mrc1, Plau, Ctsd, Fn1, Ctsl, Timp2, Igf1, and Emp1, as well as genes that are associated with apoptotic cell responses: Cd36, Pparg, Trem2, Gas6, and possibly Lrp1. In contrast, several genes that were found to be up-regulated in starry-sky TAM were also up-regulated upon classical activation, including the reparatory and pro-tumour genes Hmox1, Mmp3, and Ccl2, as well as the apoptotic cell response gene Msr1. In addition, as expected for classically-activated macrophages, expression of genes associated with inflammatory responses, including Tnf and Il6 was up-regulated, and the Arg1/Nos2 ratio was down-regulated.

Surprisingly, although many genes associated with apoptotic cell responses were down-regulated upon IFN-γ and LPS stimulation, phagocytosis of classically-activated BMDM was found to be increased compared to un-stimulated BMDM. This was not further investigated here, but a possible explanation is that although many of the genes here were found to be down-regulated, macrophages have redundant pathways for the recognition and engulfment of apoptotic cells and other genes associated with apoptotic cell clearance not investigated here may be up-regulated by classical activation.

The effect of interaction of apoptotic cells with classically activated macrophages was then assessed in co-culture assay and several TAM genes were found to be up-regulated by co-culture with apoptotic, but not with untreated or apoptosis-suppressed BL2 lymphoma cells. Subsequent assays in which a membrane was used to prevent cell-to-cell contact between macrophages and lymphoma cells, showed that expression of Gas6, Mrc1, Cd36, and Timp2 could be significantly up-regulated by co-culture with apoptotic BL2 cells, and that this was most likely mediated

through the release of soluble factors from apoptotic cells. In contrast, Pparg expression in classically-activated BMDM was only up-regulated if no membrane was present to separate the two cell types, thus suggesting that binding or engulfment of apoptotic cells was necessary to exert the effects on macrophage gene expression.

Co-culture of classically-activated BMDM with apoptotic λ-MYC cells was found to significantly decrease the expression of Axl, Plau, Anpep, and Mmp12. Delays with finding successful primers for Anpep and Mmp12 did not allow further investigation of those genes, but results as to whether the down-regulation of Axl and Plau was due to apoptotic-cell interaction were inconclusive as untreated λ-MYC, of which still large numbers of cells underwent apoptosis during the course of the assay, did have a similar effect on gene expression as apoptotic λ-MYC cells. Co-cultures performed in the presence of a transwell suggested that any observed affects were due to soluble factors released from the cells, as the presence of the membrane did not interfere in the reduction of gene expression.

Interestingly, the effect of apoptotic BL2 and λ-MYC cells on TAM genes expressed by classically-activated BMDM was not identical, suggesting that TAM in λ-MYC tumour models could differ from the starry-sky TAM signature identified in BL2 murine xenograft tumours.

Having established that apoptotic cells can affect gene expression of a small subset of TAM genes, two candidate receptors on macrophages were then assessed for their involvement. IL-4Rα and galectin-3 were selected as λ-MYC tumour models in mice in which these receptors were knocked out displayed slower tumour growth (Ford *et al.*, 2015) or reduced ability to establish tumours (unpublished findings), respectively, compared to WT mice. IL-4Rα is a component of the receptors for IL-4 and IL-13, and is necessary for alternative activation of macrophages (Colegio *et al.*, 2014; Wang and Joyce, 2010), as well as IL-4-induced proliferation of macrophages (Jenkins *et al.*, 2013). It was hypothesised that lack of either of these receptors would prevent apoptotic cell-mediated starry-sky TAM gene expression, which would cause the TAM to have a less pro-tumour phenotype, thereby slowing tumour growth down

or inhibiting it. Lack of IL-4Rα did not affect gene expression of starry-sky TAM genes or affect inflammatory cytokine expression. This indicated that tumour growth in these knockout models is down-regulated or inhibited through a different pathway. This was supported by the findings that several of the genes associated with an IL-4Rα-dependent or 'alternative activation' state, were expressed only at low levels by starry-sky TAM or not expressed at all.

Unstimulated BMDM lacking expression of galectin-3 were found to have a reduced ability to phagocytose apoptotic cells, as has been shown previously (Sano *et al.*, 2003). However, preliminary findings presented here suggest that classical activation can improve the phagocytic ability of galectin-3 deficient BMDM. Additionally, it has been shown that classical activation of macrophages by IFN-γ and LPS down-regulated galectin-3 expression (MacKinnon *et al.*, 2008). Together this may explain why no expression differences were observed between classically activated WT and LGALS3 KO BMDM in their responses to apoptotic lymphoma cells, including no differences in expression of Pparg, which was found to be dependent upon direct contact between macrophages and apoptotic cells. Time limitations prevented further exploration of the effect of apoptotic cell interaction on the phenotype of galectin-3 deficient unstimulated macrophages, but further studies will be necessary to deduce whether this may contribute to reduced tumour take rates for galectin-3 deficient mice.

In agreement with published findings (Voll *et al.*, 1997; Fadok *et al.*, 1998a), in addition to affecting expression of TAM genes, co-culture of classically-activated BMDM with apoptotic cells was also shown to reduce gene expression of the inflammatory cytokines Tnf and Il6, 3-fold and 4-18-fold, respectively. Tnf expression was solely inhibited by co-culture with apoptotic cells, as untreated or apoptosis-suppressed BL2 cells could not reduce expression. Il6 expression was also reduced by co-culture with untreated or apoptosis-suppressed BL2 cells, but this appeared to be to a lesser extend than the effect co-culture with apoptotic BL2 cells had, and expression by classically-activated BMDM co-cultured with untreated or Bcl-2-transfected lymphoma cells was significantly different than that from

classically-activated BMDM co-cultured with apoptotic BL2 cells. No differences in Tnf or Il6 expression were found for classically-activated BMDM co-cultured with apoptotic or untreated λ-MYC cells and both were capable of reducing expression. The reduction in expression of Tnf and Il6 induced by apoptotic cells appeared to be due to soluble factors released from the cells.

Interestingly, results from measurements of TNF and IL-6 cytokine release were not consistent with the gene expression results, and co-culture with apoptotic, untreated and apoptosis-suppressed cells was found to reduce release of TNF and IL-6 by classically-activated macrophages. Assessments of whether measurements were obscured by TNFα or IL-6 binding to viable lymphoma cells indicated that this was not the case. However, it has been shown that TNFα can bind to activated macrophages (Ichinose *et al.*, 1988), which was not investigated, and must be further analysed. Furthermore, transwell experiments suggested that cell-to-cell contact was necessary to reduce IL-6 release by classically-activated BMDM, but gene expression of IL-6 was not affected by the transwell. Further experiments need to be performed to elucidate whether only apoptotic cells or also viable lymphoma cells can reduce the expression of IL-6 and TNFα. Measurement of Tnf and Il6 gene expression and cytokine release at different time points during the assay may improve understanding of how their expression by classically-activated BMDM is regulated by apoptotic and/or viable cells.

In summary, it was shown in this chapter that co-culture of unstimulated and classically-activated BMDM with apoptotic lymphoma cells, but not viable lymphoma cells, can induce expression of various genes associated with the starry-sky TAM signature. Apoptotic cell co-culture up-regulated Ccl2 and Hmox1 gene expression by unstimulated BMDM, whereas classically-activated macrophages were found to up-regulate Gas6, Mrc1, Cd36, and Timp2 expression in response to co-culture with apoptotic cells. Pparg was only up-regulated by classically-activated macrophage when apoptotic cells were in direct contact with the macrophages. Furthermore, various genes were down-regulated by macrophages upon co-culture with apoptotic cells, including Fn1, Mmp12, Plau, Anpep, Abca1 and Lrp1 by

unstimulated macrophages, and Axl, Plau, Anpep and Mmp12 by classically-activated macrophages. Additionally, gene expression of the inflammatory cytokines Tnf and Il6 was up-regulated by classically-activated macrophages upon co-culture with apoptotic cells. Finally, investigation of the involvement of IL-4Rα and galectin-3 expressed by macrophages, showed that neither was involved in apoptotic-cell mediated activation of classically-activated macrophages, and IL-4Rα expression by macrophages did not affect apoptotic cell-induced activation of unstimulated macrophages. However, it was not tested if galectin-3 expression is necessary for apoptotic-cell mediated stimulation of unstimulated macrophages, and this will need to be investigated further.

Given the findings in this chapter that co-culture of classically-activated BMDM with apoptotic lymphoma cells could significantly reduce the gene and protein expression of inflammatory cytokines and the findings in Chapter 3 that pre-exposure of macrophages to apoptotic cells could reduce the cytotoxicity of macrophages induced by IFN-γ and LPS towards tumour cells, the effects of apoptotic cells on macrophage cytotoxicity were further investigated in Chapter 5.

Chapter 5 Apoptotic lymphoma cell interaction with macrophages stimulates tumour cell growth

5.1 Introduction

Results presented in Chapter 4 showed that co-culture of classically-activated macrophages with apoptotic cells, but not viable cells, could significantly increase gene expression of Timp2, Cd36, Mrc1, Pparg, and Gas6. Additionally, expression of anti-inflammatory cytokines Tnf and Il6 was found to be decreased upon co-culture with apoptotic cells. These findings are in line with previous reports that recognition and phagocytosis of apoptotic cells could suppress pro-inflammatory cytokine release *in vitro*, including release of IL-6, IL-8, IL-12, and TNFα (Voll *et al.*, 1997; Fadok *et al.*, 1998a). Additionally, engulfment of apoptotic cells by macrophages has been shown to cause the up-regulation and secretion of IL-10, TFG-β, platelet-activating factor (PAF), prostaglandins, and MMP12 and MMP2 (Voll *et al.*, 1997; Fadok *et al.*, 1998a; McDonald *et al.*, 1999; Ogden *et al.*, 2005; Ford *et al.*, 2015).

Results presented in Chapter 3 suggested that pre-exposure to apoptotic cells, but not supernatants from apoptotic cells, could reduce macrophage cytotoxicity induced by classical activation. These findings are in agreement with work published by Reiter et al. (1999), which showed that co-culture of apoptotic cells with BMDM during stimulation with IFN-γ and LPS, reduced the ability of BMDM to induce cell death in YAC-1 cells, as measured by alkaline phosphate activity. In contrast, co-culture of BMDM with necrotic cells during IFN-γ and LPS stimulation substantially increased tumour cytotoxicity of BMDM. Additionally, the suppression of anti-tumour activity was also reflected by a reduction in the release of NO (Reiter *et al.*, 1999). Other experiments have shown that pre-exposure of BMDM to phosphatidylserine-containing liposomes can suppress the activation of BMDM tumour cytotoxicity and NO secretion (Calderón *et al.*, 1994; Aramaki *et al.*, 1996).

Therefore, the aim of this chapter is to identify whether interaction with apoptotic cells can reverse the induction of a classically-activated macrophage phenotype capable of suppressing BL cell growth.

The chapter starts out to further investigate the effect of classically-activated BMDM on lymphoma cells, using a revised cytotoxicity assay from the one presented in Chapter 3 as well as a Cr51 release assay. The effect of apoptotic versus viable lymphoma cells on macrophage cytotoxicity and tumour cell growth is then studied further, followed by investigations to find out if this effect is dependent upon cell-to-cell contact, or can be mediated by soluble factors released from apoptotic lymphoma cells. Additionally, the role of galectin-3 is investigated using BMDM from LGALS3 KO mice. The chapter ends with an investigation of mediators that might be involved in classically-activated macrophage-mediated cytotoxicity.

5.2 Results

5.2.1 Classically-activated BMDM are cytotoxic for lymphoma cells

A revised cytotoxicity assay was designed that would allow for the assessment of target cell viability, as displayed in Figure 5.1. In short, BMDM were matured for 7 days, followed by removal of CSF1 for 18 hours. BMDM were then labelled with the fluorescent green membrane marker PKH67 and stimulated with IFN-γ + LPS for four hours. In the mean time, lymphoma cells for co-culture were prepared. Apoptosis was induced in BL2 and λ-MYC cells by UVB-irradiation followed by a 2 or 3-hour rest-period, respectively. Cells were then gently mixed, and added to the BMDM at a ratio of 1 macrophage to 10 lymphoma cells, without the removal of IFN-γ and LPS from the BMDM. BMDM and BL2 cells were co-cultured for 24 hours, before the lymphoma cells were removed by repeated washing steps with PBS, taking care to minimise disturbing the adherent macrophage layer. Target viable BL2 lymphoma cells, labelled with the fluorescent red membrane marker PKH26 were then added to the macrophages and co-cultured for 20 hours to assess killing. After 20 hours, all cells were removed from the plates by repeated pipetting

and the number and viability of red lymphoma target cells was assessed using a violet ratiometric membrane asymmetry probe, which detects membrane surface charge changes during apoptosis, in combination with a dead cell stain that can only enter permeabilized cells.

The results presented in Figure 5.2 confirm that IFN-γ and LPS-stimulation can indeed induce macrophage cytotoxicity. Almost 25% of the target cells became necrotic during the course of the 20-hour cytotoxicity assay when they were cultured separate from BMDM. Co-culture of target cells with unstimulated BMDM led to an increased number of viable cells, but did not affect non-viable target cell numbers. In contrast, co-culture of target cells with IFN-γ and LPS-stimulated BMDM significantly reduced the number of viable cells and increased the number of non-viable target cells. Target cell viability assessment with the ratiometric membrane asymmetry dye and dead cell stain suggested that the cells had undergone apoptosis (Figure 5.2c). This was confirmed by DAPI (4',6-diamidino-2-phenylindole) staining of the cells in the untreated and IFN-γ and LPS-stimulated BMDM-target cell co-cultures (not shown), which indicated that co-culture with IFN-γ and LPS-stimulated BMDM led to condensation of the nuclei of most target cells, a hallmark of apoptosis.

Additionally, chromium-51 (Cr51) release assays were employed to assess cytotoxicity of IFN-γ and LPS-stimulated BMDM. Many cytotoxic cells, including macrophages and NK cells induce lysis of target cells (Martin and Edwards, 1993; Damiens *et al.*, 1998; Cox *et al.*, 1992), which can be measured by chromium release from Cr51-labelled targets. BMDM were pre-treated with IFN-γ and LPS for four hours, before they were rested for 24 hours. BMDM were then washed, and co-cultured with chromium-labelled BL2 cells for 4, 8, or 24 hours at effector:target cell ratios of 100:1 to 10:1. At the end of the assay, cell-free supernatants were collected and chromium release was measured using a gamma counter. No chromium release above spontaneous release from target cells only was measured from target cells co-cultured with unstimulated or IFN-γ and LPS-stimulated BMDM for 4 or 8 hours (not shown). Only at 24 hours, chromium release above spontaneous release by

target cells was measured from target cells cultured at effector:target cell ratio 10:1, but the amount was low and there did not appear to be a difference between target cells co-cultured with unstimulated or IFN-γ and LPS-stimulated BMDM (Table 5.1). These results are in line with those presented in Figure 5.2 that suggest that IFN-γ and LPS-stimulated BMDM may induce apoptosis and not lysis of BL2 cells, and that at the end of the 20 or 24-hour co-culture, only a small number of BL2 cells have lost their membrane integrity, as shown also in Figure 5.2c.

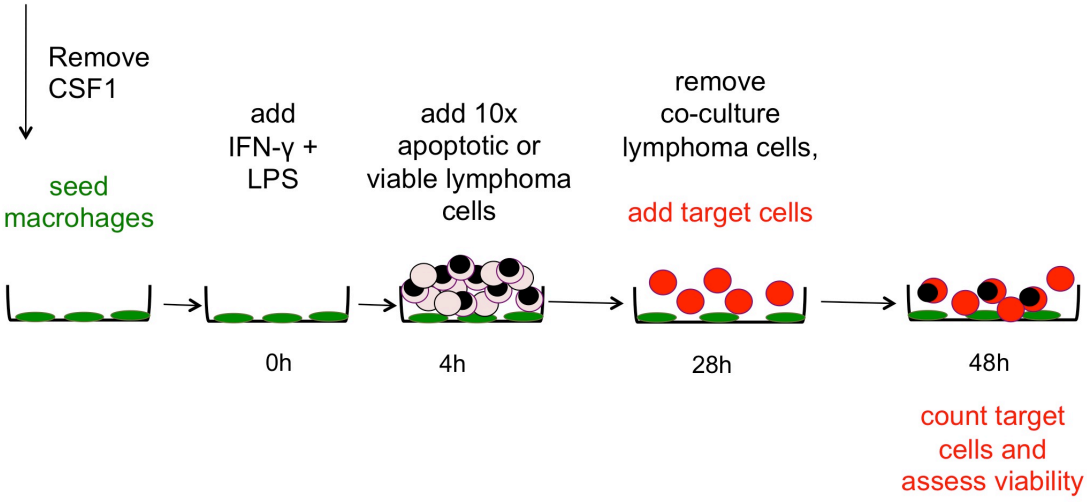

Figure 5.1 – Schematic drawing of macrophage cytotoxicity assay.
BMDM were matured *in vitro* for 8 days as previously described and CSF1 was removed for the final 18 hours. BMDM were then labelled with a PKH67 fluorescent green membrane marker and then activated by co-culture with IFN-γ and LPS for 4 hours before 10x the number of apoptotic or viable cells were added for an additional 24 hours. After 28 hours pre-treatment, co-cultured cells or media controls were removed by repeated washing and macrophage cytotoxicity was tested by the addition of BL2 lymphoma target cells that had been labelled with the fluorescent red membrane marker PKH26, at a 1:1 ratio to BMDM. Cells were co-cultured for 20 hours and at the end of the assay, the viability and number of lymphoma target cells was assessed by flow cytometry using a ratiometric membrane asymmetry probe in combination with a dead cell stain.

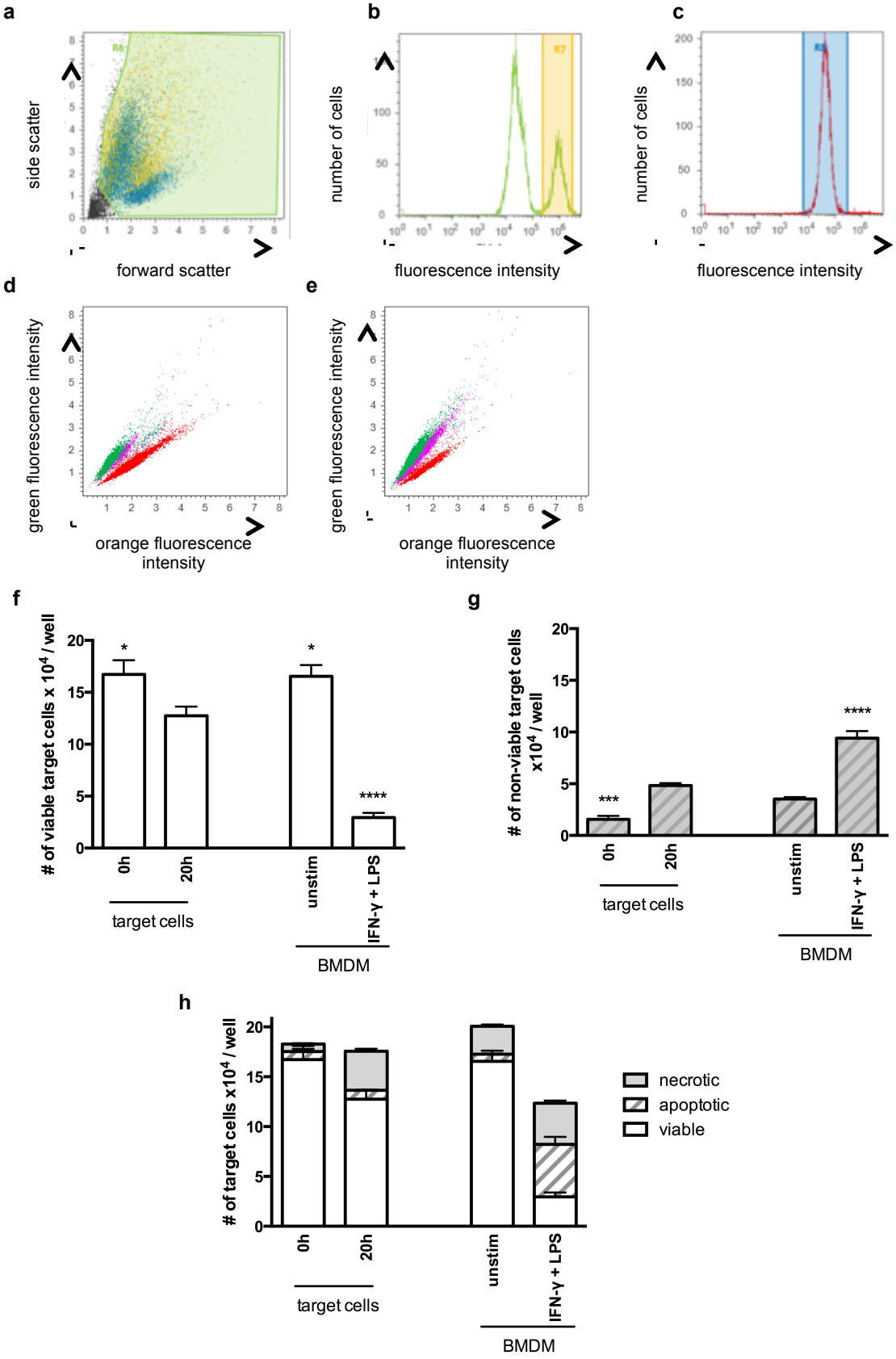
a
side scatter
forward scatter
b
number of cells
fluorescence intensity
c
number of cells
fluorescence intensity
d
green fluorescence intensity
orange fluorescence intensity
e
green fluorescence intensity
orange fluorescence intensity
f
# of viable target cells x 10^4 / well
0h
20h
unstim
IFN-γ + LPS
target cells
BMDM
g
# of non-viable target cells x10^4 / well
0h
20h
unstim
IFN-γ + LPS
target cells
BMDM
h
# of target cells x10^4 / well
necrotic
apoptotic
viable
0h
20h
unstim
IFN-γ + LPS
target cells
BMDM

Figure 5.2 – IFN-γ and LPS stimulation can induce macrophage cytotoxicity.
Mature BMDM with or without IFN-γ and LPS pre-treatment were co-cultured with target BL2 lymphoma cells in a cytotoxicity assay for 20 hours as described in Figure 5.1. At the end of the assay target lymphoma cell number and viability was assessed using a ratiometric membrane asymmetry probe in combination with a dead cell stain. (a) Forward and side scatter plot of target lymphoma cells and BMDM at the end of the assay. Gates were drawn to select all cells. (b) Green fluorescence intensity shown for all cells. Cells that were positive for green fluorescence (the macrophages labelled with PKH67 green fluorescent marker) were subtracted from the total cells. (c) From all cells minus the macrophages, red fluorescence-positive cells were then selected (the PKH26-labelled target cells). (d-e) orange fluorescence versus green fluorescence signal of F2N12S ratiometric membrane asymmetry probe for target cells co-cultured with (d) untreated macrophages or (e) IFN-γ and LPS-stimulated macrophages. Red events indicate the viable cells. Events in purple and green have undergone membrane asymmetry changes, and green events indicate cells that are also permeable. (f) viable, (g) non-viable or (h) total numbers of target cells are shown for target cells cultured alone or cultured in the presence of unstimulated or IFN-γ and LPS-stimulated BMDM. Data are means + SEM for n=6. Statistical analysis was performed using one-way ANOVA with Dunnett's multiple comparison test and all samples are compared to 20-hour target cells controls. *p<0.05, ***p<0.001, ****p<0.0001.

# of target cells added	E:T ratio	cpm in supt target cells only	cpm in supt + effectors	cpm in supt + effectors (IFN-γ+LPS)	cpm lysed controls	% lysis
0		4	4	17		
$4x10^3$	100:1	1334	737		4334	0
$4x10^3$	100:1	1334		761		0
$8x10^3$	50:1	1559	1494		8909	0
$8x10^3$	50:1	1559		1199		0
$2x10^4$	20:1	3939	3392		21690	0
$2x10^4$	20:1	3939		3250		0
$4x10^4$	10:1	5657	7705		42321	4.8
$4x10^4$	10:1	5657		7373		4.1

Table 5.1 – No difference in chromium-51 release from target cells co-cultured with unstimulated or IFN-γ and LPS-stimulated BMDM.
Mature BMDM with or without IFN-γ and LPS pre-treatment were co-cultured with target BL2 lymphoma cells labelled with Cr51 in a cytotoxicity assay for 24 hours. At the end of the assay Cr51 release from target lymphoma cells into the supernatant was measured using a gamma counter. Spontaneous release of Cr51 into the supernatant (supt) by target cells cultured without BMDM (target cells only), target cells cultured with unstimulated BMDM (+ effectors) or IFN-γ and LPS-stimulated BMDM (+ effectors (IFN-γ +LPS), or from target cells lysed with water (lysed control) is shown. % lysis is calculated as the release of Cr51 induced by effector cell co-culture as a percentage of Cr51 release from lysed cells. (cpm=counts per minute)

5.2.2 Co-culture with apoptotic cells following classical activation of macrophages can promote tumour cell growth

Having shown that classically-activated macrophages can induce apoptosis in lymphoma cells, it was then was assessed whether pre-treatment of classically-activated BMDM with apoptotic cells could affect the cell viability of target cells in a cytotoxicity assay. The assay was performed as described above. Figure 5.3 shows the results when classically-activated BMDM were pre-treated with apoptotic, untreated, or Bcl-2-transfected BL2 cells, before target BL2 cells were added. Assessment of viable target cells shows that viable target cell numbers are significantly larger when classically-activated BMDM were pre-treated with apoptotic BL2 cells compared to no pre-treatment of classically-activated BMDM before the start of the cytotoxicity assay. This was specific for pre-treatment with apoptotic cells, as pre-treatment of BMDM with untreated or apoptosis-suppressed BL2 cells did not affect viable target cell numbers. Interestingly, the total number of apoptotic and necrotic cells did not decrease.

Similar results were obtained when classically-activated BMDM were co-cultured with apoptotic or untreated λ-MYC cells, before co-culture with target BL2 cells. Co-culture with apoptotic λ-MYC, but not untreated λ-MYC cells, could significantly increase viable target cell number, without decreasing the total number of apoptotic and necrotic target cells. Collectively, these results suggest that pre-treatment of classically-activated BMDM with apoptotic cells can promote tumour cell growth.

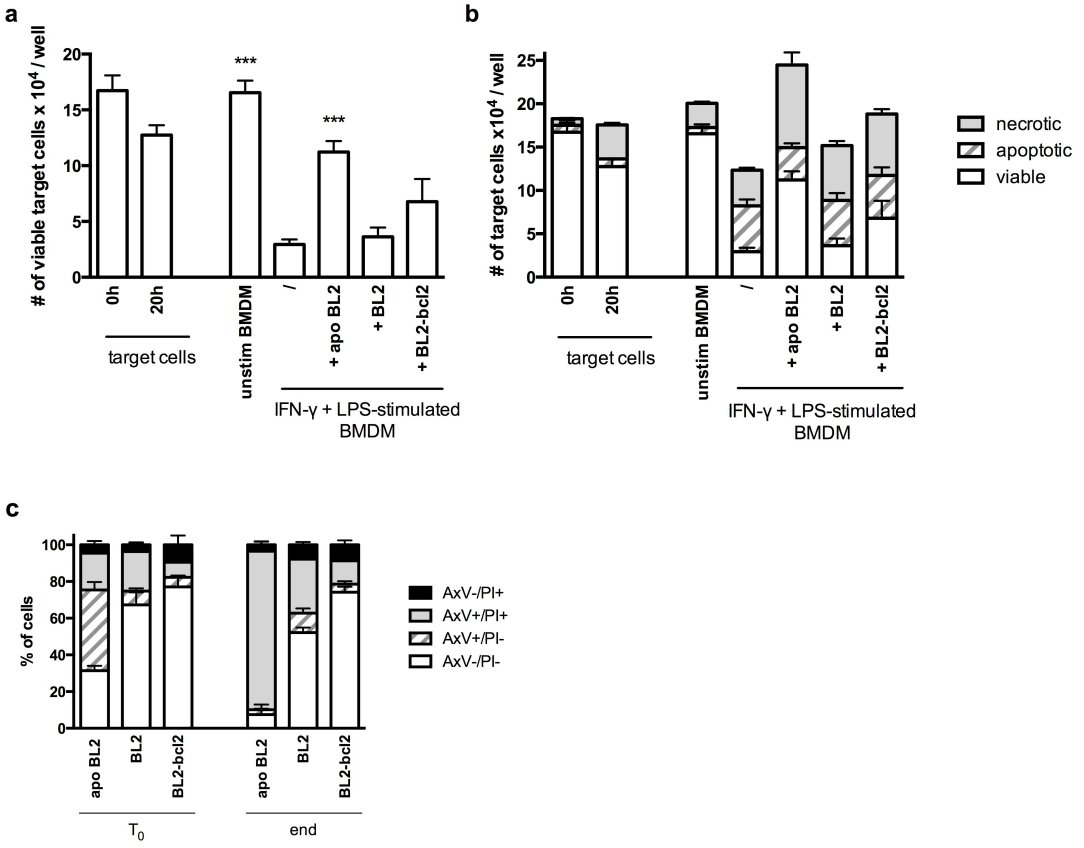

Figure 5.3 – Pre-treatment of classically activated BMDM with apoptotic BL2 cells enhances tumour cell growth.
Mature BMDM with or without IFN-γ and LPS pre-treatment were co-cultured with target BL2 lymphoma cells in a cytotoxicity assay for 20 hours as described in Figure 5.1, but rather than resting for 24 hours, BMDM were instead pre-treated with 10x apoptotic (UVB-induced) or untreated BL2 cells, or Bcl-2-transfected BL2 cells. At the end of the assay target lymphoma cell number and viability was assessed. (a) viable or (b) total numbers of target cells are shown for target cells cultured alone or cultured in the presence of unstimulated or IFN-γ and LPS-stimulated BMDM with or without additional pre-treatments with BL2 cells. Data are means + SEM for n=6. Statistical analysis was performed using one-way ANOVA with Dunnett's multiple comparison test and all co-culture samples were compared to IFNγ and LPS-stimulated BMDM. ***$p<0.001$. (c) Assessment of BL2 pre-treatment control cells by flow cytometry by simultaneous staining for Annnexin V (AxV) and propidium iodide (PI) at the time the BL2 cells were added to the macrophages (T_0) and at the end of the pre-treatment (end). Data are means + SEM for n=6.

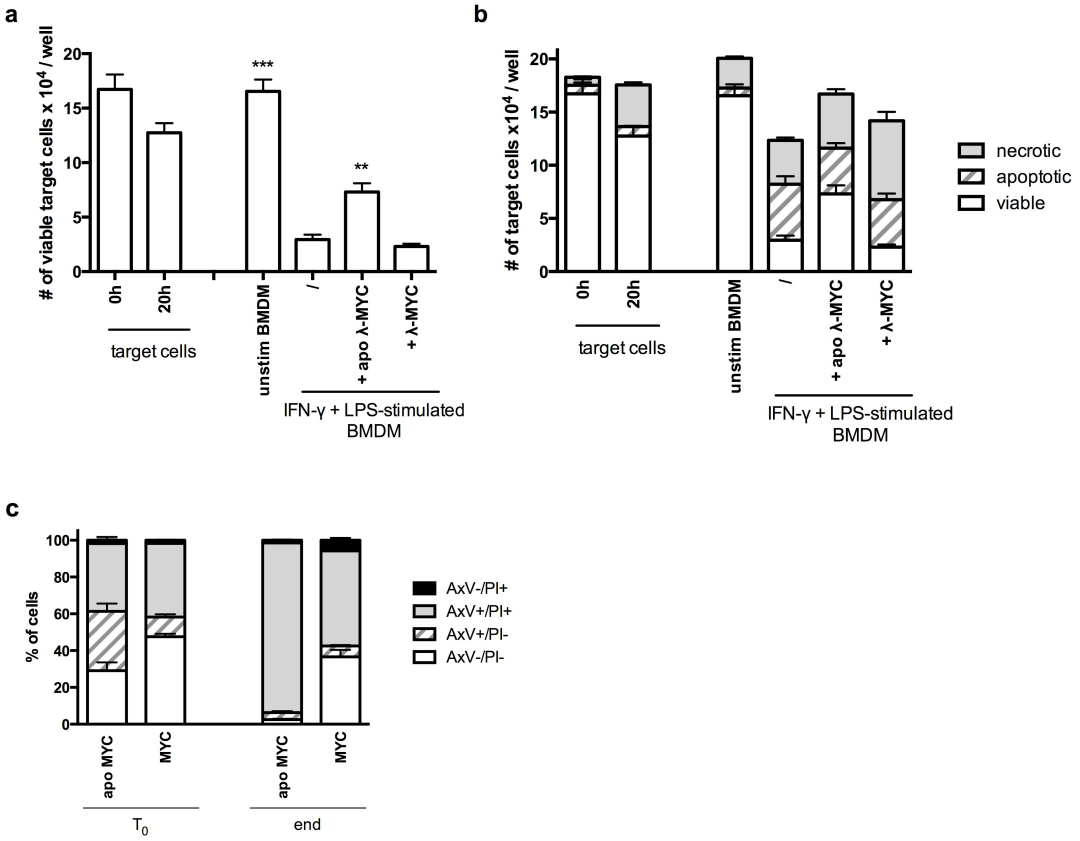

Figure 5.4 - Pre-treatment of classically activated BMDM with apoptotic λ-MYC cells enhances tumour cell growth.
Mature BMDM with or without IFN-γ and LPS pre-treatment were co-cultured with target BL2 lymphoma cells in a cytotoxicity assay for 20 hours as described in Figure 5.1, but rather than resting for 24 hours, BMDM were instead pre-treated with 10x apoptotic (UVB-induced) or untreated λ-MYC cells. At the end of the assay target lymphoma cell number and viability was assessed. (a) viable or (b) total numbers of target cells are shown for target cells cultured alone or cultured in the presence of unstimulated or IFN-γ and LPS-stimulated BMDM with or without additional pre-treatments with λ-MYC cells. Data are means ± SEM for n=6. Statistical analysis was performed using one-way ANOVA with Dunnett's multiple comparison test and all co-culture samples were compared to IFN-γ and LPS-stimulated BMDM. **p<0.01, ***p<0.001. (c) Assessment of λ-MYC pre-treatment control cells by flow cytometry by simultaneous staining for Annnexin V (AxV) and propidium iodide (PI) at the time the BL2 cells were added to the macrophages (T_0) and at the end of the pre-treatment (end). Data are means ± SEM for n=6.

5.2.3 The ability of apoptotic cells to reduce macrophage cytotoxicity is contact-dependent

Next it was investigated whether the ability of classically-activated BMDM pre-treated with apoptotic cells to promote tumour cell growth is dependent on factors released from apoptotic cells, or is contact-dependent. Classically-activated BMDM were either pre-treated directly with apoptotic or untreated BL2 cells, or the two cell

types were separated by a 0.44μm membrane, which prevents direct contact. After the pre-treatments were removed, BMDM were co-cultured directly with target lymphoma cells as before. The results are shown in Figure 5.5.

As the membrane was present only during pre-treatments of IFN-γ and LPS-stimulated BMDM with apoptotic or untreated cells and removed again for the cytotoxicity assay, it did not prevent macrophage cytotoxicity and classically-activated BMDM cultured temporarily with the membrane were also cytotoxic for lymphoma target cells. However, the presence of the membrane during pre-treatments of classically-activated BMDM with apoptotic cells significantly reduced the number of viable target cells present at the end of the assay. The total number of apoptotic and necrotic cells was not affected. Results for classically-activated BMDM pre-treated with untreated BL2 cells were not affected by the presence of the membrane during pre-treatments. This finding indicates that the promotion of tumour cell growth induced by IFN-γ and LPS-stimulated BMDM pre-treated with apoptotic lymphoma cells is dependent on cell-to-cell contact between macrophages and apoptotic cells.

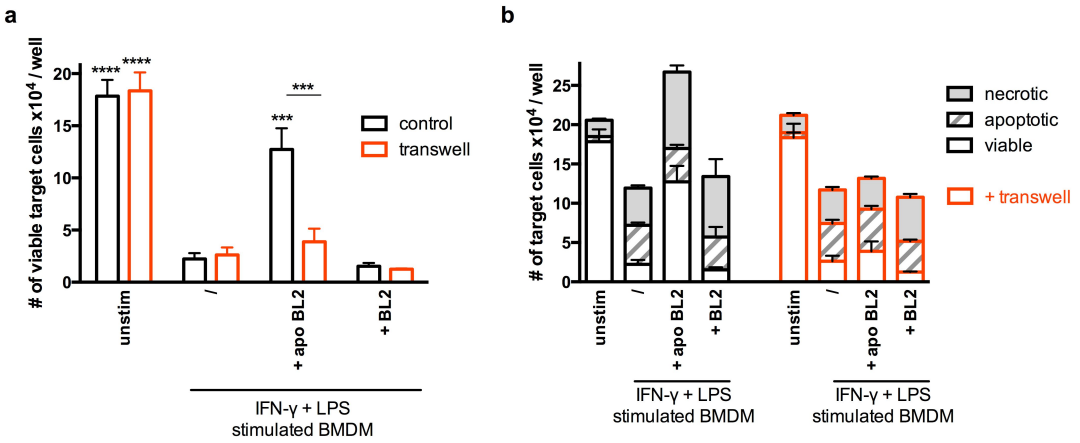

Figure 5.5 – Apoptotic cell-macrophage contact during pre-treatment of classically-activated macrophages is necessary to induce lymphoma cell growth.
Mature BMDM pre-treated with IFN-γ and LPS as described in Figure 5.1 co-cultured with 10x the number of apoptotic or viable BL2 cells, either added directly to the macrophages, or separated by a 0.44µm transwell. The ability of the macrophages to kill target lymphoma cells was then measured by the addition of an equal number of BL2 cells. (a) and (b) depict viable target cell counts (b) and total cell counts (d) of untreated BMDM and IFN-γ and LPS-stimulated cells co-cultured with or without apoptotic or viable BL2 cells in the presence or absence of a 0.44µm transwell. Data are means + SEM for n=4. Statistical analysis is shown for UT, + apo BL2, and + BL2 compared to control for with or without transwell, and comparing each of the pre-stimuli between with or without transwell using two-way ANOVA with Tukey's multiple comparisons test. *** $p<0.001$, **** $p<0.0001$.

5.2.4 Galectin-3 does not play a role in the ability of apoptotic-cell co-culture to inhibit macrophage cytotoxicity towards lymphoma cells

Experiments presented in chapter 4 and work by Sano et al. (2003) has shown that that galectin-3 plays an important role in the phagocytosis of apoptotic cells. Thus it was investigated whether galectin-3 expressed by macrophages is important for apoptotic cells to exert growth-promoting properties on classically-activated macrophages. Classically-activated WT or LGALS3 KO C57BL/6 BMDM were pre-treated with apoptotic cells or untreated BL2 cells before co-culture with lymphoma target cells. Viable and total target cell numbers at the end of the assay are displayed in Figure 5.6. Similar to WT BMDM, LGALS3 KO BMDM were cytotoxic to lymphoma cells. Furthermore, pre-treatment of classically-activated LGALS3 KO BMDM with apoptotic cells also significantly increased viable target cell numbers in the cytotoxicity assay, and, interestingly, in contrast to WT BMDM, non-viable cell numbers were significantly increased too ($p<0.01$, one-way ANOVA with Dunnett's

multiple comparison test). As before, pre-treatment of classically-activated LGALS3 KO BMDM with untreated or apoptosis-suppressed BL2 cells did not affect viable target cell numbers in the cytotoxicity assay.

Repeats of the assay with pre-treatments of classically-activated LGALS3 KO BMDM with apoptotic or viable λ-MYC cells showed a similar trend, although viable cell numbers were not significantly increased (Figure 5.7). Additionally, there appeared to be a trend that LGALS3 KO BMDM were less cytotoxic than their WT counterparts, but this was not significant.

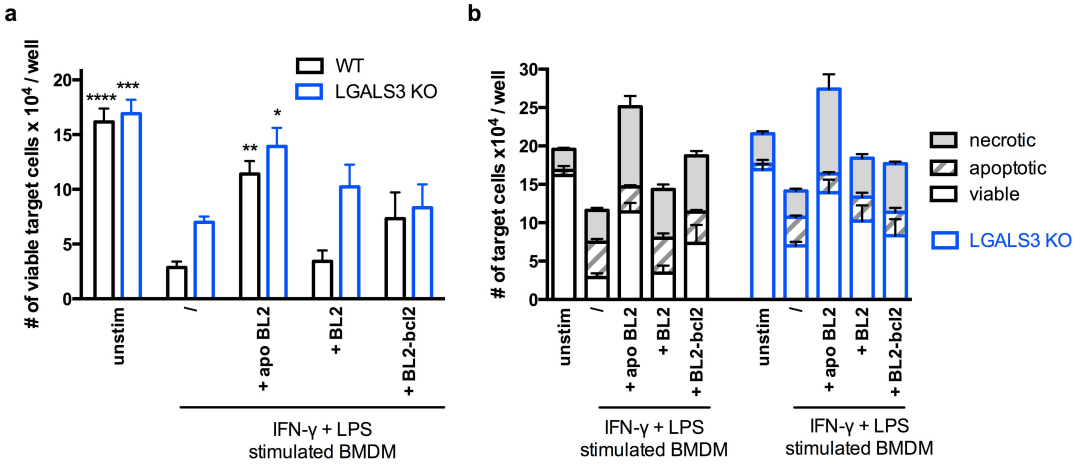

Figure 5.6 – Galectin-3 deficiency does not affect the ability of apoptotic BL2 cell pre-treated classically-activated macrophages to enhance tumour cell growth.
Mature BMDM from WT or LGALS3 KO mice, were pre-treated with IFN-γ and LPS for 4 hours before co-culture with 10x the number of apoptotic or untreated BL2 cells as described in Figure 5.3. The ability of the macrophages to kill target lymphoma cells was then measured by the addition of an equal number of BL2 cells. (a) depicts viable target cell counts (b) and total cell counts of untreated BMDM and IFN-γ and LPS-stimulated cells co-cultured with or without apoptotic or viable BL2 cells. Data are means + SEM for n=4. Statistical analysis was performed on the raw data using two-way ANOVA with Tukey's multiple comparisons test. * $p<0.05$, ** $p<0.01$, and **** $p<0.0001$.

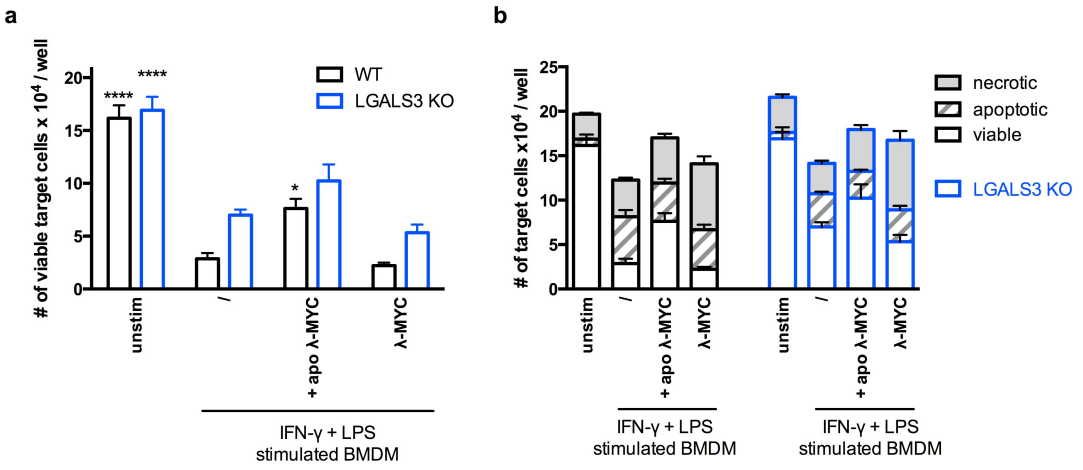

Figure 5.7 – Galectin-3 deficiency does not affect the ability of apoptotic λ-MYC cell pre-treated classically-activated macrophages to enhance tumour cell growth.
Mature BMDM from WT or LGALS3 KO mice, were pre-treated with IFN-γ and LPS for 4 hours before co-culture with 10x the number of apoptotic or untreated λ-MYC cells as described in Figure 5.4. The ability of the macrophages to kill target lymphoma cells was then measured by the addition of an equal number of BL2 cells. (a) depicts viable target cell counts (b) and total cell counts of untreated BMDM and IFN-γ and LPS-stimulated cells co-cultured with or without apoptotic or viable BL2 cells. Data are means ± SEM for n=4. Statistical analysis was performed on the raw data using two-way ANOVA with Tukey's multiple comparisons test. * $p<0.05$, and **** $p<0.0001$.

5.2.5 Nitric Oxide is released from classically-activated BMDMs, but is not decreased upon co-culture with apoptotic lymphoma cells

Further investigations were then done to elucidate what is the mediator that induces apoptosis in target cells when they are co-cultured with macrophages. Nitric oxide is known to be produced by IFN-γ and LPS-activated macrophages and can induce apoptosis in a number of cells (Jorens *et al.*, 1995; Murray and Nathan, 1999; Hibbs *et al.*, 1988; Higuchi *et al.*, 1990; Keller *et al.*, 1990; Cui *et al.*, 1994). Nitric oxide is very unstable and rapidly oxidises to nitrite (NO_2^-) and nitrate (NO_3^-) (Jorens *et al.*, 1995). Nitrite levels in the supernatants at the end of pre-treatment of classically-activated macrophages with or without apoptotic or untreated lymphoma cells were assessed using the Griess reaction, as described in Materials and Methods. Briefly, the Griess reagent reacts with nitrite, which can be spectrophotometrically quantified based on its absorbance at 548nm. The results are presented in Figure 5.8. Nitrite levels in supernatants from untreated BMDM are below detection levels, but classical activation of BMDM increases nitrite levels in the supernatants.

Interestingly, when BMDM are pre-treated with apoptotic or viable lymphoma cells, nitrite levels measured in the supernatants increase. When nitrite levels released from control lymphoma cells were assessed, it suggested that apoptosis of lymphoma cells could induce release of nitric oxide to the supernatant.

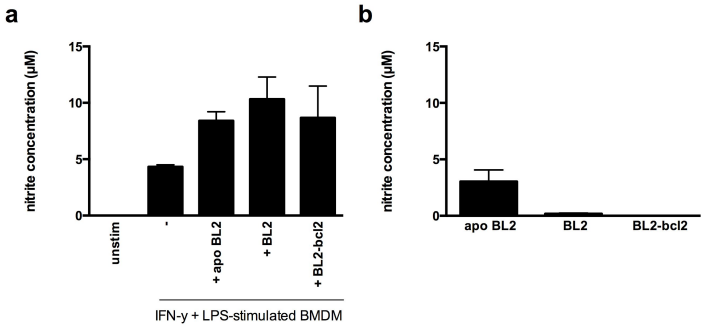

Figure 5.8 - Nitrite release by classically-activated macrophages.
Mature BMDM were pre-treated with IFN-γ and LPS for 4 hours before co-culture with 10x the number of apoptotic or untreated BL2 cells as described in Figure 5.3. Release of nitrite by (a) classically-activated BMDM co-cultures and (b) control BL2 cells was measured using the Griess reaction. Data points are means of duplicates for two independent experiments shown with the mean of the two experiments.

5.2.6 TNFα cannot induce apoptosis in lymphoma cells

Another candidate factor released from IFN-γ and LPS-stimulated macrophages that could be responsible for the induction of apoptosis in lymphoma cells is TNFα. TNFα has been shown to induce apoptosis in various tumour cells in vitro, which could be inhibited by an anti-TNFα neutralizing antibody (Urban *et al.*, 1986; Feinman *et al.*, 1987; Higuchi *et al.*, 1990). In Chapter 4, it was shown that IFN-γ and LPS-stimulated macrophages indeed up-regulate and release TNFα. Furthermore, co-culture with apoptotic cells could reduce Tnf gene expression by these macrophages. Thus, in order to test if TNFα could be the mediator that leads to apoptosis of target cells, lymphoma cells were incubated with several concentrations of TNFα, matching those found to be released from IFN-γ + LPS-stimulated BMDM in Chapter 4. After 20 hours lymphoma cell viability was assessed using the same ratiometric membrane asymmetry probe in combination with the dead cell stain employed in cytotoxicity assays. None of the concentrations of TNFα were found to

affect viable or non-viable target cell numbers, suggesting that TNFα release by classically-activated BMDM is not responsible for the induction of apoptosis in target lymphoma cells.

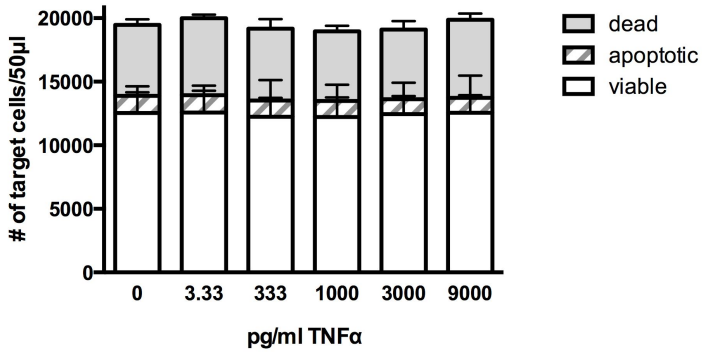

Figure 5.9 – TNFα does not induce apoptosis of lymphoma cells.
Target BL2 cells were incubated with various concentrations of TNFα for 20 hours. At the end of the assay, target cell viability was assessed. Data are means + SEM for n=2.

5.3 Discussion

Results in previous chapters showed that co-culture of classically-activated macrophages with apoptotic cells could affect the activation status of said macrophages, including the reduction of cytokine expression of Il6 and Tnf. Furthermore, pre-exposure of macrophages to apoptotic cells prior to classical activation was shown to reduce macrophage cytotoxicity. Here the effect of apoptotic cells on macrophage cytotoxicity was further investigated.

Classically-activated control macrophages were indeed found to be cytotoxic to lymphoma cells, as classically-activated macrophages significantly reduced the number of viable target cells at the end of the assay and increased the number of non-viable cells compared to target cells incubated alone. This was not due to competition for limited nutrients in the low-nutrient media, as co-culture of target cells with unstimulated BMDM did not reduce viable cell numbers, but rather significantly increased their viable target cell numbers, which suggests that co-

culture of lymphoma cells with unstimulated BMDM might induce lymphoma cell growth. However, this was not further investigated here.

Investigation of target cell viability following co-culture with classically-activated BMDM using a ratiometric dye that detects changes in membrane charge as a result of redistribution of phosphatidylserine (PS) and phosphatidylethanolamine (PE) to the outer leaflet of the cell membrane during apoptosis (Martin *et al.*, 1996), suggested that the target cells had undergone apoptosis. This was confirmed by nuclear staining of target cells with DAPI, which indicated condensation of the nuclei of target cells, another hallmark of apoptosis (Kerr *et al.*, 1972). These findings that classical activation of BMDM appears to induce apoptosis in target cells may explain why chromium-51 release assays employed to assess macrophage cytotoxicity could only detect release of isotope from labelled lymphoma cell targets after co-culture with BMDM at the effector:target cell ratio of 10:1 after 24 hours. No differences were observed between co-cultures of labelled target cells with unstimulated or IFN-γ and LPS-stimulated BMDM, which is in line with an approximately equal number of permeable target cells present after 20-hour co-culture with BMDM in the cytotoxicity assay where target cell viability was measured using the ratiometric and dead cell stain. Combined with the results that indicate classically-activated macrophages can induce apoptosis, and that both unstimulated and IFN-γ and LPS-stimulated BMDM can effectively phagocytose apoptotic cells, as presented in Chapter 4, one explanation for these results is that when classically-activated BMDM are co-cultured with such low numbers of target cells, macrophages can rapidly engulf the cells that are induced to undergo apoptosis before chromium-51 can be released.

Having shown that classically-activated BMDM could induce apoptosis in lymphoma cells, it was then investigated if pre-treatment of BMDM with apoptotic cells could interfere with macrophage cytotoxicity induced by classical activation. Experiments published by Reiter et al. (1999) have previously shown that apoptotic cells, but not necrotic cells, could reduce cytotoxic responses of IFN-γ and LPS-stimulated BMDM. However, apoptotic cell treatments were added at the same time

as classical activation stimuli, and as LPS has been shown to bind apoptotic cells, thereby preventing LPS-stimulated activation of macrophages (Ren *et al.*, 2008), it remains unclear if apoptotic cells can reverse cytotoxic responses by BMDM, or if they prevent cytotoxic activation by binding to LPS. To assess this, a cytotoxicity assay was developed in which macrophages were first classically activated by IFN-γ and LPS-stimulation for four hours, before further pre-treatments with apoptotic, viable or apoptosis-suppressed lymphoma cells. Experiments presented in Chapter 4 had previously shown that 4-hour treatment of BMDM with IFN-γ and LPS was sufficient to activate the macrophages, as measured by TNFα and IL-6 expression and release. Pre-treatment with the classical stimuli would prevent binding of apoptotic cells to LPS from interfering with the classical activation of the macrophages and possibly with the macrophages' ability to induce apoptosis in lymphoma cells. Pre-treatment of classically-activated BMDM with apoptotic cells was found to increase the number of viable target cells at the end of the assay. Interestingly, the number of non-viable cells remained the same. Further investigations revealed that this effect was specific to apoptotic cells, as untreated and cells in which apoptosis was suppressed did not have the same effect.

The substantial capacity of classically-activated BMDM to phagocytose apoptotic cells (Fadok *et al.*, 1998a; Mosser and Edwards, 2008) shown in Figure 4.7, must be taken into account when assessing these results. Indeed, small numbers of target cells seemed to have 'disappeared' when co-cultured with classically-activated BMDM compared to target cells cultured alone. These cells are likely to have been engulfed by the highly phagocytic classically-activated BMDM, as was shown in chapter 4, or they may have fallen apart as the cells became highly necrotic. Furthermore, when classically-activated BMDM are pre-treated with 10-fold numbers of apoptotic cells for 24 hours, there remains the possibility that the phagocytic capacity of these cells has been exhausted by the time the BMDM are co-cultured with target cells.

Another possibility is that incomplete removal of apoptotic cells after pre-treatment of macrophages could be responsible for the effects seen. Although multiple washes were employed, not all apoptotic pre-treatment cells could be removed without

disturbing the macrophage cell layer. Several studies have shown that apoptotic cells are capable of releasing growth factors that could enhance tumour cell growth, including fractalkine and PGE2 (Huang *et al.*, 2011; White *et al.*, 2010). Although the possibility that the remaining apoptotic cells can enhance tumour cell growth directly cannot be entirely ruled out, by the end of the pre-treatment apoptotic cells are already highly secondary necrotic and permeable, as indicated by the assessment of cell viability of control pre-treatment cells. It is highly likely that most factors released from the apoptotic or necrotic cells have already been released by the time the apoptotic-cell pre-treatments are washed away and thus would have been washed away then too. However, the possibility remains that target lymphoma cells could interact with the cell corpses.

When pre-treatments of classically-activated BMDM were performed in the presence of a membrane, the ability of the BMDM to enhance target cell growth was disabled. This does not rule out the possibility that the target cell growth response was due to unintended co-culture of target cells with cell corpses. However, in the likely case that the observed effect was due to apoptotic-cell pre-treatment-induced changes in classically-activated BMDM, this suggested cell contact between the two cell types was necessary to induce the changes.

Thus, together these finding suggest that cell-to-cell contact of classically-activated macrophages with apoptotic cells can induce macrophage-mediated tumour cell growth of target lymphoma cells, although macrophage-induced cytotoxicity may still be going on in concert in these experiments.

In Chapter 4 and elsewhere (Sano *et al.*, 2003), macrophages from galectin-3 KO mice were shown to have a lower ability to phagocytose apoptotic cells than those from wild type mice. Given the findings presented here that direct cell-to-cell contact with apoptotic cells appeared necessary to induce tumour cell growth, it was tested whether macrophage galectin-3 deficiency could prevent target cell growth induced by pre-treatment of classically-activated macrophages with apoptotic cells. No significant differences were observed in the capacity for cytotoxicity towards

lymphoma cells for classically-activated BMDM of knock-out animals compared to those from wild types. Furthermore, galectin-3 deficient classically-activated BMDM were also capable of supporting target cell growth when they were pre-treated with apoptotic cells, although interestingly, significantly larger number of dead cells were counted compared to classically-activated BMDM only. This suggests that there may be a shift in balance between growth stimulation and cytotoxicity of galectin-3-deficient classically-activated macrophages pre-treated with apoptotic cells compared to wild type, although this does not appear to result in a lower number of viable tumour cells.

The fact that no differences between wild type or galectin-3 KO BMDM-stimulated tumour cell growth are observed is maybe not surprising given the preliminary findings presented in Chapter 4 (Figure 4.23) that IFN-γ and LPS-stimulation of galectin-3 deficient macrophages may increase the phagocytic ability of galectin-3 KO BMDM. IFN-γ and LPS-stimulated galectin-3 KO BMDM might therefore be equally capable of binding and phagocytosing apoptotic cells as their wild type counterparts.

Nitric oxide has been detected in various cancers, including cervical, breast, laryngeal, central nervous system carcinomas and lymphomas (Thomsen *et al.*, 1994; 1995; Cobbs *et al.*, 1995; Taysi *et al.*, 2003; Mannick *et al.*, 1994; Zhao *et al.*, 1998). However, its effects on tumour cell growth are unclear, as NO has been shown to have tumour growth and proliferation as well as tumouricidal effects. It is likely that the effects of NO may differ per tumour dependent on NO concentration, tumour type, and the tumour microenvironment (Choudhari *et al.*, 2013; Burke *et al.*, 2013; Weigert and Brüne, 2008). Low to medium concentrations are thought to be associated with tumour growth, proliferation, angiogenesis, metastasis, and inhibition of apoptosis, whereas high levels of NO (>500nM) may promote DNA damage, oxidative stress, cytotoxicity and apoptosis (Burke *et al.*, 2013). Constitutive low level expression of NO synthase (iNOS) has been reported in Epstein-Barr virus positive human B lymphocytes, Burkitt's lymphoma cell lines, and B-cell chronic lymphocytic leukaemia, and has been associated with inhibition of apoptosis

(Mannick *et al.*, 1994; Zhao *et al.*, 1998). NO release from classically-activated macrophages has previously been shown to induce apoptosis in tumour cells (Cui *et al.*, 1994; Jorens *et al.*, 1995; Hibbs *et al.*, 1988; Keller *et al.*, 1990; Higuchi *et al.*, 1990) and apoptotic cell exposure of IFN-γ-stimulated macrophages has been shown to significantly reduce NO production. This has been shown to be mediated by phosphatidylserine (Aramaki *et al.*, 1996; Calderón *et al.*, 1994), through up-regulation of arginase II (Johann *et al.*, 2007), leading to reduced tumour cytotoxicity of liver macrophages (Daemen *et al.*, 1996). NO was therefore investigated as a possible mediator either inducing apoptosis or promoting growth of target lymphoma cells.

Nitric oxide is very unstable and rapidly oxidises to nitrite (NO_2^-) and nitrate (NO_3^-) (Jorens *et al.*, 1995), thus nitrite release from macrophages was measured. Classically-activated BMDM did release nitrite, but treatment with apoptotic as well as viable lymphoma cells appeared to lead to an increase of nitrite release. From the results presented here, it is unclear if NO was the cytotoxic agent released from classically-activated macrophages. However, as nitrite release did not follow tumour cell promotion by pre-treatment of classically-activated macrophages with apoptotic cells, it is unlikely it was the mediator inducing tumour cell growth. Interestingly, it appeared that apoptotic lymphoma cells could release nitrite. UVB-irradiation in plant cells has been shown to significantly increase NOS activity and NO release (Zhang *et al.*, 2014), and release of NO from apoptotic lymphoma cells should be investigated as a potential additional source of NO in tumours.

TNFα released from classically-stimulated macrophages has previously been shown to induce apoptosis in tumour cells (Cui *et al.*, 1994; Urban *et al.*, 1986; Higuchi *et al.*, 1990; Feinman *et al.*, 1987). In Chapter 4 it was shown to be released from classically-activated BMDM, and was thus investigated as a possible factor released from the classically-activated macrophages that could induce apoptosis in the lymphoma target cells. However, treatment of target cells with TNFα did not affect target cell viability.

In summary, results presented in this chapter indicate that apoptotic cell pre-treatment of classically-activated BMDM does not prevent macrophage-induced cytotoxicity, but instead direct contact between apoptotic cells and classically-activated macrophages can enhance tumour cell growth *in vitro*. Unfortunately, the time-scale of this project did not allow further investigation to elucidate how apoptotic cell pre-treatment of classically-activated BMDM could lead to stimulation of tumour cell growth, but possible mechanisms and growth factors that might be involved will be discussed in Chapter 7. Furthermore, additional research will be necessary to find out if apoptotic cell stimulation of macrophages can also enhance tumour cell growth in vivo.

Chapter 6 In silico gene expression comparison of starry-sky TAM to in vivo and in vitro macrophage populations

6.1 Introduction

Microarray gene expression technology has enabled the investigation of the expression of thousands of genes simultaneously. Reduction of costs for microarray gene expression technology and advances in speed have led to an abundance of microarray gene expression datasets. The challenge in making sense of these large amounts of data lies in making an analysis that increases the understanding of the cellular and molecular pathways underlying health and disease. BioLayout Express^{3D} is a powerful tool that enables the 3D visualisation of transcriptional networks generated from microarray data. The networks that are created consist of nodes that represent individual transcripts, which are connected to other transcripts depending on their expression profile across different samples. This approach gives large, highly structured network graphs, which allows for the analysis and identification of biological relationships that may be missed when datasets or transcripts are individually assessed (Freeman *et al.*, 2007; Theocharidis *et al.*, 2009).

In a previous study in our laboratory, led by Sofia Petrova, transcription profiles of micro-dissected starry-sky tumour-associated macrophages (TAM) were obtained from a mouse xenograft model of Burkitt's Lymphoma by laser capture of tissue macrophage (Mφ) populations. For comparison, tingible-body macrophages from the germinal centres of activated lymph nodes (GCM) from immunized mice and macrophages from lymph nodes (LNM) of non-immunized mice were acquired in the same way. Many genes were up or down-regulated in TAMs compared with either GCM or LNM. Our published findings show that multiple pro-tumour pathways are activated in starry-sky TAM (Ford *et al.*, 2015). Furthermore, results presented in Chapter 4 and 5 suggest that apoptotic cell interaction can shape TAM

activation signatures in macrophages and that this can lead to increased tumour cell growth. Here, BioLayout Express^{3D} is used to compare the gene expression profile of starry-sky TAM to other tissue and *in vitro* cultured monocytes and macrophages from publicly available genomics data to further the understanding of the underlying biological and molecular pathways involved.

This chapter first describes the selection and quality assessment of macrophage microarray gene expression datasets available from a public functional genomics data repository to create a macrophage dataset. It then goes on to describe the bioinformatics analysis process to non-subjectively divide the gene transcripts into clusters of genes sharing similarities in their expression and to identify the function of the main clusters. A starry-sky TAM signature was derived by comparing the whole transcription profile of starry-sky TAM to other tissue macrophages that phagocytose large numbers of apoptotic cells, namely GCM and LNM. Additionally, the starry-sky TAM were compared to resident tissue macrophages from resting lymph nodes (LNM). This signature was then overlaid on the macrophage dataset to identify the most important processes and pathways that were up-regulated in starry-sky TAM. Furthermore, it was investigated which, if any, type of macrophage in the dataset, shares the greatest similarity to the starry-sky TAM.

6.2 Results

6.2.1 Selection of murine macrophage datasets

In order to compare the gene expression of TAM to a wider variety of murine macrophages, monocyte, macrophage, and dendritic cell (DC; controls) expression datasets were searched on the National Center for Biotechnology Information's (NCBI) Gene Expression Omnibus (GEO; http://www.ncbi.nlm.nih.gov/geo/), a public functional genomics data repository. Datasets were selected based on the following criteria: 1, chip platform (Affymetrix Mouse Gene 1.0 ST Array; similar array as the one used to acquire the TAM, GCM, and LNM datasets), 2, cell type studied; 3, availability of raw data (.cel) files, and 4, availability of at least 2 replicates of each cell type within each study. In total, 226 samples were selected

from 14 individual studies. An annotated list including all the samples was then made, and information regarding the study and cell type for each sample was entered to make the interpretation of the data easier (Figure 6.1). The samples comprised a large selection of tissue macrophages including liver, lung, peritoneal, alveolar, and small intestine macrophages and microglia. Furthermore, there were a large number of BMDM and monocyte samples and also the TAM, GCM, and LNM datasets previously acquired in the lab were included. The samples are summarised in Table 6.1.

The raw data files (.cel) were then downloaded for each selected study and the quality and compatibility of the raw data was assessed. Quality and compatibility assessment is important, as (for example) changes in quality between batches of chips, differences in protocols at laboratory sites, or differences in tissue acquisition and tissue quality could potentially lead to differences in expression profiles that have no biological basis. Using the arrayQualityMetrics package in Bioconductor (http://www.bioconductor.org), the data were scored on the basis of 7 metrics. Any array suggested to be an outlier on more than one metric was removed from the dataset. Furthermore, arrays that comprised extra time points, treatments or knock-outs were removed to simplify the dataset. Figure 6.2 gives an overview of the samples that were discarded following quality assessment.

Each dataset was then normalized independently, using the robust multi-array average (RMA) expression measure (Irizarry *et al.*, 2003). Boxplots of the normalized studies are shown in Figure 6.3. Average expression was much lower for studies GSE31995, GSE42169, GSE4773, Mm20, and Mm9 and these were excluded from the macrophage dataset. Unfortunately, also the TAM, GCM, and LNM studies, which had previously been acquired in our laboratory had to be removed. Their mean expression was also much lower than that of the other datasets, most likely because they were the only ones acquired by laser capture. Because a direct comparison of TAM with the macrophage dataset was no longer possible, a different approach was taken to compare starry-sky TAM gene expression with the other macrophage samples, as detailed in section 6.2.4.

The final macrophage dataset contained all the samples that had passed the quality and compatibility assessments. These included a total of 90 samples, representing 29 individual samples (after removing duplicates), from 6 different studies. The samples are summarised in Table 6.2. The largest number of samples was from the GSE15907 study, generated as part of the Immunological Genome Project (ImmGen; www.immgem.org). This study includes samples of a variety of murine macrophages, including BMDM, various peritoneal macrophage subtypes, microglia, small intestine, liver, lung, and spleen macrophages, and various monocyte subtypes. More samples of peritoneal macrophages were provided by other studies also including LPS-treated peritoneal macrophages (GSE19340), and acetylated Low Density Lipoprotein (acLDL)-stimulated peritoneal macrophages (GSE19926). Microglia from normoxic and hypoxic conditions were available from study GSE18602, and adipose macrophages from 5 and 16-week old WT mice from GSE36669. Furthermore, one study (GSE18804) provided samples of TAM, although unlike the *in situ* starry-sky TAM profile available from our laboratory, these were of murine spleen monocytes stimulated *in vitro* by soluble factors released from human glioblastoma U-87MG (brain TAM) or colorectal adenocarcinoma HT-29 (colon TAM) tumour cells.

Sample order	Annotated list-annotation	Series	platform	Dataset Description	Pubmed ID	Chip ID	Full Chip ID	Class	Sub-type	Chip description	DatasetID
1	Mm.4:BMDM_cntrl:r1	GSE41236	Affymetrix 1.0 ST array	Bone marrow derived macropha	GSE41236	GSM1011794	GSM1011794	macrophage	BMDM	BMDM_cntrl:r1	Mm.4
2	Mm.4:BMDM_cntrl:r2	GSE41236	Affymetrix 1.0 ST array	Bone marrow derived macropha	GSE41236	GSM1011795	GSM1011795	macrophage	BMDM	BMDM_cntrl:r2	Mm.4
3	Mm.4:BMDM_cntrl:r3	GSE41236	Affymetrix 1.0 ST array	Bone marrow derived macropha	GSE41236	GSM1011796	GSM1011796	macrophage	BMDM	BMDM_cntrl:r3	Mm.4
4	Mm.4:BMDM_cntrl:r4	GSE41236	Affymetrix 1.0 ST array	Bone marrow derived macropha	GSE41236	GSM1011797	GSM1011797	macrophage	BMDM	BMDM_cntrl:r4	Mm.4
5	Mm.4:BMDM_cntrl:r5	GSE41236	Affymetrix 1.0 ST array	Bone marrow derived macropha	GSE41236	GSM1011798	GSM1011798	macrophage	BMDM	BMDM_cntrl:r5	Mm.4
6	Mm.4:BMDM_RAC2KO:r1	GSE41236	Affymetrix 1.0 ST array	Bone marrow derived macropha	GSE41236	GSM1011799	GSM1011799	macrophage	BMDM	BMDM_RAC2KO:r1	Mm.4
7	Mm.4:BMDM_RAC2KO:r2	GSE41236	Affymetrix 1.0 ST array	Bone marrow derived macropha	GSE41236	GSM1011800	GSM1011800	macrophage	BMDM	BMDM_RAC2KO:r2	Mm.4
8	Mm.4:BMDM_RAC2KO:r3	GSE41236	Affymetrix 1.0 ST array	Bone marrow derived macropha	GSE41236	GSM1011801	GSM1011801	macrophage	BMDM	BMDM_RAC2KO:r3	Mm.4
9	Mm.4:BMDM_RAC2KO:r4	GSE41236	Affymetrix 1.0 ST array	Bone marrow derived macropha	GSE41236	GSM1011802	GSM1011802	macrophage	BMDM	BMDM_RAC2KO:r4	Mm.4
10	Mm.4:BMDM_RAC2KO:r5	GSE41236	Affymetrix 1.0 ST array	Bone marrow derived macropha	GSE41236	GSM1011803	GSM1011803	macrophage	BMDM	BMDM_RAC2KO:r5	Mm.4
11	Mm.5:BMDM_cntrl:r1	GSE47733	Affymetrix 1.0 ST array	Transcriptional study of the resp	GSE47733	GSM1150711	GSM1150711	macrophage	BMDM	BMDM_cntrl:r1	Mm.5
12	Mm.5:BMDM_cntrl:r2	GSE47733	Affymetrix 1.0 ST array	Transcriptional study of the resp	GSE47733	GSM1150712	GSM1150712	macrophage	BMDM	BMDM_cntrl:r2	Mm.5
13	Mm.5:BMDM_cntrl:r3	GSE47733	Affymetrix 1.0 ST array	Transcriptional study of the resp	GSE47733	GSM1150713	GSM1150713	macrophage	BMDM	BMDM_cntrl:r3	Mm.5
14	Mm.5:BMDM_cntrl:r4	GSE47733	Affymetrix 1.0 ST array	Transcriptional study of the resp	GSE47733	GSM1151659	GSM1151659	macrophage	BMDM	BMDM_cntrl:r4	Mm.5
15	Mm.5:BMDM_cntrl:r5	GSE47733	Affymetrix 1.0 ST array	Transcriptional study of the resp	GSE47733	GSM1151660	GSM1151660	macrophage	BMDM	BMDM_cntrl:r5	Mm.5
16	Mm.5:BMDM_cntrl:r6	GSE47733	Affymetrix 1.0 ST array	Transcriptional study of the resp	GSE47733	GSM1151661	GSM1151661	macrophage	BMDM	BMDM_cntrl:r6	Mm.5
17	Mm.6:BMDM_cntrl:r1	GSE15907	Affymetrix 1.0 ST array	IMMGEN	GSE15907	GSM854317	GSM854317_	macrophage	BMDM	BMDM_cntrl:r1	Mm.6
18	Mm.6:BMDM_cntrl:r2	GSE15907	Affymetrix 1.0 ST array	IMMGEN	GSE15907	GSM854318	GSM854318_	macrophage	BMDM	BMDM_cntrl:r2	Mm.6
19	Mm.6:BMDM_cntrl:r3	GSE15907	Affymetrix 1.0 ST array	IMMGEN	GSE15907	GSM854319	GSM854319_	macrophage	BMDM	BMDM_cntrl:r3	Mm.6
20	Mm.7:BMDM_cntrl:r1	GSE31995	Affymetrix 1.0 ST array	Gene Expression data from Mou	GSE31995	GSM792470	GSM792470_	macrophage	BMDM	BMDM_cntrl:r1	Mm.7
21	Mm.7:BMDM_cntrl:r2	GSE31995	Affymetrix 1.0 ST array	Gene Expression data from Mou	GSE31995	GSM792471	GSM792471_	macrophage	BMDM	BMDM_cntrl:r2	Mm.7
22	Mm.7:BMDM_cntrl:r3	GSE31995	Affymetrix 1.0 ST array	Gene Expression data from Mou	GSE31995	GSM792472	GSM792472_	macrophage	BMDM	BMDM_cntrl:r3	Mm.7
23	Mm.7:BMDM_cntrl_1h:r1	GSE31995	Affymetrix 1.0 ST array	Gene Expression data from Mou	GSE31995	GSM792473	GSM792473_	macrophage	BMDM	BMDM_cntrl_1h:r1	Mm.7
24	Mm.7:BMDM_cntrl_1h:r2	GSE31995	Affymetrix 1.0 ST array	Gene Expression data from Mou	GSE31995	GSM792474	GSM792474_	macrophage	BMDM	BMDM_cntrl_1h:r2	Mm.7
25	Mm.7:BMDM_cntrl_1h:r3	GSE31995	Affymetrix 1.0 ST array	Gene Expression data from Mou	GSE31995	GSM792475	GSM792475_	macrophage	BMDM	BMDM_cntrl_1h:r3	Mm.7
26	Mm.7:BMDM_cntrl_3h:r1	GSE31995	Affymetrix 1.0 ST array	Gene Expression data from Mou	GSE31995	GSM792476	GSM792476_	macrophage	BMDM	BMDM_cntrl_3h:r1	Mm.7
27	Mm.7:BMDM_cntrl_3h:r2	GSE31995	Affymetrix 1.0 ST array	Gene Expression data from Mou	GSE31995	GSM792477	GSM792477_	macrophage	BMDM	BMDM_cntrl_3h:r2	Mm.7
28	Mm.7:BMDM_cntrl_3h:r3	GSE31995	Affymetrix 1.0 ST array	Gene Expression data from Mou	GSE31995	GSM792478	GSM792478_	macrophage	BMDM	BMDM_cntrl_3h:r3	Mm.7
29	Mm.7:BMDM_cntrl_6h:r1	GSE31995	Affymetrix 1.0 ST array	Gene Expression data from Mou	GSE31995	GSM792479	GSM792479_	macrophage	BMDM	BMDM_cntrl_6h:r1	Mm.7
30	Mm.7:BMDM_cntrl_6h:r2	GSE31995	Affymetrix 1.0 ST array	Gene Expression data from Mou	GSE31995	GSM792480	GSM792480_	macrophage	BMDM	BMDM_cntrl_6h:r2	Mm.7
31	Mm.7:BMDM_cntrl_6h:r3	GSE31995	Affymetrix 1.0 ST array	Gene Expression data from Mou	GSE31995	GSM792481	GSM792481_	macrophage	BMDM	BMDM_cntrl_6h:r3	Mm.7
32	Mm.7:BMDM_cntrl_12h:r1	GSE31995	Affymetrix 1.0 ST array	Gene Expression data from Mou	GSE31995	GSM792482	GSM792482_	macrophage	BMDM	BMDM_cntrl_12h:r1	Mm.7
33	Mm.7:BMDM_cntrl_12h:r2	GSE31995	Affymetrix 1.0 ST array	Gene Expression data from Mou	GSE31995	GSM792483	GSM792483_	macrophage	BMDM	BMDM_cntrl_12h:r2	Mm.7
34	Mm.7:BMDM_cntrl_12h:r3	GSE31995	Affymetrix 1.0 ST array	Gene Expression data from Mou	GSE31995	GSM792484	GSM792484_	macrophage	BMDM	BMDM_cntrl_12h:r3	Mm.7
35	Mm.7:BMDM_cntrl_24h:r1	GSE31995	Affymetrix 1.0 ST array	Gene Expression data from Mou	GSE31995	GSM792485	GSM792485	macrophage	BMDM	BMDM_cntrl_24h:r1	Mm.7

Figure 6.1 – Screenshot of part of the annotated list of macrophage datasets.
An annotated list was made of murine monocyte, macrophage, and dendritic cell expression datasets selected from NCBI's Gene Expression Omnibus (GEO). Information regarding the study and cell type for each sample was entered to ease the interpretation of the data.

Study	number of samples	Cell type
GSE15907	65	3 BMDM 3 liver Mϕ 3 lung Mϕ 3 microglia 19 monocytes 12 peritoneal Mϕ 4 small intestine Mϕ 7 small intestine lamina propria Mϕ 8 small intestine serosal Mϕ 3 spleen Mϕ
GSE18602	12	12 microglia
GSE18804	9	3 monocytes; 6 TAM
GSE19340	12	12 peritoneal Mϕ
GSE19926	8	8 peritoneal Mϕ
GSE24492	6	6 embryonic skin Mϕ
GSE27859	10	5 colonic lam. prop. Mϕ; 5 dendritic cells
GSE31995	48	48 BMDM
GSE36669	15	15 adipose Mϕ
GSE41236	10	10 BMDM
GSE42169	7	7 Alveolar
GSE47733	9	9 BMDM
Mm20	9	3 GCM 3 LNM 3 TAM
Mm9	6	6 ESDM

Table 6.1 – Summary of macrophage datasets selected from GEO.
Summary of monocyte, macrophage (Mϕ), and dendritic cell samples that were selected from NCBI's GEO database repository. Study titles refer to GEO accession number, or assigned Mm titles. Starry-sky TAM and GCM from Mm20 were later submitted to the GEO repository under accession number GSE64366.

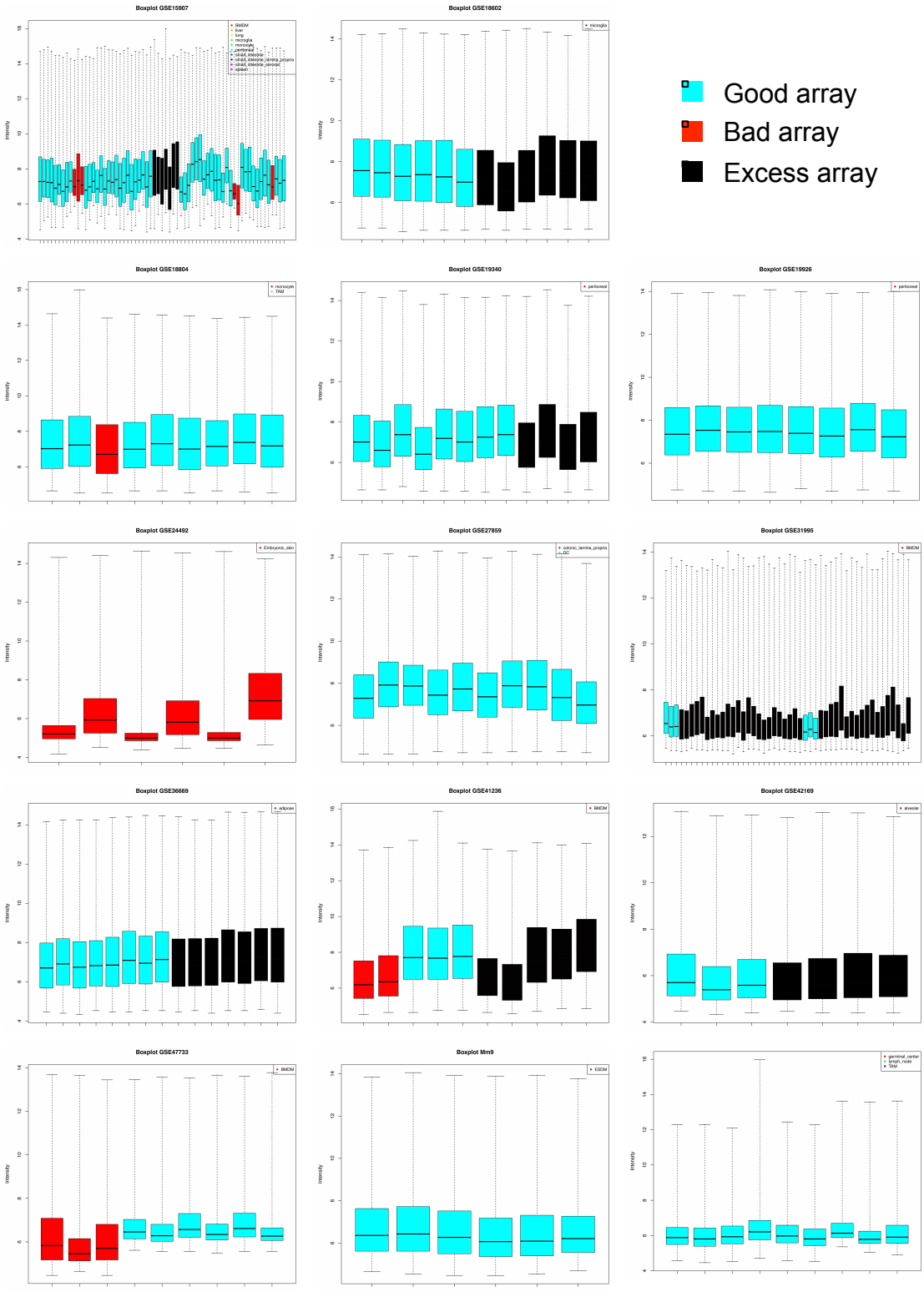
Boxplot GSE15907
Boxplot GSE18602
Boxplot GSE18804
Boxplot GSE19340
Boxplot GSE19926
Boxplot GSE24492
Boxplot GSE27859
Boxplot GSE31995
Boxplot GSE36669
Boxplot GSE41236
Boxplot GSE42169
Boxplot GSE47733
Boxplot Mm9
Intensity
Good array
Bad array
Excess array

Figure 6.2 – Pre-normalization boxplots for each study showing samples kept and discarded after quality assessment.
Using the arrayQualityMetrics package in Bioconductor the samples in each study were scored on 7 metrics. Any array suggested to be an outlier on more than one metric (bad array) was removed from the dataset. Furthermore, arrays that comprised extra time points, treatments, or knock-outs were removed to simplify the dataset (excess array). Arrays that passed the test (good array) were further assessed for compatibility.

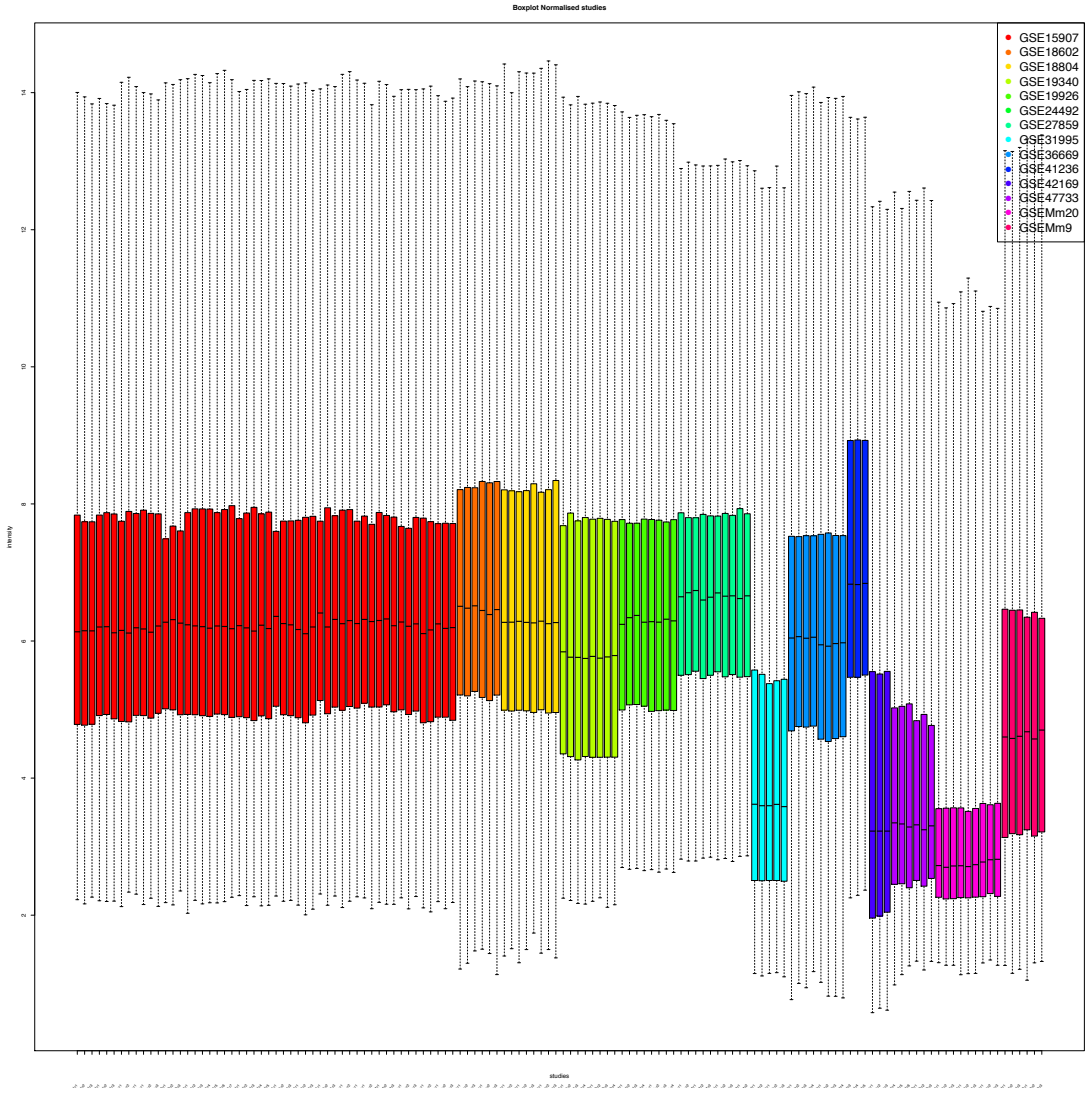

Figure 6.3 – Normalized boxplots for remaining samples after quality assessment.
Samples passing quality assessment were normalized independently, using the robust multi-array average (RMA) expression measure. Samples were colour-coded by study as indicated. Average expression was much lower for studies GSE31995, GSE42169, GSE4773, Mm20, and Mm9 and these were removed from the dataset.

Study	number of samples	Cell type
GSE15907	52	3 BMDM 3 peritoneal Mϕ 2 thioglycollate-elicited peritoneal Mϕ, F4/80hi^{+}/MHCII^{-} 1 thioglycollate-elicited peritoneal Mϕ, F4/80^{int}/MHCII^{-} 3 peritoneal Mϕ, F4/80^{int}/MCHII^{+} 3 microglia, CNS 7 small intestine lamina propria Mϕ 5 small intestine serosal Mϕ 3 liver Mϕ 3 lung Mϕ 3 spleen (red pulp) Mϕ 2 monocytes MHCII^{-}/Ly6C^{low} 3 monocytes MHCII^{int}/Ly6C^{low} 2 monocyte MHCII^{-} 1 monocyte MHCII^{+} 3 monocytes MHCII^{-}GR1^{+} 2 monocytes MHCII^{-}/CD3^{-} 3 monocytes MHCII^{-}CD3^{-}CD43^{+}
GSE18602	6	3 microglia normoxic conditions 3 microglia hypoxic conditions
GSE18804	8	2 *in vitro*-induced brain TAM 3 *in vitro*-induced colon TAM 3 spleen monocyte controls
GSE19340	8	4 peritoneal Mϕ 4 peritoneal Mϕ stimulated with LPS
GSE36669	8	4 adipose Mϕ from 5-week old WT mice 4 adipose Mϕ from 16-week old WT mice
GSE19926	8	4 peritoneal thioglycollate-elicited Mϕ 4 peritoneal thioglycollate-elicited Mϕ stimulated with acLDL

Table 6.2 – Summary of arrays included in the final macrophage dataset.
Summary of monocyte and macrophage (Mϕ) cell samples that passed quality and compatibility assessment and were included in the final macrophage dataset. Study titles refer to GEO accession numbers. Abbreviations: BMDM (bone marrow-derived macrophage), MHCII (major histocompatibility complex class II) WT (wild type), TAM (tumour-associated macrophage), acLDL (acetylated Low Density Lipoprotein).

6.2.2 Clustering of gene expression data using BioLayout Express^{3D}

Having constructed a macrophage dataset, this dataset could then be analysed using BioLayout Express^{3D}. BioLayout Express^{3D} is a powerful tool developed to generate and display large network graphs from gene expression data that is unbiased, but easy to interpret. Using the Pearson correlation coefficient, it generates a 3D network graph where transcripts (genes) are represented by nodes and are connected by edges, which represent the correlations (co-expression) between the transcripts. The graphs can then be further sub-divided non-subjectively, into sets of genes sharing similarities in their expression, so called clusters, using the Markov clustering (MCL) algorithm (van Dongen, 2000; Freeman *et al.*, 2007). When graphs are generated from large expression datasets, this often gives a highly structured graph, based on modules of co-expressed genes.

First, probesets of the microarrays were annotated using the latest annotation available from Bioconducor (March 2014) to link the AffyIDs to better understandable gene names. Then, using a Pearson threshold cut off of r=0.80, a network graph was generated of the data using BioLayout Express^{3D}. The network contained 8022 nodes and 215,224 edges (Figure 6.4a). Using the MCL algorithm, the graph was then clustered non-subjectively into clusters of genes that share similarities in their expression, using an MCL inflation value set to 2.2. High inflation values, e.g. 4, will result in many small clusters, whereas low inflation values, e.g. 1.5, will give fewer but larger, 'less clean' clusters. The recommended value for the inflation is between 1.7 and 2.2 (Theocharidis *et al.*, 2009). This gave 1061 clusters containing more than 5 nodes. Figure 6.4b shows the MCL clustered graph where the nodes in each cluster have 'collapsed' into single nodes for which the size is relative to the number of transcripts included in the cluster. Figure 6.4c shows a non-collapsed MCL clustered graph, where nodes from the same cluster have similar colours.

For the largest clusters and other clusters of interest, the gene transcripts were analysed for functions using the Functional Annotation Clustering tool on the Database for Annotation, Visualization, and Integrated Discovery (DAVID). DAVID

is a web-accessible programme that allows for identification of the function of a large group of genes. It takes information from more than 40 data sources, such as Gene Ontology, KEGG pathways, CGAP BioCarta Pathways, Entrez Gene, and UniProt, and lists all the different pathways and annotations associated with each gene. It then measures the relationship of the annotation terms based on their degree of co-association with other genes in the list. An algorithm is then applied to display similar annotations together. This allows the user to get a more insightful view of the biological function of a group of genes (Huang *et al.*, 2007; 2009b; a).

The largest cluster contained 712 genes and was associated with endocytosis and phagocytosis. This cluster will be analysed in more detail in the next section. Some of the other large clusters were associated with other broad biological processes, including mitochondria, ribosomes, and RNA processing (clusters 2, 4, 8, 9, 15, 19 and 20), cell cycle (cluster 3), extracellular matrix (5), regulation of differentiation, proliferation and cell death (clusters 6, 11), transcription (clusters 7, 10, 23), LPS-responses (Clusters 14, 32, 63, 77, 104), interferon response (cluster 28), and anti-inflammatory responses (Cluster 129). Figure 6.4c indicates some of these clusters in the network graph and for some of the clusters the mean expression of the transcripts that make up the cluster is shown for each study.

Figure 6.5 shows images from functional annotation clustering analysis of Cluster 3 using DAVID. The higher the enrichment score, the higher the similarity between the annotation categories. The p-values indicate the significance for each annotation category. A total of 69 functional annotation clusters were identified for this cluster (not all shown). As can be seen, most of the large annotation clusters were associated with the cell cycle, and included such annotation terms as cell cycle, cell division, DNA replication, condensed chromosome, DNA repair, and spindle.

Table 6.3 shows a summary of the functional annotation of the clusters, and highlights some index genes in each cluster. Index genes were arbitrarily chosen based upon analysis of individual genes using BioGPS, a gene annotation portal (www.biogps.com), as example genes of the pathways and functions associated with

that cluster. Additionally, other selected genes known to be associated with macrophages or other functions are indicated. Finally, enriched gene families are indicated when present.

6.2.2.1 Phagocyte cluster

As indicated above, the largest cluster was associated with endocytosis and phagocytosis. Figure 6.4d shows the mean expression profile of the transcripts that make up this cluster. Although the mean expression is relatively high for all samples, some samples of microglia and peritoneal macrophages, as well as brain and colon TAM and their monocyte controls, have a mean expression that is twice as high as that of the other macrophages.

In studies analysing a dataset consisting of haemopoietic and non-haemopoietic cell types (biogps.gnf.org), Hume et al. described one large expression cluster that was enriched in phagocytes (Hume *et al.*, 2010). To compare the phagocyte cluster identified in that study to the one identified in the present study, the transcripts associated with the phagocytosis cluster identified by Hume et al. were imported and overlaid onto the macrophage dataset network graph. The resulting graph is shown in Figure 6.6. Of the 469 transcripts in their phagocytosis cluster, 162 overlapped with nodes in the macrophage dataset network graph. The majority of these transcripts (112) were associated with Cluster 1, the phagocytosis cluster. The rest of the transcripts were scattered across various clusters or in no class at all.

To further analyse their phagocyte cluster, Hume et al. selected those genes in the cluster that were specifically associated with macrophages and individually analysed each gene and prescribed a putative function. This list was then used to classify some of the genes in our phagocyte cluster as presented in Table 6.4. The phagocyte cluster (Cluster 1) contained genes associated with all different processes of phagocytosis, including signalling and regulation, internalisation, vesicle formation and acidification, and digestion.

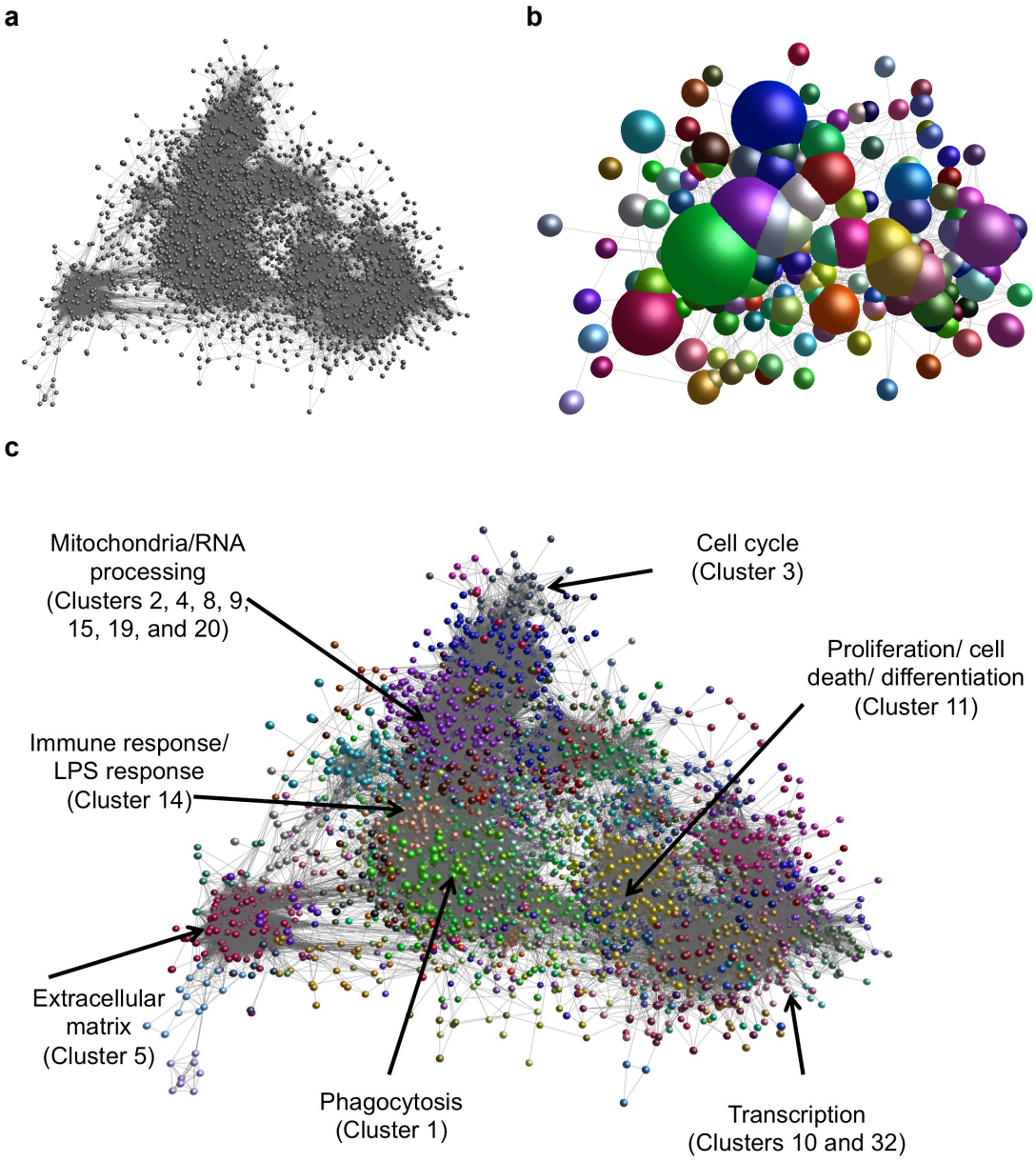
a
b
c
Mitochondria/RNA processing (Clusters 2, 4, 8, 9, 15, 19, and 20)
Cell cycle (Cluster 3)
Proliferation/ cell death/ differentiation (Cluster 11)
Immune response/ LPS response (Cluster 14)
Extracellular matrix (Cluster 5)
Phagocytosis (Cluster 1)
Transcription (Clusters 10 and 32)
d
Cluster 1

Cluster 14

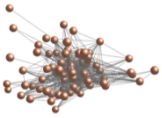

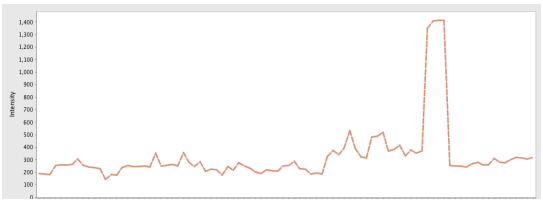

Cluster 28

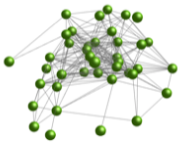

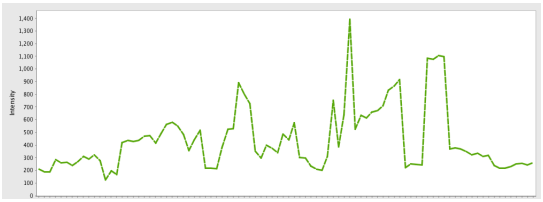

Cluster 63

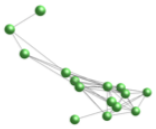

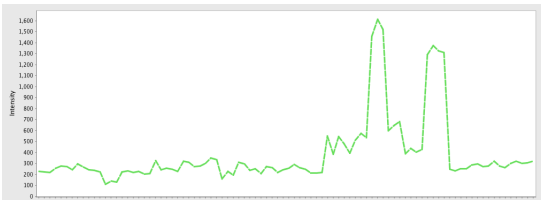

Cluster 77

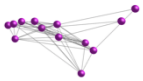

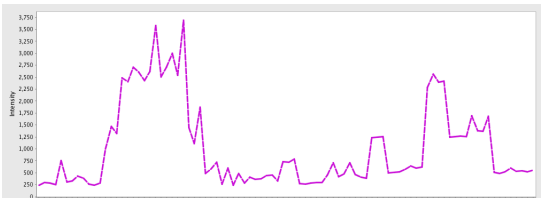

Cluster 129

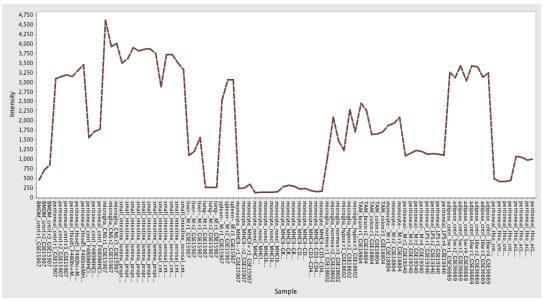

Figure 6.4 – Network analysis of macrophage dataset.
90 Samples, representing 29 mouse macrophage and monocyte populations from 6 individual studies were normalised using the RMA expression measure and the tool BioLayout Express^{3D} was used to calculate pair-wise Pearson correlation coefficients for every transcript represented on the array. A network graph was constructed using a cut off of r=0.8, where nodes represent transcripts analysed on the array, and edges represent relationships between the transcripts. (a) The resultant graph was laid out in 3-dimensional space and comprised of 8022 nodes (transcripts), connected by 215,224 edges. The graph was then clustered using the Markov clustering algorithm with an inflation value of 2.2. This resulted in 1061 clusters containing more than 5 nodes. (b) Collapsed cluster diagram where single (coloured) nodes represent a transcript cluster. The size of each node is relative to the number of transcripts contained within that cluster. (c) shows the individual nodes (transcripts) in each cluster colour-coded, and the main function of some of the larger clusters is indicated. (d) Further examples of clusters shown isolated from the main graph alongside their average expression profile of the transcripts that make up the cluster.

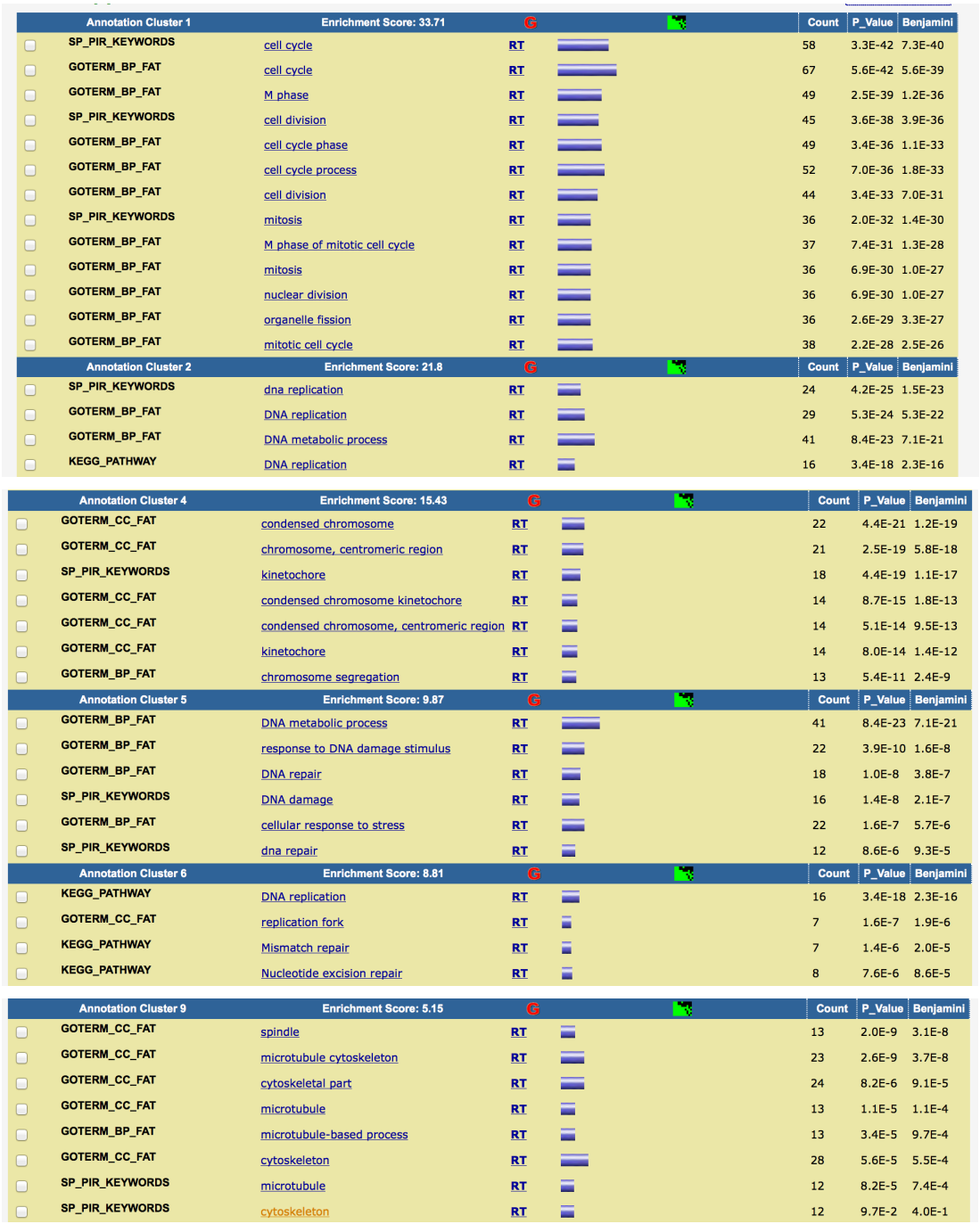

Annotation Cluster 1	Enrichment Score: 33.71			Count	P_Value	Benjamini
SP_PIR_KEYWORDS	cell cycle	RT		58	3.3E-42	7.3E-40
GOTERM_BP_FAT	cell cycle	RT		67	5.6E-42	5.6E-39
GOTERM_BP_FAT	M phase	RT		49	2.5E-39	1.2E-36
SP_PIR_KEYWORDS	cell division	RT		45	3.6E-38	3.9E-36
GOTERM_BP_FAT	cell cycle phase	RT		49	3.4E-36	1.1E-33
GOTERM_BP_FAT	cell cycle process	RT		52	7.0E-36	1.8E-33
GOTERM_BP_FAT	cell division	RT		44	3.4E-33	7.0E-31
SP_PIR_KEYWORDS	mitosis	RT		36	2.0E-32	1.4E-30
GOTERM_BP_FAT	M phase of mitotic cell cycle	RT		37	7.4E-31	1.3E-28
GOTERM_BP_FAT	mitosis	RT		36	6.9E-30	1.0E-27
GOTERM_BP_FAT	nuclear division	RT		36	6.9E-30	1.0E-27
GOTERM_BP_FAT	organelle fission	RT		36	2.6E-29	3.3E-27
GOTERM_BP_FAT	mitotic cell cycle	RT		38	2.2E-28	2.5E-26
Annotation Cluster 2	**Enrichment Score: 21.8**			**Count**	**P_Value**	**Benjamini**
SP_PIR_KEYWORDS	dna replication	RT		24	4.2E-25	1.5E-23
GOTERM_BP_FAT	DNA replication	RT		29	5.3E-24	5.3E-22
GOTERM_BP_FAT	DNA metabolic process	RT		41	8.4E-23	7.1E-21
KEGG_PATHWAY	DNA replication	RT		16	3.4E-18	2.3E-16

Annotation Cluster 4	Enrichment Score: 15.43			Count	P_Value	Benjamini
GOTERM_CC_FAT	condensed chromosome	RT		22	4.4E-21	1.2E-19
GOTERM_CC_FAT	chromosome, centromeric region	RT		21	2.5E-19	5.8E-18
SP_PIR_KEYWORDS	kinetochore	RT		18	4.4E-19	1.1E-17
GOTERM_CC_FAT	condensed chromosome kinetochore	RT		14	8.7E-15	1.8E-13
GOTERM_CC_FAT	condensed chromosome, centromeric region	RT		14	5.1E-14	9.5E-13
GOTERM_CC_FAT	kinetochore	RT		14	8.0E-14	1.4E-12
GOTERM_BP_FAT	chromosome segregation	RT		13	5.4E-11	2.4E-9
Annotation Cluster 5	**Enrichment Score: 9.87**			**Count**	**P_Value**	**Benjamini**
GOTERM_BP_FAT	DNA metabolic process	RT		41	8.4E-23	7.1E-21
GOTERM_BP_FAT	response to DNA damage stimulus	RT		22	3.9E-10	1.6E-8
GOTERM_BP_FAT	DNA repair	RT		18	1.0E-8	3.8E-7
SP_PIR_KEYWORDS	DNA damage	RT		16	1.4E-8	2.1E-7
GOTERM_BP_FAT	cellular response to stress	RT		22	1.6E-7	5.7E-6
SP_PIR_KEYWORDS	dna repair	RT		12	8.6E-6	9.3E-5
Annotation Cluster 6	**Enrichment Score: 8.81**			**Count**	**P_Value**	**Benjamini**
KEGG_PATHWAY	DNA replication	RT		16	3.4E-18	2.3E-16
GOTERM_CC_FAT	replication fork	RT		7	1.6E-7	1.9E-6
KEGG_PATHWAY	Mismatch repair	RT		7	1.4E-6	2.0E-5
KEGG_PATHWAY	Nucleotide excision repair	RT		8	7.6E-6	8.6E-5

Annotation Cluster 9	Enrichment Score: 5.15			Count	P_Value	Benjamini
GOTERM_CC_FAT	spindle	RT		13	2.0E-9	3.1E-8
GOTERM_CC_FAT	microtubule cytoskeleton	RT		23	2.6E-9	3.7E-8
GOTERM_CC_FAT	cytoskeletal part	RT		24	8.2E-6	9.1E-5
GOTERM_CC_FAT	microtubule	RT		13	1.1E-5	1.1E-4
GOTERM_BP_FAT	microtubule-based process	RT		13	3.4E-5	9.7E-4
GOTERM_CC_FAT	cytoskeleton	RT		28	5.6E-5	5.5E-4
SP_PIR_KEYWORDS	microtubule	RT		12	8.2E-5	7.4E-4
SP_PIR_KEYWORDS	cytoskeleton	RT		12	9.7E-2	4.0E-1

Figure 6.5 – Functional clustering of transcripts in Cluster 3.
The DAVID Functional Annotation tool was used to analyse all transcripts associated with Cluster 3 of the macrophage dataset. Some of the 69 function annotation clusters identified are shown here. High enrichment scores indicated high similarities between the annotation categories. P-values indicate the significance for each annotation category.

Cluster ID number	Transcript count	Putative function	Index genes	Other relevant genes	Enriched gene families
1	712	phagocytosis	Ctsb, Cd68, Cd36, Lgals3	Mfge8, P2ry2, Mmp12	cathepsins, H+ transporters
2	376	mitochondria/ribosome and RNA processing	Cdk4, Cct3, Mrpl18		chaperonins, eukaryotic translation initiation factors, mitochondrial ribosomal proteins, nucleoporins, proteasome subunits
3	292	cell cycle	Cclna2, Cdk1, Cenpa		cyclins, centromere proteins, transcription factors, histone clusters, kinesin family members
4	262	mitochondria/ribosome and RNA processing and translation/proteasome	Cct6a, Mrpl18, Polr2g		chaperonins, eukaryotic translation initiation factors, mitochondrial ribosomal proteins, polymerases, proteasome subunits
5	219	extracellular matrix	Acta2, Col1a1, Fbn1	Twist1, Cxcl12, Egfr	collagens, fibrillins
6	185	regulation of immune cell activation, proliferation, and cell death	Il10, Cd80, Pgf	CD4, CD274, Irak2, MMP9, MMP13	
7	159	transcription	Ncoa2, Sf3b1	Bclaf1	zinc-finger proteins
8	126	mitochondria/ribosome and RNA processing and translation/proteasome	Eif1b, Mrpl13, Ndufa5		eukaryotic translation initiation factors, mitochondrial ribosomal proteins, NADH dehydrogenases, proteasome subunits
9	114	mitochondria/ribosome	Atp5l, Ndufa2, Ubb, Ubc		mitochondrial ATP synthases, cytochrome c oxidase subunits, NADH hydrogenase, ribosomal proteins
10	113	transcription	Srsf5		

Cluster ID number	Transcript count	Putative function	Index genes	Other relevant genes	Enriched gene families
11	110	regulation of activation, proliferation, and cell death / transcription	Fgfr1, Bcl2, Vegfc		
12	90	?		Mertk, Vcam1	
13	82	?			
14	81	late LPS-response/regulation of cell death	Tnfsf9,Adora2a, Ifit1	Ccl5, Fas	
15	79	oxidative phosphorylation/mitochondrial/ribosome and RNA processing	Atp5g1, Mrpl23, Ndufa4		mitochondrial ATP synthases, mitochondrial ribosomal proteins, NADH dehydrogenases
16	67	intracellular protein transport	Ergic2, Rab6a	Cd200r1	
17	66	ribosome	Snord104		small nucleolar RNAs
18	61	membrane	Tmem138, Epcam		
19	61	ribosome/mitochondria/oxidative phosphorylation	Ndufa13, Rpl11		NADH dehydrogenases, ribosomal proteins
20	55	ribosome and RNA processing	Atp5g2, Rpl13		ribosomal proteins
23	49	transcription	Akna, Map3k3	Ifngr2, Il6ra, Itga4	

Cluster ID number	Transcript count	Putative function	Index genes	Other relevant genes	Enriched gene families
28	40	interferon response	Ifit2, Stat2		interferon-induced proteins
32	32	regulation of apoptosis, LPS response	Tnfaip3, Rel, Il1b		
53	18	?		Mmp2	
63	15	LPS response	Cxcl3, IL12a, Irak3, Ptges		
77	13	LPS response	Ccl3,4, Cxcl2, Cclr2, Nfkbib		cytokines
98	10			Axl, Tlr4	
104	9	early LPS-response	Cd40, Tnf, Il6, Cxcl10		
121	8	immune response	Ccr5, Ctsh, Ly86	IL4ra	
129	8	anti-inflammatory, wounding response	C1qa-c,	P2rx7	

Table 6.3 – Annotation of co-expressed gene clusters.
Clusters generated from the macrophage dataset were functionally annotated using the DAVID Functional Annotation tool. Where the function is unknown this is indicated with ?. Index genes were arbitrarily chosen to represent known functional markers within the cluster. Additionally, other genes of interest, most known to be associated with macrophages, were indicated. Additionally, enriched gene families within each cluster were also shown if present.

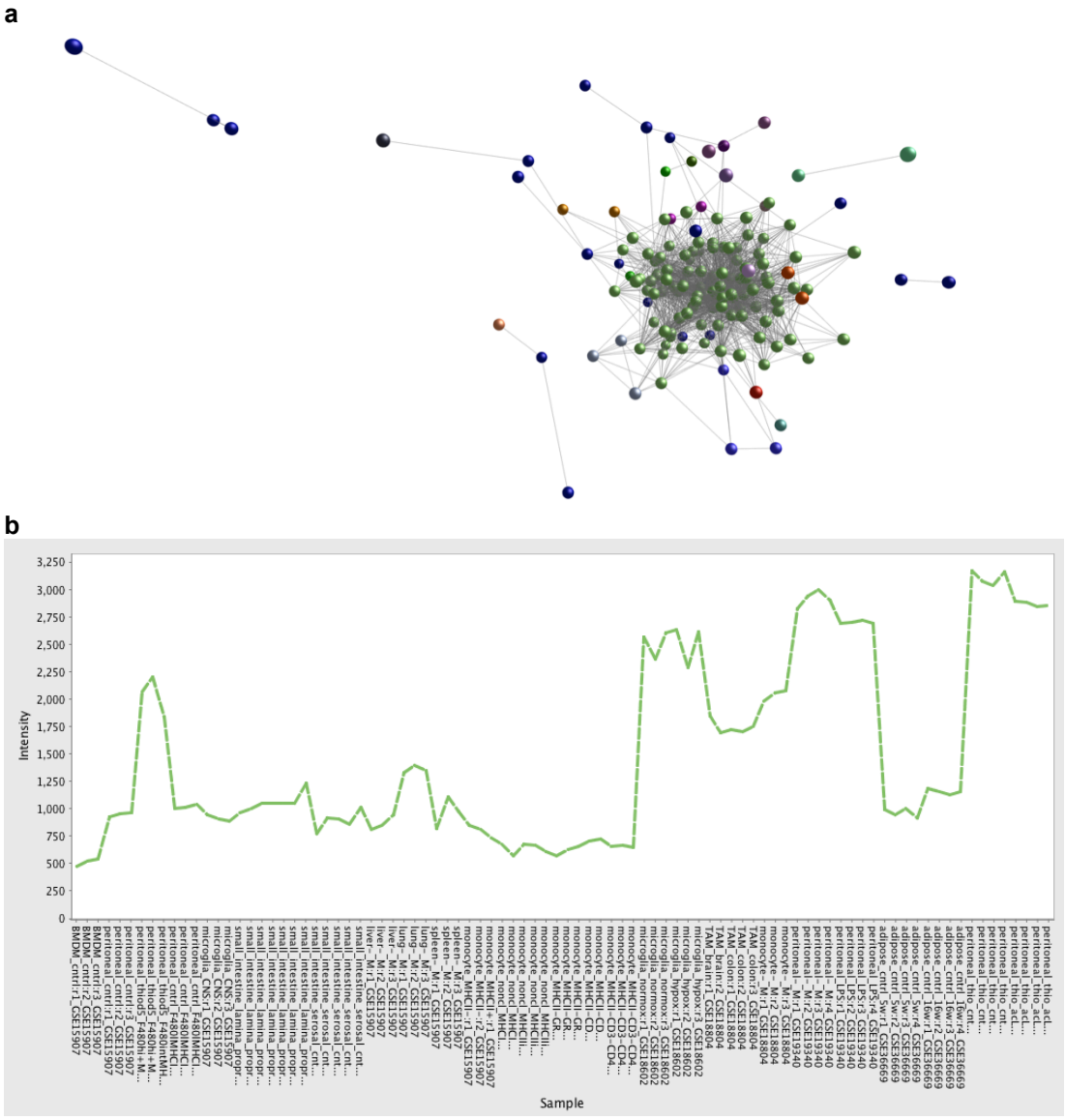

Figure 6.6 – Phagocytosis cluster identified by Hume et al. overlaid on macrophage dataset network graph.
Transcripts associated with the endocytosis/phagocytosis cluster identified by Hume et al. (2010) were imported and overlaid onto the macrophage dataset network graph created by BioLayout Express^{3D} analysis and shown in Figure 6.4. (a) The resultant graph consisted of 162 nodes, most of which (112) were associated with Cluster 1, the phagocyte cluster identified by DAVID Functional Annotation analysis and indicated in green. (b) Mean expression profile of the transcripts identified by Hume et al. that were expressed in Cluster 1 of the macrophage dataset.

Gene annotation	Present in phagocyte cluster (Cluster 1)
Transcriptional Regulation	2310044G17Rik, Cpeb4, Mdfic, Sirt2
Calcium Regulation	Mcoln1, Spsb2, Spsb4, Tpcn2, Anxa4
Signalling	Aig1, Cdkn1c, Gpr137b-ps, Htr2b, Lhfpl2, Ly9, Matk, Mvp, Plxna1, Rassf8, Rhov, Stac2, Wsb2
Cytoskeletal regulation	Capg, Klc4, Myo5a
Adhesion and Endocytic Receptors	Alcam, Cd84, Cd36, Mamdc2, Mfge8, Sdc1, Sdcbp
Vesicle trafficking (Endosomes)	Arl8b,Cd68, Fgd6, Gpnmb, Lamp1, Plekhm1, Rusc2, Samd8, Sestd1, Snx27, Stx4a, Wfs1
Proton Pump	Atp6ap1, Atp6v0a1, Atp6v0c, Atp6v0d1, Atp6v0d2, Atp6v1a, Atp6v1b2, Atp6v1c1, Atp6v1f, Atpv1g1, Atp6v1h, Rnbp
Protein degradation and processing	Ctsb, Ctsd, Ctsl, Ctsz, Fbxo32, Lonrf3, Mmp12, Psmd8, Ube2q2, Zfand2a, Anpep, Cndp2, Dpp7
Lipid Digestion and Storage	Cyp4v3, Lrp12, Npc2, Sgpl1, Soat1, Col4a3bp, Fabp5
DNA digestion	Dnase1l1, Tatdn2
Haem Digestion	Fth1
Carbohydrate digestion	Amdhd2, Galc, Galns, Gba, Gdpd1, Gusb, Hexa, Nagk, Naglu, Uap1l1

Table 6.4 – Annotation of genes enriched in phagocytosis cluster (Cluster 1).
Using annotations available from Hume et al. (2010) some of the genes in the phagocyte cluster (Cluster 1) of the macrophage dataset were classified into different processes associated with phagocytosis.

6.2.3 Clustering by macrophage type or study

In addition to viewing the macrophage dataset in a graph that clusters genes that have similar expression behaviour across the macrophage datasets, the dataset can also be viewed where each macrophage sample represents a node, and samples that have the most similar expression are clustered together. Therefore, one would predict that if samples are true repeats, they should be very similar and should cluster closely together. Furthermore, if separate studies include samples of similar macrophages

subtypes, one would expect those to cluster closely together too. If this is not the case, or in the case of a small dataset, the samples may cluster by study rather than biological function of the macrophage, as differences in protocol will play an increasing role in the expression data generated. Thus, clustering the dataset by sample may give an idea of how 'good' the dataset is.

Using a Pearson threshold cut-off of r=0.80, a network graph was generated of the data. The network contained 90 nodes, representing each of the 90 samples, and 744 edges. The network was then clustered using the MCL algorithm with an MCL inflation value set to 2.2. This gave 10 clusters. Each cluster represented samples whose expression patterns were highly correlated across the dataset. The clustered network graph is shown in Figure 6.7a. Additionally, the graph was hand-colour-coded by study and by macrophage subtype (Figure 6.7b and c).

All the duplicates, with the exception of one peritoneal macrophage that clustered with adipose macrophages (probably an outlier), clustered with each other. Because of the relatively small size of the dataset, with only 29 different samples (excluding duplicates) from only 6 different studies, there was not much overlap of different macrophage types across the studies. However, the dataset included peritoneal macrophages from three different studies, microglia from two different studies and monocytes from different studies. Although the peritoneal macrophages from all three studies did not cluster together in one group, they did appear to be closely connected and some peritoneal macrophages from each of the three studies clustered together. However, in contrast, microglia from two different studies clustered separately. Monocytes were mostly only available from one study and grouped into three separate clusters, which may reflect the different subtypes of monocytes with different expression markers included in this study. One group of monocytes from a separate study, the controls for the brain and colon TAM, clustered separately, which may be due to their being spleen monocytes, rather than the blood monocytes and mesenteric lymph node monocytes included in the largest study.

As can be deduced by comparing the graphs, the samples from the largest study (GSE15907) clustered into several other smaller clusters in addition to the monocyte clusters described above. There is one cluster that combines small intestinal lamina propria and serosal macrophages with liver macrophages, a cluster for microglia, lung macrophages and macrophages of the spleen.

Only two other clusters were identified by BioLayout Express^{3D}. One contained adipose macrophages from GSE36669. The largest cluster contained the TAM described earlier and their spleen monocyte controls, in addition to peritoneal macrophages and microglia.

Thus, the macrophage dataset clusters together some, but not all, macrophage types. Furthermore, clustering separated several macrophage subtypes from the largest study. Together these results suggest that the dataset is relatively good, although ideally more studies with more macrophage subtypes would have been included to better ensure the quality of the dataset.

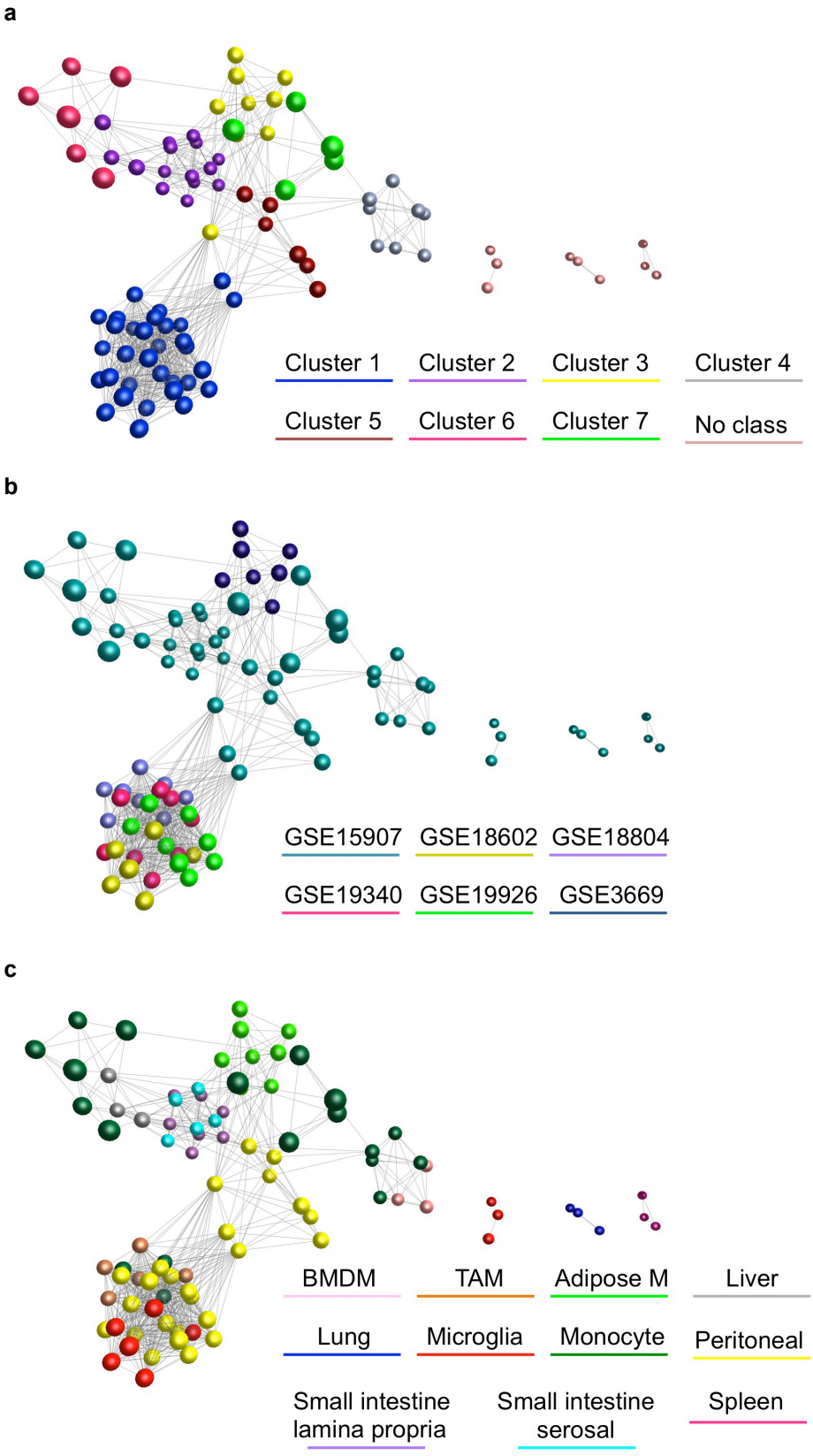
a
Cluster 1
Cluster 2
Cluster 3
Cluster 4
Cluster 5
Cluster 6
Cluster 7
No class
b
GSE15907
GSE18602
GSE18804
GSE19340
GSE19926
GSE3669
c
BMDM
TAM
Adipose M
Liver
Lung
Microglia
Monocyte
Peritoneal
Small intestine lamina propria
Small intestine serosal
Spleen

Figure 6.7 – Network clustering of macrophage dataset by samples.
BioLayout Express^{3D} was used to calculate pair-wise Pearson correlation coefficients for every study in the dataset. A network graph was constructed using a cut-off of r=0.8, where nodes represent individual studies. (a) The resultant graph was clustered using the Markov clustering algorithm with an inflation value of 2.2, and gave 10 clusters with >2 nodes. (b) Nodes are colour-coded according to the study they were part of. (c) Nodes are colour-coded according to macrophage type.

6.2.4 Analysis of starry-sky TAM up-regulated genes

Since it was not possible to directly compare the signature of starry-sky TAM from a model of Burkitt's Lymphoma (see 6.2.1), a starry-sky TAM signature was derived by comparing the whole transcription profile of TAM to its nearest normal tissue counterparts, namely tingible-body macrophages from germinal centres of activated lymph nodes (GCM) and resident tissue macrophages from resting lymph nodes (LNM), which had been acquired by the same method of laser capture dissection. This signature was then overlaid on the macrophage dataset network graph to identify the most important biological pathways up-regulated by starry-sky TAM compared to their normal counterparts.

DAVID Functional Gene Annotation analysis of the genes that were found to be up-regulated in TAM compared to GCM and LNM macrophages confirmed previous findings that the genes were associated with phagocytosis and lysosomes, the extracellular matrix, ATP synthesis, chemotaxis, inflammatory response, homeostasis, the nucleosome, inflammatory and wounding response, and angiogenesis and vasculature development.

To analyse these functions more thoroughly in various macrophage populations, these genes were then uploaded into the macrophage network graph, and it was analysed with which clusters they associated. 271 transcripts that were up-regulated in starry-sky TAM overlapped with transcripts in the macrophage dataset, of which 57 were not associated with any class. As predicted by DAVID analysis, a large number of genes up-regulated in starry-sky TAM were associated with phagocytosis, and 81 transcripts fell in the previously defined phagocyte cluster (Cluster 1). Further analysis and comparison of these gene transcripts with the annotated cluster of genes

enriched in phagocytes as defined by Hume et al. (2010) revealed that the majority of these genes (45) were associated with all aspects of endocytosis and phagocytosis, including signalling/regulation, internalisation, vesicle formation/acidification and digestion, although the largest numbers of genes appeared to be associated with vesicle formation and acidification (vesicle trafficking and proton pump) and digestion (protein degradation and processing, lipid digestion and storage and carbohydrate digestion). Gene annotation into specific categories associated with phagocytosis are presented in Table 6.5. Expression of the TAM-upregulated genes in the phagocyte cluster revealed that these genes are expressed by most monocytes and macrophages in the dataset, but are expressed highest by peritoneal macrophages and microglia. Mean expression is shown in Figure 6.8.

The second largest cluster that was associated with TAM-upregulated genes was Cluster 3 (cell cycle), which consisted entirely of histones. The macrophage dataset showed that these genes were expressed at high levels by BMDM and a subset of monocytes. BMDM are often cultured in the presence of M-CSF, and this colony stimulation factor is known to induce proliferation (Hume and MacDonald, 2012), so this is perhaps not entirely surprising. Furthermore, a subset of monocytes has been shown to be proliferative (Cheung and Hamilton, 1992). Adipose and brain and colon TAM and their control also showed above average expression of these genes, but much lower than BMDM or monocytes. Up-regulation of genes associated with the cell cycle and proliferation is in agreement with our published findings that a small proportion of starry-sky TAM proliferate *in vivo* (Ford *et al.*, 2015).

Furthermore, in agreement with the DAVID gene annotation analysis results, a large number of transcripts in cluster 5 (extracellular matrix) were up-regulated in TAM, which included collagens and fibronectins, known to contribute to the extracellular matrix architecture, and previously associated with TAM in other studies (Pollard, 2009; Chiodoni *et al.*, 2010). The average expression of these genes was highest for adipose macrophages, although peritoneal macrophages also showed a small up-regulation.

Cluster 12 showed the up-regulation of 8 genes. DAVID analysis reveals that they are mostly associated with the membrane and suggest roles in cell-cell recognition and cell-surface receptors, including Mertk and Vcam1. Mertk is a receptor for apoptotic cells (Shao *et al.*, 2009), and Vcam1 plays a role in the adhesion to endothelium (Shi and Pamer, 2011), but has also been associated with transmission of survival signals (Chen *et al.*, 2011). Mean gene expression presented in Figure 6.8 shows that these genes are highly expressed by macrophages of the spleen.

Other genes up-regulated by starry-sky TAM were scattered in small groups across various clusters. Some genes of interest are highlighted below. Cluster 14 shows up-regulation of Rsad2 and Timp1. Rsad2 is evenly expressed by all macrophages, but Timp1 appears to be associated with the LPS-response. Timp1 is a metallopeptidase inhibitor, a tissue inhibitor of matrix metalloproteinases (MMPs), a group of peptides involved in the degradation of the extracellular matrix. It has also been associated with TAM in a murine fibrosarcoma model (Biswas *et al.*, 2006). Two other genes associated with classical activation and up-regulated in TAM are Ifit2 and 3 (interferon-induced protein with tetratricopeptide repeats 2, and 3) in Cluster 28 (Mabbott *et al.*, 2010). Both genes are up-regulated in LPS-stimulated BMDM, as well as by macrophages of the small intestine. Starry-sky TAM-up-regulated Mmp2 was found in Cluster 53. Expression of this gene is high for small intestine lamina propria macrophages and adipose macrophages, but low for most of the other macrophages. Mmp2 is a collagenase, which can degrade basement membrane collagen (Liotta *et al.*, 1979). Cluster 122 contained starry-sky TAM up-regulated gene Trem2, which was shown in chapter 4 to also be up-regulated in classically-activated macrophages by co-culture with apoptotic cells. Trem2 is associated with the engulfment of bacteria (Underhill and Goodridge, 2012), but is also associated with alternatively activated macrophages (Gause *et al.*, 2013). The macrophage dataset shows that it is expressed at low levels by most monocytes, and macrophages, but increased by peritoneal macrophages and microglia. Complement components C1qa-c, associated with apoptotic cell engulfment (Ogden *et al.*, 2001; Ravichandran and Lorenz, 2007), were also up-regulated by starry-sky TAM, and found in Cluster 129. They were expressed at medium to high levels by all

macrophages, except for monocytes and BMDM. Finally, Cluster 202 contained starry-sky TAM up-regulated cytokines Ccl2, Ccl7, and Ccl12, which were expressed highly by small intestine serosal macrophages and adipose macrophages. Ccl2 is considered one of the most important factors contributing to macrophage infiltration of tumours (Murdoch, 2004).

Figure 6.8 also shows the mean expression levels of every cluster that contains TAM-up-regulated genes in one graph. As can be seen, no macrophage subset stands out for having high expression of the genes that were found to be up-regulated in TAM. Instead, some starry-sky TAM up-regulated genes are expressed at high levels by some macrophages, whereas genes associated with a different function are up-regulated by other macrophage types.

Gene annotation	Genes upregulated in TAM
Cytoskeletal regulation	Capg, Myo5a
Adhesion and Endocytic Receptors	Lgals3
Vesicle trafficking (Endosomes)	Cd68, Gpnmb, Grn, Lamp1, Lamp2 (Cluster 75), Samd8
Proton Pump	Atp6ap1, Atp6v0a1, Atp6v0c, Atp6v0d1, Atp6v0d2, Atp6v1a, Atp6v1b2, Atp6v1h
Protein degradation and processing	Ctsb, Ctsa, Ctsd, Ctsl, Ctsz, Mmp12, Anpep, Cndp2
Lipid Digestion and Storage	Nceh1 (Cluster 45), Lipa, Lpl, Lrp12, Npc2, Sgpl1, Soat1, Plin2
DNA digestion	Dnase1l1
Carbohydrate digestion	Galc, Galns, Gba, Gusb, hexa, Nagk
Calcium Regulation	Fam20c, Mcoln1, S100a1, Anxa4
Signalling	Gpr137b, Gpr137b-ps, Ly9, Trem2 (Cluster 122)

Table 6.5 – Annotation of genes in phagocyte cluster up-regulated by starry-sky TAM
Using annotations available from Hume et al. (2010) some of the genes up-regulated by starry-sky TAM that clustered in the phagocyte cluster (Cluster 1) of the macrophage dataset were classified into different processes associated with phagocytosis.

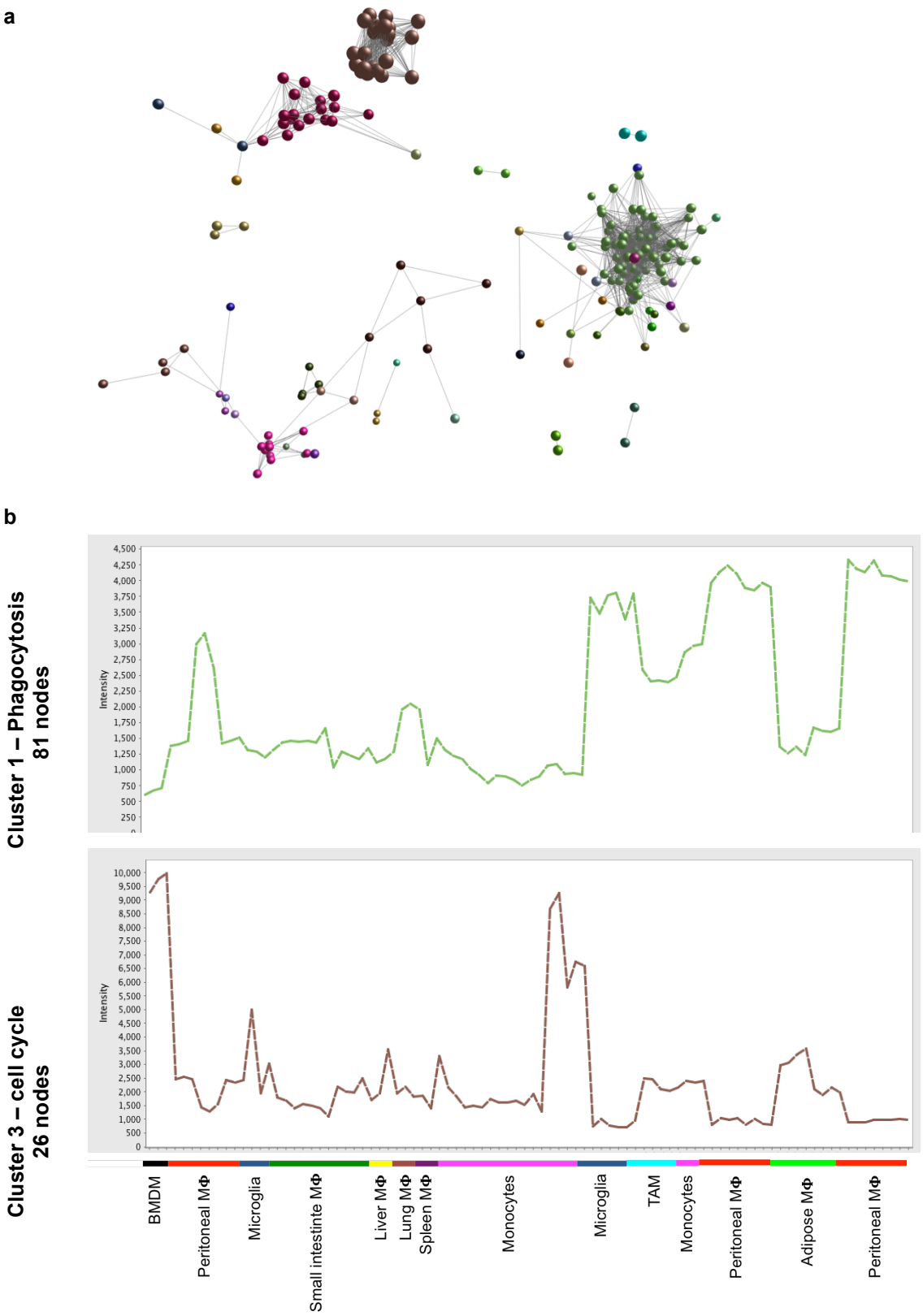
a
b
Cluster 1 – Phagocytosis
81 nodes
Cluster 3 – cell cycle
26 nodes
Intensity
BMDM
Peritoneal MΦ
Microglia
Small intestinte MΦ
Liver MΦ
Lung MΦ
Spleen MΦ
Monocytes
Microglia
TAM
Monocytes
Peritoneal MΦ
Adipose MΦ
Peritoneal MΦ

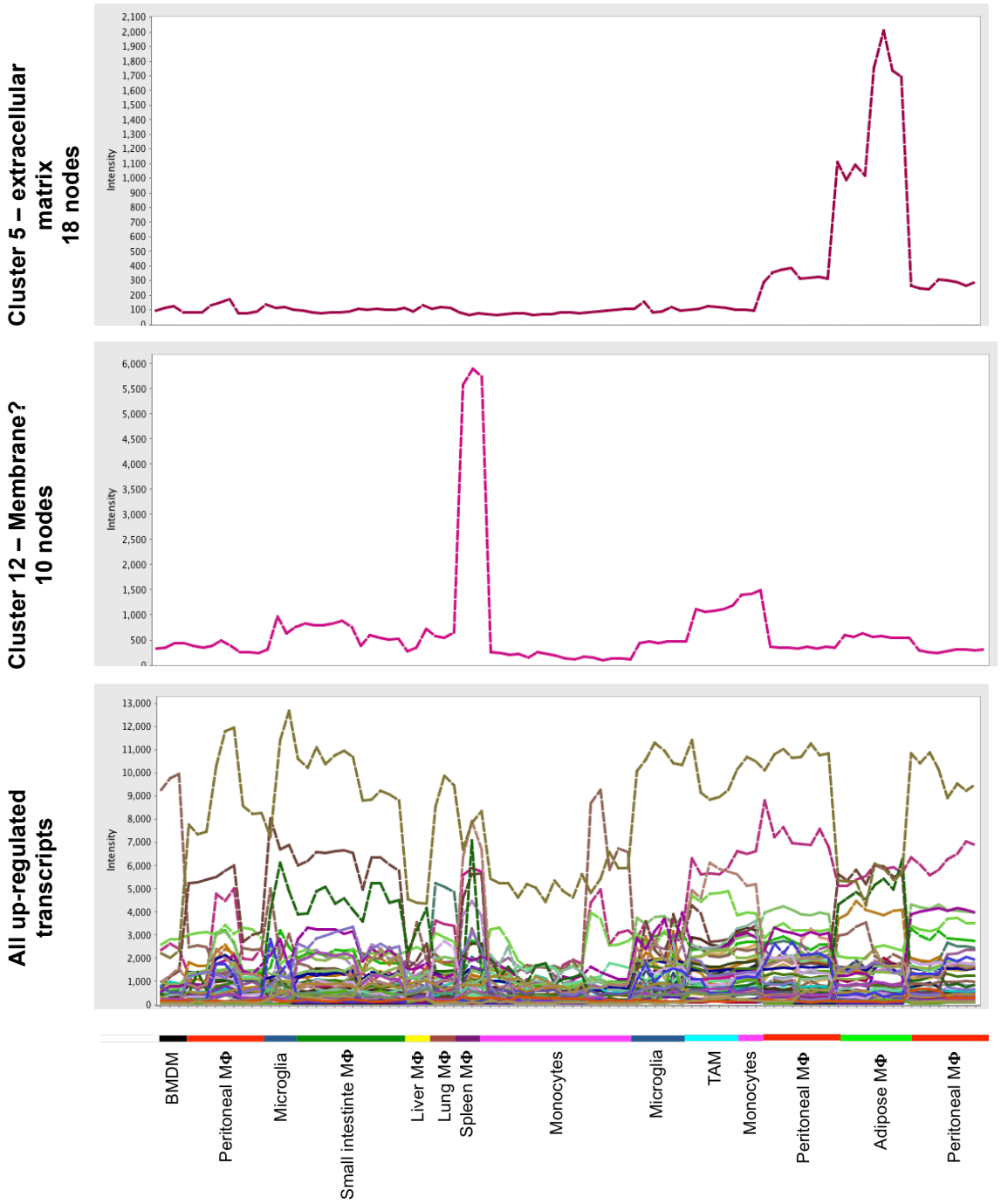

Figure 6.8 – Analysis of transcripts that are up-regulated by starry-sky TAM.
Transcripts that are up-regulated by starry-sky TAM (compared to GCM and LNM) were imported and overlaid onto the macrophage dataset network graph created created by BioLayout Express^{3D} analysis and shown in Figure 6.4. (a) The resultant graph consists of 209 nodes. (b) Mean expression profiles of starry-sky TAM transcripts for individual or all clusters. The number of nodes per cluster is indicated on the left.

6.2.5 Analysis of TAM down-regulated genes

In addition to investigating the expression of up-regulated starry-sky TAM genes, also genes that were down-regulated (compared to GCM and LNM) were analysed for their expression by the macrophages in the dataset. First DAVID gene annotation analysis was performed to identify the functions associated with these genes. The largest annotation clusters were associated with ribosomes, RNA processing, mitochondria, immune responses, proliferation/differentiation, the proteasome, and apoptosis.

Overlaying TAM down-regulated genes gave 744 genes that corresponded to genes in the macrophage network graph. As predicted by DAVID Functional Annotation Clustering, many of these genes were associated with ribosomes, RNA processing and mitochondria, and 326 genes were found in the clusters associated with these functions, including Clusters 2, 4, 8, 9, 15, 19, and 20. Figure 6.9 shows the mean expression of the transcripts in each of these clusters presented in one graph. With the exception of Cluster 9, which shows higher expression by monocytes, all gene transcripts are expressed fairly evenly by all macrophage and monocyte subtypes.

24 genes that were down-regulated by TAM were also associated with the phagocytosis cluster (Cluster 1). DAVID Functional Annotation Clustering revealed that these genes were for the most part associated with regulation of T cell activation and vesicles. Additionally, 23 transcripts were down-regulated within cluster 3, but these genes appeared to be associated with the cytoskeleton rather than with the cell cycle. These were expressed highest by BMDM, but also by subtypes of monocytes. Six genes that were down-regulated by starry-sky TAM were in the extracellular matrix cluster (Cluster 5), and expressed most highly by adipose macrophages. A total of 28 transcripts that were down-regulated by starry-sky TAM were in transcription clusters 7, 10 and 23. Expression levels were similar for all macrophages subtypes, except the Ikzf1 and Itga4 in cluster 23 were expressed at higher levels in various monocyte subtypes. Furthermore, seven transcripts that were down-regulated by starry-sky TAM, encoded five different genes that were associated with cluster 14, and were highly associated with LPS-stimulated

peritoneal macrophages. One of the genes was the chemokine Ccl5. Figure 6.9 also shows the mean expression of all starry-sky TAM down-regulated transcripts by cluster. Similar to the up-regulated starry-sky TAM genes, no macrophage subtype stands out for closely resembling the TAM by having low expression of these genes.

Combined, the results from the investigation of all starry-sky TAM up- and down-regulated genes by macrophages in the macrophage dataset suggest that no macrophage subtype included here shows very high expression of all starry-sky TAM up-regulated and low expression of down-regulated genes. Rather, different up-regulated TAM genes with different functions are associated with different macrophages. Furthermore, there was no indication that the brain and colon TAM present in the dataset closely resembled the starry-sky TAM.

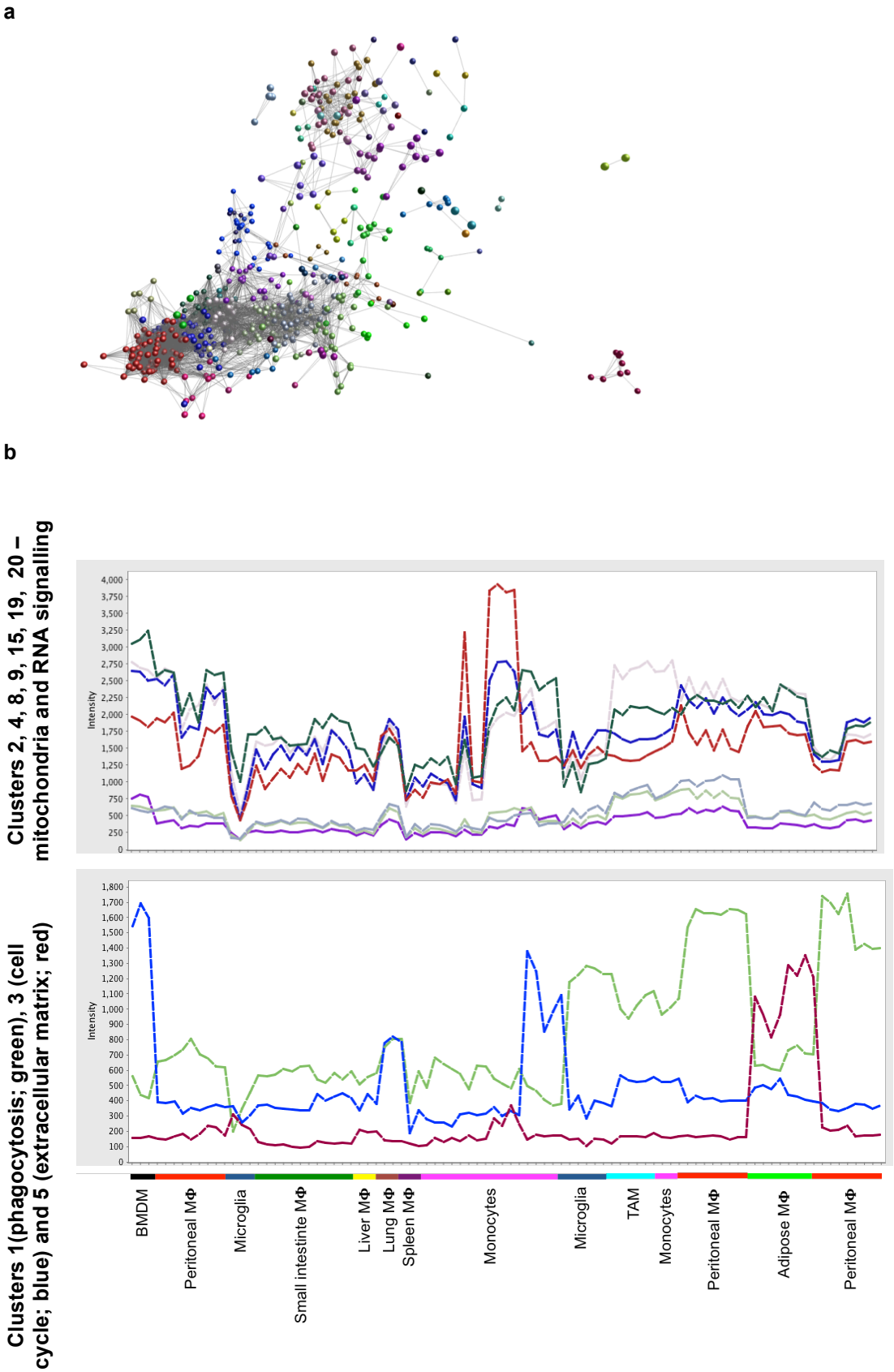
a
b
Clusters 2, 4, 8, 9, 15, 19, 20 – mitochondria and RNA signalling
Clusters 1(phagocytosis; green), 3 (cell cycle; blue) and 5 (extracellular matrix; red)
Intensity
BMDM
Peritoneal MΦ
Microglia
Small intestinte MΦ
Liver MΦ
Lung MΦ
Spleen MΦ
Monocytes
Microglia
TAM
Monocytes
Peritoneal MΦ
Adipose MΦ
Peritoneal MΦ

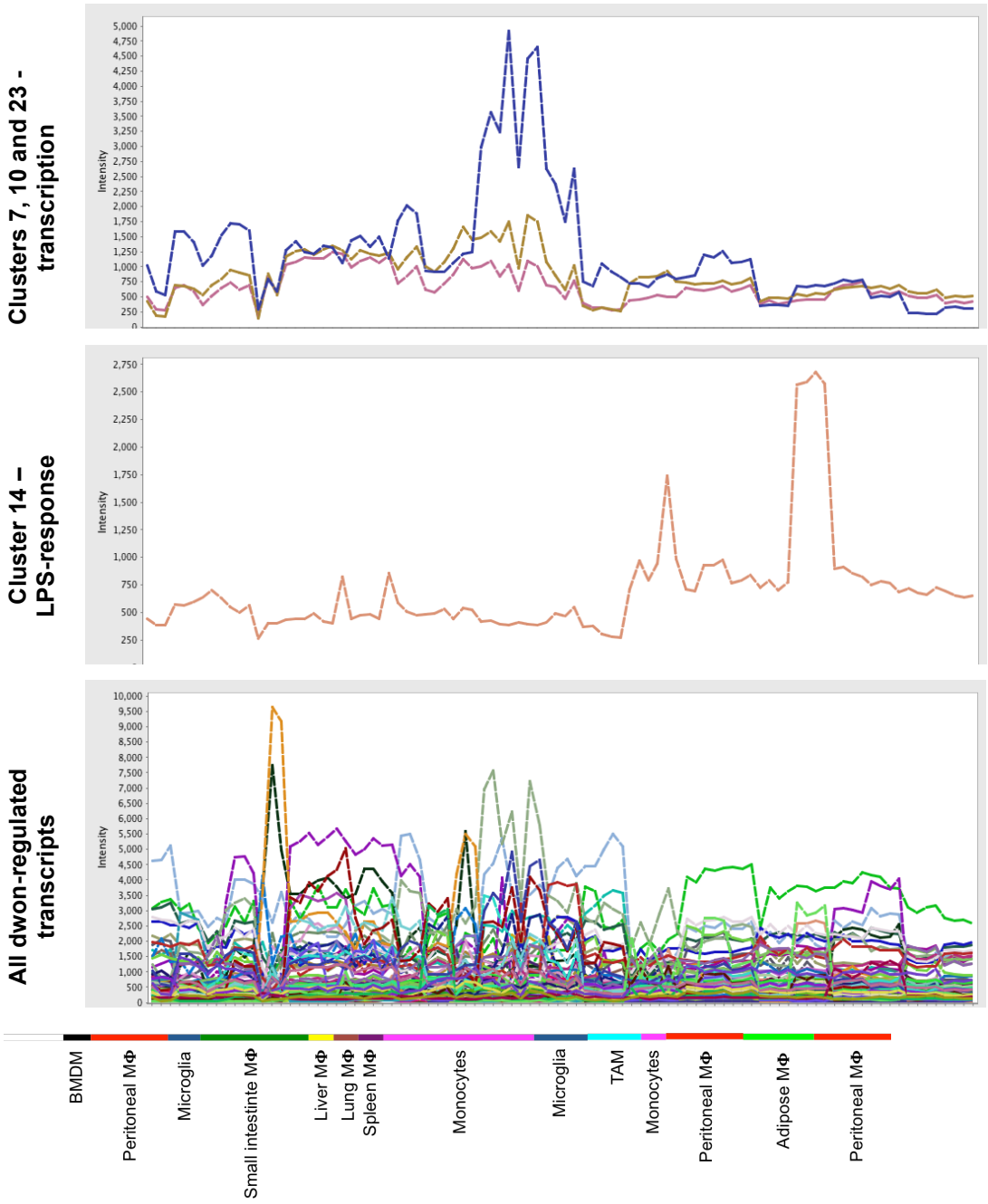

Figure 6.9 - Analysis of transcripts that are down-regulated by starry-sky TAM
Transcripts that are down-regulated by starry-sky TAM (compared to GCM and LNM) were imported and overlaid onto the macrophage dataset network graph created by BioLayout Express^{3D} analysis as shown in Figure 6.4. (a) The resultant graph consists of 744 nodes. (b) Mean expression profiles of starry-sky TAM transcripts for individual, groups, or all clusters.

6.3 Discussion

This chapter further investigated the phenotype of starry-sky TAM by comparing it to expression profiles of tissue and *in vitro* cultured monocytes and macrophages available from public databases.

First, monocyte and macrophage microarray gene expression datasets were selected from a functional genomics data repository to create a macrophage dataset. As the datasets were acquired from various different studies, they were all then subjected to rigorous quality and compatibility assessment. This was necessary to ensure that observations made from the dataset were objective and biologically relevant, and did not reflect differences in the acquisition of the sample or other technical differences. Additionally, to simplify the interpretation of the dataset, samples reflecting various time-points or irrelevant knock-outs were removed. In total, more than half the samples were removed from the dataset. Unfortunately, also the starry-sky TAM dataset, which we set out to compare to the other monocyte and macrophage subtypes had to be removed, together with the other datasets produced in our laboratory, because their mean expression levels were much lower than that of the other datasets. As described here previously, the TAM, GCM, and LNM datasets were produced from RNA derived from laser-captured microdissected macrophages. Because this method is highly labour-intensive, RNA from approximately only 1000 cells was collected, amplified, and hybridized onto microarray chips for each sample. None of the other datasets in the final macrophage dataset were acquired in this way. Monocytes were mostly isolated from peripheral blood and other tissue macrophages were collected after enzymatic digestion of tissues followed by fluorescence-activated cell sorting (FLOW), which may generate higher numbers of cells. Because more starting material could be used to generate gene expression for those cells, their mean expression levels were higher. Although these latter methods are less time consuming their resulting gene expression results may not be as accurate a representation of the actual macrophages they are supposed to resemble. Macrophages are highly plastic cells, and will respond quickly to their environments. Furthermore, enzymatic digestion has been shown to change receptor expression by macrophages and may also affect gene expression (Ford *et al.*, 1996). In contrast,

laser capture dissected starry-sky TAM and controls were taken from snap-frozen tumours and incubation of tissue samples at room temperature to 37˚C was highly limited to better preserve the *in situ* phenotype. Unfortunately, because this technique is relatively new and highly labour-intensive, no other macrophage datasets were available that had been prepared in the same way.

Following quality and compatibility assessment, bioinformatics analysis was then used to divide the gene transcripts into clusters of genes sharing similarities in their expression. The main clusters were then analysed using the online DAVID gene annotation tool to assign gene ontology information to the largest clusters and other clusters of interest. The largest cluster was highly associated with phagocytosis, and further analysis revealed that many different aspects of phagocytosis were contained in this cluster, including signalling and regulation, internalisation, vesicle formation and acidification, and digestion. This is not surprising, given that clearance of apoptotic cells and pathogens is one of the main functions of macrophages in many tissues. Some of the other large clusters were associated with broad biological processes and cellular functions, including mitochondria, ribosomes, and RNA processing, cell cycle, regulation of differentiation, proliferation and cell death, and transcription. Furthermore, one cluster was associated with extracellular matrix remodelling, and various clusters were described that were associated with classical activation by LPS and/or IFNγ.

The fact that the largest cluster in the dataset was associated with a known important biological function of macrophages also gives a positive impression of the accuracy of the dataset. Another method to assess the quality or accuracy of a dataset using BioLayout Express^{3D} is by clustering the data by sample, which clusters the samples with the greatest similarities across all transcripts together. Thus, if the gene expression of all transcripts for the samples truly represents the cells, one would expect similar subtypes of macrophages to group together, rather than the samples grouping by study. Because the final macrophage dataset was fairly small, and included macrophage datasets from only six different studies, it is difficult to assess the accuracy. However, the clustering and linking together of peritoneal

macrophages from three different studies is reassuring, as well as the division of samples from the largest study into separate clusters. However, it would have been preferable if more macrophage datasets could have been incorporated into the dataset.

Because of the incompatibility of the starry-sky TAM, an indirect comparison of TAM to the other macrophages was performed. First, starry-sky TAM gene expression profiles were compared to the profiles of tingible-body macrophages from germinal centres of activated lymph nodes as well as to resident tissue macrophages from resting lymph nodes. Up- and down-regulated genes were listed and overlaid on the macrophage dataset, thereby creating two network graphs, one for up-regulated and one for down-regulated starry-sky TAM genes. These were then individually analysed. The cluster with the highest number starry-sky TAM up-regulated genes was the phagocyte cluster. Further analysis using gene annotation presented by Hume et al. (2010) revealed that more than half of those genes were indeed involved in all different stages of phagocytosis, especially with vesicle formation and acidification, and digestion. It is not surprising that phagocytosis is up-regulated by starry-sky TAM, as the cells are known to have engulfed large numbers of apoptotic cells, which can be easily visualized by H&E staining and gives them their starry-sky histological appearance (Ford *et al.*, 2015).

Another cluster that contained starry-sky TAM up-regulated genes was the cell cycle cluster, and was highly associated with monocytes and BMDM. This is in agreement with our published findings that a small subset of TAM are proliferating (Ford *et al.*, 2015). Furthermore, many genes associated with the extracellular matrix were up-regulated in TAM, including various collagens and fibronectins. In the macrophage population these appeared to be associated with adipose and peritoneal macrophages. Research described here as well as published findings by our laboratory has shown that expression of some extracellular matrix-associated genes can be induced in macrophages by co-culture with apoptotic cells. In Chapter 4 we showed that Timp2, a metallopeptidase inhibitor, is up-regulated in classically-activated BMDM upon co-culture with apoptotic cells. Furthermore, our published research has shown that the

matrix metalloproteases Mmp12 and Mmp2 are up-regulated in macrophage cell lines upon apoptotic-cell co-culture (Ford *et al.*, 2015). Interestingly, however, Timp2, Mmp12, and Mmp2 were found not to cluster in the extracellular matrix cluster, but each of them clustered with other genes. Mmp12 was found to be associated with the phagocytic cluster, which suggests that Mmp12 up-regulation is associated with phagocytosis. Other genes that were up-regulated in TAM were scattered across different clusters, but did include both genes associated with classically-activated macrophages, and genes associated with wound-healing macrophages.

Many more genes were down-regulated by starry-sky TAM than up-regulated. Overlaying these down-regulated genes onto the macrophage dataset network graph revealed that about half were associated with general cell functions, including RNA processing and mitochondria.

Interestingly, also genes associated with the phagocyte cluster were down-regulated by TAM, but analysis of these genes using DAVID gene annotation analysis suggested they might not be involved in phagocytosis, even if their expression is highly similar to that of genes associated with phagocytosis. Furthermore, some genes were down-regulated in the cell cycle cluster, but they appeared to be associated with the cytoskeleton rather than specifically with the cell cycle, as revealed by DAVID gene annotation analysis. Other genes that were down-regulated were mostly associated with other broad cellular function clusters, although a few genes associated with LPS signalling were down-regulated by starry-sky TAM too.

No macrophage subtype from the dataset really stood out for closely resembling the starry-sky TAM profile. Rather, the starry-sky TAM phenotype reflects the activation status of a mixture of the other macrophages in the dataset. This is likely due to their unique environment compared to the other macrophages included in the dataset. However, although no single macrophage subtype expressed high levels of all the genes up-regulated by starry-sky TAM, this does not by definition mean that none of them is highly associated with the starry-sky TAM. As our published studies

have shown, MMPs that are up-regulated by starry-sky TAM are still only expressed at very low levels by those TAM. This does not make those genes less important, but it reveals the limitations of analysis using BioLayout Express^{3D} when a sample cannot be included in the dataset for direct comparison. Furthermore, gene expression levels do not tell the complete story of macrophages activation, and protein expression levels may differ from gene expression levels due to differences in translation and activation.

The brain and colon TAM that were included in the dataset did not appear to be very similar to starry-sky TAM either. This could be either because starry-sky TAM are very different from brain or colon TAM, but also because of the different ways in which the expression profiles were derived. The starry-sky TAM gene expression represented that of *in situ* TAM, whereas the brain and colon TAM were derived *in vitro* from co-culture with supernatants from cancer cells.

Thus, being unable to directly compare starry-sky TAM to other macrophages in the dataset, we could not assess if there was a macrophage subtype similar to TAM. However, further exploration of the TAM genes that were up- and down-regulated confirmed that some of the most important biological processes in TAM are associated with phagocytosis, cell cycle, and the extracellular matrix. Association with phagocytosis, and the fact that starry-sky TAM have engulfed many apoptotic cells, supports the hypothesis that interaction with apoptotic cells is highly important in driving the TAM signature, although involvement of other factors, e.g. viable tumour cells, cannot be ruled out.

Chapter 7 Discussion

7.1 Thesis objectives and summary of findings

The main objective of this thesis was to improve understanding of the role of apoptotic cells in shaping the tumour microenvironment of Burkitt's lymphoma. Specifically, the effect of apoptotic cells on the accumulation and activation of tumour-associated macrophages was investigated and how this may affect tumour growth.

Starry-sky non Hodgkin lymphoma, in particular Burkitt's Lymphoma, is characterised by high rates of apoptosis, high infiltration of macrophages, and rapid tumour growth The apoptotic cells are rapidly engulfed by tumour-associated macrophages (Hecht and Aster, 2000). A high proportion of TAM is generally associated with a poor prognosis in many cancers (Balkwill and Mantovani, 2001; Coussens and Werb, 2002; Leek *et al.*, 1996; Campbell *et al.*, 2011; Salvesen and Akslen, 1999; Ni *et al.*, 2015). Engulfment of apoptotic cells by macrophages has been found to activate downstream signalling pathways that enhance tumour cell growth, through the promotion of anti-inflammatory responses, angiogenesis, tissue remodelling and metastasis, although the dying tumour cells may also affect neighbouring tumour cells directly (Ogden *et al.*, 2005; Gregory and Pound, 2011). Recently, the *in situ* molecular signature of TAM in a xenograft model of Burkitt's lymphoma was generated, and TAM were found to be significantly enriched for transcripts encoding matrix remodelling, lipid metabolism, and phagocytosis functions, which are associated with a pro-tumour and immunosuppressive phenotype, although expression of certain inflammatory and immune response-associated molecules was increased too. Further investigations revealed that tumour cell apoptosis in co-culture assays with macrophages could up-regulate expression of active matrix remodelling mediators, in particular MMP12 and MMP2 (Ford *et al.*, 2015). The research presented here contributed to these studies, by further exploring the effects of apoptotic cells on macrophage activation and how this may affect

tumour cell growth in a series of *in vitro* experiments. Additionally, TAM activation signature was further studied *in silico*.

To further elucidate the role of apoptotic cells on macrophages activation, first the possible effects of lactoferrin were investigated in Chapter 3. Lactoferrin was identified by our laboratory to be released from apoptotic cells (Bournazou *et al.*, 2009). Because of its pleiotropic properties, including anti-inflammatory effects on macrophages (Håversen *et al.*, 2002; Crouch *et al.*, 1992; Mattsby-Baltzer *et al.*, 1996; Elass, 2002; Bournazou *et al.*, 2009), it was investigated if lactoferrin could promote the accumulation and activation of macrophages that are anti-inflammatory, immunosuppressive, and promote tumour growth, angiogenesis, and tissue remodelling.

Contrary to previous reports that lactoferrin can attract monocytes (la Rosa *et al.*, 2008), lactoferrin was not found to be able to induce chemotaxis of murine or human monocytes in Boyden chamber-like assays. Furthermore, although lactoferrin has been shown to increase the phagocytosis of parasites (Kai *et al.*, 2002; Lima and Kierszenbaum, 1985), binding assays showed that soluble lactoferrin does not enhance apoptotic cell binding to macrophages, and instead suggested that it may decrease binding, possibly due to competitive binding to a receptor that also binds apoptotic cells. Furthermore, the ability of lactoferrin to stimulate a starry-sky TAM expression profile was investigated. Only high concentrations of lactoferrin, unlikely to be clinically relevant in tumours, were found to affect macrophage activation (up-regulation of Mrc1, Mmp2, and Axl) or cytotoxicity.

As lactoferrin released from apoptotic cells in tumours appeared unlikely to affect starry-sky TAM activation, Chapter 4 investigated the direct effects of apoptotic cells on macrophages. Apoptotic cells were found to up-regulate expression of starry-sky TAM associated genes Ccl2 and Hmox1 in BMDM, and down-regulate Mmp12, Fn1, Anpep, Abca1, Lrp1, and Plau expression. Furthermore, co-culture with apoptotic cells could enhance expression of Gas6, Mrc1, Cd36, Timp2, and Pparg by classically-activated macrophages. Expression of the latter was found to be

dependent upon cell contact between apoptotic cells and macrophages. Furthermore, inflammatory responses, in particular Tnf and Il6 expression, were reduced upon co-culture with apoptotic cells. These effects were specific for co-culture with apoptotic cells, as viable cells or apoptosis-suppressed cells did not have the same effects.

Given the ability of apoptotic cells to reduce pro-inflammatory signalling, the effect of apoptotic cells on classically-activated macrophage cytotoxicity was investigated. Interestingly, pre-treatment of classically-activated macrophages did not affect the number of dead lymphoma cells, but increased the number of viable lymphoma cells, suggesting that pre-treatment with apoptotic cells could promote tumour cell growth, and this was contact-dependent. Macrophage deficiency of galectin-3, shown here and previously shown by Sano et. al (2003) to reduce macrophage phagocytosis of apoptotic cells, did not appear to play a role in apoptotic-cell mediated effects on classically-activated macrophages, but this may be due to an ability of IFN-γ and LPS-stimulation to increase the phagocytic properties of both galectin-3 KO and wild type BMDM.

Nitric oxide and TNFα were selected as potential mediators of classically-activated macrophage cytotoxicity towards lymphoma cells, but TNFα could not induce apoptosis in lymphoma cells. NO has both the ability to induce apoptosis and to act as a growth factor (Choudhari *et al.*, 2013; Burke *et al.*, 2013; Weigert and Brüne, 2008). Measurement of nitrite release from apoptotic cell-stimulated classically-activated macrophages showed it was unlikely to be released as a growth factor, but the ability of NO to induce apoptosis in lymphoma cells remains unclear.

In silico comparison of the starry-sky TAM activation signature to transcription profiles of a variety of tissue and *in vitro* cultured macrophages confirmed that a large number of TAM up-regulated transcripts were associated with phagocytosis, including some receptors for apoptotic cells, suggesting that phagocytosis of apoptotic cells is indeed an important function of TAM in BL. Additionally, regulation of the cell cycle and extracellular matrix appeared to be important functions of starry-sky TAM. Other genes up-regulated by TAM include genes

associated both with classically-activated macrophages and wound-healing macrophages, although starry-sky TAM also showed some features of classically-activated macrophages. No macrophage subset in the dataset showed activation that was very similar to starry-sky TAM, but rather the starry-sky TAM activation profile seemed to resemble a mixture of macrophages.

7.2 Lactoferrin in the tumour microenvironment

Research presented in Chapter 3 investigated lactoferrin-mediated macrophage chemoattraction and activation. In contrast to previous findings that lactoferrin can affect pro-inflammatory signalling by macrophages, only high concentrations of lactoferrin were found to stimulate expression of starry-sky TAM genes. Additionally, only high concentrations of lactoferrin could reduce macrophage cytotoxicity, although it was unclear if this was due to lactoferrin binding to LPS, thereby preventing activation of macrophages, or if it reduced the effects of classical activation by acting on macrophages separately. As high concentrations of lactoferrin are not expected to be derived from apoptotic tumour cells, lactoferrin is unlikely to affect tumourigenesis of starry-sky NHL through the accumulation and activation of tumour-associated macrophages, unless another source of lactoferrin, e.g. from infiltrating neutrophils, is present in the tumour microenvironment. No neutrophil accumulation is observed in Burkitt's lymphoma (Bournazou *et al.*, 2009), likely due to lactoferrin's ability to inhibit the migration of neutrophils (Bournazou *et al.*, 2009). However, in tumours with high levels of neutrophils, lactoferrin may play a role in the activation of TAM. Additionally, lactoferrin may be important in the activation of macrophages during the resolution of inflammation when high levels of lactoferrin are released from apoptotic neutrophils.

However, even if lactoferrin released from apoptotic tumour cells is unlikely to affect starry-sky TAM accumulation and activation, it may still play a role in the tumour microenvironment in addition to inhibiting neutrophil and eosinophil migration. Recent preliminary findings show that lactoferrin can bind to secondarily necrotic cells once they become permeable (Willems *et al.*, 2014). Persistence of uncleared apoptotic cells, perhaps through saturation of macrophage phagocytosis,

could lead apoptotic cells to become secondarily necrotic. As the cells become permeable, noxious contents may be released, which can lead to pro-inflammatory responses (Fadok *et al.*, 2001a; Voll *et al.*, 1997). Therefore, it is tempting to speculate that lactoferrin may reduce pro-inflammatory responses resulting from persistent secondarily necrotic cells, by mopping up necrotic cell-released pro-inflammatory contents by macrophages (Willems *et al.*, 2014). More research is needed to find out what lactoferrin binds to in secondary necrotic cells, but DNA is a likely candidate as lactoferrin is known to bind DNA (Bennett *et al.*, 1983). This proposed effect of lactoferrin would not only maintain an anti-inflammatory environment in tumours, but could also play a role in the resolution of inflammation, where neutrophil activation and death may lead to the release of large quantities of lactoferrin.

Finally, given lactoferrin's shown trophic properties to enhance cell growth, lactoferrin released from apoptotic cells may also affect tumourigenesis by acting directly on tumour cells. Findings in our laboratory indicate that lactoferrin cannot enhance BL cell growth (Ben Arnold; personal communication), but this should be investigated for other tumours.

In addition to its anti-inflammatory and trophic properties that may enhance tumourigenesis (Huang *et al.*, 2008; Tang *et al.*, 2010a; Grey *et al.*, 2006; Nakajima *et al.*, 2011), lactoferrin has also been shown to have many pro-inflammatory, immunostimulatory, and cell-growth inhibiting properties (Son *et al.*, 2002; Sorimachi *et al.*, 1997; Mattsby-Baltzer *et al.*, 1996; Nishiya and Horwitz, 1982; Damiens *et al.*, 1998). Oral administration and injections of lactoferrin have been shown to decrease tumour growth both in humans and mice (Varadhachary *et al.*, 2004; Wang *et al.*, 2000; Hayes *et al.*, 2005). Together, these findings suggest that lactoferrin may control both pro- and anti- inflammatory cytokine expression. Future research should focus on the question whether anti-tumour therapy leads to the release of lactoferrin from dying tumour cells, and if this negatively, or alternatively positively, affects long-term therapeutic outcome.

7.3 Apoptotic-cell stimulation of macrophages

7.3.1 Macrophage activation

Research presented in Chapter 4 investigated whether apoptotic cells can activate a starry-sky TAM phenotype in macrophages. *In vitro* co-culture of apoptotic cells with BMDM showed moderate up-regulation of mouse macrophage markers F4/80 and mannose receptor. Additionally, apoptotic cell co-culture with macrophages was shown to enhance macrophage expression of Hmox1 and Ccl2. Heme oxygenase -1 (HO-1), is an essential enzyme in heme catabolism and has been shown to stimulate expression of anti-inflammatory cytokines IL-10 and IL-1 receptor antagonist (IL-1Ra) by mouse liver, human HepG2 cells, and mouse J774.1 macrophages, and reduce TNF-α expression, which could be inhibited by Hmox1 RNA silencing (Piantadosi *et al.*, 2011). CCL2 is a strong chemoattractant for mononuclear phagocytes and has also been reported to recruit T cells, B cells, and natural killer cells (Allavena *et al.*, 1994; Qin *et al.*, 1996; Corcione *et al.*, 2002), but its ability to recruit neutrophils is weak (Rollins *et al.*, 1991). In addition to its chemoattractant properties, CCL2 has also been shown to have various trophic functions. It can promote monocyte survival through expression of anti-apoptotic proteins Bcl-2 and Bcl-x_L and inhibition of caspase-8 cleavage. Furthermore, CCL2 can enhance expression of mannose receptor on macrophages (Roca *et al.*, 2009) and it has been shown to induce proliferation of vascular smooth muscle cells (Selzman *et al.*, 2002). Perhaps paradoxically, Ccl2 expression is also up-regulated by classical activation of macrophages as shown in Chapter 4 and reported by (Mantovani *et al.*, 2004b) and this may explain why Ccl2 gene expression was not found to be further up-regulated by co-culture of classically-activated macrophages with apoptotic cells. Moreover, CCL2 has also been shown to increase intracellular Ca^{2+} levels and to induce a respiratory burst in human monocytes (Rollins *et al.*, 1991).

Although CCL2 has been shown to be released from apoptotic cells (Kobara *et al.*, 2008), to our knowledge, this is the first time it is shown that co-culture with apoptotic cells can enhance the expression of Ccl2 by macrophages. It has previously been reported that in mouse J774 macrophages apoptotic cell ingestion results in the early release of TGF-β, and that this leads to decreased synthesis and secretion of

TNFα and several chemokines (including macrophage inflammatory protein-2 (Mip-2) and Mip-1α) and increased TGF-β release. However, production of CCL2 was not found to be down-regulated after treatment with apoptotic cells, and remained the same (McDonald *et al.*, 1999).

CCL2 is abundantly expressed in tumours (Mantovani *et al.*, 2002), and is believed to be one of the most important factors contributing to macrophage infiltration (Murdoch, 2004). Overexpression of CCL2 in non-tumourigenic melanoma cells results in tumour formation, and massive monocyte/macrophage infiltration into the tumour mass in mice (Nesbit *et al.*, 2001). Thus, the results presented here may propose a new mechanism for the accumulation of TAM, i.e. that apoptotic tumour cells can attract mononuclear phagocytes and activate them to produce CCL2, thereby setting a positive feedback system to recruit more phagocytes which interact with more apoptotic cells. This may work in concert with TAM proliferation to increase the number of TAM as tumours expand.

Co-culture of apoptotic cells with unstimulated macrophages also led to reduced expression of various starry-sky associated genes, including lower expression of Fn1, Mmp12, Plau, Anpep, Abca1, and Lrp1. The down-regulation of Mmp12 is particularly interesting, as published studies have shown that co-culture of apoptotic cells with immortalized macrophage cell lines can enhance gene and protein expression of Mmp12 (Ford *et al.*, 2015). One possible explanation for the difference in results is that different phagocyte receptors may be involved in the different macrophage populations, which could lead to divergent responses.

Because BMDM were matured in the presence of apoptotic cells, which may already activate the BMDM, additionally, the ability of apoptotic cells to affect the phenotype of classically-activated macrophages was investigated. Classical activation was shown to down-regulate the expression of a large number of starry-sky TAM genes, although some genes were up-regulated as a result of classical activation. Co-culture of classically-activated macrophages with apoptotic cells could significantly up-regulate expression of Gas6, Mrc1, Cd36, Pparg, and Timp2

by classically-activated macrophages. Gas6, CD36, and Pparg, are known to be associated with apoptotic cell engulfment and processing (CD36 is an apoptotic cell receptor (Savill *et al.*, 1992), Gas6 is a bridging molecule (McCloskey *et al.*, 1997), and Pparg is a nuclear receptor regulating fatty acid storage and glucose metabolism (Hume *et al.*, 2010)) and this may be another way in which apoptotic cell-signalling may prepare macrophages for apoptotic cell clearance. Previously, ATP released by apoptotic cells has been shown to increase apoptotic cell binding to macrophages (Marques-Da-Silva *et al.*, 2011), and fractalkine released from apoptotic cells has been shown to induce expression of MFG-E8 (Miksa *et al.*, 2007), another bridging molecule. Timp2 is a metallopeptidase inhibitor, involved in extracellular matrix remodelling and has been associated with alternative activation (Welch, 2002). Mrc1 is a carbohydrate-binding receptor that is expressed by macrophages and dendritic cells and has been associated with alternative activation of macrophages (Martinez-Pomares, 2012; Franklin *et al.*, 2014). Up-regulation of Gas6, Mrc1, Cd36, and Timp2 was not prevented by the presence of a 0.44μm membrane separating the apoptotic cells and macrophages, suggesting that the up-regulation was mediated through signalling of soluble factors released from apoptotic cells. Further research will need to be carried out to find out which factors are responsible, but candidate factors include ATP, fractalkine, S1P, and CCL2. The up-regulation of Pparg was dependent upon direct contact between apoptotic cells and macrophages, and further investigations will need to reveal if binding of apoptotic cells could induce up-regulation, or if it was triggered by engulfment and/or degradation of apoptotic cells.

Moreover, some of the apoptotic cell-mediated effects on macrophage phenotype may be associated with microvesicles released from apoptotic cells, which may enhance their longevity and effective signalling range (Hochreiter-Hufford and Ravichandran, 2013). Microvesicles (or microparticles) are shedded from the membrane of apoptotic or activated cells and form a heterogeneous population of small (<1μm) vesicles (Distler *et al.*, 2005; Hugel *et al.*, 2005; Zocco *et al.*, 2014). They can be distinguished from apoptotic bodies, both in size (apoptotic bodies are many times larger) (Hristov, 2004), as well as their time of release from apoptotic cells, which happens during the early stages of apoptosis for microparticles, whereas

apoptotic bodies form during the later stages (Distler *et al.*, 2005). Microvesicles display cell surface proteins of the cell from which they originate, and may express PS on the outer membrane (Distler *et al.*, 2005; Hugel *et al.*, 2005; Zocco *et al.*, 2014). Because of their size and resemblance to the cells they originate from, microvesicles have been suggested to function as intercellular signalling vesicles. Indeed, microvesicles released from activated cells can transfer bioactive molecules and modulate processes such as inflammation, coagulation, cell proliferation, vascular function and apoptosis (Distler *et al.*, 2005; Hugel *et al.*, 2005; Zocco *et al.*, 2014; Lai *et al.*, 2015). Furthermore, cancer cell-derived microvesicles have been shown to transfer transformed characteristics of cancer cells onto normal fibroblast, including enhanced survival capacity (Antonyak *et al.*, 2011). They appear to play a role in the pathogenesis of many diseases, including cancer (Baj-Krzyworzeka *et al.*, 2006; 2007) and rheumatoid arthritis (Distler *et al.*, 2005).

Microparticles released from apoptotic cells have not been studied intensively, but they have been found to carry RNA and DNA (Reich and Pisetsky, 2009), which suggests they could be involved in intercellular signalling. Furthermore, they have been associated with the chemoattractant fractalkine (Truman *et al.*, 2008), and fractalkine-positive microvesicles have been shown to induce chemoattraction of alveolar macrophages (Truman *et al.*, 2008; Tsai *et al.*, 2014). Additionally, ICAM-3 has been shown to be released within microvesicles, and can facilitate tethering of macrophages (Torr *et al.*, 2011). Unpublished findings in our laboratory indicate that the majority of microvesicles released from apoptotic lymphoma cells are smaller than 400nm in diameter, although a small proportion of microvesicles is larger. Thus further studies are needed to determine if signalling through microvesicles released from apoptotic cells could be responsible for some of the apoptosis-mediated effects on macrophages presented here.

In Chapter 4 it was also shown that apoptotic cell co-culture down-regulated gene and cytokine expression of TNFα and IL-6 by classically-activated macrophages. Other studies have previously shown that pre-incubation with apoptotic cells, but not viable or fixed permeable cells, can increase anti-inflammatory signalling of IL-10

and decrease pro-inflammatory TNF-α, IL-1β, and IL-12 signalling in (Fadok *et al.*, 2001a; Voll *et al.*, 1997; Fadok *et al.*, 1998a). This effect was mimicked by monoclonal antibodies targeted against the thrombospondin-binding site of CD36. Moreover, antibodies specific for thrombospondin, which block the engulfment of apoptotic cells, inhibited the effects of apoptotic cells. This indicated that CD36 might be involved (Voll *et al.*, 1997). Interestingly, here it was shown that apoptotic lymphoma cells can also enhance Cd36 gene expression by classically-activated macrophages in addition to reducing Tnf and Il6 expression. This suggests that there might be a positive feedback loop, where apoptotic cell signalling through CD36 to reduce expression of Tnf and Il6, simultaneously increases the capacity of macrophages to interact with apoptotic cells by increasing CD36 expression. Thus, the importance of CD36 in apoptotic-cell mediated signalling needs to be further investigated.

7.3.2 Tumour cell growth

Research presented in Chapter 5 also investigated the ability of apoptotic cells to affect macrophage cytotoxicity. Previous studies have shown that co-culture with necrotic tumour cells can enhance cytotoxicity of unstimulated and IFN-γ and LPS-stimulated macrophages. In contrast, apoptotic cells were shown to reduce cytotoxicity of IFN-γ and LPS-stimulated macrophages, although it was unclear if this was due to apoptotic cell interaction with the macrophages or due to apoptotic cell-binding to LPS (Reiter *et al.*, 1999). Interestingly, the research presented here shows that pre-treatment of classically-activated macrophages with apoptotic lymphoma cells led to an increased number of viable lymphoma cells without affecting the total number of free non-viable cells. This was likely due to promotion of tumour growth. This effect of apoptotic cell-stimulation of classically-activated macrophages on tumour cell growth appeared to be mediated through cell-to-cell contact, although larger microvesicles (> 400nm diameter), may also play a role. It was not investigated if apoptotic-cell pre-treatment of non-activated macrophages could also enhance tumour cell growth, but findings by Reiter et al. (1999) suggested this is the case and it will be of interest to study this in more detail.

The mechanism(s) through which tumour cell growth was stimulated in the assays presented here is unknown, but a likely mechanism is through the release of growth factors from the classically-activated macrophages upon treatment with apoptotic cells. NO, known for its stimulation of tumour cell growth and tumour cell death (refs) was briefly investigated as a potential mediator of tumour cell growth (as well as tumour cell death), but results indicated that NO is unlikely to be the mediator of tumour cell growth, although its role in tumour cell death needs to be investigated further. Other factors shown to be released from TAM that can stimulate the growth and motility of tumour cells, include TGF-β, vascular endothelial growth factor (VEGF), platelet-derived growth factor (PDGF), IL-10, epidermal growth factor (EGF), fibroblast growth factor (FGF), platelet activating factor (PAF), hepatocyte growth factor (HGF) and insulin-like growth factor 1 (IGF-1) (Pollard, 2004; Leek and Harris, 2002; O'Sullivan *et al.*, 1993; Burgess, 1989; Ogden *et al.*, 2005; Ford *et al.*, 2015). NO was investigated as a potential mediator of tumour cell growth (as well as tumour cell death), but its role remained unclear and should be investigated further.

TGF-β and IGF-1 are particular candidates for stimulating the apparent tumour growth presented here, as they were found to be up-regulated by starry-sky TAM. However, Igf1 gene expression analysis presented here did not appear to be affected by co-culture of apoptotic cells with classically-activated macrophages. TGF-β has been found to be produced by macrophages upon phagocytosis of apoptotic neutrophils (Fadok *et al.*, 1998a). However, *in vitro* experiments have shown that TGF-β inhibits growth of BL cells (Spender *et al.*, 2009).

Other candidates for stimulating the apparent tumour growth are PGE2 and PAF, as production of both is up-regulated by phagocytosis of apoptotic neutrophils. (Fadok *et al.*, 1998a; Morimoto *et al.*, 2001). Furthermore, IL-10 has been shown to be released from macrophages upon stimulation with apoptotic cells and IL-10-activated macrophages increased production of the B cell survival factor, B cell-activating factor of the TNF family/B lymphocyte stimulator (BAFF/BLyS), which can enhance BL cell survival (Ogden *et al.*, 2005). Finally, phagocytosis of apoptotic

Jurkat T cells by peritoneal macrophages can lead to the secretion of VEGF, which can promote proliferation of cells.

In addition to directly enhancing tumour cell growth, some of these factors have also been shown to enhance angiogenesis, e.g. VEGF, which may be an additional way by which apoptotic cells can promote tumour growth *in vivo* (Mantovani *et al.*, 2002; Sica *et al.*, 2008b; Pollard, 2004). Stimulation of angiogenesis is one of the properties shared by many TAM (Cook and Hagemann, 2013; Noy and Pollard, 2014), and can contribute to tumour progression (Lin *et al.*, 2007).

7.4 Implications for cell death-inducing anti-cancer therapy

Although the importance of induction of apoptosis in inhibiting cancer has been established, it is increasingly becoming clear that apoptosis-inducing therapies, including radiotherapy and chemotherapy, can lead to tumour repopulation.

Various studies have indeed shown that irradiation of tumour cells can induce accelerated repopulation of the tumour. In a model of rat rhabdomyosarcoma, proliferation of tumour cells post irradiation was faster than before radiation, which resulted in enhanced tumour cell growth compared to growth of non-irradiated tumours (Hermens and Barendsen, 1969). Similar observations have been made in murine Lewis lung carcinoma models, where repopulation began immediately following γ-irradiation (Stephens *et al.*, 1978). Moreover, it has long been shown that addition of irradiated cells to tumour transplants can decrease survival time (Revesz, 1956). This has also recently been shown in a murine model of Burkitt's lymphoma (Ford *et al.*, 2015). In one experiment addition of irradiated tumour cells was shown to reduce the number of viable adenocarcinoma cells needed to give a 50% take rate in mice to 4 from 6900 without addition of irradiated tumour cells (Hewitt *et al.*, 1973), suggesting that in the presence of large numbers of apoptotic cells, e.g. after chemotherapy or radiotherapy, very small numbers of remaining viable cancer cells can be enough to repopulate the tumour.

The mechanisms for apoptotic-cell mediated tumour growth remain largely unknown and the importance and route may vary between tumour types and perhaps per tumour. Some studies suggest that apoptotic cell-mediated tumour growth may be directly attributable to the effects apoptotic tumour cells have on tumour cells, as was shown by Huang et al. (2011). Radiotherapy can induce activation of caspase-3, a key executioner of apoptosis, which was found to regulate PGE2, a growth factor that can potentially stimulate growth of surviving tumour cells. Deficiency of caspase-3 increased tumour sensitivity to radiotherapy. Furthermore, it was shown that higher levels of activated caspase-3 in tumour tissues in humans was associated with increased recurrence and death (Huang *et al.*, 2011). Additionally, Wnt and Hedgehog signalling from apoptotic cells has been shown to promote cell proliferation, and may contribute to the repopulation of tumours (Li *et al.*, 2010; Bergmann and Steller, 2010).

The results presented in this thesis that show that apoptotic cells can mediate macrophage activation, which can lead to tumour cell growth *in vitro*, demonstrate another likely mechanism by which apoptotic tumour cells can affect tumour repopulation. Indeed, several studies indicate that macrophages may play a role in this. Radiation therapy has been shown to induce an influx of macrophages into tumours (Stephens *et al.*, 1978; Russell and Brown, 2013), whereas suppression of apoptosis of lymphoma cells by transfection with Bcl-2 has been shown to decrease macrophage accumulation (Ford *et al.*, 2015). Furthermore, as was suggested in this thesis, apoptotic cell interaction with these recruited macrophages may lead to further recruitment of macrophages, possibly through the release of CCL2. Apoptotic cells may also activate tumour-promoting pathways in macrophages, including increased macrophages phagocytosis, matrix remodelling, angiogenesis, and release of growth-promoting factors. E.g. although TAM in gastrointestinal stromal tumours may limit tumour growth, imatinib-induced apoptosis in these tumours was shown to cause tumour-promoting activation of TAM (Cavnar *et al.*, 2013).

Thus to improve outcome, in addition to inducing tumour cell death, therapies should prevent apoptotic cell-mediated direct and indirect (through recruitment and activation of tumour-supportive macrophages) pro-tumour responses, and instead stimulate an immune response that can contribute to controlling and/or eradicating residual cancer cells. Various strategies can be used. One can be to inhibit apoptotic cell-induced monocytes and macrophages, and another to prevent activation of tumour-supportive macrophages and/or educate macrophages to activate a non-supportive and ideally anti-tumour phenotype. Finally, cancer cells can be stimulated to undergo immunogenic cell death, which stimulates an immune response against the cancer cells.

Inhibition of monocyte recruitment is being tested by targeting CCL2 and CSF1-mediated signalling. Antibodies to CCL2 are currently being tested in clinical trials and preliminary results have shown anti-tumour activity in advanced cancer patients (Pienta *et al.*, 2012; Sandhu *et al.*, 2013). Furthermore, combinations of chemotherapy and anti-CCL2 antibody are studied (Brana *et al.*, 2014). Additionally, inhibitors of CSF1R are showing potential at reducing macrophage migration towards irradiated tumour cells. CSF1 signalling through CSF1R is known to induce proliferation, and activation of macrophages to an alternative-like activation phenotype (Hume and MacDonald, 2012). *In vitro* macrophage migration to conditioned media from irradiated tumour cells can be blocked by an inhibitor of CSF1R. Furthermore, radiotherapy combined with this CSF1R inhibitor, suppressed tumour growth more than radiotherapy alone in a prostate cancer model (Xu *et al.*, 2013). This may be also be of importance in starry-sky TAM in Burkitt's lymphoma, as unpublished results show that CSF1R gene expression is significantly enhanced in starry-sky TAM compared to GCM.

Therapies directed at preventing apoptotic-cell activation of macrophages are mostly directed against phosphatidylserine expressed on the membrane of apoptotic cells, although, as was shown here, some soluble factors released from apoptotic cells may also be involved in inducing a pro-tumour phenotype of macrophages. Masking of phosphatidylserine by a mutant form of MFG-E8 was shown to inhibit phagocytosis

of apoptotic cells by macrophages, but could also inhibit the enhanced production of IL-10 by thioglycollate-elicited peritoneal macrophages following phagocytosis of apoptotic cells (Asano *et al.*, 2004). Furthermore, binding of Annexin V has been shown to target irradiated lymphoma cells to CD8+ dendritic cells for *in vivo* clearance, which leads to release of pro-inflammatory cytokines, and regression of tumours (Bondanza *et al.*, 2004).

Murine and rat models of prostate cancer have also shown success when chemotherapy or irradiation was combined with an anti-PS antibody, 2aG4, a variant of the human antibody bavituximab, compared to either therapy alone (He *et al.*, 2009; Yin *et al.*, 2013). Gene expression analysis showed that TAMs cultured in the presence of 2aG4 increased iNOS, inflammatory cytokines IL-12 and TNFα, and T-cell co-stimulatory molecules (CD80, CD86, and MHC class II), and decreased expression of Arg1, immunosuppressive cytokines IL-10 and TGF-β, and VEGF-A (Yin *et al.*, 2013). Bavituximab, a human anti-PS antibody, is currently being tested in clinical trials (Gerber *et al.*, 2011; Chalasani *et al.*, 2015).

Other therapies are, based on the plasticity and flexibility of macrophages (Mosser and Edwards, 2008; Hagemann *et al.*, 2008), directed at actively changing the macrophage phenotype to an anti-tumour one. Because of its potential to augment the cytotoxicity of macrophages, IFN-γ has been tested in small clinical studies, and appeared to have modest responses in small residual ovarian carcinomas after chemotherapy, although studies were too small to conclude if i.p. injections of IFN-γ improved outcome. No effect was observed in advanced ovarian carcinoma (Colombo *et al.*, 1992; Pujade-Lauraine *et al.*, 1996). These results are in line with the findings in Chapter 5 that indicate that although IFN-γ and LPS-stimulation of macrophages induces macrophage cytotoxicity, apoptotic cell stimulation of these macrophages stimulated tumour cell growth. Thus, IFN-γ may only be effective when there are low numbers of apoptotic cells in the tumour, as the apoptotic cells may also override the effects of IFN-γ on macrophages in the tumour. Alternatively, differences between human and mouse macrophages may be responsible for the minimal effects of IFN-γ in these clinical studies. Although murine macrophages

may express NO via induction of iNOS in response to IFN-γ and LPS-stimulation, human macrophages have not been shown to reliably produce nitrite by iNOS activity (Schneemann and Schoeden, 2006; Mestas and Hughes, 2004).

Finally, not all anti-cancer therapies induce tumour cell death equally. The majority of chemotherapies induce apoptotic cell death that is immunologically silent or leads to immune cell support of the tumour. However, a few treatments have been shown to induce immunogenic cell death (ICD) that stimulates an anti-tumour response through dendritic cell stimulation of T cells, which leads to favourable therapeutic responses (Kroemer *et al.*, 2013). ICD is preceded by endoplasmic reticulum (ER) stress and autophagy, which leads to distinctive properties, including the pre-apoptotic outer cell membrane exposure of calreticulin (CRT) (Zitvogel *et al.*, 2010) and other ER proteins, secretion of ATP during the blebbing phase of apoptosis, and release of nonhistone chromatin protein high-mobility group box 1 (HMGB1) (Kroemer *et al.*, 2013). ATP can lead to the recruitment of both macrophages and DC, and can stimulate DC maturation (Elliott *et al.*, 2009; Idzko *et al.*, 2007). CRT binds to transmembrane receptors, including LRP1, and leads to the engulfment by LRP1 exposing cells, which include macrophages and DC. However, as CRT is exposed on the membrane very early during ICD (before PS-exposure), simultaneous exposure by these cells of the 'don't eat me' signal CD47 appears to favour CRT-signalling through antigen presenting cells, particularly DC, that results in the production of pro-inflammatory cytokines (including IL-6, and TNFα) and to promote T cell responses. HMGB1 can bind to TLR4 and seems to be important for activating pro-inflammatory cytokine release (Kroemer *et al.*, 2013).

7.5 Tumour-associated macrophage phenotype

In silico analysis of the starry-sky TAM phenotype by comparing it against gene expression profiles of a macrophage database, confirmed that phagocytosis of apoptotic cells is likely to play an important role in these cells. Phagocytosis was shown to be the most important shared function of all macrophages, and a large group of genes overexpressed by starry-sky TAM was associated with all stages of apoptosis. Although this could be a specific feature of starry-sky TAM, known to

interact with and engulf apoptotic cells, another *in silico* study has shown that phagocytosis is a feature shared by TAM from many different human tumours. The study compared gene expression from biopsies of various different types of human cancers, including breast, colonic, diffuse large B-cell lymphoma (DLBCL), glioma, ovarian, and testicular cancer using BioLayout Express^{3D}, and showed that there was a clear signature for macrophages present in all of these cancers, which included genes associated with phagocytosis. Furthermore, this signature was also present in other cancer datasets, including gastric cancer, Hodgkin lymphoma, and skin/melanoma (Doig *et al.*, 2013). This suggests that phagocytosis of apoptotic cells is a core feature of macrophages in many different cancers, and the findings presented here may also be relevant to malignancies other than Burkitt's lymphoma or non-Hodgkin's lymphoma.

Interestingly, although the *in silico* study by Doig et al. showed that there was a clear macrophage cluster, there was no evidence of the macrophages being skewed towards a particular phenotype. In addition to genes associated with phagocytosis, the macrophage cluster contained genes involved in chemotaxis, toll-like receptors, scavenger receptors, as well as genes associated with MHC class II antigen presentation and T cell co-stimulation. Similar observations were made during the *in silico* analysis of starry-sky TAM presented here, where expression of genes associated with both LPS-mediated responses and anti-inflammatory and wounding responses were up-regulated. This may suggest that the macrophage phenotype in the tumour microenvironment is dependent on various, possibly opposing, stimuli, some enhancing tumour growth and others decreasing it, and that the balance between the two may determine outcome, which may change during development of the tumour. As increasing numbers of macrophages in tumours are mostly associated with poor prognosis (Leek *et al.*, 1996; Salvesen and Akslen, 1999; Ni *et al.*, 2015; Campbell *et al.*, 2011) this suggests that for most tumours the dominant macrophage phenotype is one that supports tumour growth. Alternatively, seemingly opposing features of the macrophage cluster in tumours may be due to different populations of macrophages, with different activation states, being present in the tumour. This has been shown to be the case in mouse mammary tumours, which were found to contain

functionally distinct subsets of TAM. Hypoxic tumour areas contained macrophages that had significant pro-angiogenic activity and their numbers increased as tumour progressed. Furthermore, they were poor antigen presenters (expressed low levels of MHC Class II), and showed increased expression of e.g. Arg1, Mrc1, Cd163, Timp2, Ctsd, Il4ra and several cytokines, including Ccl2. Outside of the hypoxic areas, macrophages expressed higher levels of MHC Class II, Il6, Il12, Il1, and Nos2. Both could suppress T-cell activation (Movahedi *et al.*, 2010).

IL-4 and IL-13 signalling through IL-4Rα has traditionally been associated with TAM (Sica *et al*., 2008a; Mantovani *et al*., 2004a; Allavena *et al*., 2008). However, more recent studies have revealed that activation signatures of TAM can be independent of alternative macrophage activation. In a recent study on TAM in a breast cancer model, TAM that were tumour-supportive and proliferative expressed only low levels of the IL-4Rα-dependent alternative activation genes Ym1, Lyve1, Fizz1, Irf4, Ccl7, Mrc1, and Ccl2 (Franklin *et al*., 2014). Although our published studies showed that expression of IL-4Rα is required for optimal pro-tumour effects of apoptotic lymphoma cells (Ford *et al*., 2015) results presented here suggest that the activation of a pro-tumour macrophage phenotype through interaction with apoptotic cells is independent of IL-4Rα expression by macrophages, although IL-4/IL-13 signalling may be involved in other NHL-promoting mechanisms. Additionally, of the IL-4Rα-dependent alternative activation genes, only Mrc1, CCL2, and CCL7 are increased in starry-sky TAM compared to GCM, and only Mrc1 is expressed at high levels, further suggesting that of IL-4Rα does not play a role in regulating starry-sky TAM activation.

In contrast, galectin-3 may play a significant role apoptotic cell activation of macrophages. Galectin-3 is expressed and released by macrophages, and up-regulated upon differentiation of monocytes into macrophages (Liu *et al*., 1995). Preliminary studies in our laboratory have shown a reduced ability of galectin-3 knockout mice to produce tumours in a λ-MYC murine lymphoma model. The reduced ability of galectin-3 deficient macrophages to phagocytose apoptotic cells shown in Chapter 4 and previously shown by (Sano *et al*., 2003), may be of great

significance here. Insufficient clearance of apoptotic cells may lead to accumulation of secondary necrotic cells, which may induce pro-inflammatory responses. Additionally, decreased apoptotic cell uptake may reduce the extent to which macrophages are activated by apoptotic cells, which may lead to a less pro-tumour phenotype that may also negatively influence tumour growth. Experiments presented here did not show a difference between IFNγ and LPS-stimulated wild type and galectin-3 macrophages co-cultured with apoptotic cells. However, IFNγ and LPS have been shown to down-regulate galectin-3 expression (MacKinnon *et al*., 2008), and preliminary results presented here seem to suggest that IFNγ and LPS stimulation may restore the phagocytic potential of galectin-3 deficient macrophages. Thus the role of galectin-3 in apoptotic-cell activation of unstimulated macrophages should be further investigated.

Although phagocytosis of apoptotic cells may be a core feature of many TAM, there are likely additional factors involved in tuning the macrophage phenotype to a tumour-supportive one. Recently, it was shown that lactic acid produced by Lewis lung carcinoma and B16 melanoma cancer cell lines could induce M2-like polarization of tumour-associated macrophages through increased expression of Arg1, Mrc1, Fizz1, Mgl1, Mgl2, and vascular endothelial growth factor (VEGF), which was independent of IL-4 and IL-13 signalling through IL-4Rα (Colegio *et al*., 2014). It has long been established that apoptotic leukaemia cells produce lactate (Tiefenthaler *et al*., 2001), and lactate release from apoptotic cells may therefore also be an important in inducing a pro-tumour phenotype of starry-sky TAM. However, the key indicators of lactate-induced genes presented by Colegio et al. are not increased in starry-sky TAM compared to GCM, and are expressed at very low levels. Of the key genes associated with lactic acid activation, including Arg1, Mrc1, Retnla (Fizz1), Lyve1, Chil3, CCL2, CCL7, only Mrc1, CCL2, and CCL7 are increased in starry-sky TAM compared to GCM, and only Mrc1 is expressed at high levels. Furthermore, it was shown here that although Gas6, Mrc1, and Cd36 up-regulation by TAM is likely mediated through the release of soluble factors from apoptotic cells, expression of Pparg and Timp2, as well as the tumour growth promoting effects, were dependent upon direct cell-cell contact between apoptotic

cells and macrophages, making it unlikely that in NHL lactate release from apoptotic cells is important in influencing the phenotype of starry-sky TAM.

7.6 Conclusion & Future Research

In summary, the studies presented in this thesis indicate that apoptotic lymphoma cells can activate macrophages that are anti-inflammatory, and promote tumour growth and tissue remodelling. Given the findings presented here that phagocytosis is one of the most important functions of starry-sky TAM, it is likely that apoptotic cells are involved in the activation of starry-sky TAM and promote tumourigenesis. This hypothesis is supported also by published studies that show that addition of irradiated BL cells to tumour transplants enhance tumour cell growth. Additionally, a murine model in which apoptosis was suppressed showed reduced tumour cell growth and a reduced accumulation of macrophages (Ford *et al.*, 2015). As many tumours have significant levels of apoptosis and phagocytosis is important for all TAM, these findings may also pertain to other types of cancer.

Of particular interest is the finding that apoptotic cell stimulation of untreated macrophages can induce Ccl2 gene expression, one of the genes up-regulated by starry-sky TAM. We propose that this is a new mechanism for the accumulation of TAM where apoptotic cells can attract mononuclear phagocytes and activate them to produce and release CCL2, thereby setting a positive feedback system to recruit more phagocytes, which can interact with more apoptotic cells. This may be acting in concert with proliferation of TAM to increase the TAM population as the tumour expands. This may be tested *in vivo* in a murine lymphoma model by comparing the effect of the depletion of apoptotic cells from, or addition of apoptotic cells to the tumour transplant in WT versus CCL2 knockout mice on the accumulation of macrophages and tumour growth.

The other main finding presented here is the ability of apoptotic cells to induce classically activated macrophages to enhance tumour cell growth. Analysis of release of growth factors from macrophages may reveal which factors are important for

tumour cell growth. Additionally, it should be tested if apoptotic lymphoma cells can also induce unstimulated macrophages to support tumour cell growth.

Whether apoptotic cell stimulation of macrophages can also enhance tumour cell growth *in vivo*, will need to be tested, e.g. by admixing unstimulated and classically-activated macrophages with or without apoptotic cells, with tumour cell injections. In addition to measuring the effects on tumour growth, the effects on angiogenesis will be of interest too. Additionally, other pro-inflammatory agents that can stimulate the TAM phenotype to a tumour-inhibiting one may be tested *in vitro* and *in vivo,* e.g. LPS, TLR agonists, or zymosan, a *Saccharomyces cerevisae* yeast cell wall particle (Ozinsky *et al.*, 2000).

The results presented here suggest that by sacrificing some tumour cells through the induction of apoptosis, tumours may hijack the developmental and wound response mechanisms of macrophages, activating them to support overall tumour growth. Additionally, it sheds a light on how apoptosis-inducing anti-cancer therapies may stimulate tumour repopulation. As our results indicate that apoptotic cells may overcome anti-tumour macrophage stimulation by activating tumour-supportive functions in macrophages, anti-cancer therapies should also focus on inhibiting apoptotic cell interaction with macrophages, or induce an immunogenic cell death that prevents pro-tumour stimulation, and instead activates the immune system to control and/or eradicate tumours.

References

Acehan D, Jiang X, Morgan DG, Heuser JE, Wang X, and Akey CW. (2002). Three-dimensional structure of the apoptosome: implications for assembly, procaspase-9 binding, and activation. *Mol. Cell* **9**: 423–432.

Adams DO, and Hamilton TA. (1984). The cell biology of macrophage activation. *Annu. Rev. Immunol.* **2**: 283–318.

Adrain C, and Martin SJ. (2001). The mitochondrial apoptosome: a killer unleashed by the cytochrome seas. *Trends Biochem. Sci.* **26**: 390–397.

Albert ML, Kim JI, and Birge RB. (2000). alphavbeta5 integrin recruits the CrkII-Dock180-rac1 complex for phagocytosis of apoptotic cells. *Nat Cell Biol* **2**: 899–905.

Aliprantis AO, Diez-Roux G, Mulder LC, Zychlinsky A, and Lang RA. (1996). Do macrophages kill through apoptosis? *Immunol. Today* **17**: 573–576.

Allavena P, Bianchi G, Zhou D, van Damme J, Jílek P, Sozzani S, *et al.* (1994). Induction of natural killer cell migration by monocyte chemotactic protein-1, -2 and -3. *Eur. J. Immunol.* **24**: 3233–3236.

Allavena P, Chieppa M, Bianchi G, Solinas G, Fabbri M, Laskarin G, *et al.* (2010). Engagement of the mannose receptor by tumoral mucins activates an immune suppressive phenotype in human tumor-associated macrophages. *Clin. Dev. Immunol.* **2010**: 547179.

Allavena P, Sica A, Solinas G, Porta C, and Mantovani A. (2008). The inflammatory micro-environment in tumor progression: The role of tumor-associated macrophages. *Critical Reviews in Oncology/Hematology* **66**: 1–9.

Andersen CL, Jensen JL, and Ørntoft TF. (2004). Normalization of real-time quantitative reverse transcription-PCR data: a model-based variance estimation approach to identify genes suited for normalization, applied to bladder and colon cancer data sets. *Cancer Res* **64**: 5245–5250.

Antonyak MA, Li B, Boroughs LK, Johnson JL, Druso JE, Bryant KL, *et al.* (2011). Cancer cell-derived microvesicles induce transformation by transferring tissue transglutaminase and fibronectin to recipient cells. *Proc. Natl. Acad. Sci. U.S.A.* **108**: 4852–4857.

ar-Rushdi A, Nishikura K, Erikson J, Watt R, Rovera G, and Croce CM. (1983). Differential expression of the translocated and the untranslocated c-myc oncogene in Burkitt lymphoma. *Science* **222**: 390–393.

Aramaki Y, Nitta F, Matsuno R, Morimura Y, and Tsuchiya S. (1996). Inhibitory effects of negatively charged liposomes on nitric oxide production from

macrophages stimulated by LPS. *Biochemical and Biophysical Research Communications* **220**: 1–6.

Arnold RR, Cole MF, and McGhee JR. (1977). A bactericidal effect for human lactoferrin. *Science* **197**: 263–265.

Arur S, Uche UE, Rezaul K, Fong M, Scranton V, Cowan AE, *et al.* (2003). Annexin I is an endogenous ligand that mediates apoptotic cell engulfment. *Developmental Cell* **4**: 587–598.

Asano K, Miwa M, Miwa K, Hanayama R, Nagase H, Nagata S, *et al.* (2004). Masking of phosphatidylserine inhibits apoptotic cell engulfment and induces autoantibody production in mice. *J Exp Med* **200**: 459–467.

Ashkenazi A, and Dixit VM. (1998). Death receptors: signaling and modulation. *Science* **281**: 1305–1308.

Baggiolini M, De Duve C, Masson PL, and Heremans JF. (1970). Association of lactoferrin with specific granules in rabbit heterophil leukocytes. *J Exp Med* **131**: 559–570.

Baj-Krzyworzeka M, Szatanek R, Weglarczyk K, Baran J, and Zembala M. (2007). Tumour-derived microvesicles modulate biological activity of human monocytes. *Immunol Lett* **113**: 76–82.

Baj-Krzyworzeka M, Szatanek R, Weglarczyk K, Baran J, Urbanowicz B, Brański P, *et al.* (2006). Tumour-derived microvesicles carry several surface determinants and mRNA of tumour cells and transfer some of these determinants to monocytes. *Cancer Immunol Immunother* **55**: 808–818.

Baker EN, and Baker HM. (2009). A structural framework for understanding the multifunctional character of lactoferrin. *Biochimie* **91**: 3–10.

Baker EN, and Baker HM. (2005). Molecular structure, binding properties and dynamics of lactoferrin. *Cell Mol Life Sci* **62**: 2531–2539.

Baker HM, Anderson BF, and Baker EN. (2003). Dealing with iron: common structural principles in proteins that transport iron and heme. *Proc. Natl. Acad. Sci. U.S.A.* **100**: 3579–3583.

Balasubramanian K, and Schroit AJ. (2003). Aminophospholipid asymmetry: a matter of life and death. *Annual review of physiology* **65**: 701–734.

Balkwill F, and Mantovani A. (2001). Inflammation and cancer: back to Virchow? *The Lancet* **357**: 539–545.

Baveye S, Elass E, Fernig DG, Blanquart C, Mazurier J, and Legrand D. (2000). Human Lactoferrin Interacts with Soluble CD14 and Inhibits Expression of Endothelial Adhesion Molecules, E-Selectin and ICAM-1, Induced by the CD14-Lipopolysaccharide Complex. *Infect Immun* **68**: 6519–6525.

Bellamy W, Takase M, Yamauchi K, Wakabayashi H, Kawase K, and Tomita M. (1992). Identification of the bactericidal domain of lactoferrin. *Biochimica et Biophysica Acta (BBA) - Protein Structure and Molecular Enzymology* **1121**: 130–136.

Bennett RM, Davis J, Campbell S, and Portnoff S. (1983). Lactoferrin binds to cell membrane DNA. Association of surface DNA with an enriched population of B cells and monocytes. *J Clin Invest* **71**: 611–618.

Bergmann A, and Steller H. (2010). Apoptosis, stem cells, and tissue regeneration. *Science Signaling* **3**: re8.

Beyenbach KW. (2006). The V-type H+ ATPase: molecular structure and function, physiological roles and regulation. *Journal of Experimental Biology* **209**: 577–589.

Bezault J, Bhimani R, Wiprovnick J, and Furmanski P. (1994). Human lactoferrin inhibits growth of solid tumors and development of experimental metastases in mice. *Cancer Res* **54**: 2310–2312.

Biswas SK, Allavena P, and Mantovani A. (2013). Tumor-associated macrophages: functional diversity, clinical significance, and open questions. *Semin Immunopathol* **35**: 585–600.

Biswas SK, Gangi L, Paul S, Schioppa T, Saccani A, Sironi M, *et al.* (2006). A distinct and unique transcriptional program expressed by tumor-associated macrophages (defective NF-kappaB and enhanced IRF-3/STAT1 activation). *Blood* **107**: 2112–2122.

Boehme SA, Lio FM, Maciejewski-Lenoir D, Bacon KB, and Conlon PJ. (2000). The chemokine fractalkine inhibits Fas-mediated cell death of brain microglia. *J Immunol* **165**: 397–403.

Bondanza A, Zimmermann VS, Rovere-Querini P, Turnay J, Dumitriu IE, Stach CM, *et al.* (2004). Inhibition of phosphatidylserine recognition heightens the immunogenicity of irradiated lymphoma cells in vivo. *J Exp Med* **200**: 1157–1165.

Bonder CS, Dickensheets HL, Finlay-Jones JJ, Donnelly RP, and Hart PH. (1998). Involvement of the IL-2 receptor gamma-chain (gammac) in the control by IL-4 of human monocyte and macrophage proinflammatory mediator production. *J Immunol* **160**: 4048–4056.

Bornkamm GW. (2009). Epstein-Barr virus and the pathogenesis of Burkitt's lymphoma: More questions than answers. *Int J Cancer* **124**: 1745–1755.

Bosisio D, Polentarutti N, Sironi M, Bernasconi S, Miyake K, Webb GR, *et al.* (2002). Stimulation of toll-like receptor 4 expression in human mononuclear phagocytes by interferon-gamma: a molecular basis for priming and synergism with bacterial lipopolysaccharide. *Blood* **99**: 3427–3431.

Botto M, Dell'Agnola C, Bygrave AE, Thompson EM, Cook HT, Petry F, *et al.*

(1998). Homozygous C1q deficiency causes glomerulonephritis associated with multiple apoptotic bodies. *Nat Genet* **19**: 56–59.

Bournazou I, Mackenzie KJ, Duffin R, Rossi AG, and Gregory CD. (2010). Inhibition of eosinophil migration by lactoferrin. *Immunol Cell Biol* **88**: 220–223.

Bournazou I, Pound JD, Duffin R, Bournazos S, Melville LA, Brown SB, *et al.* (2009). Apoptotic human cells inhibit migration of granulocytes via release of lactoferrin. *J Clin Invest* **119**: 20–32.

Brady G, MacArthur GJ, and Farrell PJ. (2008). Epstein-Barr virus and Burkitt lymphoma. *Postgraduate Medical Journal* **84**: 372–377.

Brana I, Calles A, LoRusso PM, Yee LK, Puchalski TA, Seetharam S, *et al.* (2014). Carlumab, an anti-C-C chemokine ligand 2 monoclonal antibody, in combination with four chemotherapy regimens for the treatment of patients with solid tumors: an open-label, multicenter phase 1b study. *Targ Oncol* **10**: 111–123.

Brown S, Heinisch I, Ross E, Shaw K, Buckley CD, and Savill J. (2002). Apoptosis disables CD31-mediated cell detachment from phagocytes promoting binding and engulfment. *Nature* **418**: 200–203.

Bullen JJ, Rogers HJ, and Leigh L. (1972). Iron-binding proteins in milk and resistance to Escherichia coli infection in infants. *Br Med J* **1**: 69–75.

Burgess AW. (1989). Epidermal growth factor and transforming growth factor alpha. *Br. Med. Bull.* **45**: 401–424.

Burke AJ, Sullivan FJ, Giles FJ, and Glynn SA. (2013). The yin and yang of nitric oxide in cancer progression. *Carcinogenesis* **34**: 503–512.

Calderón C, Huang ZH, Gage DA, Sotomayor EM, and Lopez DM. (1994). Isolation of a nitric oxide inhibitor from mammary tumor cells and its characterization as phosphatidyl serine. *J Exp Med* **180**: 945–958.

Callahan MK, Halleck MS, Krahling S, Henderson AJ, Williamson P, and Schlegel RA. (2003). Phosphatidylserine expression and phagocytosis of apoptotic thymocytes during differentiation of monocytic cells. *J Leukoc Biol* **74**: 846–856.

Camp V, and Martin P. (1996). The role of macrophages in clearing programmed cell death in the developing kidney. *Anat. Embryol.* **194**: 341–348.

Campbell MJ, Tonlaar NY, Garwood ER, Huo D, Moore DH, Khramtsov AI, *et al.* (2011). Proliferating macrophages associated with high grade, hormone receptor negative breast cancer and poor clinical outcome. *Breast Cancer Res. Treat.* **128**: 703–711.

Castellano F, Montcourrier P, and Chavrier P. (2000). Membrane recruitment of Rac1 triggers phagocytosis. *Journal of Cell Science* **113 (Pt 17)**: 2955–2961.

Cavnar MJ, Zeng S, Kim TS, Sorenson EC, Ocuin LM, Balachandran VP, *et al.* (2013). KIT oncogene inhibition drives intratumoral macrophage M2 polarization. *Journal of Experimental Medicine* **210**: 2873–2886.

Chalasani P, Marron M, Roe D, Clarke K, Iannone M, Livingston RB, *et al.* (2015). A phase I clinical trial of bavituximab and paclitaxel in patients with HER2 negative metastatic breast cancer. *Cancer Med* **4**: 1051–1059.

Chang CI, Liao JC, and Kuo L. (2001). Macrophage arginase promotes tumor cell growth and suppresses nitric oxide-mediated tumor cytotoxicity. *Cancer Res* **61**: 1100–1106.

Chao MP, Alizadeh AA, Tang C, Myklebust JH, Varghese B, Gill S, *et al.* (2010). Anti-CD47 Antibody Synergizes with Rituximab to Promote Phagocytosis and Eradicate Non-Hodgkin Lymphoma. *Cell* **142**: 699–713.

Chao MP, Majeti R, and Weissman IL. (2011). Programmed cell removal:a new obstacle in the road to developing cancer. *Nat Rev Cancer* **12**: 58–67.

Charrière GM, Cousin B, Arnaud E, Saillan-Barreau C, André M, Massoudi A, *et al.* (2006). Macrophage characteristics of stem cells revealed by transcriptome profiling. *Experimental Cell Research* **312**: 3205–3214.

Chekeni FB, Elliott MR, Sandilos JK, Walk SF, Kinchen JM, Lazarowski ER, *et al.* (2010). Pannexin 1 channels mediate 'find-me' signal release and membrane permeability during apoptosis. *Nature* **467**: 863–867.

Chen Q, Zhang XHF, and Massagué J. (2011). Macrophage Binding to Receptor VCAM-1 Transmits Survival Signals in Breast Cancer Cells that Invade the Lungs. *Cancer Cell* **20**: 538–549.

Chen Y, Corriden R, Inoue Y, Yip L, Hashiguchi N, Zinkernagel A, *et al.* (2006). ATP release guides neutrophil chemotaxis via P2Y2 and A3 receptors. *Science* **314**: 1792–1795.

Cheung DL, and Hamilton JA. (1992). Regulation of human monocyte DNA synthesis by colony-stimulating factors, cytokines, and cyclic adenosine monophosphate. *Blood* **79**: 1972–1981.

Cheung DL, Hart PH, Vitti GF, Whitty GA, and Hamilton JA. (1990). Contrasting effects of interferon-gamma and interleukin-4 on the interleukin-6 activity of stimulated human monocytes. *Immunology* **71**: 70–75.

Chiodoni C, Colombo MP, and Sangaletti S. (2010). Matricellular proteins: from homeostasis to inflammation, cancer, and metastasis. *Cancer Metastasis Rev.* **29**: 295–307.

Choudhari SK, Chaudhary M, Bagde S, Gadbail AR, and Joshi V. (2013). Nitric oxide and cancer: a review. *World J Surg Oncol* **11**: 118.

Cirioni O, Giacometti A, Barchiesi F, and Scalise G. (2000). Inhibition of growth of Pneumocystis carinii by lactoferrins alone and in combination with pyrimethamine, clarithromycin and minocycline. *J. Antimicrob. Chemother.* **46**: 577–582.

Cobbs CS, Brenman JE, Aldape KD, Bredt DS, and Israel MA. (1995). Expression of nitric oxide synthase in human central nervous system tumors. *Cancer Res* **55**: 727–730.

Cohen PL, Caricchio R, Abraham V, Camenisch TD, Jennette JC, Roubey RAS, *et al.* (2002). Delayed Apoptotic Cell Clearance and Lupus-like Autoimmunity in Mice Lacking the c-mer Membrane Tyrosine Kinase. *Journal of Experimental Medicine* **196**: 135–140.

Colegio OR, Chu N-Q, Szabo AL, Chu T, Rhebergen AM, Jairam V, *et al.* (2014). Functional polarization of tumour-associated macrophages by tumour-derived lactic acid. *Nature* **513**: 559–563.

Coleman ML, Sahai EA, Yeo M, Bosch M, Dewar A, and Olson MF. (2001). Membrane blebbing during apoptosis results from caspase-mediated activation of ROCK I. *Nat Cell Biol* **3**: 339–345.

Colombo N, Peccatori F, Paganin C, Bini S, Brandely M, Mangioni C, *et al.* (1992). Anti-tumor and immunomodulatory activity of intraperitoneal IFN-gamma in ovarian carcinoma patients with minimal residual tumor after chemotherapy. *Int J Cancer* **51**: 42–46.

Cook J, and Hagemann T. (2013). Tumour-associated macrophages and cancer. *Current Opinion in Pharmacology* **13**: 595–601.

Corcione A, Tortolina G, Bonecchi R, Battilana N, Taborelli G, Malavasi F, *et al.* (2002). Chemotaxis of human tonsil B lymphocytes to CC chemokine receptor (CCR) 1, CCR2 and CCR4 ligands is restricted to non-germinal center cells. *International Immunology* **14**: 883–892.

Cornish J, Callon KE, Naot D, Palmano KP, Banovic T, Bava U, *et al.* (2004). Lactoferrin Is a Potent Regulator of Bone Cell Activity and Increases Bone Formation in Vivo. *Endocrinology* **145**: 4366–4374.

Coussens LM, and Werb Z. (2002). Inflammation and cancer. *Nature* **420**: 860–867.

Coussens LM, Zitvogel L, and Palucka AK. (2013). Neutralizing Tumor-Promoting Chronic Inflammation: A Magic Bullet? *Science* **339**: 286–291.

Cox GW, Melillo G, Chattopadhyay U, Mullet D, Fertel RH, and Varesio L. (1992). Tumor necrosis factor-alpha-dependent production of reactive nitrogen intermediates mediates IFN-gamma plus IL-2-induced murine macrophage tumoricidal activity. *J Immunol* **149**: 3290–3296.

Creagh EM, Conroy H, and Martin SJ. (2003). Caspase-activation pathways in apoptosis and immunity. *Immunological Reviews* **193**: 10–21.

Crouch SP, Slater KJ, and Fletcher J. (1992). Regulation of cytokine release from mononuclear cells by the iron-binding protein lactoferrin. *Blood* **80**: 235–240.

Cui S, Reichner JS, Mateo RB, and Albina JE. (1994). Activated murine macrophages induce apoptosis in tumor cells through nitric oxide-dependent or -independent mechanisms. *Cancer Res* **54**: 2462–2467.

Daemen T, Regts J, and Scherphof GL. (1996). Liposomal phosphatidylserine inhibits tumor cytotoxicity of liver macrophages induced by muramyl dipeptide and lipopolysaccharide. *Biochimica et biophysica acta* **1285**: 219–228.

Damiens E, Mazurier J, Yazidi El I, Masson M, Duthille I, Spik G, *et al.* (1998). Effects of human lactoferrin on NK cell cytotoxicity against haematopoietic and epithelial tumour cells. *Biochimica et biophysica acta* **1402**: 277–287.

Darmon AJ, Ley TJ, Nicholson DW, and Bleackley RC. (1996). Cleavage of CPP32 by granzyme B represents a critical role for granzyme B in the induction of target cell DNA fragmentation. *J Biol Chem* **271**: 21709–21712.

Davies LC, Rosas M, Jenkins SJ, Liao C-T, Scurr MJ, Brombacher F, *et al.* (2013). Distinct bone marrow-derived and tissue-resident macrophage lineages proliferate at key stages during inflammation. *Nat Comms* **4**: 1886.

DeNardo DG, Barreto JB, Andreu P, Vasquez L, Tawfik D, Kolhatkar N, *et al.* (2009). CD4+ T Cells Regulate Pulmonary Metastasis of Mammary Carcinomas by Enhancing Protumor Properties of Macrophages. *Cancer Cell* **16**: 91–102.

Devitt A, Moffatt OD, Raykundalia C, Capra JD, Simmons DL, and Gregory CD. (1998). Human CD14 mediates recognition and phagocytosis of apoptotic cells. *Nature* **392**: 505–509.

Dinapoli MR, Calderon CL, and Lopez DM. (1996). The altered tumoricidal capacity of macrophages isolated from tumor-bearing mice is related to reduce expression of the inducible nitric oxide synthase gene. *J Exp Med* **183**: 1323–1329.

Distler JHW, Pisetsky DS, Huber LC, Kalden JR, Gay S, and Distler O. (2005). Microparticles as regulators of inflammation: novel players of cellular crosstalk in the rheumatic diseases. *Arthritis Rheum* **52**: 3337–3348.

Doig TN, Hume DA, Theocharidis T, Goodlad JR, Gregory CD, and Freeman TC. (2013). Coexpression analysis of large cancer datasets provides insight into the cellular phenotypes of the tumour microenvironment. *BMC Genomics* **14**: 469.

Doyle AG, Herbein G, Montaner LJ, Minty AJ, Caput D, Ferrara P, *et al.* (1994). Interleukin-13 alters the activation state of murine macrophages in vitro: Comparison with interleukin-4 and interferon-γ. *Eur. J. Immunol.* **24**: 1441–1445.

Duff MD, Mestre J, Maddali S, Yan ZP, Stapleton P, and Daly JM. (2007). Analysis of Gene Expression in the Tumor-Associated Macrophage. *Journal of Surgical Research* **142**: 119–128.

Dzierzak E, Medvinsky A, and de Bruijn M. (1998). Qualitative and quantitative aspects of haematopoietic cell development in the mammalian embryo. *Immunol. Today* **19**: 228–236.

Eda S, Kikugawa K, and Beppu M. (1996). Binding characteristics of human lactoferrin to the human monocytic leukemia cell line THP-1 differentiated into macrophages. *Biol. Pharm. Bull.* **19**: 167–175.

Edris B, Weiskopf K, Volkmer AK, Volkmer J-P, Willingham SB, Contreras-Trujillo H, *et al.* (2012). Antibody therapy targeting the CD47 protein is effective in a model of aggressive metastatic leiomyosarcoma. *Proceedings of the National Academy of Sciences* **109**: 6656–6661.

Elass E. (2002). Lactoferrin Inhibits the Lipopolysaccharide-Induced Expression and Proteoglycan-Binding Ability of Interleukin-8 in Human Endothelial Cells. *Infect Immun* **70**: 1860–1866.

Elliott MR, Chekeni FB, Trampont PC, Lazarowski ER, Kadl A, Walk SF, *et al.* (2009). Nucleotides released by apoptotic cells act as a find-me signal to promote phagocytic clearance. *Nature* **461**: 282–286.

Ellison RT, Giehl TJ, and LaForce FM. (1988). Damage of the outer membrane of enteric gram-negative bacteria by lactoferrin and transferrin. *Infect Immun* **56**: 2774–2781.

Fadok VA, Bratton DL, Guthrie L, and Henson PM. (2001a). Differential effects of apoptotic versus lysed cells on macrophage production of cytokines: role of proteases. *J Immunol* **166**: 6847–6854.

Fadok VA, Bratton DL, Konowal A, Freed PW, Westcott JY, and Henson PM. (1998a). Macrophages that have ingested apoptotic cells in vitro inhibit proinflammatory cytokine production through autocrine/paracrine mechanisms involving TGF-beta, PGE2, and PAF. *J Clin Invest* **101**: 890–898.

Fadok VA, de Cathelineau A, Daleke DL, Henson PM, and Bratton DL. (2001b). Loss of Phospholipid Asymmetry and Surface Exposure of Phosphatidylserine Is Required for Phagocytosis of Apoptotic Cells by Macrophages and Fibroblasts. *Journal of Biological Chemistry* **276**: 1071–1077.

Fadok VA, Warner ML, Bratton DL, and Henson PM. (1998b). CD36 is required for phagocytosis of apoptotic cells by human macrophages that use either a phosphatidylserine receptor or the vitronectin receptor (alpha v beta 3). *J Immunol* **161**: 6250–6257.

Faust N, Bonifer C, Wiles MV, and Sippel AE. (1994). An in vitro differentiation system for the examination of transgene activation in mouse macrophages. *DNA Cell Biol.* **13**: 901–907.

Feinman R, Henriksen-DeStefano D, Tsujimoto M, and Vilcek J. (1987). Tumor necrosis factor is an important mediator of tumor cell killing by human monocytes. *J*

Immunol **138**: 635–640.

Fenton MJ, Buras JA, and Donnelly RP. (1992). IL-4 reciprocally regulates IL-1 and IL-1 receptor antagonist expression in human monocytes. *J Immunol* **149**: 1283–1288.

Flecken T, and Sarobe P. (2015). Tim-3 expression in tumour-associated macrophages: a new player in HCC progression. *Gut*.

Florey O, and Haskard DO. (2009). Sphingosine 1-Phosphate Enhances Fc Receptor-Mediated Neutrophil Activation and Recruitment under Flow Conditions. *The Journal of Immunology* **183**: 2330–2336.

Ford AL, Foulcher E, Goodsall AL, and Sedgwick JD. (1996). Tissue digestion with dispase substantially reduces lymphocyte and macrophage cell-surface antigen expression. *J Immunol Methods* **194**: 71–75.

Ford CA, Petrova S, Pound JD, Voss JJLP, Melville L, Paterson M, *et al.* (2015). Oncogenic properties of apoptotic tumor cells in aggressive B cell lymphoma. *Curr. Biol.* **25**: 577–588.

Franklin RA, Liao W, Sarkar A, Kim MV, Bivona MR, Liu K, *et al.* (2014). The cellular and molecular origin of tumor-associated macrophages. *Science* **344**: 921–925.

Fraser I, Hughes D, and Gordon S. (1993). Divalent cation-independent macrophage adhesion inhibited by monoclonal antibody to murine scavenger receptor. *Nature* **364**: 343–346.

Fratelli M, Gagliardini V, Galli G, Gnocchi P, Ghiara P, and Ghezzi P. (1995). Autocrine interleukin-1 beta regulates both proliferation and apoptosis in EL4-6.1 thymoma cells. *Blood* **85**: 3532–3537.

Freeman TC, Goldovsky L, Brosch M, van Dongen S, Mazière P, Grocock RJ, *et al.* (2007). Construction, visualisation, and clustering of transcription networks from microarray expression data. *PLoS Comput. Biol.* **3**: 2032–2042.

Froelich CJ, Dixit VM, and Yang X. (1998). Lymphocyte granule-mediated apoptosis: matters of viral mimicry and deadly proteases. *Immunol. Today* **19**: 30–36.

Gaidano G, Ballerini P, Gong JZ, Inghirami G, Neri A, Newcomb EW, *et al.* (1991). p53 mutations in human lymphoid malignancies: association with Burkitt lymphoma and chronic lymphocytic leukemia. *Proc. Natl. Acad. Sci. U.S.A.* **88**: 5413–5417.

García-Montoya IA, Cendón TS, Arévalo-Gallegos S, and Rascón-Cruz Q. (2012). Lactoferrin a multiple bioactive protein: an overview. *Biochimica et biophysica acta* **1820**: 226–236.

Gardai SJ, McPhillips KA, Frasch SC, Janssen WJ, Starefeldt A, Murphy-Ullrich JE, *et al.* (2005). Cell-Surface Calreticulin Initiates Clearance of Viable or Apoptotic

Cells through trans-Activation of LRP on the Phagocyte. *Cell* **123**: 321–334.

Gause WC, Wynn TA, and Allen JE. (2013). Type 2 immunity and wound healing: evolutionary refinement of adaptive immunity by helminths. *Nat Rev Immunol* **13**: 607–614.

Gautier EL, Shay T, Miller J, Greter M, Jakubzick C, Ivanov S, *et al.* (2012). Gene-expression profiles and transcriptional regulatory pathways that underlie the identity and diversity of mouse tissue macrophages. *Nat. Immunol.* **13**: 1118–1128.

Gerber DE, Stopeck AT, Wong L, Rosen LS, Thorpe PE, Shan JS, *et al.* (2011). Phase I Safety and Pharmacokinetic Study of Bavituximab, a Chimeric Phosphatidylserine-Targeting Monoclonal Antibody, in Patients with Advanced Solid Tumors. *Clinical Cancer Research* **17**: 6888–6896.

Geser A, de Thé G, Lenoir G, Day NE, and Williams EH. (1982). Final case reporting from the Ugandan prospective study of the relationship between EBV and Burkitt's lymphoma. *Int J Cancer* **29**: 397–400.

Ginhoux F, Greter M, Leboeuf M, Nandi S, See P, Gokhan S, *et al.* (2010). Fate Mapping Analysis Reveals That Adult Microglia Derive from Primitive Macrophages. *Science* **330**: 841–845.

Giuffrè G, Barresi V, Skliros C, Barresi G, and Tuccari G. (2007). Immunoexpression of lactoferrin in human sporadic renal cell carcinomas. *Oncology reports* **17**: 1021–1026.

Gordon S, and Taylor PR. (2005). Monocyte and macrophage heterogeneity. *Nat Rev Immunol* **5**: 953–964.

Gordon S. (2003). Alternative activation of macrophages. *Nat Rev Immunol* **3**: 23–35.

Gordon S. (1999). Macrophage-restricted molecules: role in differentiation and activation. *Immunol Lett* **65**: 5–8.

Gordon S. (2007). The macrophage: past, present and future. *Eur. J. Immunol.* **37 Suppl 1**: S9–17.

Green DR, and Reed JC. (1998). Mitochondria and apoptosis. *Science* **281**: 1309–1312.

Green DR, Ferguson T, Zitvogel L, and Kroemer G. (2009). Immunogenic and tolerogenic cell death. *Nat Rev Immunol* **9**: 353–363.

Gregory CD, and Pound JD. (2011). Cell death in the neighbourhood: direct microenvironmental effects of apoptosis in normal and neoplastic tissues. *The Journal of pathology* **223**: 177–194.

Gregory CD, and Pound JD. (2010). Microenvironmental influences of apoptosis in

vivo and in vitro. *Apoptosis* **15**: 1029–1049.

Gregory CD, Rossi AG, Bournazou I, Zhuang L, and Willems JJLP. (2011). Leukocyte migratory responses to apoptosis: the attraction and the distraction. *Cell Adh Migr* **5**: 293–297.

Grey A, Zhu Q, Watson M, Callon K, and Cornish J. (2006). Lactoferrin potently inhibits osteoblast apoptosis, via an LRP1-independent pathway. *Molecular and Cellular Endocrinology* **251**: 96–102.

Grey A. (2004). The Low-Density Lipoprotein Receptor-Related Protein 1 Is a Mitogenic Receptor for Lactoferrin in Osteoblastic Cells. *Molecular Endocrinology* **18**: 2268–2278.

Grimsley C, and Ravichandran KS. (2003). Cues for apoptotic cell engulfment: eat-me, don't eat-me and come-get-me signals. *Trends in Cell Biology* **13**: 648–656.

Gude DR, Alvarez SE, Paugh SW, Mitra P, Yu J, Griffiths R, *et al.* (2008). Apoptosis induces expression of sphingosine kinase 1 to release sphingosine-1-phosphate as a 'come-and-get-me' signal. *The FASEB Journal* **22**: 2629–2638.

Gumienny TL, Brugnera E, Tosello-Trampont A-C, Kinchen JM, Haney LB, Nishiwaki K, *et al.* (2001). CED-12/ELMO, a novel member of the CrkII/Dock180/Rac pathway, is required for phagocytosis and cell migration. *Cell* **107**: 27–41.

Gutierrez MI, Bhatia K, Cherney B, Capello D, Gaidano G, and Magrath I. (1997). Intraclonal molecular heterogeneity suggests a hierarchy of pathogenetic events in Burkitt's lymphoma. *Annals of oncology* **8**: 987–994.

Hackam DJ, Rotstein OD, Zhang WJ, Demaurex N, Woodside M, Tsai O, *et al.* (1997). Regulation of phagosomal acidification. Differential targeting of Na+/H+ exchangers, Na+/K+-ATPases, and vacuolar-type H+-atpases. *J Biol Chem* **272**: 29810–29820.

Hagemann T, Lawrence T, McNeish I, Charles KA, Kulbe H, Thompson RG, *et al.* (2008). 'Re-educating' tumor-associated macrophages by targeting NF- B. *Journal of Experimental Medicine* **205**: 1261–1268.

Hall SE, Savill JS, Henson PM, and Haslett C. (1994). Apoptotic neutrophils are phagocytosed by fibroblasts with participation of the fibroblast vitronectin receptor and involvement of a mannose/fucose-specific lectin. *J Immunol* **153**: 3218–3227.

Hanayama R, Tanaka M, Miwa K, Shinohara A, Iwamatsu A, and Nagata S. (2002). Identification of a factor that links apoptotic cells to phagocytes. *Nature* **417**: 182–187.

Hanayama R, Tanaka M, Miyasaka K, Aozasa K, Koike M, Uchiyama Y, *et al.* (2004). Autoimmune disease and impaired uptake of apoptotic cells in MFG-E8-deficient mice. *Science* **304**: 1147–1150.

Haridas M, Anderson BF, and Baker EN. (1995). Structure of human diferric lactoferrin refined at 2.2 A resolution. *Acta Crystallogr. D Biol. Crystallogr.* **51**: 629–646.

Hart SP, Dransfield I, and Rossi AG. (2008). Phagocytosis of apoptotic cells. *Methods* **44**: 280–285.

Hashizume S, Kuroda K, and Murakami H. (1983). Identification of lactoferrin as an essential growth factor for human lymphocytic cell lines in serum-free medium. *Biochimica et biophysica acta* **763**: 377–382.

Hayday AC, Gillies SD, Saito H, Wood C, Wiman K, Hayward WS, *et al.* (1984). Activation of a translocated human c-myc gene by an enhancer in the immunoglobulin heavy-chain locus. *Nature* **307**: 334–340.

Hayes TG, Falchook GF, Varadhachary GR, Smith DP, Davis LD, Dhingra HM, *et al.* (2005). Phase I trial of oral talactoferrin alfa in refractory solid tumors. *Invest New Drugs* **24**: 233–240.

Håversen L, Ohlsson BG, Hahn-Zoric M, Hanson LÅ, and Mattsby-Baltzer I. (2002). Lactoferrin down-regulates the LPS-induced cytokine production in monocytic cells via NF-κB. *Cell Immunol* **220**: 83–95.

He J, Yin Y, Luster TA, Watkins L, and Thorpe PE. (2009). Antiphosphatidylserine Antibody Combined with Irradiation Damages Tumor Blood Vessels and Induces Tumor Immunity in a Rat Model of Glioblastoma. *Clinical Cancer Research* **15**: 6871–6880.

Hecht JL, and Aster JC. (2000). Molecular biology of Burkitt's lymphoma. *J. Clin. Oncol.* **18**: 3707–3721.

Henson PM, and Hume DA. (2006). Apoptotic cell removal in development and tissue homeostasis. *Trends in Immunology* **27**: 244–250.

Herbomel P, Thisse B, and Thisse C. (1999). Ontogeny and behaviour of early macrophages in the zebrafish embryo. *Development* **126**: 3735–3745.

Hermens AF, and Barendsen GW. (1969). Changes of cell proliferation characteristics in a rat rhabdomyosarcoma before and after x-irradiation. *European Journal of Cancer* **5**: 173–189.

Hesse M, Modolell M, La Flamme AC, Schito M, Fuentes JM, Cheever AW, *et al.* (2001). Differential Regulation of Nitric Oxide Synthase-2 and Arginase-1 by Type 1/Type 2 Cytokines In Vivo: Granulomatous Pathology Is Shaped by the Pattern of L-Arginine Metabolism. *The Journal of Immunology* **167**: 6533–6544.

Hewitt HB, Blake E, and Proter EH. (1973). The effect of lethally irradiated cells on the transplantability of murine tumours. *Br J Cancer* **28**: 123–135.

Hibbs JB, Taintor RR, Vavrin Z, and Rachlin EM. (1988). Nitric oxide: a cytotoxic

activated macrophage effector molecule. *Biochemical and Biophysical Research Communications* **157**: 87–94.

Higuchi M, Higashi N, Taki H, and Osawa T. (1990). Cytolytic mechanisms of activated macrophages. Tumor necrosis factor and L-arginine-dependent mechanisms act synergistically as the major cytolytic mechanisms of activated macrophages. *J Immunol* **144**: 1425–1431.

Hochreiter-Hufford A, and Ravichandran KS. (2013). Clearing the dead: apoptotic cell sensing, recognition, engulfment, and digestion. *Cold Spring Harbor Perspectives in Biology* **5**: a008748.

Hoeffel G, Wang Y, Greter M, See P, Teo P, Malleret B, *et al.* (2012). Adult Langerhans cells derive predominantly from embryonic fetal liver monocytes with a minor contribution of yolk sac-derived macrophages. *Journal of Experimental Medicine* **209**: 1167–1181.

Hoffer PB, Miller-Catchpole R, and Turner DA. (1979). Demonstration of lactoferrin in tumor tissue from two patients with positive gallium scans. *J. Nucl. Med.* **20**: 424–427.

Hopkinson-Woolley J, Hughes D, Gordon S, and Martin P. (1994). Macrophage recruitment during limb development and wound healing in the embryonic and foetal mouse. *Journal of Cell Science* **107 (Pt 5)**: 1159–1167.

Hristov M. (2004). Apoptotic bodies from endothelial cells enhance the number and initiate the differentiation of human endothelial progenitor cells in vitro. *Blood* **104**: 2761–2766.

Huang DW, Sherman BT, and Lempicki RA. (2009a). Bioinformatics enrichment tools: paths toward the comprehensive functional analysis of large gene lists. *Nucleic Acids Research* **37**: 1–13.

Huang DW, Sherman BT, and Lempicki RA. (2009b). Systematic and integrative analysis of large gene lists using DAVID bioinformatics resources. *Nat Protoc* **4**: 44–57.

Huang DW, Sherman BT, Tan Q, Kir J, Liu D, Bryant D, *et al.* (2007). DAVID Bioinformatics Resources: expanded annotation database and novel algorithms to better extract biology from large gene lists. *Nucleic Acids Research* **35**: W169–75.

Huang N, Bethell D, Card C, Cornish J, Marchbank T, Wyatt D, *et al.* (2008). Bioactive recombinant human lactoferrin, derived from rice, stimulates mammalian cell growth. *In Vitro Cell. Dev. Biol. Anim.* **44**: 464–471.

Huang Q, Li F, Liu X, Li W, Shi W, Liu F-F, *et al.* (2011). Caspase 3–mediated stimulation of tumor cell repopulation during cancer radiotherapy. *Nature Medicine* **17**: 860–866.

Hugel B, Martínez MC, Kunzelmann C, and Freyssinet J-M. (2005). Membrane

microparticles: two sides of the coin. *Physiology (Bethesda)* **20**: 22–27.

Hughes DA, and Gordon S. (1998). Expression and function of the type 3 complement receptor in tissues of the developing mouse. *J Immunol* **160**: 4543–4552.

Hume DA, and MacDonald KPA. (2012). Therapeutic applications of macrophage colony-stimulating factor-1 (CSF-1) and antagonists of CSF-1 receptor (CSF-1R) signaling. *Blood* **119**: 1810–1820.

Hume DA, Summers KM, Raza S, Baillie JK, and Freeman TC. (2010). Functional clustering and lineage markers: Insights into cellular differentiation and gene function from large-scale microarray studies of purified primary cell populations. *Genomics* **95**: 328–338.

Hume DA. (2006). The mononuclear phagocyte system. *Current Opinion in Immunology* **18**: 49–53.

Ichinose Y, Bakouche O, Tsao JY, and Fidler IJ. (1988). Tumor necrosis factor and IL-1 associated with plasma membranes of activated human monocytes lyse monokine-sensitive but not monokine-resistant tumor cells whereas viable activated monocytes lyse both. *J Immunol* **141**: 512–518.

Idzko M, Hammad H, van Nimwegen M, Kool M, Willart MAM, Muskens F, *et al.* (2007). Extracellular ATP triggers and maintains asthmatic airway inflammation by activating dendritic cells. *Nature Medicine* **13**: 913–919.

Ieni A, Barresi V, Grosso M, Rosa MA, and Tuccari G. (2009). Lactoferrin immuno-expression in human normal and neoplastic bone tissue. *J Bone Miner Metab* **27**: 364–371.

Irizarry RA, Hobbs B, Collin F, Beazer-Barclay YD, Antonellis KJ, Scherf U, *et al.* (2003). Exploration, normalization, and summaries of high density oligonucleotide array probe level data. *Biostatistics* **4**: 249–264.

Jackson M, Taylor AH, Jones EA, and Forrester LM. (2010). The culture of mouse embryonic stem cells and formation of embryoid bodies. *Methods Mol. Biol.* **633**: 1–18.

Jaiswal S, Jamieson CHM, Pang WW, Park CY, Chao MP, Majeti R, *et al.* (2009). CD47 Is Upregulated on Circulating Hematopoietic Stem Cells and Leukemia Cells to Avoid Phagocytosis. *Cell* **138**: 271–285.

Jalalinadoushan M, Peivareh H, and Azizzadeh Delshad A. (2004). Correlation between Apoptosis and Histological Grade of Transitional Cell Carcinoma of Urinary Bladder. *Urol J* **1**: 177–179.

Jenkins SJ, Ruckerl D, Cook PC, Jones LH, Finkelman FD, van Rooijen N, *et al.* (2011). Local Macrophage Proliferation, Rather than Recruitment from the Blood, Is a Signature of TH2 Inflammation. *Science* **332**: 1284–1288.

Jenkins SJ, Ruckerl D, Thomas GD, Hewitson JP, Duncan S, Brombacher F, *et al.* (2013). IL-4 directly signals tissue-resident macrophages to proliferate beyond homeostatic levels controlled by CSF-1. *Journal of Experimental Medicine* **210**: 2477–2491.

Jersmann HPA, Ross KA, Vivers S, Brown SB, Haslett C, and Dransfield I. (2003). Phagocytosis of apoptotic cells by human macrophages: analysis by multiparameter flow cytometry. *Cytometry A* **51**: 7–15.

Ji ZS, and Mahley RW. (1994). Lactoferrin binding to heparan sulfate proteoglycans and the LDL receptor-related protein. Further evidence supporting the importance of direct binding of remnant lipoproteins to HSPG. *Arterioscler. Thromb.* **14**: 2025–2031.

Johann AM, Barra V, Kuhn AM, Weigert A, Knethen von A, and Brüne B. (2007). Apoptotic cells induce arginase II in macrophages, thereby attenuating NO production. *The FASEB Journal* **21**: 2704–2712.

Johann AM, Weigert A, Eberhardt W, Kuhn A-M, Barra V, Knethen von A, *et al.* (2008). Apoptotic cell-derived sphingosine-1-phosphate promotes HuR-dependent cyclooxygenase-2 mRNA stabilization and protein expression. *J Immunol* **180**: 1239–1248.

Jorens PG, Matthys KE, and Bult H. (1995). Modulation of nitric oxide synthase activity in macrophages. *Mediators of Inflammation* **4**: 75–89.

Juncadella IJ, Kadl A, Sharma AK, Shim YM, Hochreiter-Hufford A, Borish L, *et al.* (2013). Apoptotic cell clearance by bronchial epithelial cells critically influences airway inflammation. *Nature* **493**: 547–551.

Kai K, Komine K-I, Komine Y, Kuroishi T, Kozutsumi T, Kobayashi J, *et al.* (2002). Lactoferrin stimulates A Staphylococcus aureus killing activity of bovine phagocytes in the mammary gland. *Microbiol. Immunol.* **46**: 187–194.

Kamranvar SA, Gruhne B, Szeles A, and Masucci MG. (2007). Epstein–Barr virus promotes genomic instability in Burkitt's lymphoma. *Oncogene* **26**: 5115–5123.

Kane SV, Sandborn WJ, Rufo PA, Zholudev A, Boone J, Lyerly D, *et al.* (2003). Fecal lactoferrin is a sensitive and specific marker in identifying intestinal inflammation. *Am. J. Gastroenterol.* **98**: 1309–1314.

Kawakami H, and Lönnerdal B. (1991). Isolation and function of a receptor for human lactoferrin in human fetal intestinal brush-border membranes. *Am. J. Physiol.* **261**: G841–6.

Kawane K, Fukuyama H, Yoshida H, Nagase H, Ohsawa Y, Uchiyama Y, *et al.* (2003). Impaired thymic development in mouse embryos deficient in apoptotic DNA degradation. *Nat. Immunol.* **4**: 138–144.

Keller R, Geiges M, and Keist R. (1990). L-arginine-dependent reactive nitrogen

intermediates as mediators of tumor cell killing by activated macrophages. *Cancer Res* **50**: 1421–1425.

Keller R. (1973). Cytostatic elimination of syngeneic rat tumor cells in vitro by nonspecifically activated macrophages. *J Exp Med* **138**: 625–644.

Kerr JF, Wyllie AH, and Currie AR. (1972). Apoptosis: a basic biological phenomenon with wide-ranging implications in tissue kinetics. *Br J Cancer* **26**: 239–257.

Kinchen JM, and Ravichandran KS. (2007). Journey to the grave: signaling events regulating removal of apoptotic cells. *Journal of Cell Science* **120**: 2143–2149.

Kinchen JM, and Ravichandran KS. (2008). Phagosome maturation: going through the acid test. *Nat Rev Mol Cell Biol* **9**: 781–795.

Kinchen JM, Doukoumetzidis K, Almendinger J, Stergiou L, Tosello-Trampont A, Sifri CD, *et al.* (2008). A pathway for phagosome maturation during engulfment of apoptotic cells. *Nat Cell Biol* **10**: 556–566.

Klimp AH, Hollema H, Kempinga C, van der Zee AG, de Vries EG, and Daemen T. (2001). Expression of cyclooxygenase-2 and inducible nitric oxide synthase in human ovarian tumors and tumor-associated macrophages. *Cancer Res* **61**: 7305–7309.

Kobara M, Sunagawa N, Abe M, Tanaka N, Toba H, Hayashi H, *et al.* (2008). Apoptotic myocytes generate monocyte chemoattractant protein-1 and mediate macrophage recruitment. *J Appl Physiol* **104**: 601–609.

Kobayashi N, Karisola P, Peña-Cruz V, Dorfman DM, Jinushi M, Umetsu SE, *et al.* (2007). TIM-1 and TIM-4 Glycoproteins Bind Phosphatidylserine and Mediate Uptake of Apoptotic Cells. *Immunity* **27**: 927–940.

Kothakota S, Azuma T, Reinhard C, Klippel A, Tang J, Chu K, *et al.* (1997). Caspase-3-generated fragment of gelsolin: effector of morphological change in apoptosis. *Science* **278**: 294–298.

Kovalchuk AL, Qi CF, Torrey TA, Taddesse-Heath L, Feigenbaum L, Park SS, *et al.* (2000). Burkitt lymphoma in the mouse. *J Exp Med* **192**: 1183–1190.

Kreider T, Anthony RM, Urban JF, and Gause WC. (2007). Alternatively activated macrophages in helminth infections. *Current Opinion in Immunology* **19**: 448–453.

Kroemer G, Galluzzi L, Kepp O, and Zitvogel L. (2013). Immunogenic Cell Death in Cancer Therapy. *Annu. Rev. Immunol.* **31**: 51–72.

Kuipers ME, de Vries HG, Eikelboom MC, Meijer DK, and Swart PJ. (1999). Synergistic fungistatic effects of lactoferrin in combination with antifungal drugs against clinical Candida isolates. *Antimicrobial Agents and Chemotherapy* **43**: 2635–2641.

la Rosa de G, Yang D, Tewary P, Varadhachary A, and Oppenheim JJ. (2008). Lactoferrin acts as an alarmin to promote the recruitment and activation of APCs and antigen-specific immune responses. *J Immunol* **180**: 6868–6876.

Lacy-Hulbert A. (2009). Comparative Characterization of Non-professional and Professional Phagocyte Responses to Apoptotic Cells. *Phagocytosis of Dying Cells: From Molecular Mechanisms to Human Diseases*: 189–215.

Lai FW, Lichty BD, and Bowdish DME. (2015). Microvesicles: ubiquitous contributors to infection and immunity. *J Leukoc Biol* **97**: 237–245.

Lauber K, Bohn E, Kröber SM, Xiao Y-J, Blumenthal SG, Lindemann RK, *et al.* (2003). Apoptotic cells induce migration of phagocytes via caspase-3-mediated release of a lipid attraction signal. *Cell* **113**: 717–730.

Leek RD, and Harris AL. (2002). Tumor-associated macrophages in breast cancer. *J Mammary Gland Biol Neoplasia* **7**: 177–189.

Leek RD, Lewis CE, Whitehouse R, Greenall M, Clarke J, and Harris AL. (1996). Association of macrophage infiltration with angiogenesis and prognosis in invasive breast carcinoma. *Cancer Res* **56**: 4625–4629.

Lennon-Dumenil AM, Bakker AH, Maehr R, Fiebiger E, Overkleeft HS, Rosemblatt M, *et al.* (2002). Analysis of Protease Activity in Live Antigen-presenting Cells Shows Regulation of the Phagosomal Proteolytic Contents During Dendritic Cell Activation. *Journal of Experimental Medicine* **196**: 529–540.

Leoncini L, Del Vecchio MT, Megha T, Barbini P, Galieni P, Pileri S, *et al.* (1993). Correlations between apoptotic and proliferative indices in malignant non-Hodgkin's lymphomas. *Am. J. Pathol.* **142**: 755–763.

Levay PF, and Viljoen M. (1995). Lactoferrin: a general review. *Haematologica* **80**: 252–267.

Leveugle B, Mazurier J, Legrand D, Mazurier C, Montreuil J, and Spik G. (1993). Lactotransferrin binding to its platelet receptor inhibits platelet aggregation. *Eur J Biochem* **213**: 1205–1211.

Li F, Huang Q, Chen J, Peng Y, Roop DR, Bedford JS, *et al.* (2010). Apoptotic cells activate the 'phoenix rising' pathway to promote wound healing and tissue regeneration. *Science Signaling* **3**: ra13.

Li H, Zhu H, Xu CJ, and Yuan J. (1998). Cleavage of BID by caspase 8 mediates the mitochondrial damage in the Fas pathway of apoptosis. *Cell* **94**: 491–501.

Lichanska AM, and Hume DA. (2000). Origins and functions of phagocytes in the embryo. *Experimental Hematology* **28**: 601–611.

Lichanska AM, Browne CM, Henkel GW, Murphy KM, Ostrowski MC, McKercher SR, *et al.* (1999). Differentiation of the mononuclear phagocyte system during mouse

embryogenesis: the role of transcription factor PU.1. *Blood* **94**: 127–138.

Lima MF, and Kierszenbaum F. (1985). Lactoferrin effects on phagocytic cell function. I. Increased uptake and killing of an intracellular parasite by murine macrophages and human monocytes. *J Immunol* **134**: 4176–4183.

Lin EY, Li J-F, Bricard G, Wang W, Deng Y, Sellers R, *et al.* (2007). Vascular endothelial growth factor restores delayed tumor progression in tumors depleted of macrophages. *Mol Oncol* **1**: 288–302.

Liotta LA, Abe S, Robey PG, and Martin GR. (1979). Preferential digestion of basement membrane collagen by an enzyme derived from a metastatic murine tumor. *Proc. Natl. Acad. Sci. U.S.A.* **76**: 2268–2272.

Liu FT, Hsu DK, Zuberi RI, Kuwabara I, Chi EY, and Henderson WR. (1995). Expression and function of galectin-3, a beta-galactoside-binding lectin, in human monocytes and macrophages. *Am. J. Pathol.* **147**: 1016–1028.

Liu G, Bi Y, Wang R, Shen B, Zhang Y, Yang H, *et al.* (2013). Kinase AKT1 Negatively Controls Neutrophil Recruitment and Function in Mice. *The Journal of Immunology* **191**: 2680–2690.

Liu X, Kim CN, Yang J, Jemmerson R, and Wang X. (1996). Induction of apoptotic program in cell-free extracts: requirement for dATP and cytochrome c. *Cell* **86**: 147–157.

Livak KJ, and Schmittgen TD. (2001). Analysis of Relative Gene Expression Data Using Real-Time Quantitative PCR and the 2−ΔΔCT Method. *Methods* **25**: 402–408.

Luo X, Budihardjo I, Zou H, Slaughter C, and Wang X. (1998). Bid, a Bcl2 interacting protein, mediates cytochrome c release from mitochondria in response to activation of cell surface death receptors. *Cell* **94**: 481–490.

Lupetti A, Dissel JT, Brouwer CPJM, and Nibbering PH. (2008). Human antimicrobial peptides' antifungal activity against Aspergillus fumigatus. *Eur J Clin Microbiol Infect Dis* **27**: 1125–1129.

Mabbott NA, Kenneth Baillie J, Hume DA, and Freeman TC. (2010). Meta-analysis of lineage-specific gene expression signatures in mouse leukocyte populations. *Immunobiology* **215**: 724–736.

Machnicki M, Zimecki M, and Zagulski T. (1993). Lactoferrin regulates the release of tumour necrosis factor alpha and interleukin 6 in vivo. *Int J Exp Pathol* **74**: 433–439.

MacKinnon AC, Farnworth SL, Hodkinson PS, Henderson NC, Atkinson KM, Leffler H, *et al.* (2008). Regulation of alternative macrophage activation by galectin-3. *J Immunol* **180**: 2650–2658.

MacMicking JD, Nathan C, Hom G, Chartrain N, Fletcher DS, Trumbauer M, *et al.*

(1995). Altered responses to bacterial infection and endotoxic shock in mice lacking inducible nitric oxide synthase. *Cell* **81**: 641–650.

Mader JS, Richardson A, Salsman J, Top D, de Antueno R, Duncan R, *et al.* (2007). Bovine lactoferricin causes apoptosis in Jurkat T-leukemia cells by sequential permeabilization of the cell membrane and targeting of mitochondria. *Experimental Cell Research* **313**: 2634–2650.

Mahmoud SMA, Lee AHS, Paish EC, Macmillan RD, Ellis IO, and Green AR. (2012). Tumour-infiltrating macrophages and clinical outcome in breast cancer. *Journal of Clinical Pathology* **65**: 159–163.

Majeti R, Chao MP, Alizadeh AA, Pang WW, Jaiswal S, Gibbs KD Jr., *et al.* (2009). CD47 Is an Adverse Prognostic Factor and Therapeutic Antibody Target on Human Acute Myeloid Leukemia Stem Cells. *Cell* **138**: 286–299.

Mannick JB, Asano K, Izumi K, Kieff E, and Stamler JS. (1994). Nitric oxide produced by human B lymphocytes inhibits apoptosis and Epstein-Barr virus reactivation. *Cell* **79**: 1137–1146.

Mantovani A, Allavena P, and Sica A. (2004a). Tumour-associated macrophages as a prototypic type II polarised phagocyte population: role in tumour progression. *Eur. J. Cancer* **40**: 1660–1667.

Mantovani A, Bottazzi B, Colotta F, Sozzani S, and Ruco L. (1992). The origin and function of tumor-associated macrophages. *Immunol. Today* **13**: 265–270.

Mantovani A, Jerrells TR, Dean JH, and Herberman RB. (1979). Cytolytic and cytostatic activity on tumor cells of circulating human monocytes. *Int J Cancer* **23**: 18–27.

Mantovani A, Sica A, Sozzani S, Allavena P, Vecchi A, and Locati M. (2004b). The chemokine system in diverse forms of macrophage activation and polarization. *Trends in Immunology* **25**: 677–686.

Mantovani A, Sozzani S, Locati M, Allavena P, and Sica A. (2002). Macrophage polarization: tumor-associated macrophages as a paradigm for polarized M2 mononuclear phagocytes. *Trends in Immunology* **23**: 549–555.

Marques-Da-Silva C, Burnstock G, Ojcius DM, and Coutinho-Silva R. (2011). Purinergic receptor agonists modulate phagocytosis and clearance of apoptotic cells in macrophages. *Immunobiology* **216**: 1–11.

Martin JH, and Edwards SW. (1993). Changes in mechanisms of monocyte/macrophage-mediated cytotoxicity during culture. Reactive oxygen intermediates are involved in monocyte-mediated cytotoxicity, whereas reactive nitrogen intermediates are employed by macrophages in tumor cell killing. *J Immunol* **150**: 3478–3486.

Martin SJ, Finucane DM, Amarante-Mendes GP, O'Brien GA, and Green DR.

(1996). Phosphatidylserine externalization during CD95-induced apoptosis of cells and cytoplasts requires ICE/CED-3 protease activity. *J Biol Chem* **271**: 28753–28756.

Martinez-Pomares L. (2012). The mannose receptor. *J Leukoc Biol* **92**: 1177–1186.

Mattsby-Baltzer I, Roşeanu A, Motaş C, Elverfors J, Engberg I, and Hanson LÅ. (1996). Lactoferrin or a Fragment Thereof Inhibits the Endotoxin-Induced Interleukin-6 Response in Human Monocytic Cells. *Pediatr Res* **40**: 257–262.

McBride HM, Rybin V, Murphy C, Giner A, Teasdale R, and Zerial M. (1999). Oligomeric complexes link Rab5 effectors with NSF and drive membrane fusion via interactions between EEA1 and syntaxin 13. *Cell* **98**: 377–386.

McCloskey P, Fridell YW, Attar E, Villa J, Jin Y, Varnum B, *et al.* (1997). GAS6 mediates adhesion of cells expressing the receptor tyrosine kinase Axl. *J Biol Chem* **272**: 23285–23291.

McDonald PP, Fadok VA, Bratton D, and Henson PM. (1999). Transcriptional and translational regulation of inflammatory mediator production by endogenous TGF-beta in macrophages that have ingested apoptotic cells. *J Immunol* **163**: 6164–6172.

Messmer UK, Ankarcrona M, Nicotera P, and Brüne B. (1994). p53 expression in nitric oxide-induced apoptosis. *FEBS Lett* **355**: 23–26.

Mestas J, and Hughes CCW. (2004). Of Mice and Not Men: Differences between Mouse and Human Immunology. *The Journal of Immunology* **172**: 2731–2738.

Metz-Boutigue MH, Jollès J, Mazurier J, Schoentgen F, Legrand D, Spik G, *et al.* (1984). Human lactotransferrin: amino acid sequence and structural comparisons with other transferrins. *Eur J Biochem* **145**: 659–676.

Mevorach D, Zhou JL, Song X, and Elkon KB. (1998). Systemic exposure to irradiated apoptotic cells induces autoantibody production. *J Exp Med* **188**: 387–392.

Mielgo A, and Schmid MC. (2013). Impact of tumour associated macrophages in pancreatic cancer. *BMB Rep* **46**: 131–138.

Miki H, Suetsugu S, and Takenawa T. (1998). WAVE, a novel WASP-family protein involved in actin reorganization induced by Rac. *EMBO J.* **17**: 6932–6941.

Miksa M, Amin D, Wu R, Ravikumar TS, and Wang P. (2007). Fractalkine-induced MFG-E8 leads to enhanced apoptotic cell clearance by macrophages. *Mol Med* **13**: 553–560.

Miyanishi M, Tada K, Koike M, Uchiyama Y, Kitamura T, and Nagata S. (2007). Identification of Tim4 as a phosphatidylserine receptor. *Nature* **450**: 435–439.

Mochizuki H, Goto K, Mori H, and Mizuno Y. (1996). Histochemical detection of apoptosis in Parkinson's disease. *J. Neurol. Sci.* **137**: 120–123.

Moffatt OD, Devitt A, Bell ED, Simmons DL, and Gregory CD. (1999). Macrophage recognition of ICAM-3 on apoptotic leukocytes. *J Immunol* **162**: 6800–6810.

Moldoveanu T, Grace CR, Llambi F, Nourse A, Fitzgerald P, Gehring K, *et al.* (2013). BID-induced structural changes in BAK promote apoptosis. *Nature Structural and Molecular Biology* **20**: 589–597.

Molyneux EM, Rochford R, Griffin B, Newton R, Jackson G, Menon G, *et al.* (2012). Burkitt's lymphoma. *Lancet* **379**: 1234–1244.

Montuenga LM, and Pio R. (2007). Tumour-associated macrophages in nonsmall cell lung cancer: the role of interleukin-10. *European Respiratory Journal* **30**: 608–610.

Moreira S, Stramer B, Evans I, Wood W, and Martin P. (2010). Prioritization of Competing Damageand Developmental Signals by Migrating Macrophages in the Drosophila Embryo. *Current Biology* **20**: 464–470.

Morimoto K, Amano H, Sonoda F, Baba M, Senba M, Yoshimine H, *et al.* (2001). Alveolar macrophages that phagocytose apoptotic neutrophils produce hepatocyte growth factor during bacterial pneumonia in mice. *Am. J. Respir. Cell Mol. Biol.* **24**: 608–615.

Morris L, Graham CF, and Gordon S. (1991). Macrophages in haemopoietic and other tissues of the developing mouse detected by the monoclonal antibody F4/80. *Development* **112**: 517–526.

Mosser DM, and Edwards JP. (2008). Exploring the full spectrum of macrophage activation. *Nat Rev Immunol* **8**: 958–969.

Movahedi K, Laoui D, Gysemans C, Baeten M, Stange G, Van den Bossche J, *et al.* (2010). Different Tumor Microenvironments Contain Functionally Distinct Subsets of Macrophages Derived from Ly6C(high) Monocytes. *Cancer Res* **70**: 5728–5739.

Mukhtar RA, Moore AP, Tandon VJ, Nseyo O, Twomey P, Adisa CA, *et al.* (2012). Elevated Levels of Proliferating and Recently Migrated Tumor-associated Macrophages Confer Increased Aggressiveness and Worse Outcomes in Breast Cancer. *Ann Surg Oncol* **19**: 3979–3986.

Murdoch C. (2004). Mechanisms regulating the recruitment of macrophages into hypoxic areas of tumors and other ischemic tissues. *Blood* **104**: 2224–2234.

Murray HW, and Nathan CF. (1999). Macrophage microbicidal mechanisms in vivo: reactive nitrogen versus oxygen intermediates in the killing of intracellular visceral Leishmania donovani. *J Exp Med* **189**: 741–746.

Muzio M, Chinnaiyan AM, Kischkel FC, O'Rourke K, Shevchenko A, Ni J, *et al.* (1996). FLICE, a novel FADD-homologous ICE/CED-3-like protease, is recruited to the CD95 (Fas/APO-1) death--inducing signaling complex. *Cell* **85**: 817–827.

Nagata S, Hanayama R, and Kawane K. (2010). Autoimmunity and the Clearance of Dead Cells. *Cell* **140**: 619–630.

Nakajima K-I, Kanno Y, Nakamura M, Gao X-D, Kawamura A, Itoh F, *et al.* (2011). Bovine milk lactoferrin induces synthesis of the angiogenic factors VEGF and FGF2 in osteoblasts via the p44/p42 MAP kinase pathway. *Biometals* **24**: 847–856.

Nakano T, Ishimoto Y, Kishino J, Umeda M, Inoue K, Nagata K, *et al.* (1997). Cell adhesion to phosphatidylserine mediated by a product of growth arrest-specific gene 6. *J Biol Chem* **272**: 29411–29414.

Nakaya M, Tanaka M, Okabe Y, Hanayama R, and Nagata S. (2006). Opposite effects of rho family GTPases on engulfment of apoptotic cells by macrophages. *J Biol Chem* **281**: 8836–8842.

Naot D, Grey A, Reid IR, and Cornish J. (2005). Lactoferrin--a novel bone growth factor. *Clin Med Res* **3**: 93–101.

Napirei M, Karsunky H, Zevnik B, Stephan H, Mannherz HG, and Möröy T. (2000). Features of systemic lupus erythematosus in Dnase1-deficient mice. *Nat Genet* **25**: 177–181.

Naresh KN, Lakshminarayanan K, Pai SA, and Borges AM. (2001). Apoptosis index is a predictor of metastatic phenotype in patients with early stage squamous carcinoma of the tongue: a hypothesis to support this paradoxical association. *Cancer* **91**: 578–584.

Nathan C. (2008). Metchnikoff's Legacy in 2008. *Nat. Immunol.* **9**: 695–698.

Neri A, Barriga F, Inghirami G, Knowles DM, Neequaye J, Magrath IT, *et al.* (1991). Epstein-Barr virus infection precedes clonal expansion in Burkitt's and acquired immunodeficiency syndrome-associated lymphoma. *Blood* **77**: 1092–1095.

Nesbit M, Schaider H, Miller TH, and Herlyn M. (2001). Low-Level Monocyte Chemoattractant Protein-1 Stimulation of Monocytes Leads to Tumor Formation in Nontumorigenic Melanoma Cells. *The Journal of Immunology* **166**: 6483–6490.

Newman SL, Henson JE, and Henson PM. (1982). Phagocytosis of senescent neutrophils by human monocyte-derived macrophages and rabbit inflammatory macrophages. *J Exp Med* **156**: 430–442.

Nguyen T, Brunson D, Crespi CL, Penman BW, Wishnok JS, and Tannenbaum SR. (1992). DNA damage and mutation in human cells exposed to nitric oxide in vitro. *Proc. Natl. Acad. Sci. U.S.A.* **89**: 3030–3034.

Ni Y-H, Ding L, Huang X-F, Dong Y-C, Hu Q-G, and Hou Y-Y. (2015). Microlocalization of CD68(+) tumor-associated macrophages in tumor stroma correlated with poor clinical outcomes in oral squamous cell carcinoma patients. *Tumour Biol.* **36**: 5291–5298.

Nishiya K, and Horwitz DA. (1982). Contrasting effects of lactoferrin on human lymphocyte and monocyte natural killer activity and antibody-dependent cell-mediated cytotoxicity. *J Immunol* **129**: 2519–2523.

Norrby K, Mattsby-Baltzer I, Innocenti M, and Tuneberg S. (2001). Orally administered bovine lactoferrin systemically inhibits VEGF165-mediated angiogenesis in the rat. *Int J Cancer* **91**: 236–240.

Noy R, and Pollard JW. (2014). Tumor-Associated Macrophages: From Mechanisms to Therapy. *Immunity* **41**: 49–61.

O'Sullivan C, Lewis CE, Harris AL, and McGee JO. (1993). Secretion of epidermal growth factor by macrophages associated with breast carcinoma. *Lancet* **342**: 148–149.

Obeid M, Tesnière A, Ghiringhelli F, Fimia GM, Apetoh L, Perfettini J-L, *et al.* (2007). Calreticulin exposure dictates the immunogenicity of cancer cell death. *Nature Medicine* **13**: 54–61.

Ogden CA, deCathelineau A, Hoffmann PR, Bratton D, Ghebrehiwet B, Fadok VA, *et al.* (2001). C1q and mannose binding lectin engagement of cell surface calreticulin and CD91 initiates macropinocytosis and uptake of apoptotic cells. *J Exp Med* **194**: 781–795.

Ogden CA, Pound JD, Batth BK, Owens S, Johannessen I, Wood K, *et al.* (2005). Enhanced apoptotic cell clearance capacity and B cell survival factor production by IL-10-activated macrophages: implications for Burkitt's lymphoma. *J Immunol* **174**: 3015–3023.

Ohbu M, Saegusa M, and Okayasu I. (1995). Apoptosis and cellular proliferation in oesophageal squamous cell carcinomas: differences between keratinizing and nonkeratinizing types. *Virchows Archiv* **427**: 271–276.

Oldenborg PA, Zheleznyak A, Fang YF, Lagenaur CF, Gresham HD, and Lindberg FP. (2000). Role of CD47 as a marker of self on red blood cells. *Science* **288**: 2051–2054.

Ondrejka SL, and Hsi ED. (2015). Pathology of B-Cell Lymphomas: Diagnosis and Biomarker Discovery. In: Cancer Treatment and Research. Vol. 165. Cham: Springer International Publishing. p 27–50.

Onozaki K, Matsushima K, Kleinerman ES, Saito T, and Oppenheim JJ. (1985). Role of interleukin 1 in promoting human monocyte-mediated tumor cytotoxicity. *J Immunol* **135**: 314–320.

Ozinsky A, Underhill DM, Fontenot JD, Hajjar AM, Smith KD, Wilson CB, *et al.* (2000). The repertoire for pattern recognition of pathogens by the innate immune system is defined by cooperation between toll-like receptors. *Proc. Natl. Acad. Sci. U.S.A.* **97**: 13766–13771.

Park D, Tosello-Trampont A-C, Elliott MR, Lu M, Haney LB, Ma Z, *et al.* (2007). BAI1 is an engulfment receptor for apoptotic cells upstream of the ELMO/Dock180/Rac module. *Nature* **450**: 430–434.

Park S-Y, Jung M-Y, Kim H-J, Lee S-J, Kim S-Y, Lee B-H, *et al.* (2008a). Rapid cell corpse clearance by stabilin-2, a membrane phosphatidylserine receptor. *Cell death and differentiation* **15**: 192–201.

Park S-Y, Kim S-Y, Jung M-Y, Bae DJ, and Kim I-S. (2008b). Epidermal Growth Factor-Like Domain Repeat of Stabilin-2 Recognizes Phosphatidylserine during Cell Corpse Clearance. *Molecular and Cellular Biology* **28**: 5288–5298.

Peter C, Waibel M, Radu CG, Yang LV, Witte ON, Schulze-Osthoff K, *et al.* (2008). Migration to apoptotic 'find-me' signals is mediated via the phagocyte receptor G2A. *J Biol Chem* **283**: 5296–5305.

Petrova S. (2012). The cellular microenvironment in Burkitt's lymphoma: Gene expression profiling of Tumour-Associated Macrophages *in situ*, PhD Thesis. *University of Edinburgh.*

Piantadosi CA, Withers CM, Bartz RR, MacGarvey NC, Fu P, Sweeney TE, *et al.* (2011). Heme Oxygenase-1 Couples Activation of Mitochondrial Biogenesis to Anti-inflammatory Cytokine Expression. *Journal of Biological Chemistry* **286**: 16374–16385.

Pienta KJ, Machiels J-P, Schrijvers D, Alekseev B, Shkolnik M, Crabb SJ, *et al.* (2012). Phase 2 study of carlumab (CNTO 888), a human monoclonal antibody against CC-chemokine ligand 2 (CCL2), in metastatic castration-resistant prostate cancer. *Invest New Drugs* **31**: 760–768.

Pollard JW. (2009). Trophic macrophages in development and disease. *Nat Rev Immunol* **9**: 259–270.

Pollard JW. (2004). Tumour-educated macrophages promote tumour progression and metastasis. *Nat Rev Cancer* **4**: 71–78.

Pujade-Lauraine E, Guastalla JP, Colombo N, Devillier P, François E, Fumoleau P, *et al.* (1996). Intraperitoneal recombinant interferon gamma in ovarian cancer patients with residual disease at second-look laparotomy. *J. Clin. Oncol.* **14**: 343–350.

Qian B, Deng Y, Im JH, Muschel RJ, Zou Y, Li J, *et al.* (2009). A Distinct Macrophage Population Mediates Metastatic Breast Cancer Cell Extravasation, Establishment and Growth. *PLoS ONE* **4**: e6562.

Qian B-Z, and Pollard JW. (2010). Macrophage Diversity Enhances Tumor Progression and Metastasis. *Cell* **141**: 39–51.

Qin S, Larosa G, Campbell JJ, Smith Heath H, Kassam N, Shi X, *et al.* (1996). Expression of monocyte chemoattractant protein-1 and interleukin-8 receptors on

subsets of T cells: correlation with transendothelial chemotactic potential. *Eur. J. Immunol.* **26**: 640–647.

Rae F, Woods K, Sasmono T, Campanale N, Taylor D, Ovchinnikov DA, *et al.* (2007). Characterisation and trophic functions of murine embryonic macrophages based upon the use of a Csf1r–EGFP transgene reporter. *Developmental Biology* **308**: 232–246.

Ravichandran KS, and Lorenz U. (2007). Engulfment of apoptotic cells: signals for a good meal. *Nat Rev Immunol* **7**: 964–974.

Ravichandran KS. (2010). Find-me and eat-me signals in apoptotic cell clearance: progress and conundrums. *Journal of Experimental Medicine* **207**: 1807–1817.

Reich CF, and Pisetsky DS. (2009). The content of DNA and RNA in microparticles released by Jurkat and HL-60 cells undergoing in vitro apoptosis. *Experimental Cell Research* **315**: 760–768.

Reiter I, Krammer B, and Schwamberger G. (1999). Cutting edge: differential effect of apoptotic versus necrotic tumor cells on macrophage antitumor activities. *J Immunol* **163**: 1730–1732.

Ren Y, Xie Y, Jiang G, Fan J, Yeung J, Li W, *et al.* (2008). Apoptotic cells protect mice against lipopolysaccharide-induced shock. *J Immunol* **180**: 4978–4985.

Revesz L. (1956). Effect of tumour cells killed by x-rays upon the growth of admixed viable cells. *Nature* **178**: 1391–1392.

Richmond A. (2002). NF-κB, chemokine gene transcription and tumour growth. *Nat Rev Immunol* **2**: 664–674.

Riento K, and Ridley AJ. (2003). Rocks: multifunctional kinases in cell behaviour. *Nat Rev Mol Cell Biol* **4**: 446–456.

Roca H, Varsos ZS, Sud S, Craig MJ, Ying C, and Pienta KJ. (2009). CCL2 and Interleukin-6 Promote Survival of Human CD11b+ Peripheral Blood Mononuclear Cells and Induce M2-type Macrophage Polarization. *Journal of Biological Chemistry* **284**: 34342–34354.

Rodriguez-Manzanet R, Sanjuan MA, Wu HY, Quintana FJ, Xiao S, Anderson AC, *et al.* (2010). T and B cell hyperactivity and autoimmunity associated with niche-specific defects in apoptotic body clearance in TIM-4-deficient mice. *Proceedings of the National Academy of Sciences* **107**: 8706–8711.

Rollins BJ, Walz A, and Baggiolini M. (1991). Recombinant human MCP-1/JE induces chemotaxis, calcium flux, and the respiratory burst in human monocytes. *Blood* **78**: 1112–1116.

Russell JS, and Brown JM. (2013). The irradiated tumor microenvironment: role of tumor-associated macrophages in vascular recovery. *Front Physiol* **4**: 157.

Salvesen HB, and Akslen LA. (1999). Significance of tumour-associated macrophages, vascular endothelial growth factor and thrombospondin-1 expression for tumour angiogenesis and prognosis in endometrial carcinomas. *Int J Cancer* **84**: 538–543.

Sandhu SK, Papadopoulos K, Fong PC, Patnaik A, Messiou C, Olmos D, *et al.* (2013). A first-in-human, first-in-class, phase I study of carlumab (CNTO 888), a human monoclonal antibody against CC-chemokine ligand 2 in patients with solid tumors. *Cancer Chemother Pharmacol* **71**: 1041–1050.

Sano H, Hsu DK, Apgar JR, Yu L, Sharma BB, Kuwabara I, *et al.* (2003). Critical role of galectin-3 in phagocytosis by macrophages. *J Clin Invest* **112**: 389–397.

Savill J, Dransfield I, Gregory C, and Haslett C. (2002). A blast from the past: clearance of apoptotic cells regulates immune responses. *Nat Rev Immunol* **2**: 965–975.

Savill J, Dransfield I, Hogg N, and Haslett C. (1990). Vitronectin receptor-mediated phagocytosis of cells undergoing apoptosis. *Nature* **343**: 170–173.

Savill J, Hogg N, Ren Y, and Haslett C. (1992). Thrombospondin cooperates with CD36 and the vitronectin receptor in macrophage recognition of neutrophils undergoing apoptosis. *J Clin Invest* **90**: 1513–1522.

Savill J. (1997). Apoptosis in resolution of inflammation. *J Leukoc Biol* **61**: 375–380.

Scaffidi C, Fulda S, Srinivasan A, Friesen C, Li F, Tomaselli KJ, *et al.* (1998). Two CD95 (APO-1/Fas) signaling pathways. *EMBO J.* **17**: 1675–1687.

Schlegel RA, Krahling S, Callahan MK, and Williamson P. (1999). CD14 is a component of multiple recognition systems used by macrophages to phagocytose apoptotic lymphocytes. *Cell death and differentiation* **6**: 583–592.

Schneemann M, and Schoeden G. (2006). Macrophage biology and immunology: man is not a mouse. *J Leukoc Biol* **81**: 579–579.

Schrijvers DM. (2005). Phagocytosis of Apoptotic Cells by Macrophages Is Impaired in Atherosclerosis. *Arteriosclerosis, Thrombosis, and Vascular Biology* **25**: 1256–1261.

Schulz C, Perdiguero EG, Chorro L, Szabo-Rogers H, Cagnard N, Kierdorf K, *et al.* (2012). A Lineage of Myeloid Cells Independent of Myb and Hematopoietic Stem Cells. *Science* **336**: 86–90.

Scott RS, McMahon EJ, Pop SM, Reap EA, Caricchio R, Cohen PL, *et al.* (2001). Phagocytosis and clearance of apoptotic cells is mediated by MER. *Nature* **411**: 207–211.

Sebbagh M, Renvoizé C, Hamelin J, Riché N, Bertoglio J, and Bréard J. (2001). Caspase-3-mediated cleavage of ROCK I induces MLC phosphorylation and

apoptotic membrane blebbing. *Nat Cell Biol* **3**: 346–352.

Segawa K, Kurata S, Yanagihashi Y, Brummelkamp TR, Matsuda F, and Nagata S. (2014). Caspase-mediated cleavage of phospholipid flippase for apoptotic phosphatidylserine exposure. *Science* **344**: 1164–1168.

Selzman CH, Miller SA, Zimmerman MA, Gamboni-Robertson F, Harken AH, and Banerjee A. (2002). Monocyte chemotactic protein-1 directly induces human vascular smooth muscle proliferation. *Am J Physiol Heart Circ Physiol* **283**: H1455–H1461.

Shao W-H, Zhen Y, Eisenberg RA, and Cohen PL. (2009). The Mer receptor tyrosine kinase is expressed on discrete macrophage subpopulations and mainly uses Gas6 as its ligand for uptake of apoptotic cells. *Clinical Immunology* **133**: 138–144.

Shepard JL, and Zon LI. (2000). Developmental derivation of embryonic and adult macrophages. *Curr. Opin. Hematol.* **7**: 3–8.

Shi C, and Pamer EG. (2011). Monocyte recruitment during infection and inflammation. *Nat Rev Immunol* **11**: 762–774.

Shimura S, Yang G, Ebara S, Wheeler TM, Frolov A, and Thompson TC. (2000). Reduced infiltration of tumor-associated macrophages in human prostate cancer: association with cancer progression. *Cancer Res* **60**: 5857–5861.

Shinoda I, Takase M, Fukuwatari Y, Shimamura S, Köller M, and König W. (1996). Effects of lactoferrin and lactoferricin on the release of interleukin 8 from human polymorphonuclear leukocytes. *Biosci. Biotechnol. Biochem.* **60**: 521–523.

Sica A, Allavena P, and Mantovani A. (2008a). Cancer related inflammation: The macrophage connection. *Cancer Letters* **267**: 204–215.

Sica A, and Mantovani A. (2012). Macrophage plasticity and polarization: in vivo veritas. *J Clin Invest* **122**: 787–795.

Sica A, Larghi P, Mancino A, Rubino L, Porta C, Totaro MG, *et al.* (2008b). Macrophage polarization in tumour progression. *Seminars in Cancer Biology* **18**: 349–355.

Sica A, Saccani A, Bottazzi B, Polentarutti N, Vecchi A, Van Damme J, *et al.* (2000). Autocrine production of IL-10 mediates defective IL-12 production and NF-κB activation in tumor-associated macrophages. *J Immunol* **164**: 762–767.

Skommer J, Brittain T, and Raychaudhuri S. (2010). Bcl-2 inhibits apoptosis by increasing the time-to-death and intrinsic cell-to-cell variations in the mitochondrial pathway of cell death. *Apoptosis* **15**: 1223–1233.

Son K-N, Park J, Chung C-K, Chung DK, Yu D-Y, Lee K-K, *et al.* (2002). Human Lactoferrin Activates Transcription of IL-1β Gene in Mammalian Cells. *Biochemical and Biophysical Research Communications* **290**: 236–241.

Sorimachi K, Akimoto K, Hattori Y, Ieiri T, and Niwa A. (1997). Activation of macrophages by lactoferrin: secretion of TNF-alpha, IL-8 and NO. *Biochem. Mol. Biol. Int.* **43**: 79–87.

Sorokin SP, Hoyt RF, Blunt DG, and McNelly NA. (1992). Macrophage development: II. Early ontogeny of macrophage populations in brain, liver, and lungs of rat embryos as revealed by a lectin marker. *The Anatomical Record* **232**: 527–550.

Spender LC, O'Brien DI, Simpson D, Dutt D, Gregory CD, Allday MJ, *et al.* (2009). TGF-β induces apoptosis in human B cells by transcriptional regulation of BIK and BCL-XL. *Cell death and differentiation* **16**: 593–602.

Steidl C, Lee T, Shah SP, Farinha P, Han G, Nayar T, *et al.* (2010). Tumor-associated macrophages and survival in classic Hodgkin's lymphoma. *N Engl J Med* **362**: 875–885.

Steijns JM, and van Hooijdonk AC. (2000). Occurrence, structure, biochemical properties and technological characteristics of lactoferrin. *Br. J. Nutr.* **84 Suppl 1**: S11–7.

Stein M, Keshav S, Harris N, and Gordon S. (1992). Interleukin 4 potently enhances murine macrophage mannose receptor activity: a marker of alternative immunologic macrophage activation. *J Exp Med* **176**: 287–292.

Stephens TC, Currie GA, and Peacock JH. (1978). Repopulation of gamma-irradiated Lewis lung carcinoma by malignant cells and host macrophage progenitors. *Br J Cancer* **38**: 573.

Sun B, Sun Y, Wang J, Zhao X, Wang X, and Hao X. (2006). Extent, relationship and prognostic significance of apoptosis and cell proliferation in synovial sarcoma. *Eur. J. Cancer Prev.* **15**: 258–265.

Surh CD, and Sprent J. (1994). T-cell apoptosis detected in situ during positive and negative selection in the thymus. *Nature* **372**: 100–103.

Tang L, Cui T, Wu JJ, Liu-Mares W, Huang N, and Li J. (2010a). A rice-derived recombinant human lactoferrin stimulates fibroblast proliferation, migration, and sustains cell survival. *Wound Repair and Regeneration* **18**: 123–131.

Tang L, Wu JJ, Ma Q, Cui T, Andreopoulos FM, Gil J, *et al.* (2010b). Human lactoferrin stimulates skin keratinocyte function and wound re-epithelialization. *Br. J. Dermatol.* **163**: 38–47.

Taylor RC, Cullen SP, and Martin SJ. (2008). Apoptosis: controlled demolition at the cellular level. *Nat Rev Mol Cell Biol* **9**: 231–241.

Taysi S, Uslu C, Akcay F, and Sutbeyaz MY. (2003). Malondialdehyde and Nitric Oxide Levels in the Plasma of Patients with Advanced Laryngeal Cancer. *Surgery Today* **33**: 651–654.

Tennant I, Pound JD, Marr LA, Willems JJLP, Petrova S, Ford CA, *et al.* (2013). Innate recognition of apoptotic cells: novel apoptotic cell-associated molecular patterns revealed by crossreactivity of anti-LPS antibodies. *Cell death and differentiation* **20**: 698–708.

Theocharidis A, van Dongen S, Enright AJ, and Freeman TC. (2009). Network visualization and analysis of gene expression data using BioLayout Express(3D). *Nat Protoc* **4**: 1535–1550.

Thiede B, Treumann A, Kretschmer A, Söhlke J, and Rudel T. (2005). Shotgun proteome analysis of protein cleavage in apoptotic cells. *Proteomics* **5**: 2123–2130.

Thomas LL, Xu W, and Ardon TT. (2002). Immobilized lactoferrin is a stimulus for eosinophil activation. *J Immunol* **169**: 993–999.

Thomsen LL, Lawton FG, Knowles RG, Beesley JE, Riveros-Moreno V, and Moncada S. (1994). Nitric oxide synthase activity in human gynecological cancer. *Cancer Res* **54**: 1352–1354.

Thomsen LL, Miles DW, Happerfield L, Bobrow LG, Knowles RG, and Moncada S. (1995). Nitric oxide synthase activity in human breast cancer. *Br J Cancer* **72**: 41–44.

Tiefenthaler M, Amberger A, Bacher N, Hartmann BL, Margreiter R, Kofler R, *et al.* (2001). Increased lactate production follows loss of mitochondrial membrane potential during apoptosis of human leukaemia cells. *Br. J. Haematol.* **114**: 574–580.

Togawa J-I, Nagase H, Tanaka K, Inamori M, Nakajima A, Ueno N, *et al.* (2002). Oral administration of lactoferrin reduces colitis in rats via modulation of the immune system and correction of cytokine imbalance. *J. Gastroenterol. Hepatol.* **17**: 1291–1298.

Torr EE, Gardner DH, Thomas L, Goodall DM, Bielemeier A, Willetts R, *et al.* (2011). Apoptotic cell-derived ICAM-3 promotes both macrophage chemoattraction to and tethering of apoptotic cells. *Cell death and differentiation* **19**: 671–679.

Tosello-Trampont AC, Nakada-Tsukui K, and Ravichandran KS. (2003). Engulfment of Apoptotic Cells Is Negatively Regulated by Rho-mediated Signaling. *Journal of Biological Chemistry* **278**: 49911–49919.

Truman LA, Ford CA, Pasikowska M, Pound JD, Wilkinson SJ, Dumitriu IE, *et al.* (2008). CX3CL1/fractalkine is released from apoptotic lymphocytes to stimulate macrophage chemotaxis. *Blood* **112**: 5026–5036.

Tsai RK, and Discher DE. (2008). Inhibition of 'self' engulfment through deactivation of myosin-II at the phagocytic synapse between human cells. *The Journal of Cell Biology* **180**: 989–1003.

Tsai W-H, Shih C-H, Feng S-Y, Li I-T, Chang S-C, Lin Y-C, *et al.* (2014). CX3CL1(+) Microparticles Mediate the Chemoattraction of Alveolar Macrophages

toward Apoptotic Acute Promyelocytic Leukemic Cells. *Cell Physiol Biochem* **33**: 594–604.

Tung Y-T, Chen H-L, Yen C-C, Lee P-Y, Tsai H-C, Lin M-F, *et al.* (2013). Bovine lactoferrin inhibits lung cancer growth through suppression of both inflammation and expression of vascular endothelial growth factor. *J. Dairy Sci.* **96**: 2095–2106.

Underhill DM, and Goodridge HS. (2012). Information processing during phagocytosis. *Nat Rev Immunol* **12**: 492–502.

Ura S, Masuyama N, Graves JD, and Gotoh Y. (2001). Caspase cleavage of MST1 promotes nuclear translocation and chromatin condensation. *Proc. Natl. Acad. Sci. U.S.A.* **98**: 10148–10153.

Urban JL, Shepard HM, Rothstein JL, Sugarman BJ, and Schreiber H. (1986). Tumor necrosis factor: a potent effector molecule for tumor cell killing by activated macrophages. *Proc. Natl. Acad. Sci. U.S.A.* **83**: 5233–5237.

van der Strate BW, Beljaars L, Molema G, Harmsen MC, and Meijer DK. (2001). Antiviral activities of lactoferrin. *Antiviral Res.* **52**: 225–239.

van Dongen S. (2000). Graph clustering by flow simulation, PhD thesis. *University of Utrecht*.

van Furth R, Cohn ZA, Hirsch JG, Humphrey JH, Spector WG, and Langevoort HL. (1972). The mononuclear phagocyte system: a new classification of macrophages, monocytes, and their precursor cells. *Bull. World Health Organ.* **46**: 845–852.

Van Ginderachter JA, Movahedi K, Hassanzadeh Ghassabeh G, Meerschaut S, Beschin A, Raes G, *et al.* (2006). Classical and alternative activation of mononuclear phagocytes: Picking the best of both worlds for tumor promotion. *Immunobiology* **211**: 487–501.

Van Snick JL, and Masson PL. (1976). The binding of human lactoferrin to mouse peritoneal cells. *J Exp Med* **144**: 1568–1580.

Vandivier RW, Ogden CA, Fadok VA, Hoffmann PR, Brown KK, Botto M, *et al.* (2002). Role of surfactant proteins A, D, and C1q in the clearance of apoptotic cells in vivo and in vitro: calreticulin and CD91 as a common collectin receptor complex. *J Immunol* **169**: 3978–3986.

Varadhachary A, Wolf JS, Petrak K, O'Malley BW, Spadaro M, Curcio C, *et al.* (2004). Oral lactoferrin inhibits growth of established tumors and potentiates conventional chemotherapy. *Int J Cancer* **111**: 398–403.

Varin A, and Gordon S. (2009). Alternative activation of macrophages: Immune function and cellular biology. *Immunobiology* **214**: 630–641.

Verreck FAW, de Boer T, Langenberg DML, Hoeve MA, Kramer M, Vaisberg E, *et al.* (2004). Human IL-23-producing type 1 macrophages promote but IL-10-

producing type 2 macrophages subvert immunity to (myco)bacteria. *Proc. Natl. Acad. Sci. U.S.A.* **101**: 4560–4565.

Vieira OV, Bucci C, Harrison RE, Trimble WS, Lanzetti L, Gruenberg J, *et al.* (2003). Modulation of Rab5 and Rab7 Recruitment to Phagosomes by Phosphatidylinositol 3-Kinase. *Molecular and Cellular Biology* **23**: 2501–2514.

Vogel HJ. (2012). Lactoferrin, a bird's eye view. *Biochem. Cell Biol.* **90**: 233–244.

Volkman A, and Gowans JL. (1965). The origin of macrophages from bone marrow in the rat. *Br J Exp Pathol* **46**: 62–70.

Voll RE, Herrmann M, Roth EA, Stach C, Kalden JR, and Girkontaite I. (1997). Immunosuppressive effects of apoptotic cells. *Nature* **390**: 350–351.

Wada N, Zaki MAA, Hori Y, Hashimoto K, Tsukaguchi M, Tatsumi Y, *et al.* (2011). Tumour-associated macrophages in diffuse large B-cell lymphoma: a study of the Osaka Lymphoma Study Group. *Histopathology* **60**: 313–319.

Wakabayashi H, Abe S, Okutomi T, Tansho S, Kawase K, and Yamaguchi H. (2009). Cooperative anti-Candida effects of lactoferrin or its peptides in combination with azole antifungal agents. *Microbiol. Immunol.* **40**: 821–825.

Wally J, and Buchanan SK. (2007). A structural comparison of human serum transferrin and human lactoferrin. *Biometals* **20**: 249–262.

Walmer DK, Padin CJ, Wrona MA, Healy BE, Bentley RC, Tsao MS, *et al.* (1995). Malignant transformation of the human endometrium is associated with overexpression of lactoferrin messenger RNA and protein. *Cancer Res* **55**: 1168–1175.

Walusansa V, Okuku F, and Orem J. (2012). Burkitt lymphoma in UGANDA, the legacy of Denis Burkitt and an update on the disease status. *Br. J. Haematol.* **156**: 757–760.

Wang H, Grand RJ, Milner AE, Armitage RJ, Gordon J, and Gregory CD. (1996). Repression of apoptosis in human B-lymphoma cells by CD40-ligand and Bcl-2: relationship to the cell-cycle and role of the retinoblastoma protein. *Oncogene* **13**: 373–379.

Wang H-W, and Joyce JA. (2010). Alternative activation of tumor-associated macrophages by IL-4. *Cell Cycle* **9**: 4824–4835.

Wang MB, Strasnick B, and Zimmerman MC. (1992). Extranodal American Burkitt's lymphoma of the head and neck. *Arch. Otolaryngol. Head Neck Surg.* **118**: 193–199.

Wang WP, Iigo M, Sato J, Sekine K, Adachi I, and Tsuda H. (2000). Activation of intestinal mucosal immunity in tumor-bearing mice by lactoferrin. *Jpn. J. Cancer Res.* **91**: 1022–1027.

Weigert A, and Brüne B. (2008). Nitric oxide, apoptosis and macrophage polarization during tumor progression. *Nitric Oxide* **19**: 95–102.

Weigert A, Tzieply N, Knethen von A, Johann AM, Schmidt H, Geisslinger G, *et al.* (2007). Tumor cell apoptosis polarizes macrophages role of sphingosine-1-phosphate. *Mol Biol Cell* **18**: 3810–3819.

Weinberg GA. (1994). Iron chelators as therapeutic agents against Pneumocystis carinii. *Antimicrobial Agents and Chemotherapy* **38**: 997–1003.

Weiskopf K, and Weissman IL. (2015). Macrophages are critical effectors of antibody therapies for cancer. *MAbs* **7**: 303–310.

Welch JS. (2002). TH2 Cytokines and Allergic Challenge Induce Ym1 Expression in Macrophages by a STAT6-dependent Mechanism. *Journal of Biological Chemistry* **277**: 42821–42829.

White GE, Tan TCC, John AE, Whatling C, McPheat WL, and Greaves DR. (2010). Fractalkine has anti-apoptotic and proliferative effects on human vascular smooth muscle cells via epidermal growth factor receptor signalling. *Cardiovascular Research* **85**: 825–835.

Willems JJLP, Arnold BP, and Gregory CD. (2014). Sinister self-sacrifice: the contribution of apoptosis to malignancy. *Front Immunol* **5**: 299.

Willingham SB, Volkmer J-P, Gentles AJ, Sahoo D, Dalerba P, Mitra SS, *et al.* (2012). The CD47-signal regulatory protein alpha (SIRPa) interaction is a therapeutic target for human solid tumors. *Proceedings of the National Academy of Sciences* **109**: 6662–6667.

Wood W, Turmaine M, Weber R, Camp V, Maki RA, McKercher SR, *et al.* (2000). Mesenchymal cells engulf and clear apoptotic footplate cells in macrophageless PU.1 null mouse embryos. *Development* **127**: 5245–5252.

Wynn TA, Chawla A, and Pollard JW. (2013). Macrophage biology in development, homeostasis and disease. *Nature* **496**: 445–455.

Xu J, Escamilla J, Mok S, David J, Priceman S, West B, *et al.* (2013). CSF1R Signaling Blockade Stanches Tumor-Infiltrating Myeloid Cells and Improves the Efficacy of Radiotherapy in Prostate Cancer. *Cancer Res* **73**: 2782–2794.

Xu XX, Jiang HR, Li HB, Zhang TN, Zhou Q, and Liu N. (2010). Apoptosis of stomach cancer cell SGC-7901 and regulation of Akt signaling way induced by bovine lactoferrin. *J. Dairy Sci.* **93**: 2344–2350.

Yamada Y, Amagasaki T, Jacobsen DW, and Green R. (1987). Lactoferrin binding by leukemia cell lines. *Blood* **70**: 264–270.

Yin Y, Huang X, Lynn KD, and Thorpe PE. (2013). Phosphatidylserine-Targeting Antibody Induces M1 Macrophage Polarization and Promotes Myeloid-Derived

Suppressor Cell Differentiation. *Cancer Immunology Research* **1**: 256–268.

Zhang J-J, Li X-Q, Sun J-W, and Jin S-H. (2014). Nitric oxide functions as a signal in ultraviolet-B-induced baicalin accumulation in Scutellaria baicalensis suspension cultures. *Int J Mol Sci* **15**: 4733–4746.

Zhao H, Dugas N, Mathiot C, Delmer A, Dugas B, Sigaux F, *et al.* (1998). B-cell chronic lymphocytic leukemia cells express a functional inducible nitric oxide synthase displaying anti-apoptotic activity. *Blood* **92**: 1031–1043.

Zhuang L, Pound JD, Willems JJLP, Taylor AH, Forrester LM, and Gregory CD. (2012). Pure populations of murine macrophages from cultured embryonic stem cells. Application to studies of chemotaxis and apoptotic cell clearance. *J Immunol Methods* **385**: 1–14.

Zimecki M, Artym J, Chodaczek G, Kocieba M, and Kruzel M. (2005). Effects of lactoferrin on the immune response modified by the immobilization stress. *Pharmacol Rep* **57**: 811–817.

Zitvogel L, Kepp O, Senovilla L, Menger L, Chaput N, and Kroemer G. (2010). Immunogenic Tumor Cell Death for Optimal Anticancer Therapy: The Calreticulin Exposure Pathway. *Clinical Cancer Research* **16**: 3100–3104.

Zocco D, Ferruzzi P, Cappello F, Kuo WP, and Fais S. (2014). Extracellular vesicles as shuttles of tumor biomarkers and anti-tumor drugs. *Front Oncol* **4**: 267.

Zou H, Li Y, Liu X, and Wang X. (1999). An APAF-1-cytochrome c multimeric complex is a functional apoptosome that activates procaspase-9. *J Biol Chem* **274**: 11549–11556.